Determination of genes involved in the microRNA turnover in *Arabidopsis thaliana*

FIRAS LOUIS

Supervisors: Pr Tamas Dalmay and Pr Simon Moxon

A thesis submitted for the degree of Doctor of Philosophy (PhD)

School of Biological Sciences, University of East Anglia, Norwich, United Kingdom

December 2023

Abstract

microRNAs are short 21-24nt small RNAs responsible of the regulation of proteins level in both plants and animals and as crucial regulators, they need to be tightly regulated. In plants, miRNAs are transcribed from a MIR gene and form a long transcript with a stem-loop structure necessary for processing into a smaller dsRNA by the Dicing body. The duplex is then methylated by *HEN1* that confers protection against 3' nucleases. One of the two strands is loaded into its partner, an ARGONAUTE protein to form the RISC complex that degrades complementary mRNAs. miRNAs can then be truncated by SDN1 or urydilated by HESO1 and/or URT1 to promote their degradation. However, SDN1 cannot degrade urydilated miRNAs and the protein responsible is still unknow. During my PhD, I tried to uncover this protein by a screening assay using a GFP transgene targeted by miR395 in low sulphur conditions and by rescuing the *hen1* background with different candidate genes predicted to interact with HESO1. While the screening assay did not produce sufficient results and needs some improvements, the other approach led us to a small phenotypic rescue of the *hen1* background by *sua*, which is a splicing factor, despite not having a miRNA level increase in the vegetative stage. The alternative splicing analysis between *sua* and the wild type (Col-0) highlighted an unknown nuclease (namely *RNase X*), homologous to a human *RNase P* subunit whose function have been transferred to PRORPs in plants. The mutant shows a higher level of some miRNAs, an increased tailing and has a better fitness compared to Col-0, indicative of the importance of this gene. While more needs to be uncovered on this *RNase X*, the results suggest that it regulates a subset of miRNAs and that it may be involved in the degradation of a subset of U-tailed miRNAs.

Contents

Abbreviations

ABI: Abscisic Acid Insensitive

AGO: ARGONAUTE

AP2: APETALA2

ARF: Auxin Response Factor

cDNA: complementary DNA

CERK1: Chitin Elicitor Receptor Kinase 1

DCL: DICER-Like

DNA: Deoxyribonucleic Acid

dsRNA: double stranded RNA

EMS: Ethyl Methanesulfonate

ER: Early Response mutant

FRET/FLIM: Fluorescence Resonance Energy Transfer/Fluorescence Lifetime Imaging

GFP: Green Fluorescent Protein

GO: Gene Ontology

GOI: Gene Of Interest

HAT: High Affinity Transporter

HEN1: HUA Enhancer 1

HESO1: HEN1 Suppressor 1

HI[number]: HESO1 Interactor [number]

HKG: Housekeeping Gene

HYL1: Hyponastic Leaves 1

LAT: Low Affinity Transporter

LR: Late Response mutant

LS: Low Sulphur condition

$MgSO_4$: Magnesium Sulphate

miPEP: miRNA-encoded peptide

miRNA/miR[number]: microRNA

miRNA*: passenger miRNA

miTRATA: microRNA Truncation and Tailing Analysis

mRNA: messenger RNA

NEXT: Nuclear Exosome Targeting

nt: nucleotide

NTF2: Nuclear Transport Factor 2

ORF: Open Reading Frame

PCR: Polymerase Chain Reaction

Pi: inorganic Phosphate

POI: Protein of Interest

Pre-miR/pre-miRNA/premiR[number]: precursor miRNA

Pri-miR/pri-miRNA/primiR[number]: primary miRNA

PRORP: proteinaceous RNAse P or PROtein-only RNase P

pv: (days) post vernalisation

RT-qPCR: Reverse Transcriptase quantitative Polymerase Chain Reaction

RICE: RISC-Interacting Clearing Exonuclease

RISC: RNA-induced Silencing Complex

RNA: Ribonucleic Acid

RNA Pol II: RNA polymerase II

RPP38: Ribonuclease P protein subunit P38

SAM: Shoot Apical Meristem

SDN: Small-RNA Degrading Nuclease

siRNA: small interfering RNA

SLIM1: Sulphur Limitation 1

SNC4: Suppressor of NPR1-1, Constitutive 4

snoRNA: small nucleolar RNA

SPL: Squamosa Promoter Binding Protein-Like

sRNA: small RNA

SUA: Suppressor of ABI3-5

SUC2: Sucrose Transport Protein 2

SULTR: Sulphur Transporter

TAIR: The Arabidopsis Information Resource (website)

TDMD: Target Directed microRNA Degradation

SOV: Suppressor Of Varicose

T-DNA: Transfer DNA

TE : Transposable Element

TOE1: Target Of Early Activation Tagged 1

UTR: Untranslated Region

URT1: UTP:RNA Uridylyltransferase 1

WT: Wild Type

Y2H: Yeast Two Hybrid

Acknowledgements

Firstly, I would like to thank Tamas Dalmay for giving the opportunity to do my PhD at UEA, allowing me to continue working on miRNAs in *Arabidopsis* after my Master. This PhD shaped me in many ways and strengthened my insatiable curiosity and I could not have managed it without proper support. Another thanks to Tamas for the Ziggurat challenge, I had tons of fun on weird sports, especially the Quidditch, and it was a very welcomed weekly mental break during my last year. I also thank the members of the Dalmay laboratory for helping me settle in the laboratory, especially Yvonne Ridge and Maria-Elena Mannarelli who answered many questions, offered their help without any complains and sometimes called me a star to make my weeks better. A huge thanks is due to Dr Rocky Payet, who put down the bases of this PhD, helped me with some of my analysis, was a great mentor, trusted confidant and without him, this work would not exist.

I also received immeasurable support from my family and friends who stayed abroad, who despite not understanding all of what I was doing, kept me asking if I was progressing so I can rant about work. Special mention to my sister who kept asking me if I found my fluorescent gene and to Anthony for intense discussions and awful jokes over video games. I also met great friends in the UK, and I would like to thank Anya for her incredible mental support and the Smashing Cocks: Daniel, Keanu and Mellieha. We had great times together smashing shuttlecocks over dramas or intense sperm discussions, foraging, eating cheese and so on. Maybe the real treasure was not to answer a 20-year-old question but the friends we made along the way.

Final thanks are for Aaron Swartz and Alexandra Elbakyan/Sci-hub for their fights for accessible Science and providing papers that even UEA cannot access. Knowledge should be freely available to everyone, especially in developing countries.

On a lighter note, I want to finish this section with a famous quote from Richard Feynman which resonate a lot with me: "*I have a friend who's an artist and has sometimes taken a view which I don't agree with very well. He'll hold up a flower and say: ''look how beautiful it is," and I'll agree. Then he says: ''I as an artist can see how beautiful this is but you as a scientist take this all apart and it becomes a dull thing," and I think that he's kind of nutty.*

First of all, the beauty that he sees is available to other people and to me too, I believe. Although I may not be quite as refined aesthetically as he is … I can appreciate the beauty of a flower. At the same time, I see much more about the flower than he sees. I could imagine the cells in there, the complicated actions inside, which also have a beauty. I mean it's not just beauty at this dimension, at one centimetre; there's also beauty at smaller dimensions, the inner structure, also the processes. The fact that the colours in the flower evolved in order to attract insects to pollinate it is interesting; it means that insects can see the colour. It adds a question: does this aesthetic sense also exist in the lower forms? Why is it aesthetic? All kinds of interesting questions which the science knowledge only adds to the excitement, the mystery and the awe of a flower. It only adds. I don't understand how it subtracts.".

Chapter I] Introduction

According to the classic model of molecular biology, firstly enunciated by Jacob & Monod, (1961), gene expression is mostly controlled by a set of transcription factors which are proteins that bind to the promoting region of a coding gene leading to its activation or its inhibition (Yu & Gerstein, 2006). More recently, non-coding small RNAs (sRNAs) emerged as a set of molecules with an essential regulation role (He & Hannon, 2004). There are two main types of sRNAs: small interfering RNAs (siRNAs) and microRNAs (miRNAs). Plant siRNAs are around 24 nucleotides (nt) long and have a significant role in preventing proliferation of transposable elements (TEs) (Hollister et al., 2011). miRNAs, that are the focus of the rest of this thesis, are 21-24 nt long and regulate gene expression at a post-transcriptional level (Bartel, 2004).

1) An impactful discovery at the origin of a new field of research

The story of microRNAs starts with in 1993 in *Caenorhabditis elegans* when Lee et al., (1993) found that *LIN-4* acts negatively on the protein coding gene *LIN-14* during the first larval stage. *LIN-4* does not encode for a protein and its two transcripts (22 and 61 nt) possess complementarity sequences with the 3' untranslated region (3'UTR) of *LIN-14* showing what will later be confirmed for the mode of actions of miRNAs. It is only seven years later that another sRNA (*let-7*) will be described in *C. elegans* to downregulate five genes (*LIN-14*, *LIN-28*, *LIN-41*, *LIN-42* and *DAF-12*) through RNA-RNA interactions with their 3'UTRs (Reinhart et al., 2000). Those breakthroughs opened a new field of research and massive discoveries about miRNAs followed during the following two years including part of their processing pathway (Bernstein et al., 2001; Cerutti et al., 2000) and ~150 new miRNAs were discovered in animals (including *Homo sapiens* and *Drosophila melanogaster*) following two criteria emerging from the shared features with *LIN-4* and *let-7*: an RNA size between 21 and 24 nt detectable by northern blot and have a complementarity with flanking regions of protein coding genes.

In plants, 16 miRNAs were also discovered in *Arabidopsis thaliana* (Reinhart et al., 2002) with eight of them were found identical in rice, thus conserved. Moreover, Bernstein et al., (2001) showed that mutation in the *Dicer* homologue (responsible for miRNAs' processing) avoid miRNAs' accumulation, demonstrating similarities in the miRNA pathway between plants and animals. The criteria for the identification of miRNAs in plants changed multiple times with new discoveries but most of the researchers followed Meyers' criteria since 2008 (Meyers et al., 2008). Those main criteria are: 1) One or more miRNA/miRNA* duplexes (a double stranded RNA composed of the miRNA and its complementary strand, the miRNA*) with two nucleotides 3' overhang to allow methylation of the duplexes. 2) Validation of both the mature miRNA and its miRNA* (by sequencing or northern blot or qPCR). 3) The duplex must have less than 4 mismatches. miRNAs are stored in different databases (Fromm et al., 2020) and the most used is miRBase (Griffiths-Jones, 2006) (http://www.mirbase.org/, current version: 22.1). An update to Meyers criteria was proposed in 2018 (Axtell & Meyers, 2018) to reduce the number of false positives present in the databases, which advise confirmation only by sRNAseq, to keep only miRNAs from 20 to 24 nt with enhanced evidence needed for the miRNAs of a size of 23 or 24 nt.

The miRNA field of research exploded by looking at miRNAs in a plethora of organisms, by determining the mechanisms behind the biogenesis and turnover, the mode of action, the stress responses, the conservation of the machinery of miRNAs, etc. Many differences were found between plants and animals, especially in the machinery while the repertoires of miRNAs are conserved within kingdoms. Our understanding of those small molecules drastically changed and new discoveries keep arising on a regular basis with potential use in treating diseases (Ho et al., 2022; Saiyed et al., 2022) or improving crops (Chen et al., 2021; Djami-Tchatchou et al., 2017; Raza et al., 2023).

2) Biogenesis and mode of action

miRNAs are expressed in both plants and animals from a MIR gene transcribed by the *RNA Polymerase II* (*RNA Pol II*) leading to a single strand primary miRNA (pri-miRNA or pri-miR), which undergo several modifications like the addition of a 3' poly-A tail, a 5' capping and/or

splicing out introns for some of them (roughly half of *Arabidopsis*' miRNAs)(Szarzynska et al., 2009). The pri-miRNA folds into a characteristic hairpin structure and is further processed in different ways between animal and plants to finally produce a mature miRNA that targets a mRNA, with different complementarity depending on the kingdom.

In animals, the pri-miRNA is processed by a complex composed of the endonucleases III Drosha (Lee et al., 2003) and Pasha in Drosophila and *C. elegans* (Denli et al., 2004) and Drosha and DGCR8 in Bilaterians (Han et al., 2004; Landthaler et al., 2004) to cut the stem and make a precursor miRNA (pre-miRNA or pre-miR) that is exported to the cytoplasm by the protein Exportin 5 (Yi et al., 2003). Then, the pre-miRNA is shortened of its loop by Dicer to form a 21-24 nucleotides double stranded RNA, called the miRNA/miRNA* duplex (Hutvágner et al., 2001; Ketting et al., 2001). The miRNA is the guide strand which is loaded into an ARGONAUTE protein (usually AGO1 in Drosophila and AGO2 in mammalian) to form the miRISC complex (Alisch et al., 2007; Bernstein et al., 2003; Kataoka et al., 2001; Schwarz et al., 2003), while the miRNA* is the passenger strand and is usually not loaded and released in the cytoplasm to be degraded (Figure 1). In plants, the whole processing of the pri-miRNA happens in the nucleus with the Dicing Body cutting the pri-miRNA's stem into the pre-miRNA and also the pre-miRNA's loop into the same double stranded RNA (Fang & Spector, 2007; Rogers & Chen, 2013). The Dicing Body is composed of a multitude of proteins with the main proteins being SERRATE (Homologue of Ars2 that binds to Drosha and Pasha/DGCR8) (Laubinger et al., 2008; Lobbes et al., 2006; Yang et al., 2006), HYL1 (Dong et al., 2008; Han et al., 2004; Yang et al., 2014) and DCL1 (for *Dicer-Like 1*) (Dong et al., 2008; W. Park et al., 2002; Reinhart et al., 2002). The key difference between animals and plants is that plants miRNA/miRNA* duplex get methylated by HEN1 in their 3' ends to protect the miRNAs from early degradation and promote their stability in the AGO1 as a loss of *HEN1* shows a huge decrease in miRNA's level (Yang et al., 2006; Yu et al., 2005). The miRNA/miRNA* duplex is then exported to the cytoplasm by the protein HASTY (Mee et al., 2005; Papp et al., 2003), homolog of Exportin 5, to have the guide strand loaded in AGO1 and the passenger strand released to be degraded (Liu et al., 2020) (Figure 1).

Once loaded, miRNAs target one or multiple mRNA targets with more or less complementarity mainly depending on the system studied. Indeed, in animals, targets recognition primarily relies on a seed sequence of 7 nucleotides in position 2-8 of the miRNA targeting the 3'-UTR

of mRNA (Forman & Coller, 2010; Grimson et al., 2007) while in plants, the miRNA requires almost perfect complementarity within the Open Reading Frames (ORFs) of its target (Voinnet, 2009). This has an impact on the mode of action of the RISC complex with two possible outcomes: translation inhibition or target cleavage. If there is almost complete complementarity, the endonucleolytic activity is triggered on AGO1's PIWI domain, that cleaves the mRNA in two, leaving it vulnerable to degradation (Ameres & Zamore, 2013; Iwakawa & Tomari, 2013; Liu et al., 2014; Rhoades et al., 2002). This does not happen when there is only a seed binding, which causes a translation inhibition by preventing the ribosomes to bind to the mRNA (Bartel, 2009; Lai, 2002). This action is not performed by AGO alone but requires a partnership with GW182 (Eulalio et al., 2008) in Drosophila, TNRC6 in Vertebrates (Pfaff et al., 2013; Zipprich et al., 2009) and SUO in plants (Yang et al., 2012) and its enrolment calls for other proteins that degrade the poly-A tail of the mRNA leading to its degradation (Fabian & Sonenberg, 2012; Meister et al., 2005). The choice of mode of action depends on a tiny loop in the PIWI domain which differs between plants and animals (Xiao et al., 2023). This complementarity difference influences the number of targets a miRNA can have with plant miRNAs having few targets (Bartel, 2009; Liu et al., 2014; Rhoades et al., 2002) while in animals, miRNAs have several targets (Nozawa et al., 2016; Simkin et al., 2020).

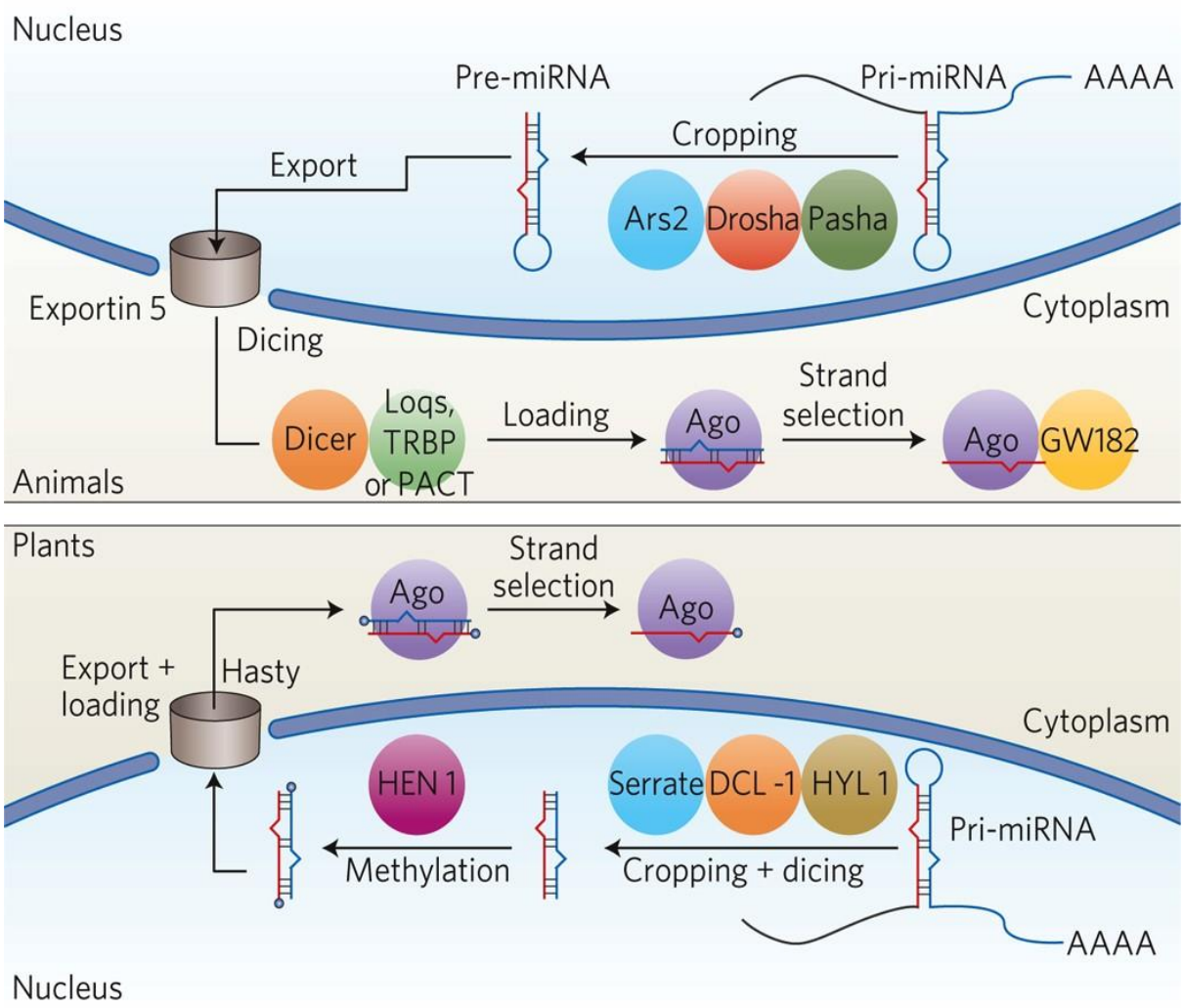

Figure 1: miRNA biogenesis pathway in animals and plants. In both systems, the primary miRNA (pri-miRNA) is transcribed from a MIR gene, forms a characteristic hairpin structure, is poly-adenylated on the 3'-end and capped on the 5'end. In animals, the pri-miRNA's stem is removed by Drosha, Pasha/DGCR8 and Ars2 to form the precursor miRNA (pre-miRNA) that is exported by Exportin 5 to the cytoplasm to have its loop removed by Dicer to form a miRNA/miRNA duplex. Only one of the strand is loaded into a protein ARGONAUTE (AGO) to form the miRISC complex. In plants, the processing of the pri-miRNA into the pre-miRNA and into the miRNA/miRNA* duplex is performed by the Dicing Body composed of SERRATE, HYL1 and DCL1. The duplex is protected by a 2-O-methylation done by HEN1 to increase their stability before their export into the cytoplasm by HASTY. The guide strand is then loaded into AGO1. In animals, GW182 (TNRC6 in Vertebrates) is required for the action of the miRISC complex. From Moran et al. (2017) with permission of the publisher.*

3) miRNAs as key regulators: Some examples of miRNAs' implication in plants

The first miRNA was discovered in *C. elegans* and was involved in the larvae developmental timing (Lee et al., 1993). miRNAs have a significant impact on plants due to their regulatory roles, from plant development and reproduction to the ability to respond to biotic and abiotic stresses. Losing miRNAs or proteins involved in their processing induces huge developmental effects, showing the very important role of those small non-coding RNAs. Indeed, the null mutant for *DCL1* exhibits abnormal patterns formation during embryogenesis after the eight-cell stage (Nodine & Bartel, 2010) and mutants for *AGO1*, *HEN1* and *HYL1* shows reduced level of miRNAs and atypical leaf phenotypes, poor fertility, late flowering and prematurely open flowers (Bohmert et al., 1998; Jover-Gil et al., 2012). The overall decrease in miRNAs showed many phenotypic changes that reduce fitness but as miRNAs are downregulating a target according to their short sequences, it is clear that each miRNA has a specific role by targeting specific transcripts. Looking at those miRNAs and their targets specifically allowed us to unveil important pathways in plant development, reproduction, and stress response.

3.1) miRNAs in plant development

In plants, development is dependent on genetic factors but also the environment and miRNAs have a huge role in the development and reproduction (Dong et al., 2022) (Figure 2). The regulatory network between miRNAs and their targets during development is huge (Chen et al., 2018; Li & Zhang, 2016; Singh et al., 2018; Wu, 2013) and also depends on environmental factors such as temperature and light like in flowering time (Lee et al., 2010).

The most famous and routinely tested miRNAs are miR156 and miR172, involved in plant development and the transition from vegetative to reproductive stage (Schoor et al., 2021; Spanudakis & Jackson, 2014; Teotia & Tang, 2015). miR156 is expressed in young plants during the vegetative stage and repress SPL (*SQUAMOSA Promoter Binding Protein-Like*) transcription factors to maintain a juvenile phase as an overexpression of miR156/157 reduces the level of SPLs, leading to a late flowering of *Arabidopsis* (Gandikota et al., 2007;

Wang et al., 2009) and rice (Xie et al., 2006). This phenotype was essentially rescued by having an *SPL3* without the target site of miR156, showing that those two are involved in plant maturation (Wu & Poethig, 2006). As the plant gets older, miR156 expression is decreased and the level of its targets increases, leading to a juvenile to adult transition and the apparition of the stem (Cheng et al., 2021). At that moment, miR172 starts to get expressed to promote the flowering by targeting the *APETALA2* (*AP2*) transcription factors. A study showed that overexpression of miR172 induced early flowering while overexpression of *AP2* delays it (Aukerman & Sakai, 2003). The interesting part comes from the promotion of miR172's expression by SPLs, especially SPL9 and SPL10 in *Arabidopsis,* which acts redundantly. As miR156 is slowly downregulated in the plant, the numbers of SPLs transcription factors increase and induce the expression of miR172 that then induces flower development. This is known as the miR156-SPL-miR172 pathway and is recognized as the key pathway to the juvenile to adult transition in plants (Schoor et al., 2021; Wu et al., 2009). But miR156 has also many other roles in stress response (Yuan et al., 2023), while Zhao et al., (2017) found that the particular yellow colour in the petals of *Paeonia lactiflora* might be regulated by miR156 targeting *SPL1* and not because of the sap pH or the metal elements present in soil like previously thought.

Hormones also play a significant role in plant development and are unsurprisingly regulated by miRNAs like *Auxin*, one of the five main phytohormones. miR160 targets different *Auxin Response Factors* (*ARFs*), involved in the production of the hormone, leading to its regulation (Hao et al., 2022). Silencing of miR160 increases the level of *ARF16* and *ARF17* and shows many phenotypic defects as abnormal leaf shapes and symmetry, early infertile flowering, and shorter roots (Mallory et al., 2005). Meanwhile, overexpressing miR160 represses the expression of *ARF10* and *ARF16* with the same strength as the *arf10/arf16* double mutant, with roots malformations and loss of gravity-sensing (Wang et al., 2005).

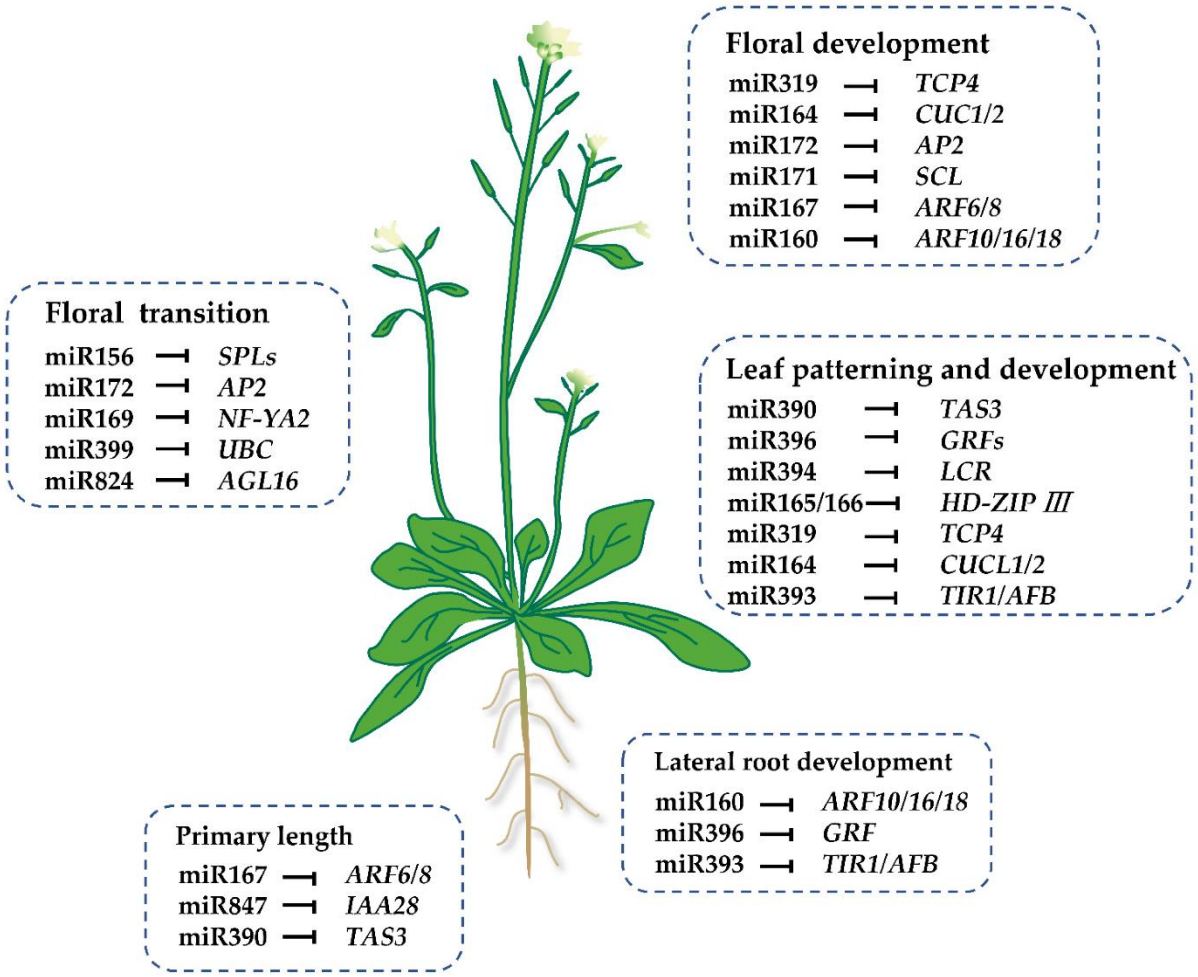

Figure 2: Roles of miRNAs in plant development. miRNAs are grouped in their roles and associated with their targets. From Teng et al. (2023) in open access.

3.2) miRNAs involved in nutrient stress response: miR395 and miR399 in the regulation of Sulphur and Phosphate uptake and assimilation

miRNAs are not only involved in plant development but also involved in stress responses, both biotic and abiotic, with a plethora of miRNAs in play. miRNAs are of key interest for agronomic plants as understanding and detecting these molecules can help agronomists to have the correct response (Samynathan et al., 2023).

Alongside Carbon (C), Hydrogen (H) and Oxygen (O), plants need 14 mineral nutrients, divided into two groups, to maintain their growth and development (Nath & Tuteja, 2016). Six macronutrients, required in substantial amounts, are composed of Nitrogen (N), Phosphorus (P), Potassium (K), Calcium (Ca), Magnesium (Mg) and Sulfur (S) while micronutrients are

present in small quantity. Mineral nutrients are extracted from soil and transported through the plant with several specific transporters. Deficiency in mineral nutrients induces morphological defects and reduced yield (Zhao et al., 1999) which is a real problem in crops species (McGrath & Zhao, 1996). miRNAs have key roles in maintaining nutrient homeostasis in plants. Sulfate (SO_4^{2-}) is extracted from soil by the High Affinity Transporters (*HATs*) SULTR1;1, induced significantly even under short periods of low Sulfur conditions (Takahashi et al., 2000) and SULTR1;2 which is constitutively expressed (Yoshimoto et al., 2002). After assimilation, Sulfur is transported through the plant in the xylem by two Low Affinity Transporters (LATs) called SULTR2;1 and SULTR2;2 (Kirschner et al., 2018; Takahashi et al., 2000). Kataoka et al., (2004) found that the Sulfur uptake by another transporter called SULTR3;5, constitutively expressed in Arabidopsis, was minor when the gene is expressed alone but greatly increases SO_4^{2-} uptake when it is co-expressed with *SULTR2;1* with a Sulfate uptake activity three times higher than SULTR2;1 expressed alone. Sulfur homeostasis needs to be regulated and the expression of *SULTR1;1* and *SULTR2;1* is under control of a transcription factor: *SULPHURLIMITATION1* (*SLIM1*) which controls the transcription of those genes but also triggers the synthesis of miR395 in low Sulfur conditions in *Arabidopsis* (Kawashima et al., 2009; Maruyama-Nakashita et al., 2006) (Figure 3). Under low Sulfur conditions, miR395 is expressed in both roots and shoots and targets the LAT *SULTR2;1* and three ATP Sulphurylases involved in the Sulfur metabolism pathway (*APS1*, *APS3* and *APS4*). Kawashima et al., (2009) found that, under low Sulfur conditions, the expression of *SULTR2;1* is reduced in leaves as expected but increased in the roots which is the opposite results predictable since it is targeted by miR395. This is due to the exact localisation of those two molecules in the roots. Indeed, *SULTR2;1* is predominantly expressed in xylem parenchyma cells (Takahashi et al., 1997, 2000) while the targeting miRNA is mainly found in phloem companion cells. However, fragments of *SULTR2;1* mRNA cleaved by miR395 were found in roots indicating that both are expressed in the same cells, thus the separation is not strict and the transcription of *SULTR2;1* may occur in phloem companion cells and is repressed by miR395 only in those cells under low Sulfur conditions to maintain the expression level of *SULTR2;1* only in the Xylem as proposed by the authors. Taken together, those results show the crucial role of miR395 in Sulfur homeostasis under low Sulfur conditions and under the control of SLIM1, by limiting the Sulfur uptake and transportation from roots to shoots by

targeting *SULTR2;1* and by decreasing Sulfur metabolism by targeting ATP Sulphurylases (Q. Li et al., 2020).

Like in the Sulfur uptake system, Phosphorus, in the form of Pi, HPO_4^{2-} or $H_2PO_4^-$, is taken from soil by two HATs: PHT1;1 and PHT1;4, (Shin et al., 2004) while its transport from roots to shoots is promoted by the LAT PHT2;1 (Versaw & Harrison, 2002) (Figure 3). Overaccumulation of Pi in plant is toxic and can lead to symptoms as chlorosis (less chlorophyll synthesized) and necrosis in the mature leaves (Aung et al., 2006). To avoid such damage, the protein PHO2, also known as UBC24, is synthesized during normal Pi conditions and add ubiquitin to the transporters PHT1 (including PHT1;1 and PHT1;4) which are then degraded so less Pi is taken from soil and thus maintaining Pi homeostasis (Delhaize & Randall, 1995). However, during low Pi conditions, miR399 is transcribed to target *PHO2* therefore the HATs are no longer downregulated and thus increasing the global Pi influx from the roots (Aung et al., 2006; Fujii et al., 2005). miR399 is a long-distance regulator during Pi starvation because it is more expressed at first in the shoots than the roots (Hackenberg et al., 2013; Khan et al., 2014; Lin et al., 2008), it is present in the vascular system where *PHO2* is expressed. Aung et al. (2006) and Lin et al. (2008) showed shoots to roots movement in a reciprocal grafting experiment between a wild type *Arabidopsis* and a miR399 overexpressing transgenic plant. However, to avoid overaccumulation of miR399, plants induce the expression of *IPS1* which is targeted by miR399 but contain a bulge in the middle of the pairing region preventing the repression operated by the RISC (Franco-Zorrilla et al., 2007). The regulation of Pi homeostasis during Pi starvation by miRNA is not only controlled by miR399 but also by miR827 in the same way. Indeed, miR827 targets another ubiquitin ligase (*NLA*) responsible of the degradation of *PHT1* group members in *Arabidopsis* (Kant et al., 2011) but miR827 targets two proteins of the *PHT5* group in rice (Lin et al., 2018). Based on target prediction analysis, Lin et al. (2018) predicted that miR827 targets *PHT5* homologs in angiosperms but targets *NLA* in Brassicaceae and Cleomaceae showing an interesting target shifting of miR827 during evolution.

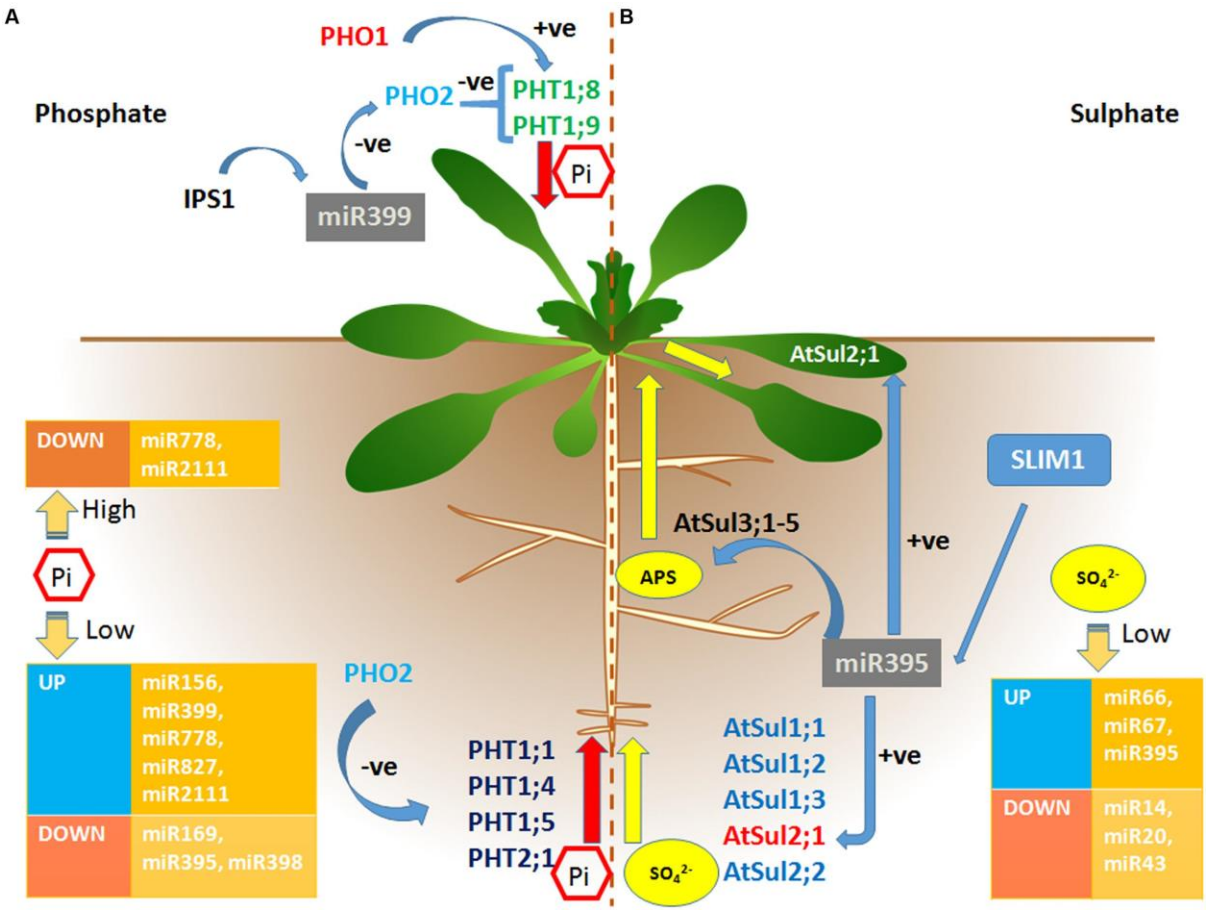

Figure 3: Regulation of the Sulfate and Phosphate pathways by miRNAs. A. Phosphate pathway. B. Sulfate pathway. From Kumar et al. (2017) in open access.

4) Maintaining the equilibrium of miRNAs

With such important roles, miRNAs must be tightly regulated and degraded when their action is no longer necessary. Compared to their biogenesis, there is more mystery regarding miRNA degradation, especially in plants. In plants, miRNA level is controlled at multiple steps during their lifetime ranging from their synthesis, loading into the AGO protein or after the RISC sliced the complementary target with numerous ways of regulation (Figure 4).

As mentioned previously, plant miRNAs are transcribed from a *MIR* gene by the *Pol II* into a pri-miRNA. Recently, Lauressergues et al. (2015, 2022) discovered that most pri-miRs seems to be translated into a miPEP, a short peptide with the ability to upregulate the production of the miRNA it originated from. Indeed, after being transcribed from the MIR gene, the transcript can be alternatively spliced into either a long or a short transcript. The long transcript will lead to the previously known pathway of maturation giving a mature miRNA while the short transcript is exported to the cytoplasm and translated by a ribosome, forming a miPEP. The authors also showed that this mechanism seems to be conserved as they tested to induce, in three different plants species, a higher level of the conserved miR156a (81%-97% sequence identity of the 5'arm sequence between the three species) and of a less conserved miRNA, miR167a (51%-71% sequence identity) using the sequences of the miPEP of the other species (*Arabidopsis thaliana* vs *Arabidopsis thaliana*, *Arabidopsis thaliana* vs *Brassica rapa*, *Brassica rapa* vs *Brassica olera*, etc). After treatment, the first miRNA was more expressed in all plants in all the experiments while the level of miR167a was just increased in the plants treated with their own miPEP showing the conservation of this mechanism but also the importance of the sequence for targeting the correct miR gene. This was also shown in *Vitis vinifera* where miR172b and miR3635b are induced by cold stress and the increase of *miPEP172b* and *miPEP3635b* increases overall cold tolerance (Chen et al., 2022). On top of being spliced, pri-miRs can also be degraded, if their action is no longer necessary, by the Nuclear Exosome Targeting (NEXT) 3' exonuclease which is triggered by SERRATE as they bind together (Bajczyk et al., 2020). Knocking out *NEXT* increases the level of pri-miRs but not the level of mature miRNAs, showing that *NEXT* does not process the pri-miRNAs but only

degrades them. Pri-miRs can be protected from the action of exonucleases by MAC5, which also promotes their processing by SERRATE by interacting with the latter (Li et al., 2020).

Pri-miRs that are processed by the Dicing Body become pre-miRNAs that needs further processing. However, errors can occur during the first trimming of the stem of the pri-miRNA and two pathways have been proposed for the future of incorrectly processed pre-miRs: reparation or degradation (Song et al., 2019). Like with miRNAs, *HESO1* can uridylate pre-miRNAs (8.3% of all pre-miRs) which triggers their degradation as the authors showed that uridylation of pre-miRs was almost gone in the *heso1* mutant and restored when the mutant was complemented with *HESO1*. Over the tailing analysis, they noticed an equivalent portion of cytidylated pre-miRs (8.2%) which was later found to be the repairing system of incorrectly processed pre-miRs. The authors then looked at the level of pre-miRs cytidylation in the 10 nucleotidyltransferase proteins (*NTPs*) single mutants known in *Arabidopsis* (Zhao et al., 2012) and found a decrease of pre-miRs cytidylation in *ntp6* and *ntp7*. Surprisingly, *HESO1* is also involved in the cytidylation of pre-miRs, with 4% of cytidylated pre-miRs in *heso1* against 8% in the wild type (WT), giving it another potential role in miRNAs processing pathways.

After getting shortened by the Dicing Body, the double stranded miRNA needs to be stabilised by the addition of a 2'-O-methyl group at their 3'-end protecting them from 3'-5' exoribonucleases and from the action of TUTases like HESO1 and URT1 (Figure 4). This step, specific to plants and at least one Cnidaria is conducted by the small RNA methyltransferase HEN1 (HUA ENHANCER 1) discovered in plants in 2005 (Li et al., 2005; Yu et al., 2005) and in the Cnidaria *Nematostella vectensis* in 2018 (Modepalli et al., 2018). This step is crucial in plants as the mutant shows drastically reduced levels of miRNAs and pleiotropic phenotypes with reduced organ size, altered leaf shape, late flowering and decreased female fertility (Chen et al., 2002; Park et al., 2002) and is often used for crosses in publications studying the turnover of miRNAs (Tu et al., 2015; Wang et al., 2015, 2018; Zhao et al., 2012). Further investigations in plants showed a preference for 21-24nt RNA duplexes with a 2 nucleotides overhangs (Yang et al., 2006). Tsai et al. (2014) found that *HEN1* expression is light dependent and that *hen1* mutant plants are light-hypersensitive showing inhibition of stem growth. In the case of the duplex not being methylated, the 3'-5' exoribonuclease ATRM2, found by Wang et al. (2018), provoke its degradation. Indeed, the *atrm2-hen1* background showed a

partial suppression of *hen1* morphological defects with an increase of miRNAs level and thus a lower expression of the targets, confirming its implication in the regulation of miRNA turnover pathway. However, the study showed that there was no increase of trimming of miRNAs with a unfunctional *atrm2*, even in *hen1/heso1/urt1* background, where miRNAs can be easily truncated, suggesting that *ATRM2* is not capable of degrading miRNAs. Finally, the authors found an increase in the level of miRNA* in *atrm2* mutants compared to their relative controls (like *hen1/atrm2* vs *hen1*) indicating that *ATRM2* acts on the miRNA/miRNA* duplex and this action is probably performed just before the loading into *AGO1* as they interact with each other. Therefore, *ATRM2* is a checking the correct methylation of the duplex before the loading into the miRISC, reinforcing the importance of methylation in plants miRNAs.

To be active and achieve its role, a miRNA must be loaded into an ARGONAUTE (AGO) protein mainly AGO1 for plants miRNAs (Vaucheret et al., 2004) . The loading happens in both the nucleus and cytoplasm (Wang et al., 2019) and requires the Chaperone protein HSP90 (Iki et al., 2010) coupled with ATP to open the AGO1 and leave enough space for the duplex to be loaded. The miRNA duplex is then separated with the guide strand being kept while the passenger strand is cleaved by AGO1 and released in the cytoplasm to be further degraded. Very recently, Liu et al., (2020) discovered that the 5'-3' exoribonuclease XRN4 is involved in the degradation of some miRNA* in *Arabidopsis*. It is known that *XRN* genes are involved in the degradation of sRNAs in animals (Nagarajan et al., 2013) and that XRN2 and XRN3 are required for the pri-miRNA processing and for the miRNA loop degradation in plants (Kurihara, 2017). From this, they wanted to test the level of sRNAs in *xrn4* knockout plants and observed an increase of 21-nucleotide sRNAs level including 32 miRNA*. To check if XRN4 act before or after the miRNA* precursor processing step, they looked at the level of pri-miRNAs for the selected *MIR* genes in the mutant. The results showed an accumulation of certain pri-miRNA* compared to the WT but with levels below the accumulation level of the corresponding miRNA*s. They also showed no significant difference between the level of pre-miRNAs between the mutant and the WT and found that XRN4 localizes in P-bodies (in the cytoplasm) while the transcription of miRNAs and their processing happens in the nucleus. Taken together, these results demonstrate the role of *XRN4* in the degradation of miRNA*s in P-bodies and that the process is downstream of the miRNA precursor processing step.

However, it is still unclear why and how XRN4 is responsible of the degradation of only a subset of miRNA*s and if other similar proteins act cooperatively with XRN4.

Once operational, the plant miRISC operates by targeting mRNA with almost full complementarity to the loaded miRNA. The slicing, by the AGO1 PIWI domain, often happens between position 10 and 11 of the miRNA relative to its 5-end (Park & Shin, 2014). The complex can then be stabilized or weakened, and miRNAs degraded through different pathways.

Stabilization is driven by RISC-Interacting Clearing Exonucleases (RICEs) by degrading the uridylated products of the miRISC slicing as they were shown to degrade single stranded RNA *in vitro* but not miRNA nor miRNA* *in vitro* and the expression of the inactive RICE1 protein showed a decrease in miRNA level and an increase in the level of cleaved and uridylated mRNA products from the miRISC (Zhang et al., 2017).

Usually, in Eukaryotes, proteins are degraded following either the Ubiquitin-Proteasome pathway (addition of Ubiquitin which act as markers for rapid degradation by the proteasome) or the Lysosomal proteolysis (absorption by a lysosome containing digestive enzymes, it can also fuse with the autophagosome) (Cooper, 2000; Lilienbaum, 2013). AGO1 can be degraded following both pathways as it was shown to be ubiquitylated and an inhibition of autophagy leads to a non-degradation of *AGO1* (Derrien et al., 2012). A possible prior step controlling the AGO1 loading is performed by the F-box protein FBW2, which assemble a complex called SCF that target unloaded AGO1 protein and promote their degradation (Hacquard et al., 2022). A previous study showed that the mutant *fbw2* had an increased level of AGO1 and overexpressing *FBW2* reduced the level of AGO1 proteins but not the level of mRNA (Earley et al., 2010), which is regulated by miR168 (Dalmadi et al., 2021). Hacquard et al. (2022) also showed that when AGO1 is not degraded correctly, it binds to random sRNAs and makes off-targets cleavages, showing the importance of *FBW2* in the quality control of RNA silencing. However, it is still unknown which protein degradation pathways this FBW2/SCF triggers and if miRNAs are degraded within the miRISC when this step is not taken.

Even though in animals, miRNAs do not undergo post-transcriptional modifications before their RISC loading like the methylation in plants, they are considered as stable molecules especially when they are loaded in the RISC complex with commonly half-lives superior to 24h (Marzi et al., 2016). However, their turnover rate is dependent of their own role and the cell type they are in (Marzi et al., 2016), for example, faster decay in neuronal cells was shown in the retinal cells of mouse (Krol et al., 2010). In plants, miRNAs are considered as stable molecule thanks to their 3'-methylation. However, two main ways of impairing this steadiness have been described: 3' truncation and 3' uridylation, which mark for degradation. Among all the exoribonucleases, dispatched in six super-families (RNR, DEDD, RBN, PDX, RRP4 and 5PX) (Zuo, 2001), only one family of enzyme from the DEDD super-family was found to degrade methylated miRNAs. Indeed, the 3'-truncation of methylated miRNAs is operated by the 3'-5' exoribonucleases SDN1/2/3, mainly SDN1, even if the miRNA is loaded in the RISC complex (Ramachandran & Chen, 2008). Knock outs of *sdn1/2/3* showed an overall increased level of miRNAs while it was scarcer on single mutant, showing their redundancy. The authors also showed that SDN1 degrades unmethylated miR173 faster than the methylated version *in vitro*, indicating the importance of the methylation in miRNA turnover but also showing that it is not the perfect protection. They also calculated that 1 molecule of SDN1 can degrade 14 molecules of miRNAs. The product of this degradation is a 9 nucleotides miRNA *in vitro* but *in vivo*, the miRNA is only degraded by a few nucleotides (Yu et al., 2017), indicating that SDNs are more important for the unmethylation of miRNAs than their proper degradation when loaded in AGO1 at least. Recently, the crystal structure of SDN1 was unveiled (Chen et al., 2018) and in vitro results suggest that SDN1 can trim miRNAs bound to AGO1 due to its interaction with the PAZ domain of AGO1 in an RNA-independent manner. Animal miRNAs are found to be degraded by truncation induced by several exoribonucleases. Indeed, the 5'-3' exoribonuclease XRN1 is responsible for the degradation of some passenger strands (miRNA*) in *C. elegans* (Chatterjee et al., 2011) but also of specific miRNAs like miR382 in human (Bail et al., 2010). Alongside XRN1, its paralogue XRN2 is one of the various enzymes responsible for miRNA degradation in animals and knockout of *xrn1* or *xrn2* showed an increase in the overall miRNAs' level in *C.elegans* (Chatterjee et al., 2011; Chatterjee & Großhans, 2009).

After removal of the methylation, plants miRNAs are left unprotected and are subject to uridylation. Two enzymes are responsible for the 3'-urydilation of miRNAs in plants: HESO1 (HEN1 SUPPRESSOR 1) and URT1 (URYDYLYTRANSFERASE 1). HESO1 was found to uridylate non-methylated miRNAs in *hen1* background (Zhao et al., 2012), and the double mutant *hen1-heso1* phenotypically rescued the *hen1* background, showing that miRNAs are degraded after U-tailing. Surprisingly, in *hen1-heso1* double mutants, some U-tailed miRNAs remained, suggesting another protein is involved in this process. This observation led to the discovery of *URT1* (Tu et al., 2015; Wang et al., 2015). In *hen1-heso1-urt1* triple mutants, no U-tailed miRNAs have been found alongside an increasing 3'-5' trimming (Wang et al., 2015), highlighting that no other TUTases (enzymes adding Uridine nucleotide to RNA) are involved in miRNA's U-tailing and also the balance between uridylation and truncation. Also, those reports showed that HESO1 and URT1 act cooperatively and do not compete as their preferred substrate is not the same. Indeed, URT1 prefers A-ending miRNAs as HESO1 works better on U-ending miRNAs thus HESO1 may be increasing the length of the U-tail created by URT1. Moreover, the tailing of miRNAs in plants reduces the slicing activity of AGO1 (Tu et al., 2015). In animals, several TUTases, that can be triggered by the protein LIN28 (Chang et al., 2013), are responsible for the addition of Uridine on miRNAs marking them for a rapid degradation (Knouf et al., 2013; Thornton et al., 2014).

Very recently, Han & Mendell (2023) discovered that the structure of AGO also plays a role in the stability of miRNAs in both plants and animals. Indeed, the 3' extremity of the miRNA is hidden in the PAZ domain of the ARGONAUTE when it's loaded and is only exposed in plants during the binding between the miRNA and its mRNA target. Because plant RISC needs an almost perfect complementarity with the target, part of the miRNA gets out of the PAZ domain during the binding, letting the 3' end exposed to truncation or tailing, making HEN1's action primordial for the protection of miRNAs, especially with SDN1 interacting with the PAZ domain, as well. One way to degrade miRNAs in animals is the Target-Directed miRNA Degradation (TDMD), which occurs when the miRNA binds with perfect complementarity its target in the miRISC complex, leaving its 3' end outside of the complex. As the animal miRNAs do not have a 3' end protection like plants' methylation, the miRNA is then vulnerable to enzymatic processes and is degraded (Ghini et al., 2018; Sheu-Gruttadauria et al., 2019). A similar pathway was discovered in plants, which happens only to a subset of miRNAs, called

Target Mimicry. It was found that IPS1, involved in Pi starvation response (Fujii et al., 2005), was targeted by miR399 but exhibited a bulge on the cleavage site of the miRNA resulting in a non-cleavage and sequestration of miR399 (Franco-Zorrilla et al., 2007). The authors showed that overexpressing IPS1 results in a decrease in the level of miR399 and reduced Pi content in the roots. This discovery led to the artificial target mimicry field which design "sponges" to sequester specific miRNAs and increase the level of their targets to either understand the functions of miRNAs or for crop improvements (Peng et al., 2018; Gupta, 2015; Todesco et al., 2010).

As uridylation only act as a marker and TUTases are unable of nuclease activity, there must be one or more protein(s) responsible of the degradation of uridylated miRNAs. In animals, Dis3l2, a 3'-5' exoribonuclease, was found to be responsible of the degradation of the uridylated miRNA pre-let-7 in mouse embryonic stem cells *in vivo*, and thus is proposed as the protein responsible of the degradation of uridylated miRNAs in animals (Chang et al., 2013; Ustianenko et al., 2013; Yang et al., 2020). In the algae *Chlamydomonas*, *RRP6* degrades miRNAs uridylated by the nucleotidyltransferase *MUT68*, shown *in vitro*, and knocking out *MUT68* increases miRNA level and *rrp6* mutant expose a miRNA accumulation *in vivo* (Ibrahim et al., 2010). The closest homolog in plants is *SOV* (*SUPPRESSOR OF VARICOSE*) but was found inactive in the *Arabidopsis thaliana* ecotype Col-0 reducing drastically its probability to be the correct enzyme for this role in plants (Zhang et al., 2010) while *SDN1* does not work on U-tailed miRNAs (Ramachandran & Chen, 2008). In conclusion, the enzyme responsible for the degradation of uridylated miRNAs remains unknown (Figure 4).

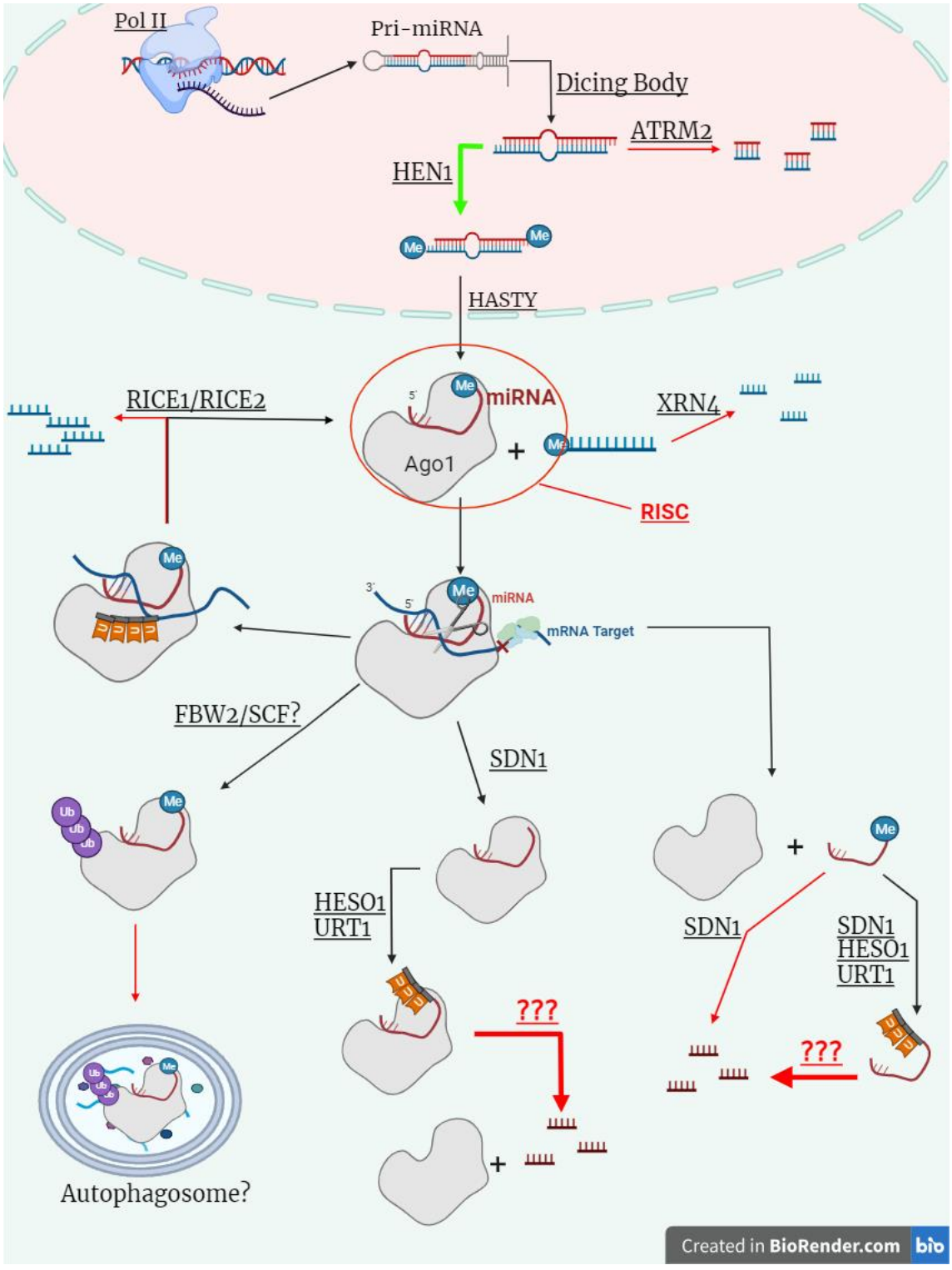

Figure 4: Overview of plant miRNA lifecycle. A microRNA is transcribed from a MIR gene in the form of the primary miRNA (pri-miRNA) with the characteristic stem-loop structure which is recognised by the Dicing body responsible of its cleavage into a precursor miRNA (pre-miRNA (not shown)) and then into a double stranded miRNA. The double stranded miRNA is then methylated by HEN1, a crucial step for miRNA protection. If not methylated, the double stranded RNA is degraded by ATRM2.The miRNA is

then exported to an AGO1 to form the RISC complex, the guide strand is loaded and the passenger strand is released in the cytoplasm. A subset of those is degraded by XRN4. After degrading the complementary mRNA, the RISC complex can be stabilised and reused thanks to the actions of RICE1 and RICE2 or tagged for degradation by FBW2/SCF to be degraded by the autophagosome. miRNA protection can be removed by SDN1, which can also degrade unloaded miRNAs. Once unmethylated, the miRNA is subject to uridylation by HESO1 and/or URT1 which promotes its degradation by unknown nuclease(s). This figure was made with BioRender.

5) Alternative splicing in plants

5.1) Introduction

Because plants cannot move to escape to environmental changes and predation, they evolved to adapt locally to the several types of stress like temperature change, drought, salt stress, etc by regulating specialised genes expression (Becklin et al., 2016; Gratani, 2014; Guerra et al., 2015). While the most evident way is to modulate the expression within the genome with promoters of genes activated by stress pathways, regulating the mRNA level by sRNAs can be another way to downregulate the number of proteins translated and thus affect the stress response like explained previously with the Sulfur pathway and miR395. One of the other possibilities is to alternatively splice the mRNA to make new proteins that can have a better response to a stress (Filichkin et al., 2015; Reddy et al., 2013).

In Eukaryotes, alternative splicing is an evolutionary highly conserved mechanism that consists in the removal of the introns and joining the exons of a precursor messenger RNA (pre-mRNA) to form a mature mRNA. Yet, an immature pre-mRNA can have multiples introns and exons and, depending on the splicing, multiple isoforms can arise from that process, which complexify the transcriptome and permit a better response to the environment with the same number of genes (Ben-Dov et al., 2008; Maniatis & Tasic, 2002; Matlin et al., 2005; Sibley et al., 2016).

This mechanism is widespread in genomes as estimations in plant indicate that almost 90% of genes contains introns (Shang et al., 2017) and 42-70% of them, including *MIR* genes, are alternatively spliced (Chamala et al., 2015; Marquez et al., 2012; Reddy et al., 2013), while

95% of human genes are alternatively spliced (Pan et al., 2008). Those numbers are forever changing, with potentially more events to discover as looking at several tissues, new sequencing techniques and new tools to predict them are developed and many false positives are predicted by bioinformatics (Hayer et al., 2015). In 2003, only 1.2% of *Arabidopsis*' genes was predicted to undergo alternative splicing (Zhu et al., 2003), which drastically increased to 61% in 2012 (Syed et al., 2012).

On each pre-mRNA, this process involves 5 small nuclear RNAs (*U1*, *U2*, *U4*, *U5* and *U6*) and more than 200 proteins which form the spliceosome (Albaqami & Reddy, 2018; Matera & Wang, 2014; Will & Lührmann, 2011). The spliceosome is formed on splice sites, recognized by site combination of two pairs of nucleotides on each end of the intron. The most common is GU-AG with 97.9% of the canonical splice site combination in plants pre-mRNA, 98.3% in animals and 98.7% in fungi (Frey & Pucker, 2020). Intron-containing genes can end in many different isoforms according to the splicing event they undergo, with five different futures: (1) skipped exon (SE) where an exon is not retained making a shorter mRNA, (2) alternative 5' splice site (A5SS) where the spliceosome recognizes an alternative splice site in the exon preceding the intron instead of the intron itself making a shorter mRNA, (3) alternative 3' splice site (A3SS) where the target site is recognised in the exon following the intron making a shorter mature mRNA, (4) intron retention (IR) where a full intron is kept by the spliceosome making a longer mRNA and (5) mutually exclusive exons (MEE) where an exon is kept but another one is removed, so the mature mRNA never contains both of the exons at the same time (Figure 5).

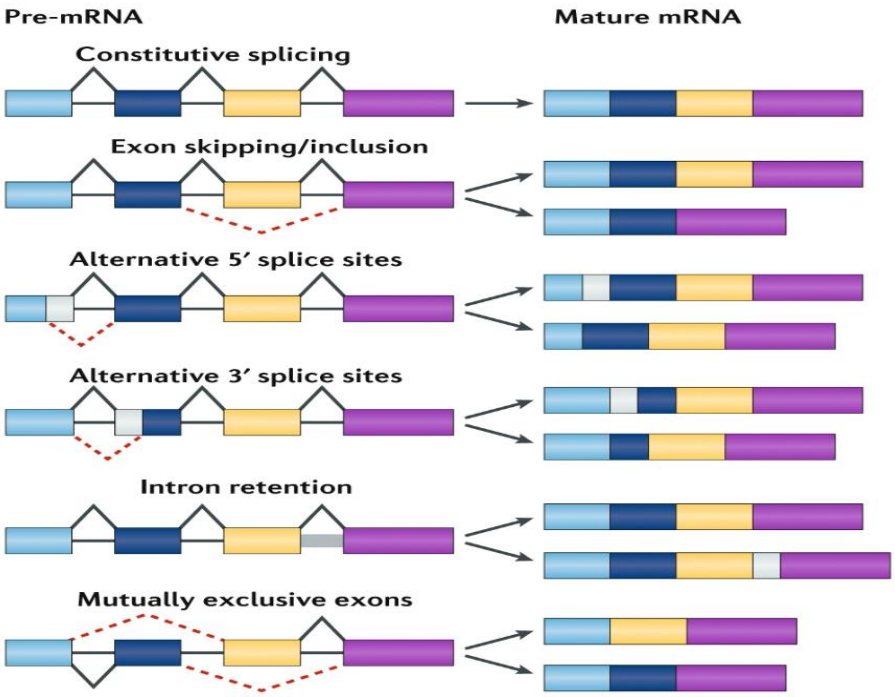

Figure 5: Main types of alternative splicing events. Boxes represent the exons, and the lines represent the introns. Black bended lines represent the constitutive splicing, and the red bended doted lines represent the alternative splicing. From Frankiw et al. (2019) with permission of the publisher.

While alternative splicing is conserved among Eukaryotes, the proportion of the events differs between kingdoms: In plants, intron retention is the most common event with 56% of events in *Arabidopsis* and 53.5% in rice (Wang & Brendel, 2006), while skipped exon events prevail in animals with up to 25% of events in *Drosophila* (Daines et al., 2011; Gibilisco et al., 2016) and 35% in humans (Wang et al., 2008) compared to the 8% and 13.8% in *Arabidopsis* and rice respectively (Wang & Brendel, 2006).

Alternatively spliced mRNA can then undergo several paths: (1) Being translated into a protein following the central dogma of molecular biology (Crick, 1958; Pramanik et al., 2021), (2) Being degraded, in the cytoplasm, by the Non-Mediated Decay (NMD) pathway, which is the mRNA surveillance pathway which degrades premature mRNA or incorrectly spliced mRNA that would have a premature STOP codon for example (Drechsel et al., 2013; Kervestin & Jacobson, 2012) or (3) being held captive in the nucleus to be protected from the NMD and for a later use (Jia et al., 2020).

Despite being well studied, alternative splicing still has a lot of mysteries to unfold concerning the transcriptome and proteome complexity, especially in plants which are less studied than animals and yeast in that domain.

5.2) Alternative splicing at the origin of everything

In plants, alternative splicing is responsible for the response to many stresses and of sensing the environment, acting in the circadian clock (Filichkin et al., 2010; Seo et al., 2012) or like a thermometer sensing temperature changes (Dikaya et al., 2021; Lee et al., 2013; Posé et al., 2013), allowing them to grow effectively (Shang et al., 2017). It has been shown that genes related to stress responses harbour no or few introns, which is logical because transcription and post-transcriptional modifications are time-consuming processes which defy the point of a rapid response (Jeffares et al., 2008; Speth et al., 2018; Swinburne & Silver, 2008; Zhu et al., 2016). For example, *HAB1* is a gene encoding a protein interacting with SnRK2/OST1 to regulate ABA signalling, a crucial hormone in plants, and exists in two forms, HAB1.1 and HAB1.2 which contains an extra intron. Both have antagonistic effects with HAB1.1 turning off ABA signalling while HAB1.2 does not interact with SnRK2/OST1 and leaves the ABA level unchanged (Zhan et al., 2015). The spliceosome alone is not responsible of all responses as *SR45* controls alternative splice site and where the spliceosome assembles. The mutant *sr45* showed pleiotropic defects like late flowering, leaf and flower morphology defects and even in ABA and Glucose signalling (Ali et al., 2007; Carvalho et al., 2010).

Alternative splicing is also involved in miRNA expression with 71 out of 1229 *Arabidopsis* miRNAs and 401 out of 2669 rice miRNAs being intronic miRNAs i.e. located in introns of host genes (Yang et al., 2012). In animals, the level of expression of intronic miRNAs matches the host protein, and it was proposed that *Drosha* processes the excised intron containing the miRNA (Baskerville & Bartel, 2005; Wang et al., 2009). Similar expression results were shown in plants, but we still don't know the processing details of those intronic miRNAs (Yang et al., 2012)but we can also assume that those short introns are also processed by the Dicing body. Examples of intronic miRNAs are miR400, miR162a and miR838. miR400 is contained in the intron of a gene (*AT1G32583*) and is constitutively expressed in normal conditions as the

intron is spliced out. However, in heat stress conditions, the intron is retained and the level of miR400 decrease drastically (Yan et al., 2012). miR162a and miR838 regulate the expression of *DCL1*, responsible for miRNA processing, and are both located in gene introns, *AT5G08185* and *DCL1* respectively with miR162 targeting directly the *DCL1* mRNA by sequence complementarity (Xie et al., 2003). *DCL1* can regulate its own mRNA and triggers the liberation of miR838 which will downregulate *DCL1* in a negative feedback loop (Rajagopalan et al., 2006). This specific feedback loop with the miRNA inside *DCL1* sequence was also described in other plants with miR838 in *Medicago truncatula*, miR1047 in *Physcomitrella patens* and miRc-7 in *Carica papaya* (Axtell et al., 2007; Liang et al., 2013; Tworak et al., 2016), and thus despite different miRNA sequences, even between *Arabidopsis thaliana* and *Medicago truncatula*, suggesting a divergent evolution and showing the importance of regulating *DCL1*. Finally, ~50% of *Arabidopsis* genes contains introns that are spliced out by the spliceosome in direct communication with the miRNA dicing body, especially *SERRATE* (Stepien et al., 2017), adding another layer of importance of the alternative splicing in plants.

6) Aims and objectives of the PhD

The aim of the PhD is to answer a 20-year-old question and fill a big knowledge gap in the lifecycle of plant miRNA: What degrades urydilated miRNAs? Indeed, as mentioned before, after a miRNA completed its role of targeting a mRNA to be degraded, the miRNA needs to be degraded as well. Among the multiple degradation pathways, the main one is the removal of the methylation protection by SDN1, followed by an urydilation of the miRNA by HESO1 and/or URT1. As SDN1 cannot degrades urydilated miRNAs, another protein must be involved in that role and remains unknown.

To achieve this, I used two main approaches using a GFP screening assay based on the degradation of miR395 and a candidate approach, analysing mutants of HESO1 predicted interactors crossed in a *hen1* background to look for phenotypic and miRNA level rescues. As the project went on, I also analysed the alternative splicing of *sua* to get one more candidate to analyse and obtain mRNA sequencing data requested in Zhang et al. (2014).

Chapter II] Genetic screen to identify genes involved in the miRNA turnover

1) Introduction

The objective is to find the protein(s) responsible for miRNAs' turnover. There are different approaches in biology for genes characterization described in Alonso & Ecker (2006) and this chapter describes a forward genetic screen. The Forward genetics approach involves generating a mutant population, looking for a mutant phenotype and after selection of candidate mutants, identifying the genes involved in the process. The Dalmay laboratory created a transgene that contain a *Green Fluorescence Protein (GFP)* gene carrying a miR395 target site at its 3'UTR and driven by the SUCROSE-TRANSPORTER2 (SUC2) promoter. This *pSUC2:GFP:395* transgene is targeted by miR395, specifically expressed in phloem companion cells during Low Sulfur (LS) condition. The SUC2 promoter is only active in the phloem companion cells, therefore GFP expression is restricted to those cells. In LS media, GFP accumulation is downregulated by the expression of miR395, and no fluorescence can be seen. Once Sulfur, in the form of 30mM $MgSO_4$, is added to the media, the transcription of miR395 is switched off and the existing miRNA molecules start to be degraded, therefore the transgene is derepressed and fluorescence appear (Figure 6A).

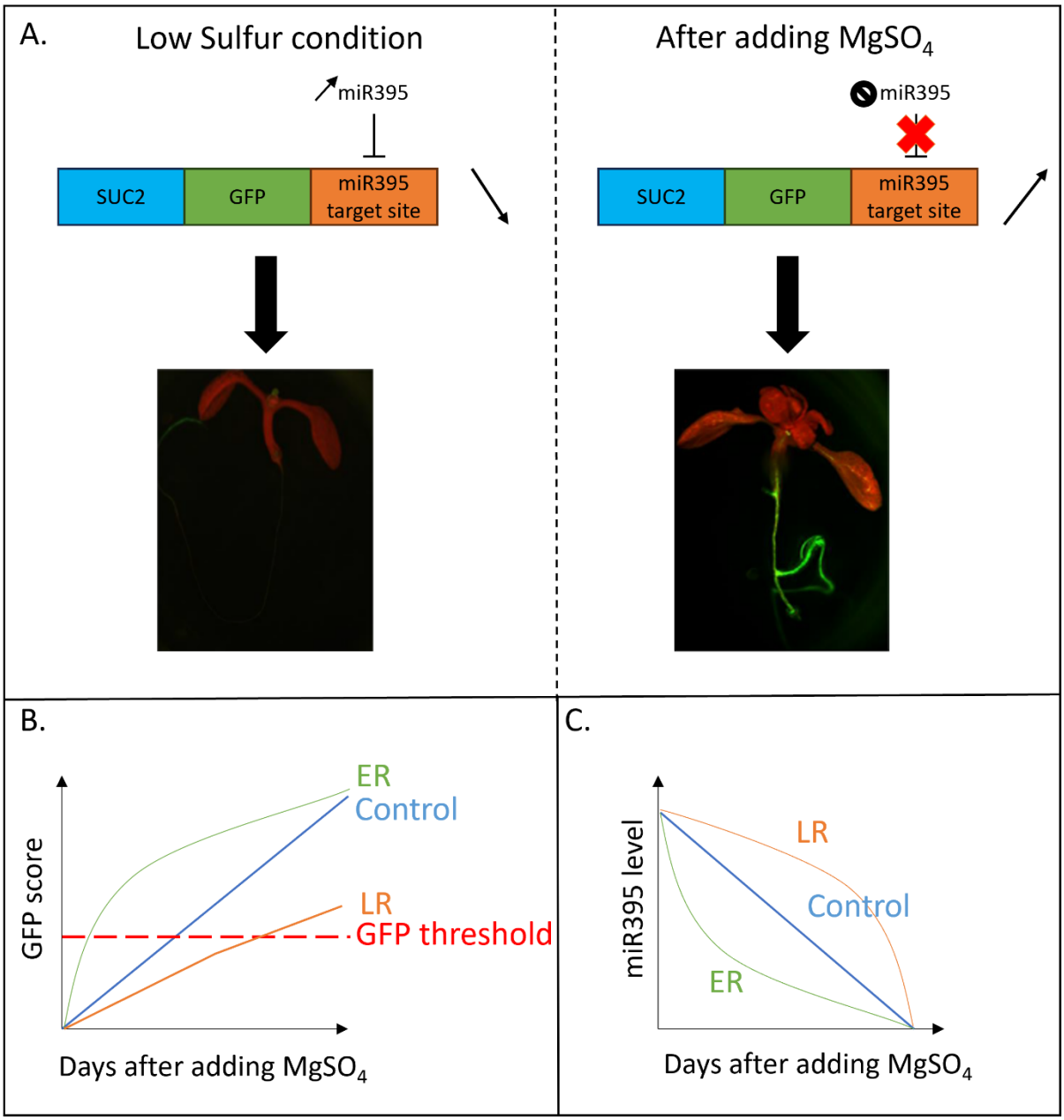

Figure 6: Graphical summary of the GFP screening. A. Left panel: the transgene RNA is targeted and downregulated by miR395, expressed in Low Sulfur condition, leading to an absence of fluorescence in the root. Right panel: After adding $MgSO_4$, the transcription of miR395 is stopped and the existing molecules are degraded. This induces an increase in the transgene transcript level and an apparition of the GFP, which happen in three days in the control. B. Model graph showing the trend of the GFP expression depending on the background after adding $MgSO_4$. An Early Response (ER) mutant will pass the GFP threshold faster than the control and a Late Response (LR) mutant will pass the GFP threshold after the control. C. Model graph of the level of miR395 after adding $MgSO_4$. In an Early Response mutant, miR395 will be degraded faster and its level going down faster than the control and a Late Response mutant will degrade miR395 more slowly and its level will go down slower than the control.

Since transgene silencing can be maintained by *RNA-directed RNA polymerase 6* (*RDR6*) (Dalmay et al., 2000, 2001), I am screening a GFP marker gene in a *rdr6* mutant background to ensure that GFP expression is derepressed in the absence of miR395. The fluorescence recovery can be observed in wild type plants (WT) 3 days after adding $MgSO_4$. Plants carrying a mutation in the miRNA turnover pathway should express either faster (ER for Early Response) or slower (LR for Late Response) GFP recovery and these mutants are selected as candidates. Indeed, a faster recovery would indicate a faster degradation of miR395, thus the genes responsible for miRNAs' degradation are more expressed suggesting that the mutation affects their own repressors or miR395 can be degraded more slowly in late response mutants because the mutation affects a gene involved in the degradation of the miRNA (Figures 6B, 6C).

However, mutations in other genes, not participating in the miRNA's turnover, may lead to the same phenotypes because mutations in the Sulfur assimilation pathway can cause the change of miR395 level (Liang & Yu, 2010). Mutations in proteins involved in Sulfur sensing or assimilation (SULTR1;1 and SULTR1;4 for example) can alter the correct transcription of SLIM1 and thus miR395 expression (SLIM1 is responsible of miR395 upregulation in LS condition) therefore the GFP transgene can exhibit different GFP recovery phenotype if the mutation occur in genes involved in the Sulfur assimilation pathway. To solve this issue, the measure of the level of miRNA involved in other starvation pathways can later be measured, like miR399 involved in the phosphate assimilation pathway by growing the candidate in low phosphate condition.

2) The screening assay

My part in this project starts with the screening assay. Every week, ~150-300 EMS mutated M2 pSUC2:GFP:395/*rdr6* seeds containing were sowed in LS media to trigger the transcription of miR395. 6 days later, the media was replenished with Sulfur, in the form of 30mM $MgSO_4$, to stop the production of miR395 and trigger their degradation. The plants were observed under fluorescence microscope (450 nm light) at 8 timepoints (-1, 0, 1, 2, 5, 7, 9, 12 where 0 is when Sulfur was replenished) and the GFP intensity of each plant was subjectively scored according to table 1 while being voice recorded and transcribed back into a spreadsheet.

Table 1: Scoring system used for the GFP screening assays.

Score	Microscope observation
0	No GFP fluorescence.
1	Very faint GFP fluorescence.
2	Faint GFP fluorescence in some parts of the roots.
3	GFP fluorescence in the roots and a bit in the aerial part.
4	Bright GFP fluorescence across the plant.
5	Very bright GFP fluorescence in the whole plant.

In total. ~2500 seeds were sowed, which ~1600 germinated and only ~1000 survived to the twelfth day of the screening (Figure 7.A) representing only 40-50% of the starting material (Figure 7.B).

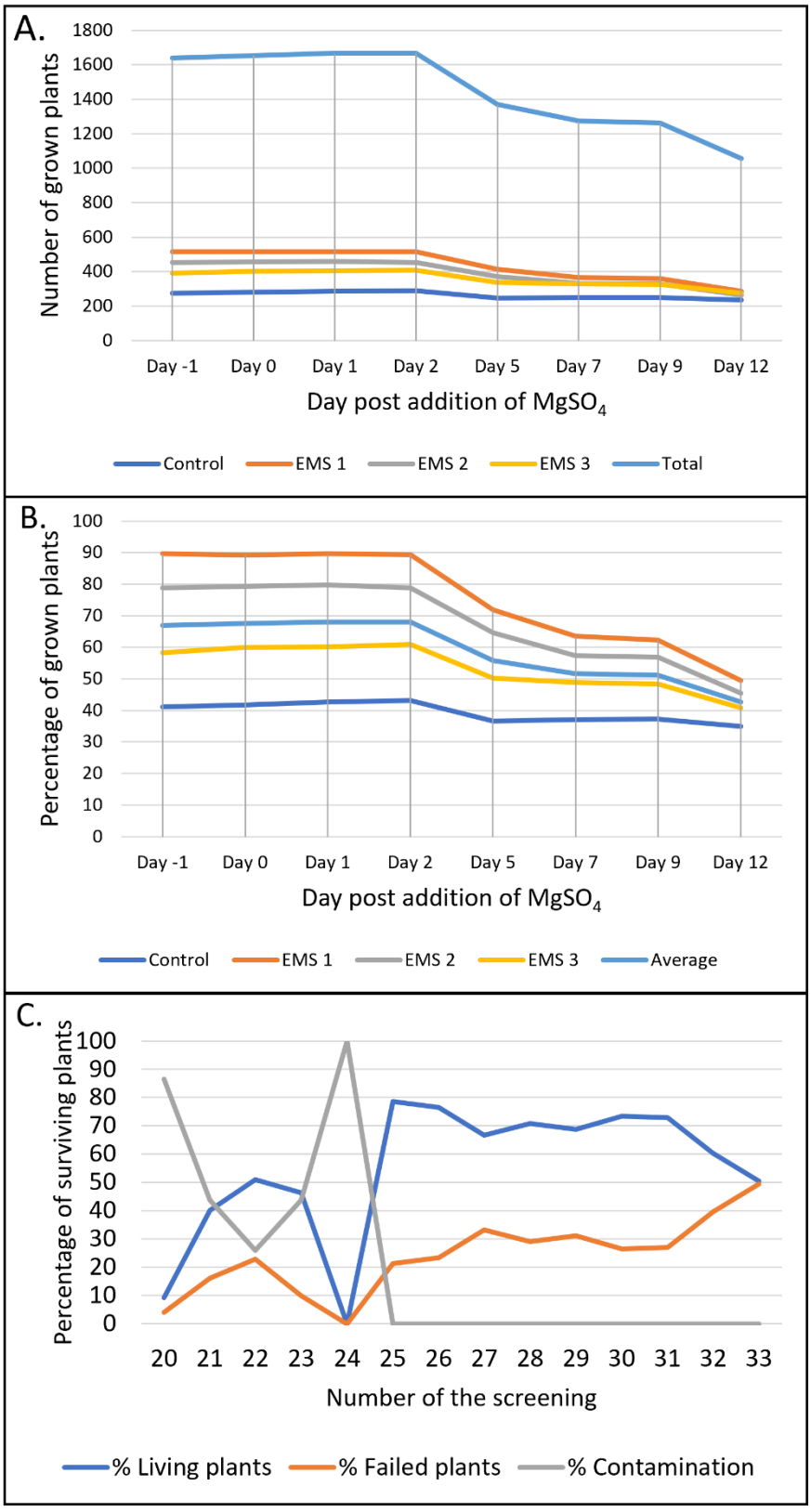

Figure 7: Summary of the plants used in the screenings. A. Number of grown plants from all screening assays at different timepoints. B. Percentage of grown plants from all screening assays at different timepoints. C. Plant survivability after 12 days of GFP screening. The "failed

plants" indicate plants which did not germinate, had no roots or the seed was absent in the 48 well plate.

Plant survivability was impaired at the beginning of the screening by fungal/bacterial contamination coming from the bottle of $MgSO_4$, explaining the drop of grown plants at Day 5 (Figures 7.A, 7.B) and overall, by growth issues with 20% to 50% of the seeds not germinating or with no roots to analyse referred as "% Failed plants" in Figure 7.C.

After 14 independent screenings, 40 potential candidates were recorded and transferred on MS media then soil but only 13 produced seeds (1 ER, 12 LR) (Figure 8). To those 13 candidates were added 19 candidates (8 ER, 9 LR and 2 unknown) previously found by other members of the group but not yet analysed.

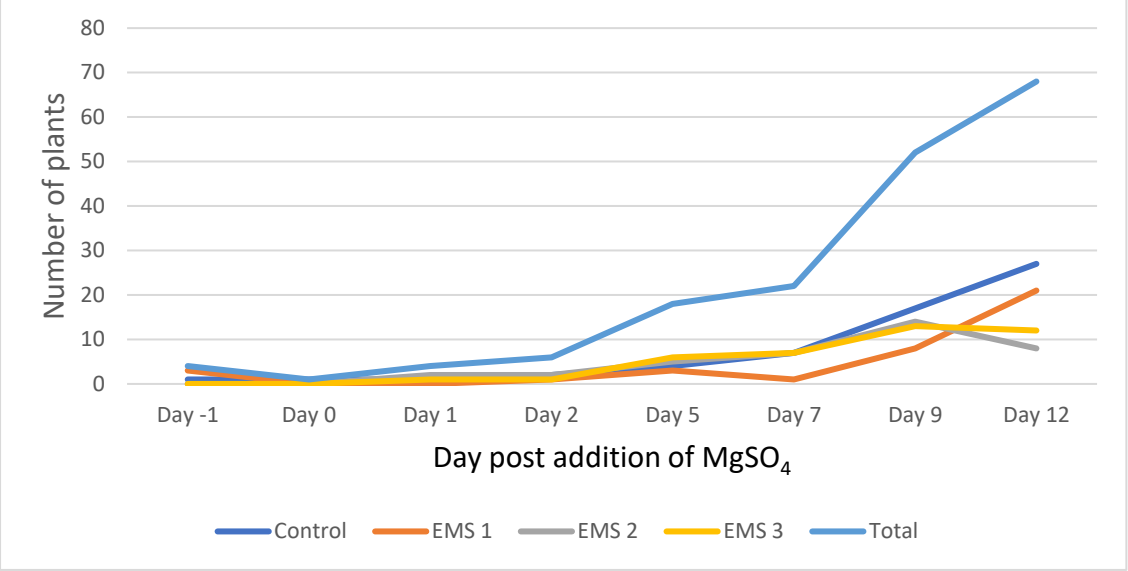

Figure 8: Number of plants that scored the set GFP threshold of 3 at the different days of the screening after replenishing the media with Sulfur.

As the screening was subjective, to confirm the potential of a candidate, RT-qPCR was performed to measure the level of miR395 in a three timepoints experiment.

3) Confirmation of the fluorescent phenotype by RT-qPCR

To confirm the outcome of the screening assay, the plants were first transferred to soil to produce seeds. Then, three biological replicates containing a pool of ~20 plants were grown on LS media on square Petri dishes for 14 days, then replenished with 30mM $MgSO_4$. The roots were cut at three timepoints: 0h, 24h and 48h after Sulfur replenishing, as previous work showed no difference in the level of miR395 between the 48h timepoint and the 72h timepoint. The RNA was extracted using Tri Reagent and Chloroform, measured by Nanodrop and 500ng of RNA was cleaned by a DNase treatment followed by cDNA synthesis.

Since miRNAs are only 21-24 nt long, standard primers routinely used for PCRs cannot be used. Several techniques were designed to complement the miRNAs into cDNA like the addition of A-tails and U-tails (Balcells et al., 2011; Mei et al., 2012; Shi & Chiang, 2005) to elongate the length of all miRNAs but the most common technique is the use of stem-loop RT primer. This consists in designing a stem-loop structure with one of the extremities complementary to a miRNA (or family of miRNAs) and use a reverse transcriptase to make cDNA (Benes & Castoldi, 2010; Chen et al., 2005). Standard PCR primers can then be designed on the product. We decided to follow an improved version called the '2-tailed hemiprobe' protocol from Androvic et al. (2017). The method is improved by the complementarity of the miRNA to both extremities of the stem-loop hemiprobe, allowing a much higher specificity (Figures 9.A, 9.B). A Reverse Transcriptase then elongates the 3' end of the hemiprobe to form cDNA (Figure 9.C) and PCR primers are designed to match both extremities of the hairpin structure (Figure 9.D).

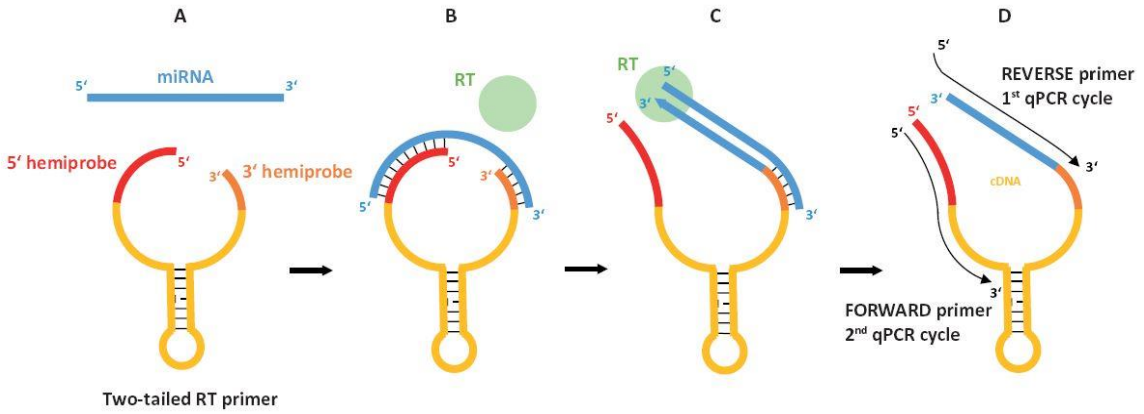

*Figure 9: Schematic of Two-tailed RT-qPCR. (**A**) Two-tailed RT primer having two hemiprobes connected by a hairpin folding sequence. (**B**) The hemiprobes bind cooperatively, one at each end of the target miRNA, forming a stable complex. (**C**) Reverse transcriptase binds the 3'-end of the hybridized Two-tailed RT primer and elongates it to form tailed cDNA. (**D**) The cDNA is amplified by RT-qPCR using two target-specific primers. From Androvic et al. (2017) with permission of the publisher.*

The RT-qPCR machine was set up to perform a quantitative mode and gave amplification plots and melt curves graphs to verify the proper run of the RT-qPCR. For the actual quantification, Ct values for Actin (housekeeping gene) and for miR395 were measured, and analysed following the Pfaffl method (Pfaffl, 2001).

After the RT-qPCR analysis, 6 mutants were chosen, 2 of them were Early Response mutants, 3 Late Response and 1 was expressing a surprising high level of miR395 at 0h, which was considered of interest for the Sulfur pathways and further tested (Figures 10, 11).

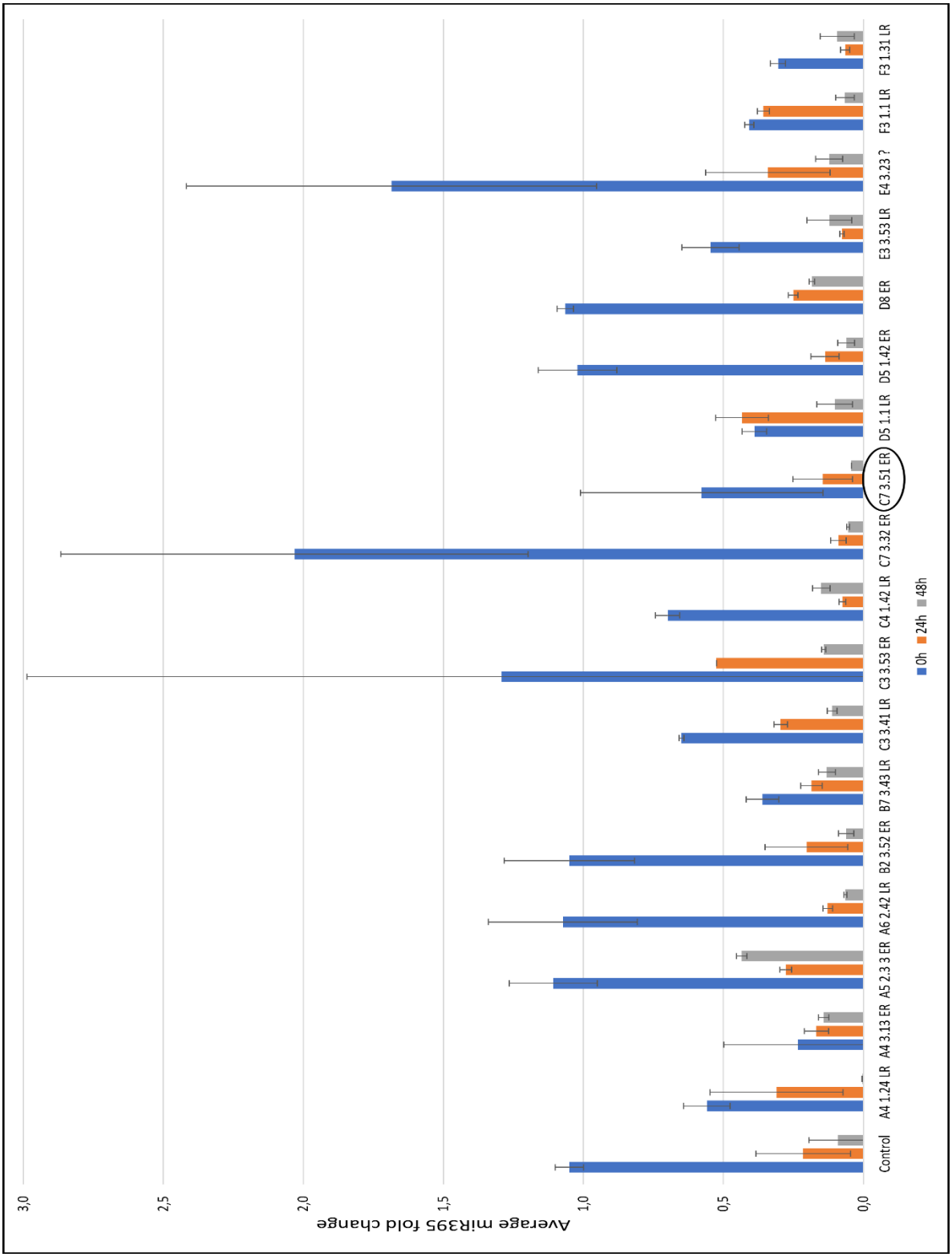

Figure 10: Average expression of miR395 after replenishing the media with $MgSO_4$. Average fold change of miR395 at 0h, 24h and 48h after replenishing the media with $MgSO_4$ compared to the control 0h for the first set of candidates following the Pfaffl method. The error bars represent the standard deviation. Note: some results were omitted from the two figures to make them more readable as some values were too big and crushed down the totality of the graph.

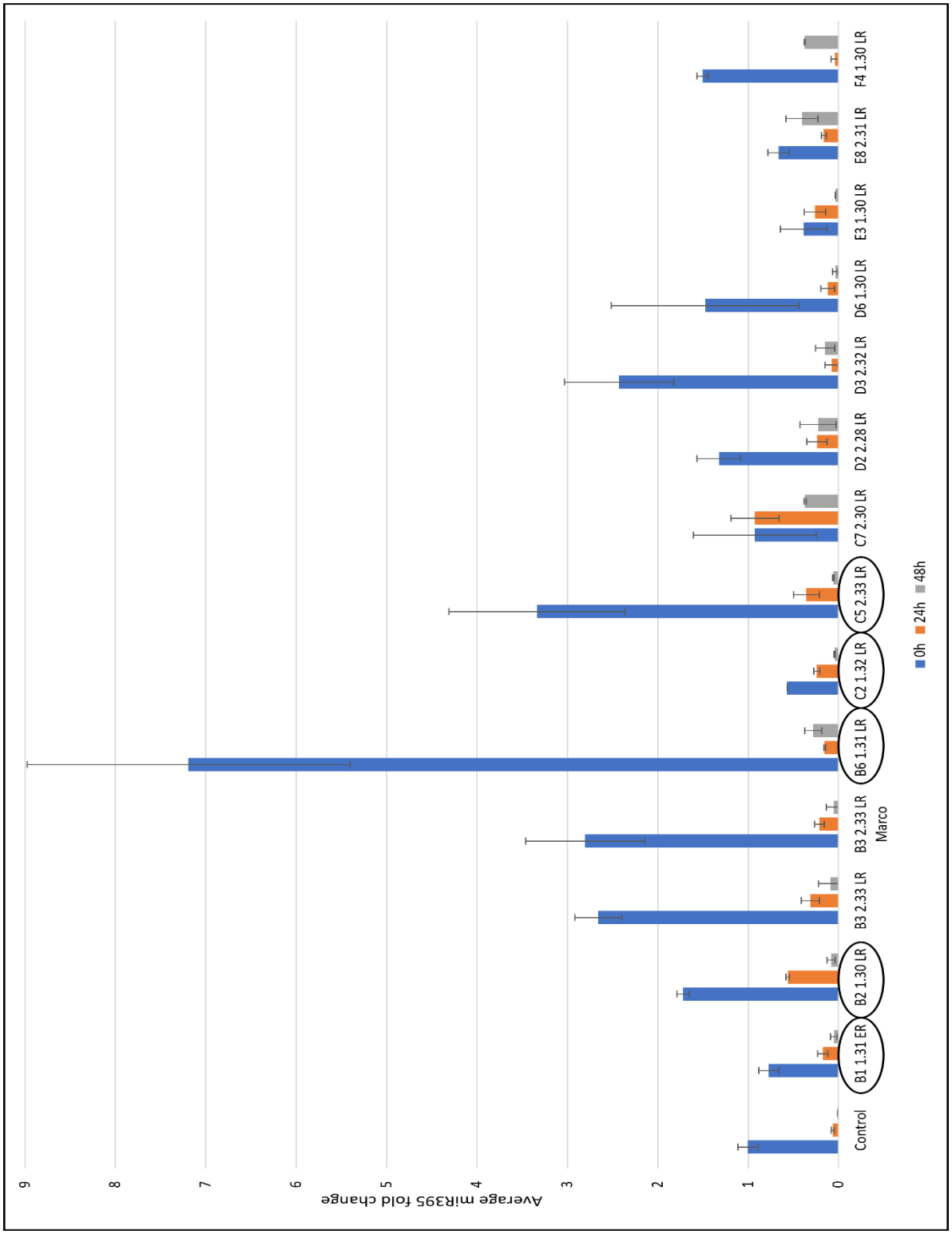

Figure 11: Average expression of miR395 after replenishing the media with $MgSO_4$. Average fold change of miR395 at 0h, 24h and 48h after replenishing the media with $MgSO_4$ compared to the control 0h for the first set of candidates following the Pfaffl method. The error bars represent the standard deviation. Note: some results were omitted from the two figures to make them more readable as some values were too big and crushed down the totality of the graph.

The next step was to have a clearer view of the degradation curve. 96 well plates are a limitation in this objective as 3 biological replicates for each timepoint is a minimum and only allow 3 timepoints and a control on the same plate with 4 technical replicates and both miR395 and Actin tested. In consequence, we decided to carry out for northern blots, which allow a more flexible design. Also, using another technique to test the level of miRNAs make the validation of candidates more robust.

4) Confirmation of the RT-qPCR candidates with Northern Blot

Northern blot experiments were then performed with 5 or 6 timepoints to further investigate the degradation rate of miR395 in the Early and Late Response mutants. In the same way as the RT-qPCR assays, 3 biological replicates composed of a pool of ~20 plants of the different mutants and a control were grown in LS media and replenished with $MgSO_4$ after 2-3 weeks and the RNA extracted from the roots at different timepoints. As there were less mutants to validate, I decided to increase the number of timepoints (0h, 3h, 6h, 15h, 24h and 48h) to have a better view of the degradation curve in both the control and the mutants. Sometimes, the amount of RNA extracted was too low, so I increased the duration of growth before adding $MgSO_4$ from 2 to 3 weeks and to have a bigger volume of root tissues Some of the experiments started with the seedlings growing on MS media first, then transferred on LS media for a week to induce the Sulfur starvation. Northern blots were done using 1-5 µg of total RNA and the membrane was incubated overnight with γ-^{32}P labelled probe against U6 (housekeeping gene used for normalisation) or against miR395. After several washes, the membrane was put in a cassette containing a Fujifilm, that detects the gamma particles emitted by the membrane. The film was scanned after a variable amount of time being exposed to the radioactive membrane using the scanner Typhoon 9500 FLA, and the intensity of the bands were manually measured using ImageQuant. The expression level of miR395 was calculated by normalising the signal intensity of miR395 to the signal intensity of U6.

4.1) Analysis of the mutant with high miR395 level at 0h

The mutant B6 1.31 LR was found to have an expression level of miR395 seven times higher than the control at the 0h timepoint. To verify this result and to determine if this mutant could

be involved in the Sulfur pathway, the levels of miR395 in plants grown on LS media or MS media were compared. All plants (3 biological replicates of Col-0, rdr6 and B6 1.31LR) were grown on MS media then transferred after two weeks to either MS or LS media for 96h and the RNA extracted from their roots.

The level of miR395 was increased after transferring from MS to LS media showing the deficiency in Sulfur in the LS media and showing that 96h is enough to induce starvation and miR395 expression. This protocol was also used for the analysis of the other mutants as plants grown first on MS media showed a bigger root volume, thus increasing the amount of RNA extracted.

As shown by the northern blot, there is no significant difference in the level of miR395 in the mutant B6 1.31 LR compared to both controls growing in the LS media (Figure 12). Therefore, I concluded that this mutant was a false positive. The RT-qPCR result might come from the normalisation with the housekeeping gene, which is Actin, but in the Northern blot, U6 is used. If the EMS mutation(s) appeared in the Actin gene and its related pathway, then the normalisation of miR395 is biased and may have led to a very high level of miR395 expression.

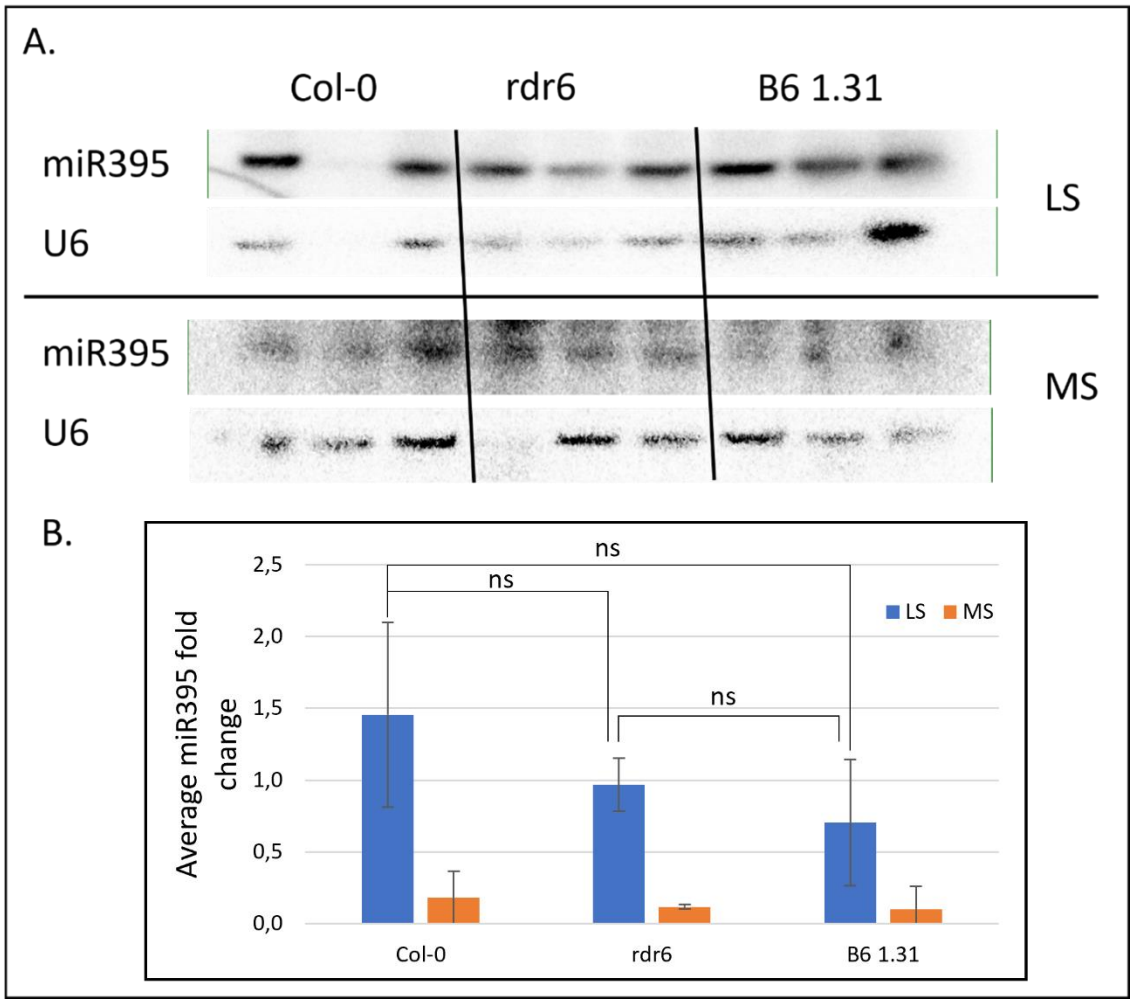

Figure 12: Analysis of the expression of miR395. A. Northern blots of miR395 and U6 in plants grown on MS media then transferred to LS or MS media. Each condition was performed with 3 biological replicates of each background. B. Average expression of miR395 in those plants, normalised by U6.

The bands for miR395 in the MS northern blot seem strong but it is because of how ImageQuant works: the initial image is cropped on the area of interest, i.e., where miR395 or U6 is, to create another file. When opening this file, ImageQuant removes some background noise and is amplifying the bands to allow the analysis, making it look stronger than they are. Figure 13 being the initial scan for miR395.

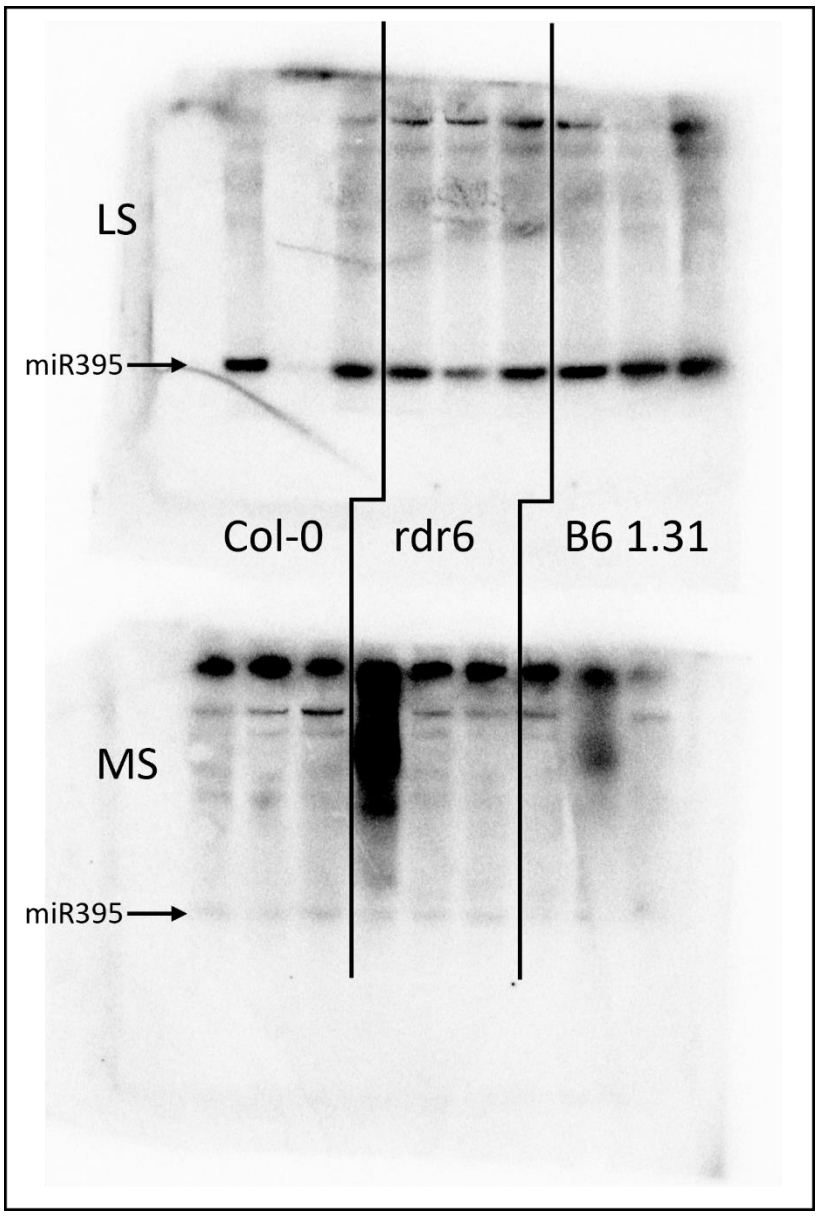

Figure 13: Northern blots showing miR395 in plants grown on MS media and transferred to MS media or LS media for starvation. Each condition was performed with 3 biological replicates of each background.

4.2) Analysis of the early response mutants

For the candidates that expressing slower or faster GFP recovery and gave positive results by RT-qPCRs, I then proceeded to further validation by increasing the number of timepoints from 3 to 5-6 and used northern blots to calculate the degradation rate of miR395. Two early responses candidates were chosen for this analysis: C7 3.51 (ER1) and B1 1.31 (ER2). A few northern blots were carried out for each mutant as neither the control (*rdr6*) nor the

candidates produced a good degradation pattern of miR395, making it hard to calculate a degradation rate to compare the wild type and the mutants (Figures 14, 15).

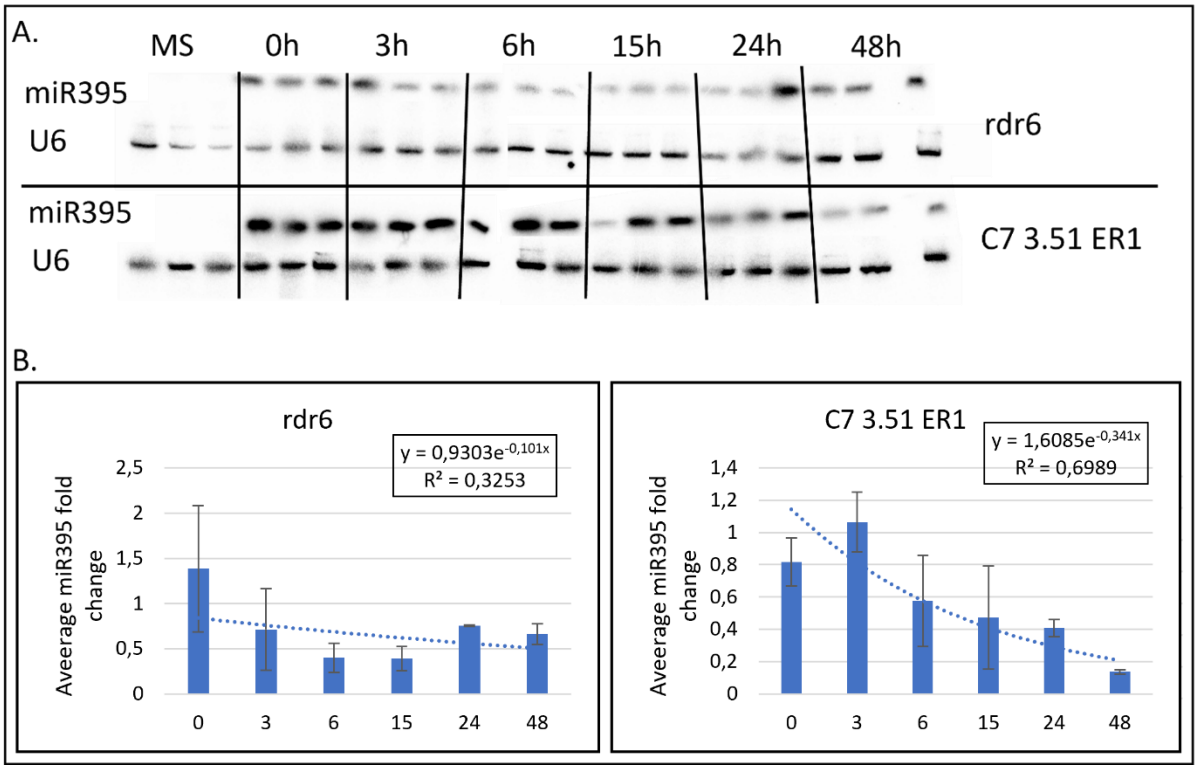

Figure 14: Analysis of the expression of miR395 in rdr6 and C7 3.51 ER1. A. Northern blots of miR395 and U6 in a 6 timepoint experiment. B. Average expression of miR395 in rdr6 and the mutant C7 3.51 ER1, normalised by U6. Note: the MS values for miR395 equals 0 in calculation spreadsheet, so they are not represented in the graph to produce the degradation curve.

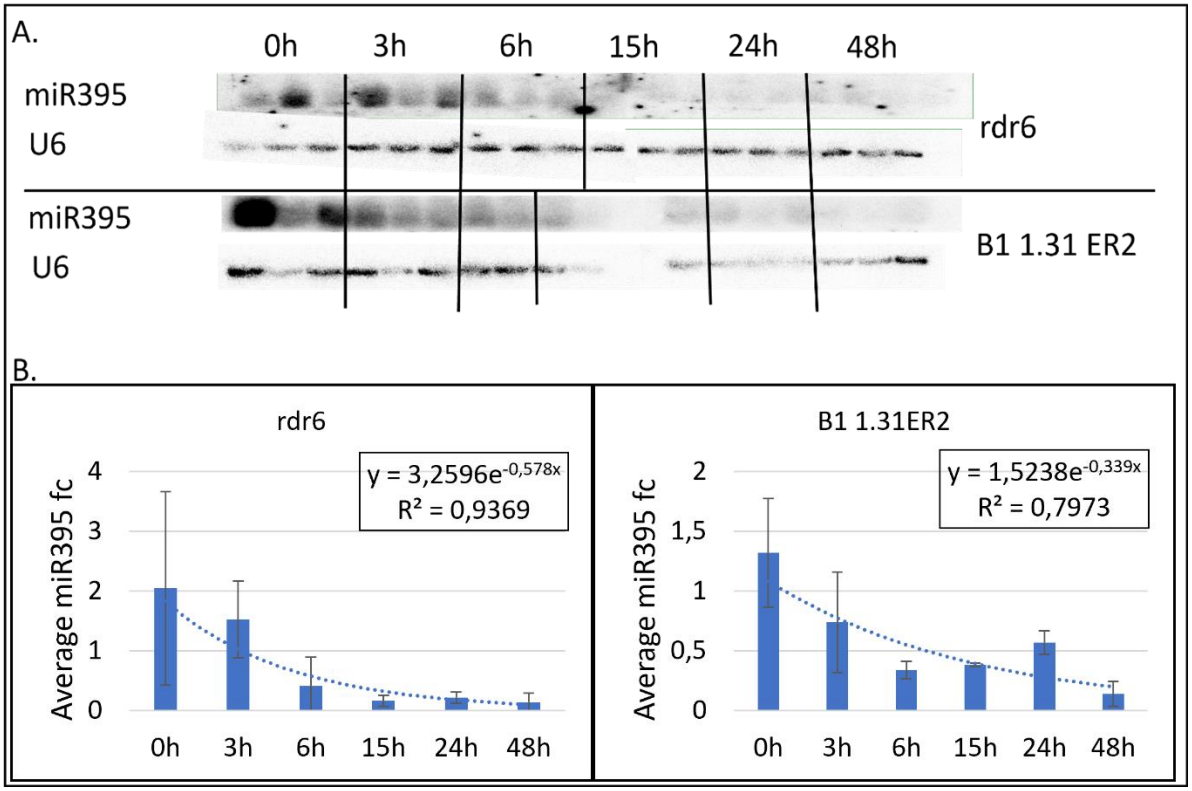

Figure 15: Analysis of the expression of miR395 in rdr6 and B1 1.31 ER2. A. Northern blots of miR395 and U6 in a 6 timepoint experiment. B. Average expression of miR395 in rdr6 and the mutant B1 1.31 ER2, normalised by U6. fc = fold change.

4.3) Analysis of the late response mutants

In the same way as the early response mutants, three late response candidates were chosen: C5 2.33 (LR1), B2 1.30 (LR2) and C2 1.32 (LR3).

The first late response mutant to be tested was C5 2.33 LR1. In the same way as the early response mutant, a 5 timepoints experiment was performed but did not validate the RT-qPCR results (Figure 16).

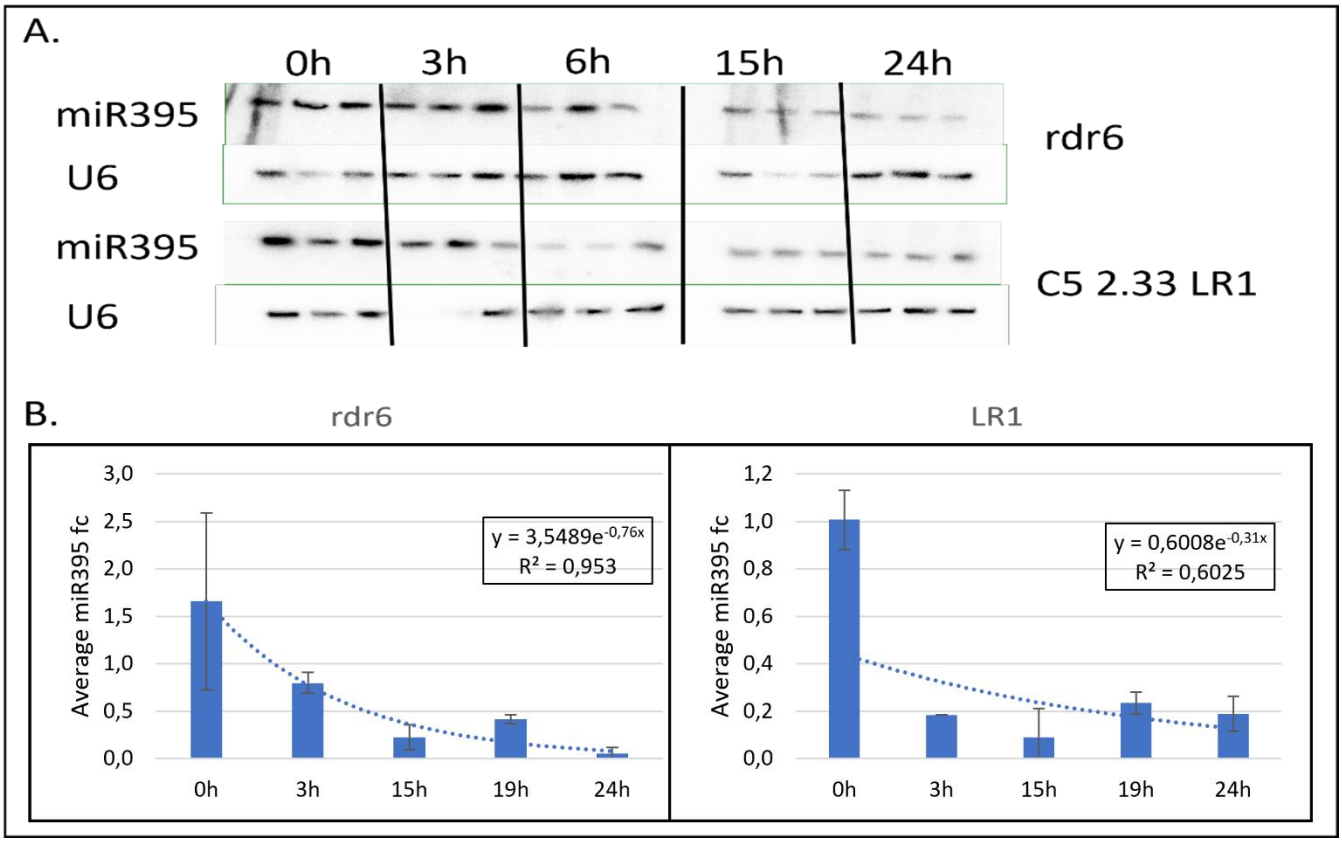

Figure 16: Analysis of the expression of miR395 in rdr6 and C5 2.33 LR1. A. Northern blots of miR395 and U6 on a 5 timepoint experiment. B. Average expression of miR395 in rdr6 and the mutant C5 2.33 LR1, normalised by U6. fc = fold change

The second late response mutant, B2 1.30 LR2 showed the best degradation curve of all the candidates (Figure 17).

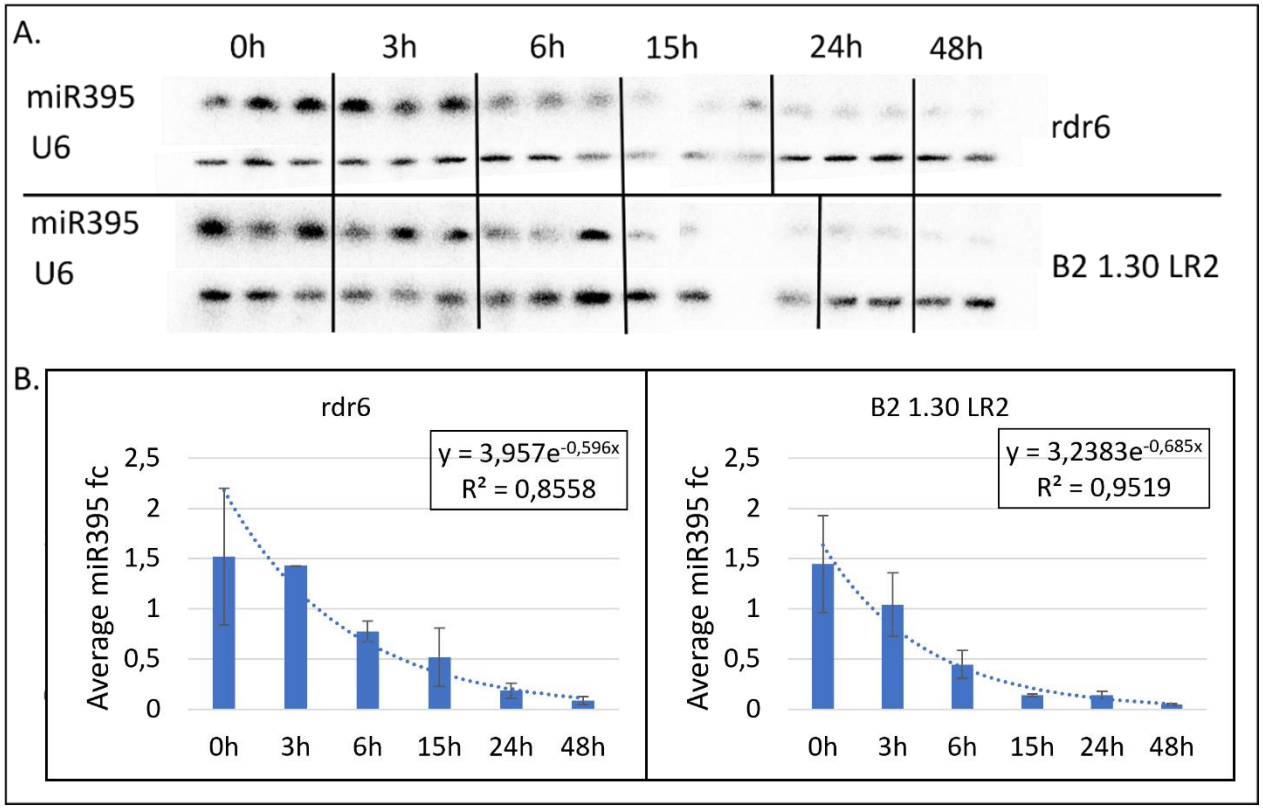

Figure 17: Analysis of the expression of miR395 in rdr6 and B2 1.30 LR2. A. Northern blots of miR395 and U6 on a 6 timepoint experiment. B. Average expression of miR395 in rdr6 and the mutant B2 1.30 LR2, normalised by U6. fc = fold change

Surprisingly, the exposure time of the Fujifilm to the membrane alters the value of the slope (Table 2). This is due to the processing by ImageQuant. Despite this, the slope values are too similar and B2 1.30 LR2 is considered a false positive from the screening assay.

Table 2: Degradation slope of miR395 in rdr6 and B2 1.30 LR2 at different exposure times.

Exposure time for miR395	Slope	R^2
rdr6 1h	-0.587x	0.9362
LR2 1h	-0.571x	0.9578
rdr6 3h	-0.596x	0.9422
LR2 3h	-0.685x	0.9610

Finally, the third tested late response candidate, C2 1.32 LR3, did not show a good degradation response due to its 24h timepoint and because of the control as well (Figure 18).

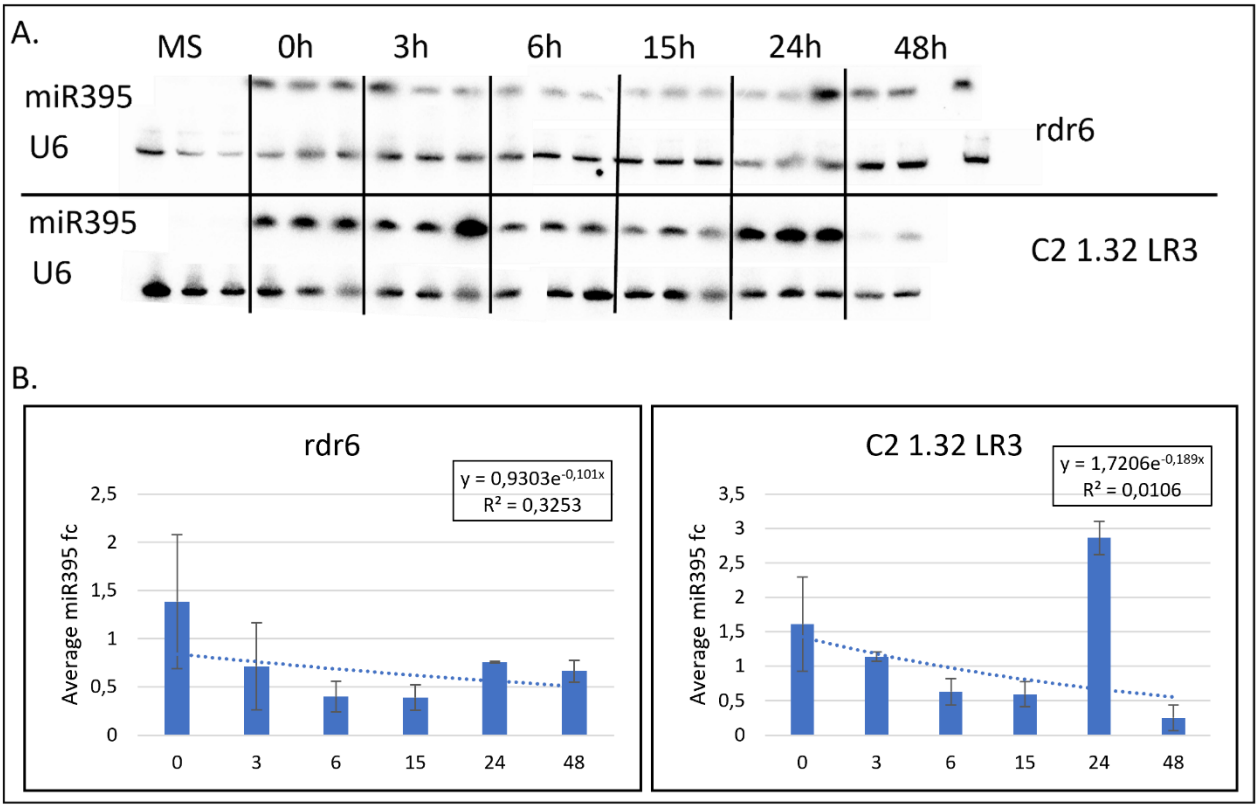

Figure 18: Analysis of the expression of miR395 in rdr6 and C2 1.32 LR3. A. Northern blots of miR395 and U6 on a 6 timepoint experiment. B. Average expression of miR395 in rdr6 and the mutant C2 1.32 LR3, normalised by U6. Note: the MS values for miR395 equals 0 in calculation spreadsheet, so they are not represented in the graph to produce the degradation curve. fc = fold change

5) Discussion

At first, contamination was jeopardizing my screens and even completely killed off all seedlings in my screening N° 24 (Figure 7.C). After making new media, and changing my sterilisation protocol, it turned out the main source of contamination was coming from the $MgSO_4$ solution. Therefore, after each experiment, the $MgSO_4$ bottle was autoclaved, which solved the problem. Loss of candidates continued during the transfer of candidates to MS media then to soil for seed collection, as some of them perished because of the transfer stress or the media got contaminated reducing the number of candidates to analyse.

Despite having a good starting number of screened plants (Maple & Møller, 2007) with ~2500 seeds screened that gave 40 candidates, only 13 survived and produced seeds. Unfortunately, even after adding 19 other candidates picked by the previous PhD student, Dr Rocky Payet, the validation of the mutants from the screenings was not achieved neither by RT-qPCR nor Northern blot and we decided to put an end to this project to focus on the candidate approach. Different points can also be raised to support this decision.

The first step of the GFP screening assay rest on a subjective judgement of the fluorescence intensity. As such, a lot of false positives were picked up and some potential candidates could have been lost in the first stage as well. However, it is not realistic to carry out an accurate measurement of miR395 level in every single seedling. Also, during the assays, the eyes must first accommodate to the darkness in the room and acknowledge which intensity correspond to which score. For that, the control (plants having the transgene but not EMS mutated) was always assayed first to calibrate the eyes but even the control was not flawless and lots of the control plants were not expressing the GFP correctly, even 7 days after Sulfur replenishment when all the plants should express the GFP correctly. Quantification of the intensity by computer may improve this step of the pipeline even though the calibration would still be mostly subjective. Unfortunately, increasing the number of screenings would induce extra labour, as each seedlings must be individually examined over long periods of time and increasing the quantity of seedlings to monitor needs to consider the extra work done by a single person. Another point that can be raised is that the day 12 was the last day of screening because the aerial parts would later grow and hide the roots from being seen, which may have led to a loss of potential late response or very late response mutants that would have shown GFP recovery at a later timepoint. It could also have been interesting to look again at the GFP expression in the candidates to validate the data from the screening before starting the quantification of miR395.

Following the screening, one of the main problems was the quantity of RNA extracted from the roots. Indeed, plants grown on LS media tends to have shorter roots, so less RNA was obtained and while it was not a problem with RT-qPCR, Northern blots requires a lot of RNA

to provide the best results, even if I managed to have results with less than 1 µg of RNA per biological replicate. Also, since roots tissues were used, sometimes an accumulation of starch was found after drying the RNA pellet making it hard to dissolve in water. The solution was to centrifuge the samples and collect the supernatant containing the RNA, but a lot of RNA was still lost in the process and lots of variations in the RNA concentration between biological replicates would occur. The presence of starch was irregular making it hard to foresee and thus troubleshoot. As for the root's length, growing plants on MS media before transferring them on LS media to starve on Sulfur for a few days seemed to be an effective way to increase the size of the roots, thus the level of RNA.

The RNA shortage first led us to use RT-qPCR as ~50 ng was necessary to perform it. The plate design changed a few times to ultimately fit the control at 0h and the 3 timepoints of the mutants, with each three biological replicates and four technical replicates for each one of them. Half the plate was measuring the level of miR395 and the other half Actin as the housekeeping gene for later normalization. As experienced in the other project and discussed later, the stability and abundance of the housekeeping genes may vary with the plant background. Actin was chosen to be the housekeeping gene for normalisation, but it could have been mutated during the EMS treatment or its regulation changed because of a mutated regulator leading to the false positives' discovery. This is solved during the northern blots using U6 where U6 is seen, and its abundance calculated by ImageQuant allowing a better normalisation. During the northern blot stage, the time series experiment was gradually improved by either increasing the number of timepoints to smooth the degradation curve and increase its R^2, increase the number of plants per biological replicate or changing the volume of $MgSO_4$ added to the media. The use of an LNA probe for miR395 did not improve the northern blot results variability. Indeed, the results were very variable, especially with RT-qPCR, while the controls seemed to be always very different, and I could see high variability of the results (not shown) despite not changing the parameters between two experiments and this is a point to improve if this pipeline is used again.

It is important to note that even if I did not manage to get an interesting candidate, this screening is functional and allowed the previous PhD student to discovery a post transcriptional gene silencing mutant, called *msm1* (unpublished data).

Chapter III] Identifying HESO1 interacting proteins

1) Introduction

After testing the Forward genetics approach with the screening assay, we decided to go for the Reverse genetics approach. This starts with several candidate genes obtained through various ways (interaction with protein with known functions, gene homology, etc), create a collection of mutants via plant transformation (crossing, directed deletions or point mutations, etc) and select the GOI candidates (Aklilu, 2021). It is relatively easy to create a collection of *Arabidopsis thaliana* mutants since the availability of the SALK lines (http://signal.salk.edu/). This project is based on the creation of a loss of functions for all the genes in *S.cerevisiae* to allow researchers to effectively choose genes of interest (Giaever et al., 2002; Ross-Macdonald et al., 1999; Winzeler et al., 1999). This was then applied to *A. thaliana* by José M. Alonso et al. (2003). They inserted over 225000 *Agrobacterium* 'transferred DNA' (T-DNA) in the genome of *Arabidopsis* to identify 21700 mutated genes over the 29500 predicted genes. Knowing the GOI, PCR primers targeting the T-DNA insert and the WT, designed to verify the insertion (Figure 19), can be easily collected from the SALK website which automatically design both PCR primers pairs based on the SALK line number (O'Malley et al., 2015).

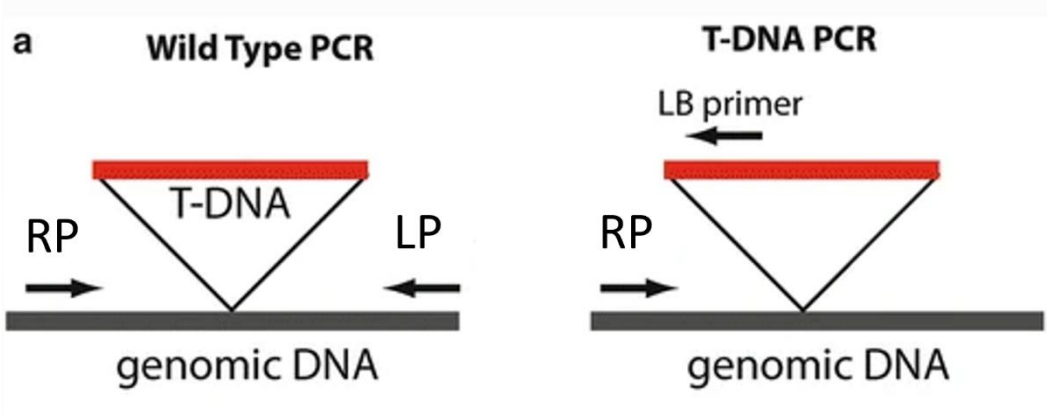

Figure 19: Two PCR master mixes are prepared, one containing the RP (Right Primer) and the LP (Left Primer) primers that will amplify the wild type gene and the second one containing the RP and LB (Left Border) primers that will show the T-DNA insertion and a portion of the wild type gene. The PCR is performed with both sets of master mixes, then the products are

mixed and loaded on an agarose gel. The first set of primers giving a long product (WT), visualized by a higher band and the second set a short product (SALK mutant) giving the lower band, heterozygous plants will have the two bands present. Modified from O'Malley et al., (2015).

This second project is based on the Arabidopsis Interactome Map Project (Dreze et al., 2011), another collaborative project that highlighted, in *Arabidopsis*, ~6200 interactions between ~2700 proteins based on verified interactions in yeast two-hybrid system (Y2H). This system is based on the reconstitution of a transcription factor by the expression of a DNA-binding domain to its activation domain (Dreze et al., 2010; Fields & Song, 1989). By adding the sequence of the proteins of interest to the sequence of those two parts, the transcription factor can only be activated if the two protein interacts between them leading to a visible phenotype that depends on the strength of the interaction. With the help of bioinformatics to condense the huge dataset (https://thebiogrid.org/) (showing the multiple interactions for one protein, drawing the interactome, etc), the Arabidopsis Protein Interactome Network is clearer than ever before and finding predictions of proteins interacting with a protein of interest (POI) became a formality in *Arabidopsis*.

For this project, we will look at six genes predicted to interact with HESO1, namely *HIX* for *HESO1 INTERACTOR X* (with *X*= 1 to 6) (Figure 20), to determine if any of them is involved in the miRNA pathways. For that, we will start looking at a phenotypic rescue of *hen1* by crossing the different mutants in this background. Indeed, as HEN1 is responsible for the protection of mature miRNAs, they are severely under-expressed in a *hen1* background leading to a severe phenotype. However, Zhao et al. (2012) showed that knocking out *HESO1* in a *hen1* background led to a phenotypic recovery as the miRNAs were less U-tailed, thus less prone to degradation. Our hypothesis is that if any of the interactors is involved in miRNA turnover, we should observe a phenotypic rescue of *hen1*. The level of some miRNAs will also be assessed by northern blots.

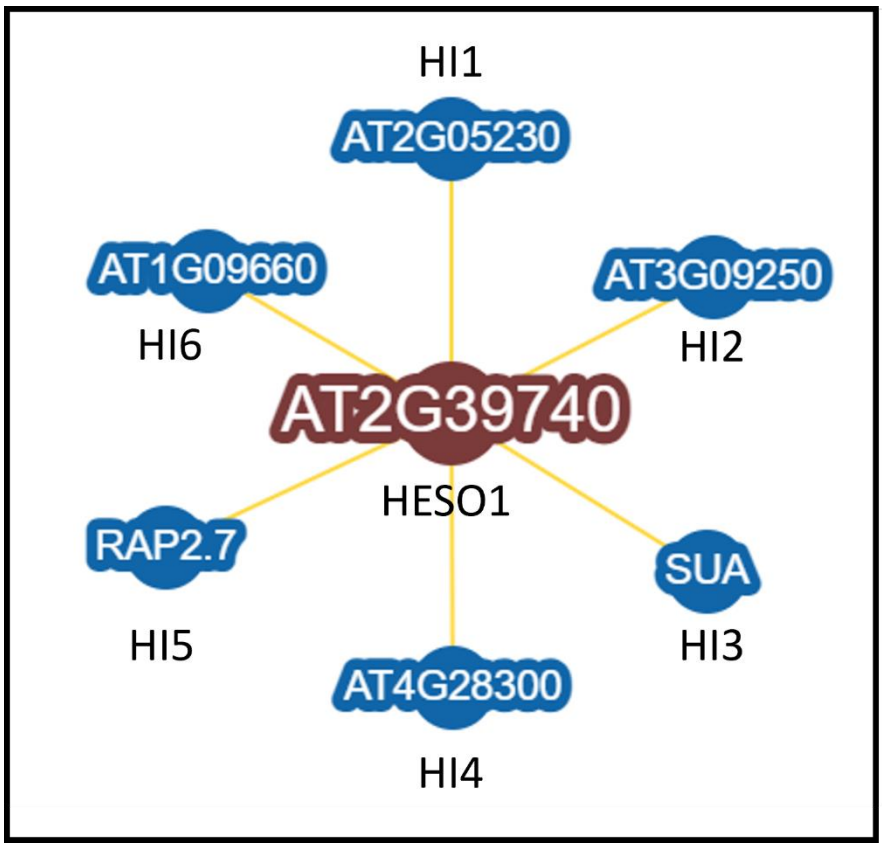

Figure 20: Predicted interactors of HESO1 according to BioGrid.

2) Isolation of the SALK lines and crosses with *hen1*

The SALK mutants from the six genes of interest were ordered and named accordingly as in Table S4 and represented in Figure 21.

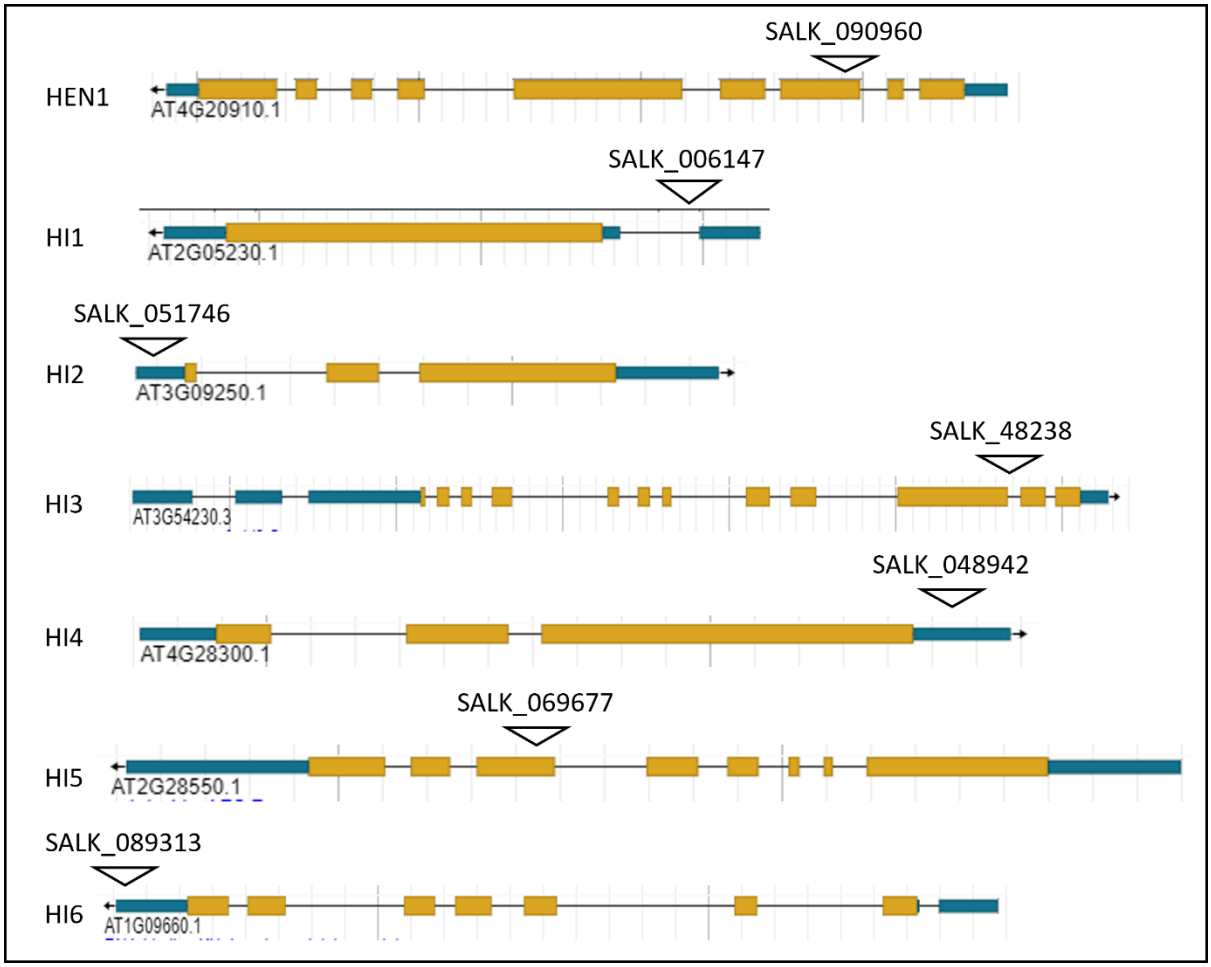

Figure 21: Locations of the SALK T-DNA inserts in the different mutants ordered. The green boxes represent the 3'-UTR and the 5'-UTR while the yellow boxes represent the CDS, the black lines are the intronic regions.

Upon receiving the SALK lines, the SALK seeds are not necessarily all homozygous for the T-DNA insert, therefore the first step is to obtain homozygous lines of each mutant, which was done previously by the laboratory. DNA from a single leaf was extracted and the verification of the homozygous single mutant for each candidate was performed by the genotyping PCR as described in Figure 19, and the future plants that will be used for the crossings are coming from the seeds of those single mutant plants (Figure 22).

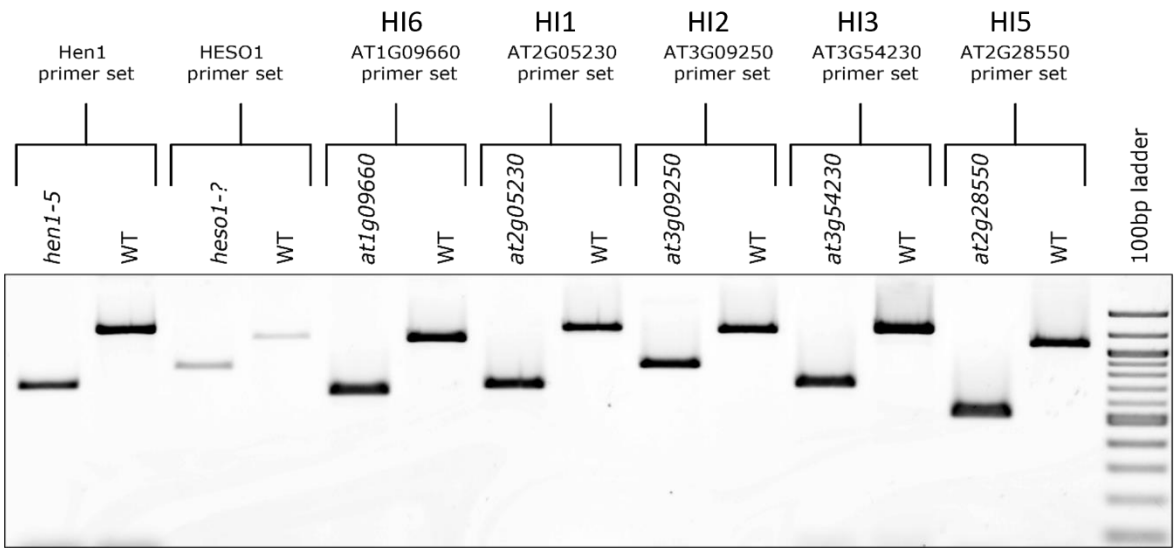

Figure 22: Gel showing the genotyping PCR results for the HESO1 interactors, hen1 and heso1. Two PCRs were performed on each samples, with either the corresponding LP and RP primers or the corresponding RP and LB primers. The products were then mixed accordingly before being loaded into an agarose gel and going through electrophoresis. Col-0 was used as the negative control (WT). The homozygous mutant contains a T-DNA insert that makes the PCR product smaller and thus migrating a bigger distance than the WT in the agarose gel. In the case the plant is heterozygous, both bands in the well would show. The 100 bp ladder ranges at 100, 200, 300, 400, 500, 600, 700, 800, 900, 1000, 1200, 1500 bp.

After selection of the homozygous mutants, the selected lines were crossed with the *hen1* line to monitor a phenotypic change (Zhao et al., 2012). For the crosses, homozygous mutants were grown under short day conditions for about a month to prevent asynchronous flowering of the different lines. They were then moved to long day conditions, which triggers the transition from vegetative phase to reproductive phase, where the flowers are produced. As *Arabidopsis thaliana* performs self-fertilisation during the flower opening (Charlesworth & Vekemans, 2005), crosses need to be done on unopened flowers. Under a microscope, the process starts with the receiving plant (i.e., the female) with the removal of opened flowers and siliques if any are already present. Then, with forceps, the removal of the meristem buds to prevent the stem to continue growing with unwanted flowers, leaving two to three unopened flowers. The petals and stamens were delicately removed, leaving only the carpel ready to receive pollen from the donating plant (i.e., the male). From the male plant, opened flowers were picked and the petals removed to see the anthers that were then gently rubbed on the pistils of the receiving plant, several rubs were performed with different male anthers

to ensure proper fertilisation. The pistils were covered to protect them from unwanted pollen and taped to differentiate them from each other. The success of the crosses could be verified three to four days later with the start of production of a silique. Usually, the *hix* plants were receiver and *hen1* plants donors as the siliques of *hen1* are very small and do not provide a good yield (Wang et al., 2015; Wei et al., 2020). Seeds were collected from those siliques, the F1 generation grown, and the plants were genotyped by PCR to verify the success of the crosses. Successful F1 lines were kept and the seeds from their self-fertilization were used to produce the F2. Finally, the F2 seeds were sown at a bigger scale to look for double homozygous containing the SALK T-DNA insert in both *hen1* and *hix* genes. Plants without both impaired genes were discarded while the double mutants were kept for further experiments. In the end, the double mutants obtained were *hi2/hen1*, *hi3/hen1*, *hi5/hen1* and *hi6/hen1* and used as the base for the future experiments.

3) Phenotypic analysis

One of the objectives was to observe a phenotypic rescue of the *hen1* background. Over the numerous ways to measure the phenotype in *Arabidopsis* (Boyes et al., 2001), I decided to measure the rosette diameter as a reflection of the vegetative growth and the siliques' length for the reproductive part. As Arabidopsis rosette is not a perfect circle, I measured the two biggest leaves to measure the rosette diameter in four biological replicates of each available background. Siliques were measured in triplicates of each background as *hen1* siliques are scarce on the stem and few of them manages to grow to their full size. The rosette measurements were done every three or four days from day 15 post vernalization (pv) to day 35 pv (Figure 23) while the siliques were measured once a least one replicate of each background produced a dozen siliques to make sure to take the longest one, except for *hi3/hen1* which was measured later due to the loss of the plants after the phenotyping measurement (Figure 25).

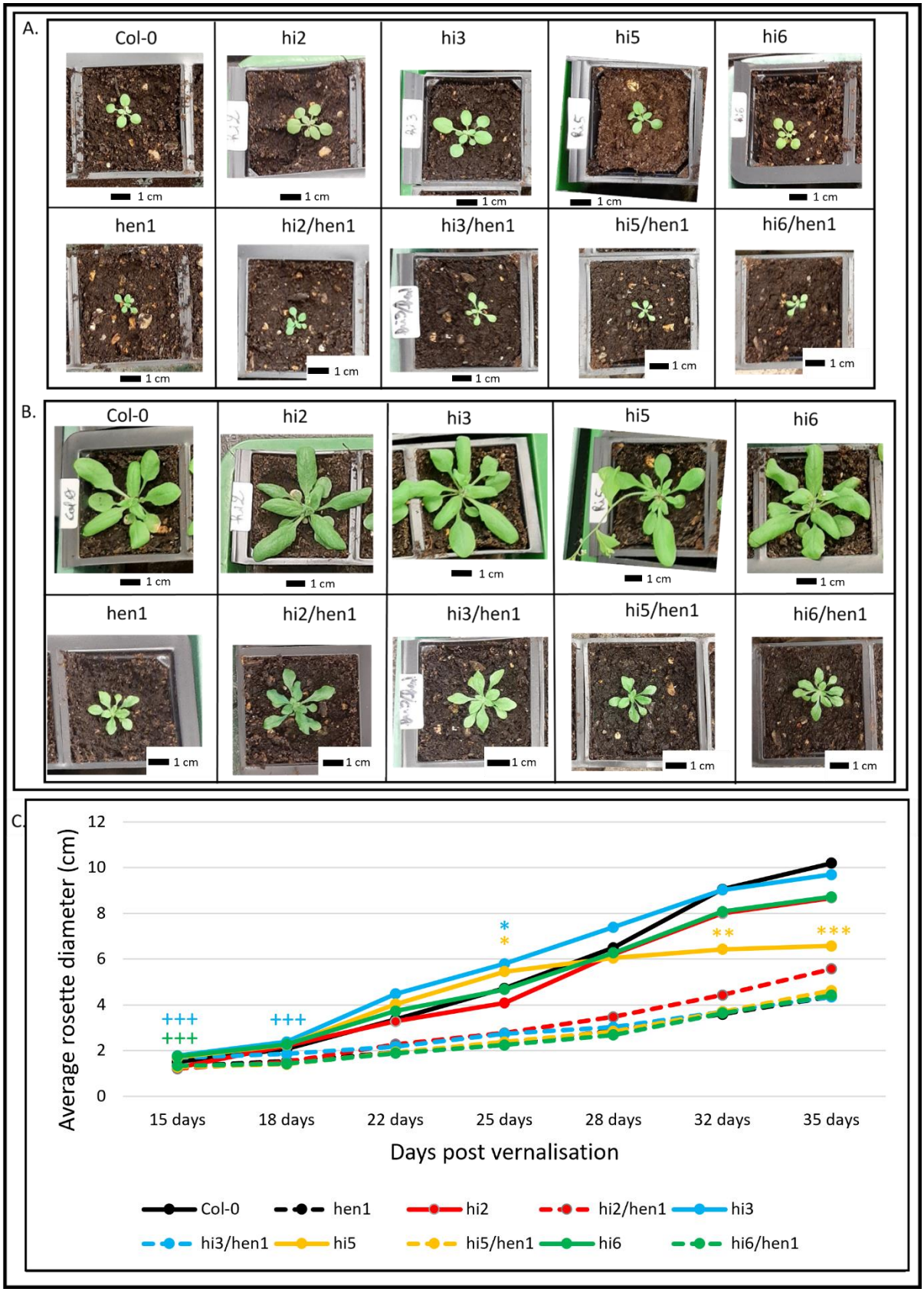

Figure 23: Phenotypic analysis. A. Pictures of the different genotypes at Day 18 after vernalization. B. Pictures of the different genotypes at Day 28 after vernalization. C. Average rosette diameter of the different backgrounds at different timepoints after vernalization. The

rosette diameter was calculated by summing the two longest rosette leaves of 4 biological replicates. Coloured asterisks represent statistical comparison and significance between the Col-0 control and the corresponding single mutant (for example, blue asterisk is the comparison between hi3 and Col-0) while the coloured crosses represent statistical comparison and significance between the hen1 control and the corresponding double mutant (for example, blue asterisk is the comparison between hi3/hen1 and hen1) (two-tailed t-test, p-value < 0.05).

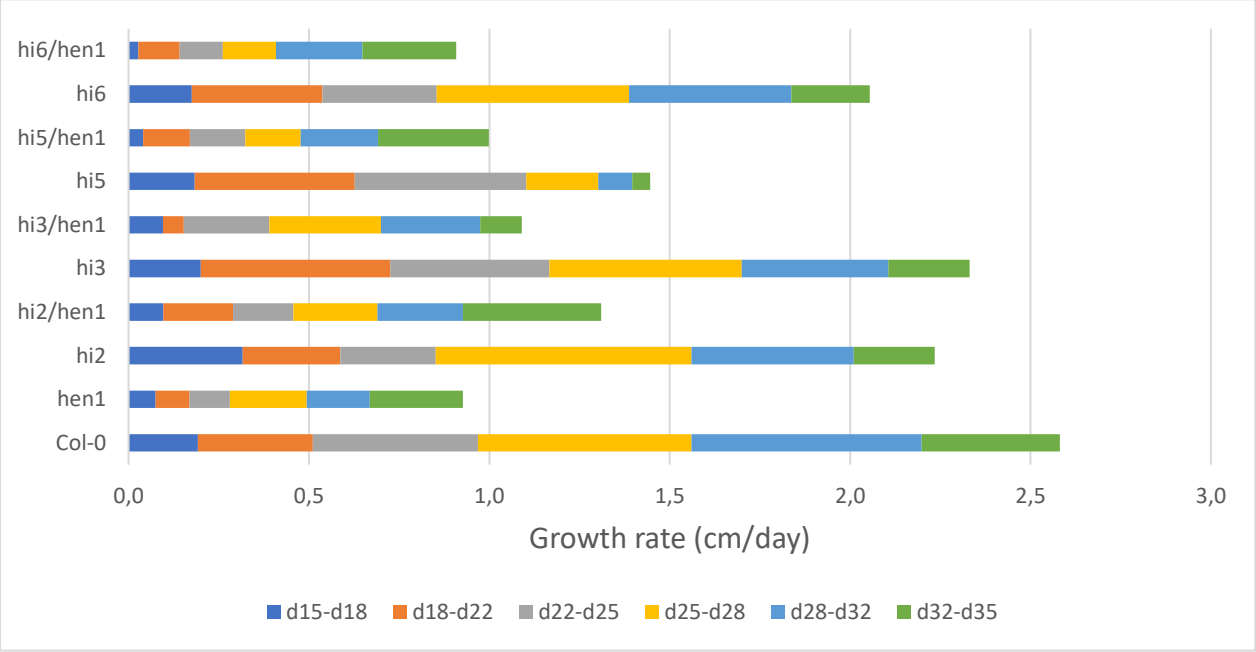

Figure 24: Average growth rate of the different tested backgrounds over periods of 3 or 4 days. Growth rate was calculated as the average rosette diameter at the most recent timepoint minus the average rosette diameter at the older timepoint divided by the number of days separating them.

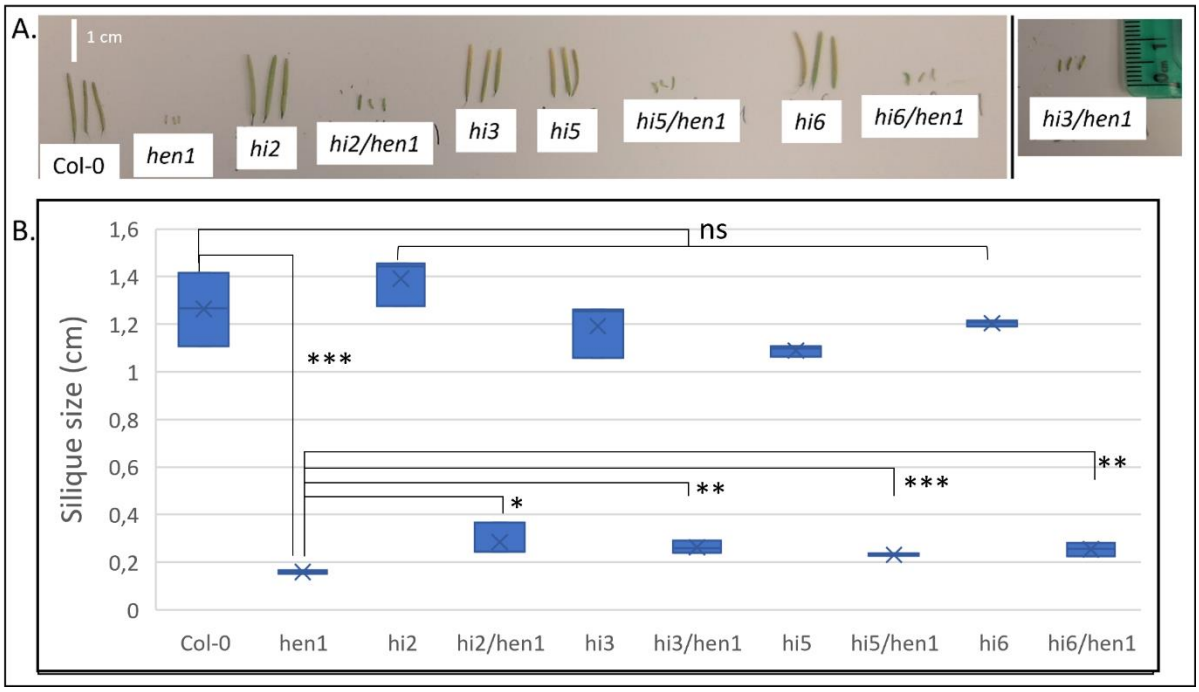

Figure 25: Silique length in the different genotypes. A. 3 siliques measured for each backgrounds, hi3/hen1 was not measured at the same time than the other backgrounds but the images are on the same scale. B. Graph of the three measured siliques in A. Brackets and asterisks represent statistical comparison and significance (two-tailed t-test, p-value < 0.05), ns: not significant.

The single mutant hi2 did not show a phenotypic difference to Col-0 (Figure 23) although it slowed down its growth speed past Day 28 pv (Figure 24). The siliques are the longest of all the tested backgrounds, but the difference compared to the WT is not significant (Figure 25). As for the double mutant, *hi2/hen1* seems to have the best phenotypic rescue considering the rosette diameter, the growth speed and the silique size (Figures 23, 24, 25), giving us the best candidate from that perspective.

hi3 had the biggest rosette diameter until it got caught up by the WT at the end of the experiment (Figures 23, 24) while its siliques are smaller than Col-0 (Figure 25). While the double mutant *hi3/hen1* was growing better at the early stages of the observations than *hen1*, in the end of the experiment, they have the same size (Figures 23). The interesting part of *hi3/hen1* is witnessable at the reproductive stage with slightly bigger silique (Figure 25) but most importantly an early production of the stem in *hi3/hen1* compared to *hen1* (Figure 26), thus of the flowering production time, which led us to continue working on that gene.

Figure 26: Small phenotypic rescue of hen1 by hi3. Picture of hen1 and hi3/hen1 at day 52 after vernalisation.

The smallest of the single mutants is *hi5*, almost having the same size as *hi2/hen1* at Day 35 pv (Figure 23). It seems to have stopped growing after Day 28 pv, or at least reduced growing drastically (Figure 24). It became the fastest background to have reached its final rosette size, thus started producing its reproductive system as shown by the visible stem in Figure 23. Even if *hi5* was the first to reach reproduction stage, its siliques were the smallest of the single mutants (Figure 25). The double mutant *hi5/hen1* looks like the single *hen1* in all measured vegetative points but had bigger siliques (Figures 22, 23, 24).

Finally, *hi6* showed similar vegetative growth to *hi2* (Figures 23, 24) but smaller siliques (Figure 25). The double mutant is comparable to *hen1* (Figures 22, 23) with only slightly bigger siliques to make the difference (Figure 25).

The phenotypic analysis on its own cannot give us a conclusion and the complementary step was to measure the level of some miRNAs in the different mutants.

4) Quantification of the level of miRNAs in the mutants

The second objective was to measure the level of some miRNAs, despite the lack of big phenotypic rescue in case the rescue was not phenotypically visible with my criteria but could have been detectable at the miRNA level. I chose to test miRNAs that are routinely investigated: miR156, miR166 and miR390 (Mee et al., 2005; Wang et al., 2018; Wu et al., 2013), but also two "special" miRNAs that are miR158a and miR319a. Indeed, miR158a is not fully methylated in the wild type and miR319a is less sensible to tailing and trimming (Zhai et al., 2013). The experiments shown on Figure 27 and Figure 28 were done independently.

Beside of the γ-^{32}P trace visible in all the miRNAs blots, making the quantification of Col-0 and *hen1* complicated, none of the double mutants showed a rescue in any of the tested miRNAs (Figure 27). The amount of loaded RNA and/or its transfer from the acrylamide gel to the membrane was an issue as shown by the very variable amount of U6. However, the level of miRNAs in the single mutant *hi6* is significantly higher than Col-0, but not in the double mutant *hi6/hen1* compared to *hen1* and indicates that the role of this gene could happen upstream the methylation step by HEN1 and might act as a stabilizer and could increase the efficiency of HEN1.

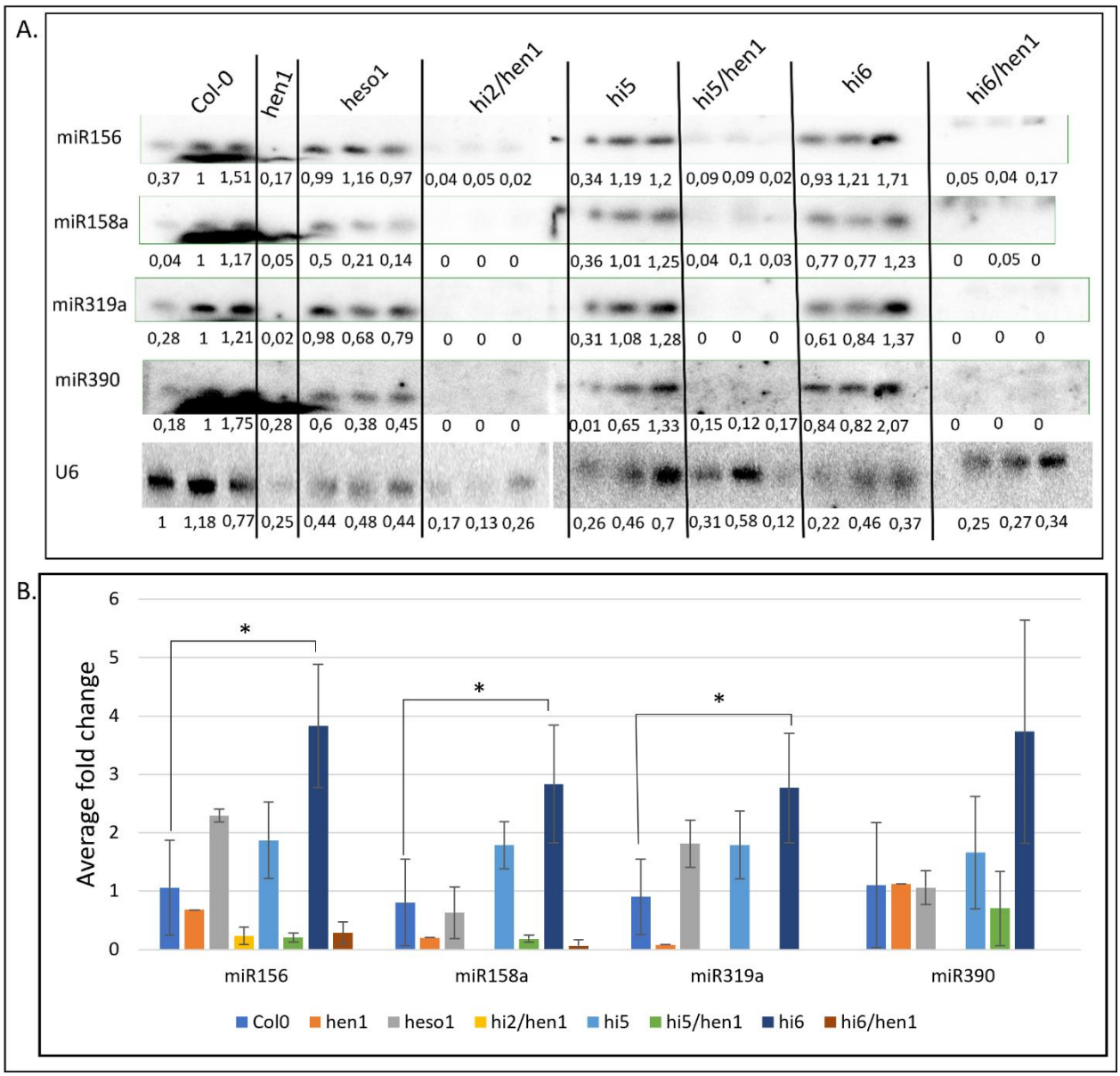

Figure 27: Analysis of miRNA expression in different Arabidopsis backgrounds. A. Northern blots of miR156, miR158a, miR319a, miR390 and U6 for loading control. 5 µg of RNA loaded. B. Average expression of the different tested miRNAs in the different backgrounds, normalized by U6. Asterisks represent statistical comparison and significance (two-tailed t-test, p-value < 0.05). Comparisons with hen1 cannot be achieved because there is only one biological replicate, other comparisons with Col-0 were not significative and not shown to keep the graph clear.

The same results were observed with *hi3* and *hi3/hen1* with a noticeable higher level of the "special" miRNAs in the the *hen1* backgrounds (Figure 28).

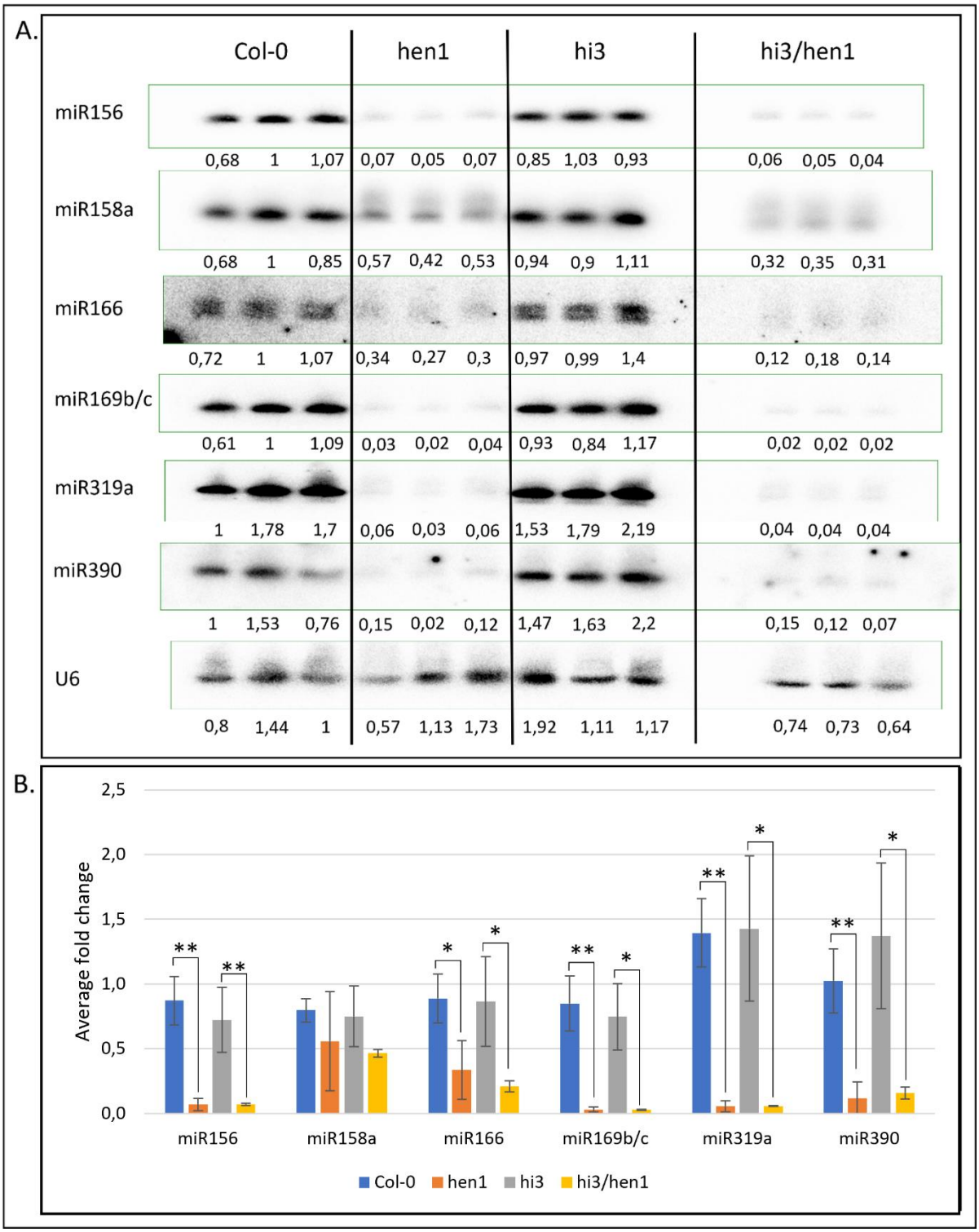

Figure 28: Analysis of miRNA expression in different Arabidopsis backgrounds. A. Northern blots of miR156, miR158a, miR166, miR169b/c, miR319a, miR390 and U6 for loading control. 10 µg of RNA loaded. B. Average expression of the different tested miRNAs in the different backgrounds, normalized by U6. Asterisks represent statistical comparison and significance (two-tailed t-test, p-value < 0.05). Other comparisons were not significative and not shown to keep the graph clear.

5) Discussion

The idea of using the yeast-two hybrid approach to get new candidates of interest was good as a candidate approach is easier than screening assays and working on 6 candidates seems feasible in the PhD timeframe, although highly dependent on the reproductive capability of the mutants and the methods used. Nonetheless, those interactions were discovered in yeast-two assays where false positive results are very common (Auerbach & Stagljar, 2005; Srere, 1999). It also does not necessarily expose what happens in reality in the plant cells, independently of any kind of stress responses, cascade reactions involving complexes or even cells localization, where proteins in different subcellular compartments can be predicted to interact together in yeast-two assay even if inside a plant cell, those would never meet. In the same way as in a yeast-two hybrid, Ehlert et al. (2006) developed a two-hybrid assay in *Arabidopsis* protoplast to propose an *in vivo* approach of high-throughput protein-protein interactions. Using that approach over yeast allowed them to demonstrate new interactions that were not shown using the yeast approach, which are more likely to happen as the interactions are happening in the living plants. *In vivo* confirmation of the interaction between *HESO1* and its individual interactors should have been done and was planned if the miRNAs analysis showed a candidate of interest. Before a proper interaction experiment, a simple co-localization experiment with one gene containing one fluorescent marker sequence such as GFP or mCherry and the other gene, another fluorescent marker could be a good preliminary experiment. Indeed, observation under a fluorescent microscope would then show the localization, which can already reject the result of the yeast-two hybrid assay if the proteins are not co-localized in the same cells or show different sub-cellular locations. Then, if the proteins co-localize, we could have confirmed the interaction using for example the FRET/FLIM technique (Long et al., 2017, 2018; Weidtkamp-Peters & Stahl, 2017).

Unfortunately, two double mutants (*hi1/hen1* and *hi4/hen1*) could not be obtained. However, improvement on selection be made. *hen1* plants are very defective but if there is a rescue in miRNA level, it cannot be missed as shown in Zhao et al., (2012). This background makes it very difficult to keep the plants alive, as any kind of stress can be detrimental for those plants because they cannot respond effectively. It also takes a long time to get the double mutants

as the *hen1* plants flower later than the WT, and the siliques are very small, thus containing few seeds. The double mutant for *hi1/hen1* and *hi4/hen1* were obtained at some point but some of the few seeds available for seed increase did not germinate or the plants did not survive until seed collection, losing months of progress. For future work on double mutants, I recommend keeping a heterozygous *hen1* background in a homozygous version of the other gene as a backup for an easier re-selection than starting from the F1 which will produce a lot of unwanted background and making the selection more tedious.

While *hi1/hen1* and *hi4/hen1* could not be obtained in time, their functions do not make them prime candidates for being involved in miRNA turnover. *HI1* is predicted to be a DNAJ heat shock N-terminal domain-containing protein but no studies were done on this gene to either validate this prediction or to find any potential other role. DNAJ proteins bind to HSP70 chaperone proteins to help the stabilisation of newly formed proteins (Frydman, 2003), so *HI1* is very unlikely to bind RNA, thus miRNAs nor be involved in their turnover. *HI4* was uncharacterized when this experiment started but was recently found to be involved in the allowance of water sensing by the embryo (Dorone et al., 2021). Renamed *FLOE1* by the authors, it is expressed during embryo development and is at its higher concentration in the mature desiccated state. *FLOE1* rapidly condensate when exposed to water and this is reversible when dried again, mimicked when exposed to lowering concentrations of salted water, showing a gradual emergence of the condensed form. The authors also showed that *FLOE1* reduce germination rate when water is limited. Overall, *FLOE1* is a water sensor that help the seed making the decision to germinate or not, depending on environmental conditions, thus it is not a good candidate for playing a role in miRNA degradation. This shows the limitations of the yeast-two hybrids experiment as none of those two proteins would interact with RNA, making an interaction with *HESO1* futile.

In retrospect, as in Boyes et al. (2001), counting the number of leaves every one to two days may have been a better phenotypic measurement to add for the vegetative part as the leaves length may vary quite a lot. For the reproductive part, stem size was measured at some timepoints, but it presented a huge variability, same for the apparition of flowers. Some *hen1* plants took over three months before starting to produce the stem and some only two despite

the vernalization of the seeds and the plants growing in the same tray, thus in the exact same conditions.

The northern blots showed that none of the remaining candidates could rescue the level of miRNAs in a *hen1* background, despite *hi2/hen1* and *hi3/hen1* having a slightly better phenotype than *hen1*, either in the vegetative part or in the reproductive part. According to TAIR, *HI2* is predicted to be part of the *Nuclear Transport Factor 2* (*NTF2*) family (Araport11) but it is not confirmed yet. *NTF2* genes are present in yeast and animals and are responsible of the transport of *Ran*-GDP inside the cells. Three *NTF2* genes are present in Arabidopsis, *NTF2a*, *NTF2b* and *NTL* (for *NTF2-like*), which only *NTF2a* and *NTF2b* can replace the function of *NTF2* in yeast, with the same role to bind to Arabidopsis *Ran*, showing a highly conserved protein (Zhao et al., 2006). While *Ran* has a lot of functions in a cell, like nuclear envelope formation (Hetzer et al., 2000) or nucleus-cytoplasm transport (Zhang et al., 1999), miRNAs are not part of any of this process making *HI2* very unlikely to perform any role in miRNAs lifecycle. However, according to GO predictions, *HESO1* is located both in the cytoplasm and the nucleus, *HI2* could interact with *HESO1* for its transfer between the two compartments, but again, interactions in yeast-two hybrids assays does not mean that the interactions are truly happening in *Arabidopsis* and are yet to be confirmed *in vivo*. *HI2*'s function made me choose to not continue working on it but, microscope experiments at the cellular level may show new results explaining the size increase of the rosette in the *hen1* background.

Northern blots, or at minima RT-qPCR, could also have been performed on the stem and reproductive tissues and not just on seedlings rosette. Looking at miRNAs involved in the reproduction in those tissues, like miR172, may show a rescue in those miRNAs in *hi3/hen1*, which could explain the small phenotypic rescue. However, working on the reproductive parts of Arabidopsis in a *hen1* background is very complicated for the reasons already mentioned above.

Our most interesting candidate *HI3*, namely *suppressor of ABI3-5* or *SUA,* is a splicing factor with many potential roles. It was first discovered as a splicing factor of *ABSCISIC ACID INSENSITIVE 3* (*ABI3-5*) (Sugliani et al., 2010). *ABI3* regulates seed maturation and exist in two isoform *ABI3-α* and *ABI3-β* and the proportion of each is regulated by *SUA*. It was also showed

to splice *SNC4* and *CERK1*, responsible of immune response in *Arabidopsis thaliana* (Zhang et al., 2014). *SUA* is at 45% homologous to the human splicing factor *RBM5* responsible of the splicing apoptosis genes *Fas* and *c-FLIP* and can interfere during the spliceosome assembly process (Bonnal et al., 2008). With such diverse roles and with maybe more to discover, we hypothesize that *SUA* may alternatively splice actors of miRNA biogenesis like *AAR2* (Fan et al., 2022) and will be discussed more in details in the next chapter.

HI5 is called *TARGET OF EARLY ACTIVATION TAGGED 1* (*TOE1*) is a conserved transcription factor involved in the phase transition between vegetative and reproductive stages (Wu et al., 2009) as well as in stress response (Licausi et al., 2013) and trichome formation (Liu et al., 2023). *TOE1* is a fast-growing mutant as shown by Zhang et al. (2015), who did the phenotypic assay on the mutant. The phase transition is also explained by the targeting of *FLOE1* by miR172 which act as an antagonist to miR156 (Wu et al., 2009). It was also shown in the *dwarf5* mutant, where a loss of function of *DWARF5* reduces the level of miR172, thus increasing the level of *TOE1*, showing a delayed phase transition in the mutant (Zhou et al., 2023). Unfortunately, the level of miR172 was not tested in northern blots but, as *hi5* did not rescue any other miRNAs in the *hen1* background and had no effect on *hen1*'s phenotype, it is safe to say that it is not involved in miRNA turnover.

Lastly, *HI6* showed neither interesting phenotypic rescue of *hen1* nor did it increase the level of miRNAs in *hen1*. However, the single mutant showed a high level of miRNAs making it interesting for this project. *HI6*, more commonly known as *ATKH1* is an RNA-binding protein part of the large KH family containing 30 members in *Arabidopsis* with unknown functions for most of them (Lorković & Barta, 2002; Zhang et al., 2022). The only known point about *ATKH1* is that it is downregulated in abscisic acid (ABA) and salicylic acid (SA) treatments, but not all the KH proteins are (Zhang et al., 2022). A lot needs to be discovered about that conserved family, but we could hypothesize that *HI6* may interact upstream of *HEN1* mediated methylation like *MOS2*, which is a similar RNA binding protein that binds to pri-miRNA to increase the processing efficiency of pri-miRNAs (Wu et al., 2013). However, the following experiments did not show any satisfactory results and the level of methylation, which was supposed to be measured by mass spectrometry, was not done due to technical and time constraints. Therefore, I decided not to include the few experiments that were done as they

do not bring any results and consider *HI6* as not a mutant to focus on for the aim of this project, but it might be interesting to further explore this gene in the context of miRNA biogenesis.

To conclude, the candidate approach was a little more successful than the screening approach with one mutant to work on: *SUA*. Despite not having a miRNA level rescue, the small reproductive rescue of *hen1* by *hi3* and its role of splicing factor may unveil new discoveries that cannot be caught by northern blots.

Chapter IV] The splicing factor *SUA*, the padlock to the miRNA turnover?

1) Introduction

Following the candidate approach interrogating the proteins interacting with HESO1, the last remaining candidate of this approach is the splicing factor *SUA*, which was *HI3* in the previous chapter. Firstly described by Sugliani et al. (2010), the *SUPPRESSOR OF ABI3-5* (*SUA*) was found to influence the splicing of the gene *ABI3* (*ABSCISIC ACID INSENSITIVE 3*) in two functional transcripts *ABI3-α* and *ABI3-β*. *ABI3* regulates the seed maturation in flowering plants (To et al., 2006), shown by the *abi3-5* mutant that displays green seeds with reduced longevity, among other disadvantageous aspects (Ooms et al., 1993). In WT plants, *SUA* represses the removal of a 77 nucleotides long intron, leading to the long *ABI3-α* transcript being the major transcript present. In *abi3-5*, which is not a complete loss of function mutant, *ABI3-α* is still the major transcript but *ABI3-β*, which has the intron removed has an increased level of a functional protein. In the double mutant *abi3-5/sua*, the *ABI3-β* transcript is the most abundant and rescue drastically the phenotype with brown seeds, increased longevity, and the return of sensitivity to ABA. Finally, by overexpressing *SUA* in the double mutant *abi3-5/sua*, they showed a decrease in *ABI3-β* transcript and an enhanced phenotype. *SUA* is thus in control of the splicing, with other splicing factors of *ABI3* and as stated by the authors and by my phenotypic experiments, *sua* does not show any strong phenotypes, suggesting that other splicing factors act redundantly to it or that *SUA* regulates only a specific set of genes. It could have many more roles, not yet identified, especially in stress conditions.

SUA was later found to be involved in plant immunity by alternatively splicing *SNC4* and *CERK1* (Zhang et al., 2014). *CERK1* is involved in the perception of fungal chitin (Miya et al., 2007; Wan et al., 2008) and bacterial peptidoglycan (Willmann et al., 2011). A loss-of-function mutant of *snc4* exhibit no phenotype difference to the WT (Hayashi et al., 2008) but a gain-of-function in *snc4-1D* exhibited a constitutive expression of defence markers and showed a greater pathogen resistance (Bi et al., 2010). Zhang et al. (2014) showed that the expression level of *snc4-1D* was greatly reduced in *sua/snc4* double mutant compared to the *snc4* single mutant as well as the expression of *scn4-1D* was lower in the single mutant *sua* compared to

the WT and was accompanied by a retention of an intron in *SNC4* in the *sua* mutant. They also looked at the proportion of *CERK1* transcripts in WT and in *sua* and found an increased number of a retained intron form in *sua*. Finally, they infected Col-0 and *sua* plants with the bacteria *Pseudomonas syringae* and observed a higher level of infection supported by the single mutant compared with the WT.

SUA is homologous to the human *RNA Binding Motif Protein 5* (*RBM5*), sharing 45% sequence similarity (Sugliani et al., 2010). *RBM5* regulates the splicing of an apoptosis gene (Bonnal et al., 2008) and disturbs the formation of the spliceosomal assembly after the formation of the prespliceosomal complex (Behzadnia et al., 2007). Starting from this observation, Sugliani et al. (2010) also showed, in yeast two-hybrid assay and *in vivo*, the interaction between *SUA* and the spliceosomal factor *U2AF65*, showing a similar role to the human protein.
Splicing is an important step in miRNA biogenesis. Indeed, emerging intron containing pri-miRNAs are spliced into mature pri-miRNAs (Yu et al., 2017) or into miPEP (Lauressergues et al., 2015, 2022). This occurs in the Dicing Complex, composed of many actors but the main ones are *DCL1*, *SERRATE* and *HYL1*. Studies found that *SERRATE* affects the correct splicing of pri-miRNAs with the *serrate* mutant having more pri-miRNAs with defective splicing and an overall reduced level of miRNA (Laubinger et al., 2008; Yang et al., 2006). *HYL1* was found to splice a subset of pri-miRNAs (Szarzynska et al., 2009) and was found recently to be regulated through phosphorylation by the splicing factor *AAR2* (Fan et al., 2022). *AAR2* is a conserved eukaryote protein which splices pre-mRNA and the *Arabidopsis aar2* mutant shows hundreds of retained intron events compared to the WT, in addition of an overall decrease of 21 and 24 nucleotides sRNA accumulation. However, as only roughly half of the *Arabidopsis* MIR genes contain introns (Stepien et al., 2017; Szweykowska-Kulinska et al., 2013), an overall decrease in all miRNA accumulation is indicative that this reduction is not from the splicing function of *AAR2* but rather from *HYL1* phosphorylation.

Taken together, these results shows that *SUA* plays a general role in splicing in *Arabidopsis* and more roles could be uncovered in the miRNA field.

2) Is SUA involved in miRNA biogenesis?

Notwithstanding of having the same overall level of tested miRNAs between Col-0 and *sua*, on the same northern blot membrane used in Chapter III]4), we can see extra signal higher up on the membrane that could be the pre-miR and the pri-miR (Figure 29).

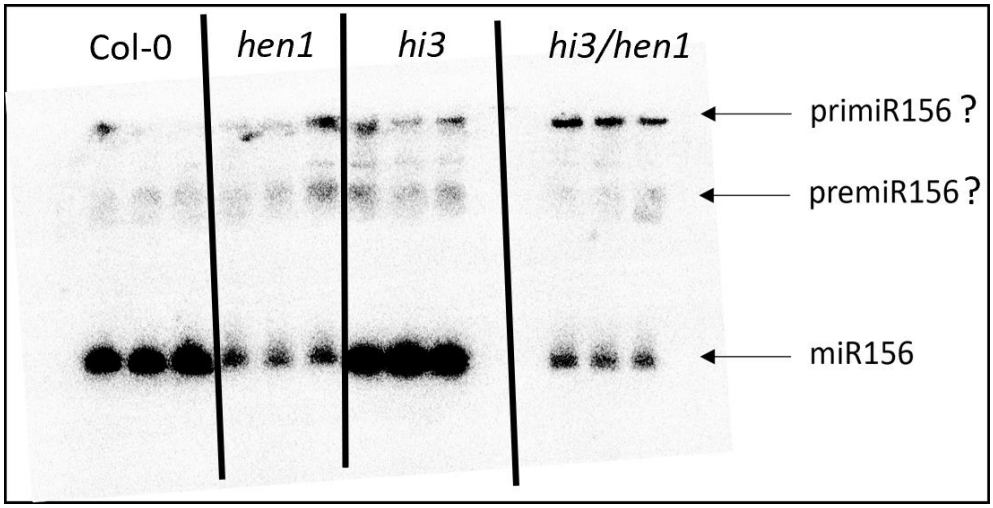

Figure 29: Picture of the complete membrane after incubating overnight a radio-labelled probe targeting miR156.

Indeed, the probe that targets the miRNA would automatically target the pre-miR and pri-miR as they contain the same sequence, but no ladder was used to confirm the size of the bands. Starting for the postulate that the bands are indeed the pre-miR and the pri-miR, the results showed that there is no difference in the level of the tested pre-miRs (Figure 30) but the level of pri-miRNAs was significantly higher in *hi3/hen1* compared to all the other samples tested (Figure 31), which is surprising as *HEN1* methylate only the miRNA duplex, so we would expect to see the same results, at minima, in *hi3* but that is not the case.

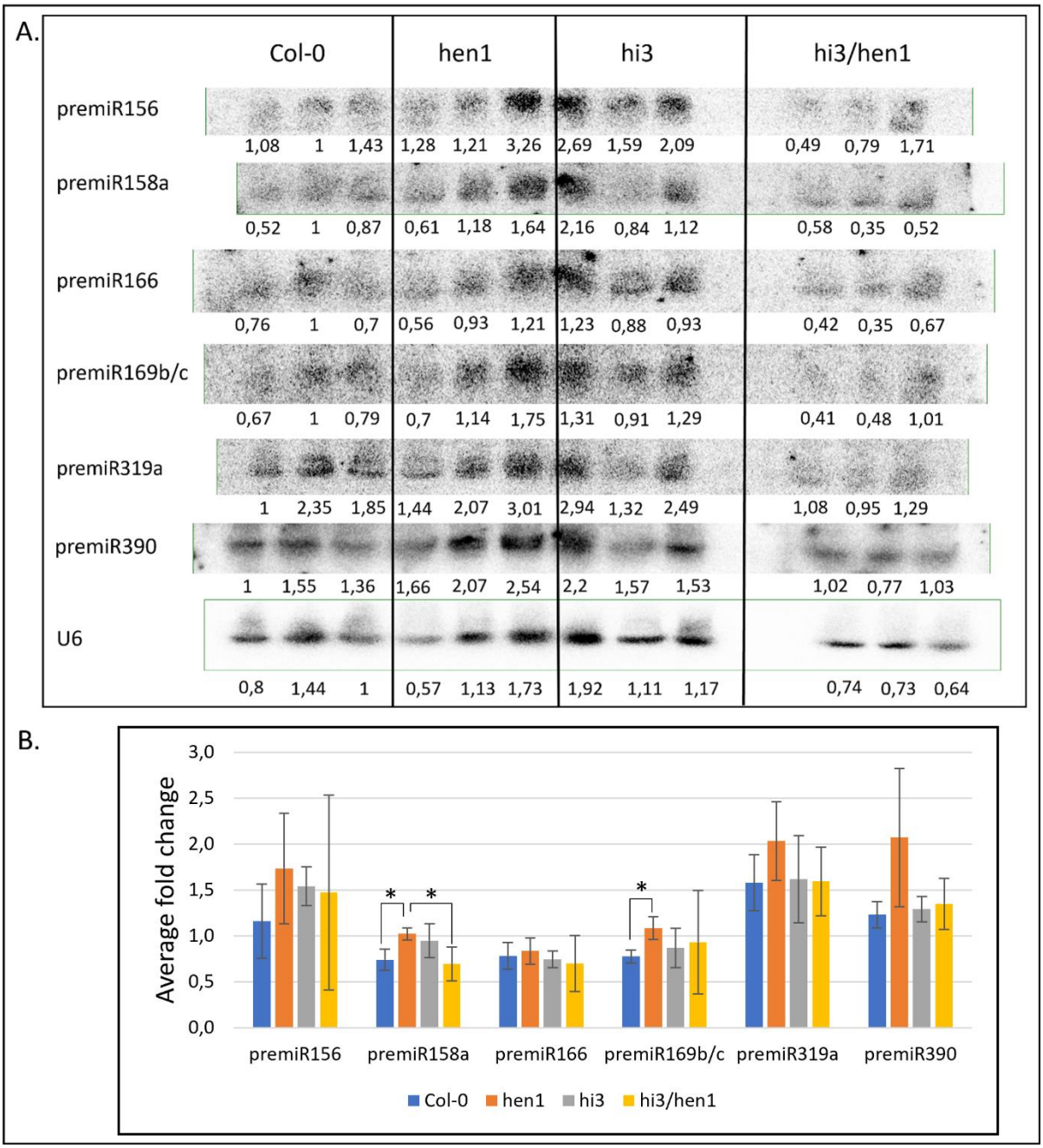

Figure 30: Analysis of potential pre-miRNA expression in different Arabidopsis backgrounds. A. Northern blots of premiR156, premiR158a, premiR166, premiR169b/c, premiR319a, premiR390 and U6 for loading control. 10 µg of RNA loaded. B. Average expression of the different tested pre-miRNAs in the different backgrounds, normalized by U6. Asterisks represent statistical comparison and significance (two-tailed t-test, p-value < 0.05). Other comparisons were not significative and not shown to keep the graph clear.

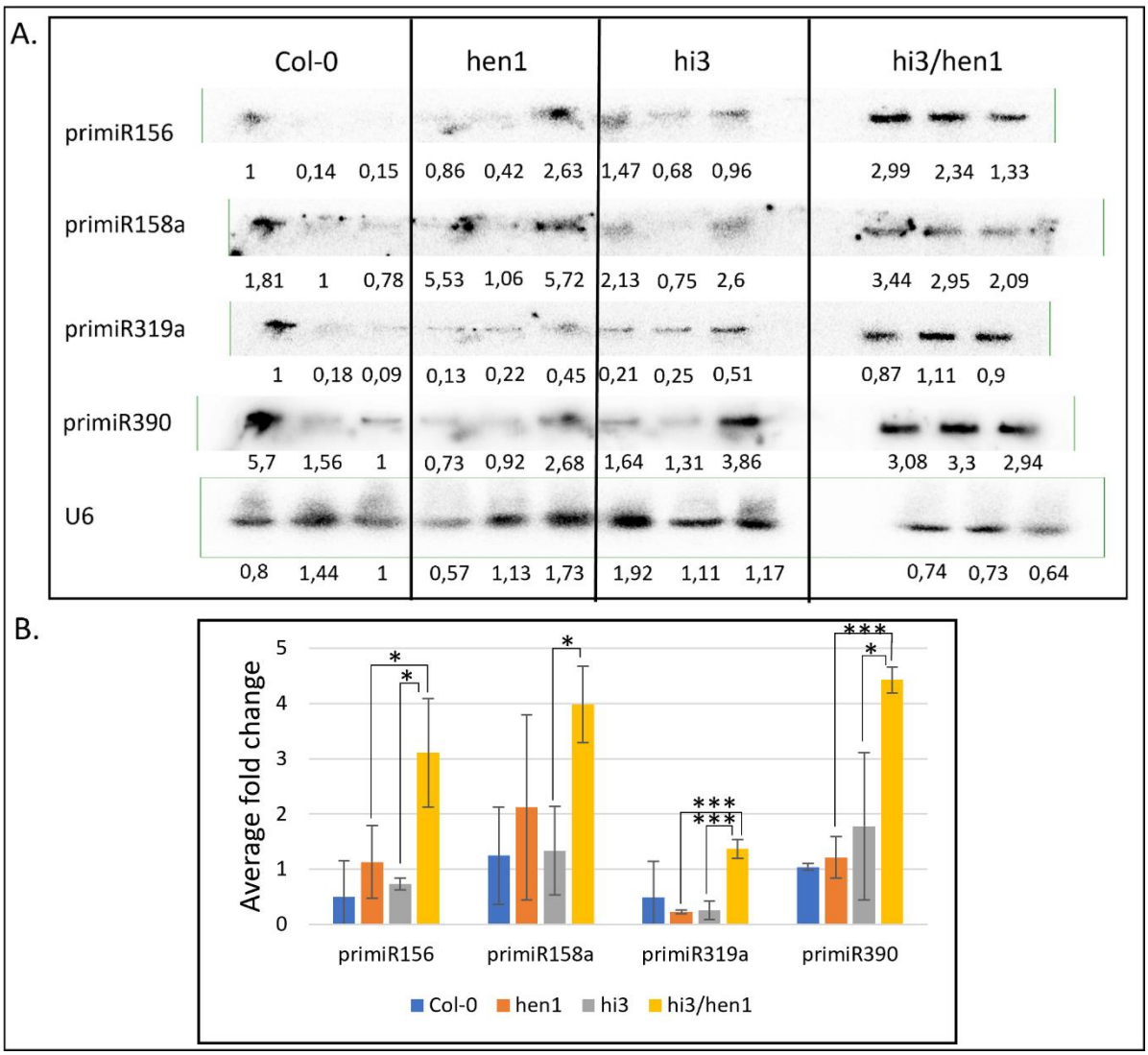

Figure 31: Analysis of potential pri-miRNA expression in different Arabidopsis backgrounds. A. Northern blots of primiR156, primiR158a, primiR319a, primiR390 and U6 for loading control. 10 µg of RNA loaded. B. Average expression of the different tested pri-miRNAs in the different backgrounds, normalized by U6. Asterisks represent statistical comparison and significance (two-tailed t-test, p-value < 0.05). Other comparisons were not significative and not shown to keep the graph clear.

As there is no ladder to confirm the size of the bands, which also appears to be the wells containing all the remaining total RNA that did not go inside the gel, I did RT-qPCR on primiR156 and primiR390 to challenge those results (Figure 32).

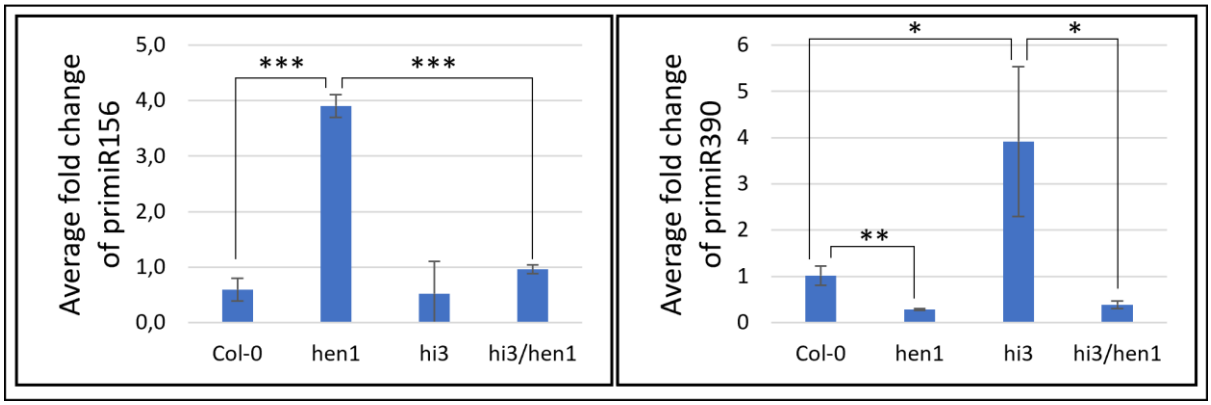

Figure 32: RT-qPCR results of the level of primiR156 and primiR390. 3 biological replicates were used, and Actin was the housekeeping gene used for normalization. Asterisks represent statistical comparison and significance (two-tailed t-test, p-value < 0.05). Other comparisons were not significative and not shown to keep the graph clear.

The RT-qPCR results showed that there is not a higher level of primiR156 and primiR390 in *hi3/hen1* compared to the other backgrounds (Figure 32). This means that the visible bands on the membrane contained RNA, which is targeted by the different northern blot probes, and not only targeting the pri-miRNAs. As the two techniques gave opposite results, we cannot validate if the higher level of pri-miRNAs in *hi3/hen1* is true, and we will simply reject the hypothesis of *sua* being involved in the pre-miRNA and the pri-miRNA processing.

3) Analysis of *sua* transcriptome

As our first hypothesis was rejected, I investigated the second, which stated that *SUA* is responsible for the correct splicing of mRNA(s) that translate to protein(s) involved in the processing or the degradation of miRNAs. To verify that, Illumina mRNA sequencing was done on three biological replicates of Col-0 and *sua* to quantify the transcriptome and qualify the difference in alternative splicing between the two backgrounds. We received the cleaned data from Novogene, composed of paired reads of 150bp with, on average, 66 million reads per sample, and started to align them to the genome (TAIR10) using STAR (Dobin et al., 2013, version 2.7.9a), which also indexed the genome one step sooner. The resulting files were used with SALMON (Patro et al., 2017, Version 1.9) to quantify the level of mRNA and those were normalized using DESeq2 (Love et al., 2014, version 1.41.12). The count matrix data generated

by SALMON was also used on iDEP (Ge et al., 2018, version 1.1) to generate the figures and gather information that were not given by the other tools.

The samples distributed equally (Figure 33.A) but the PCA showed that the third replicate of Col-0 was clustering more with sua than the other two replicates (Figure 33.B), which may have altered the analysis and can be seen on the heatmap (Figure 33.C). I decided to keep it in the analysis, while staying aware of it in the differential expression analysis.

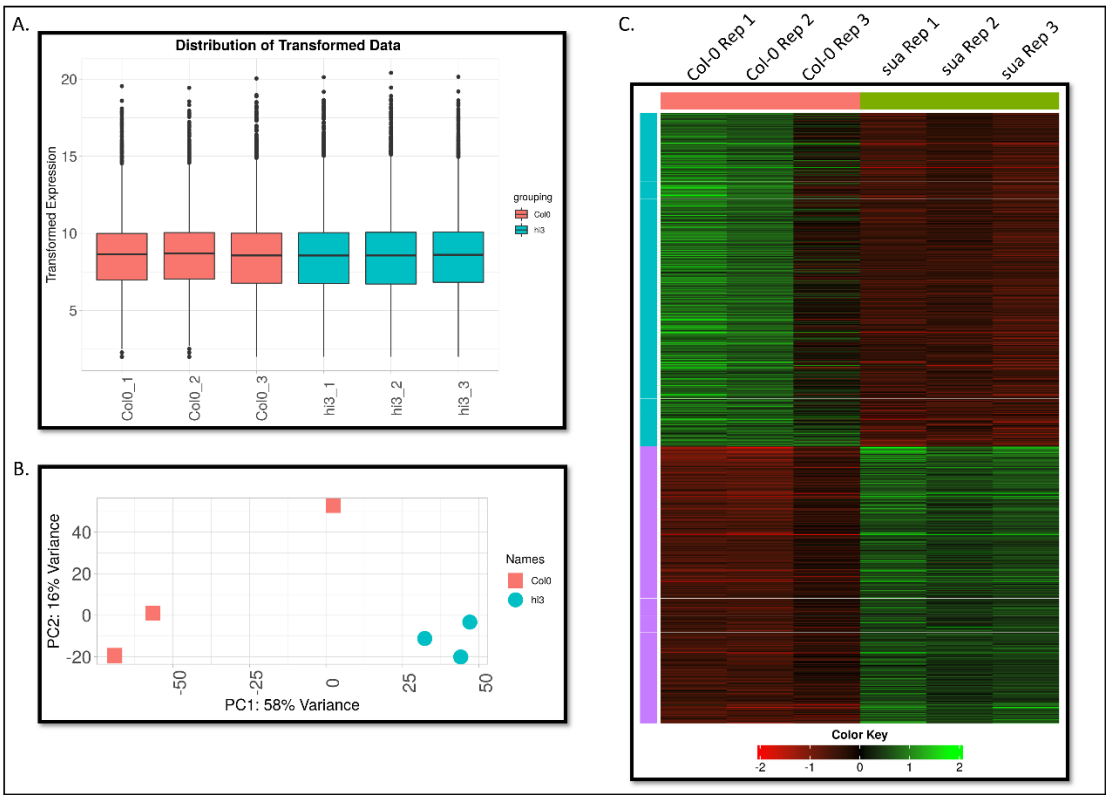

Figure 33: Analysis of the Illumina sequencing. A. Distribution of the transformed data. B. PCA of the sequenced samples. C. Heatmap of the differentially expressed genes in the sequenced samples.

Nevertheless, DESeq2 differential analysis showed that 2015 genes were downregulated in *sua* and 1671 upregulated compared to Col-0 when looking at genes with a 0.05 FDR cutoff and a minimal of 1.5-fold change difference between the two backgrounds (Figures 34.A, 34.B.). Enrichment analysis showed that over the 1671 upregulated genes in *sua*, the most occurring KEGG pathways were related to plant hormone signalling, zeatin production, autophagy, and plant-pathogen interactions while in terms of GO Biological Process, it is

related to different stress responses (abiotic, oxygen level and hormones) (Figures 34.C, 34.D). Those terms are abnormal, because the plants did not grow in any stressful conditions and thus should not be the main term resulting from the analysis. In terms of the downregulated KEGG pathways in *sua* compared to Col-0, there are pathways involved in the central dogma of biology with DNA replication, RNA degradation, ribosome biogenesis and nucleotide excision repair (Figure 34.C). The same can be seen with the GO Biological Process with nucleic acid metabolic process, RNA processing and ribosome biogenesis, as well as different cell organization involved (organelles, microtubules, chromosomes, etc) (Figure 34.D). Those being downregulated in *sua* compared to Col-0 showing its importance as a splicing factor.

A.

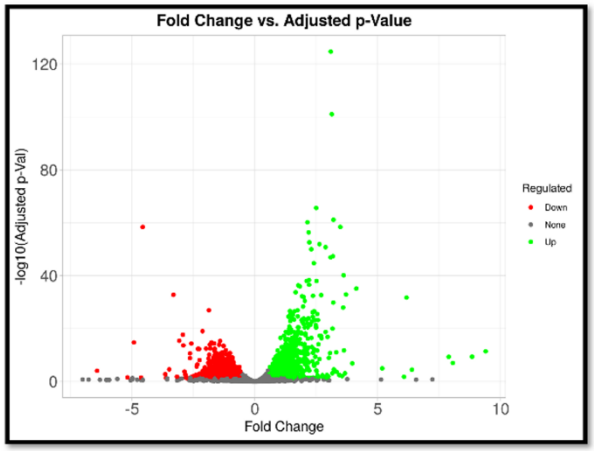

B.

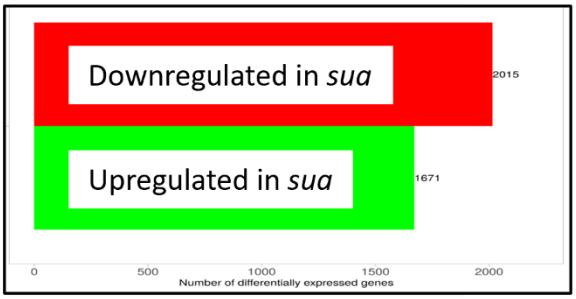

C.

Grp.	Adj.Pval	Fold	Pathway (Click for more info)
Upregulated	8.59E-6	2.5	Plant hormone signal transduction
	2.31E-3	2.6	MAPK signaling pathway-plant
	6.52E-3	4.6	Zeatin biosynthesis
	1.70E-2	3.6	Autophagy-other
	2.58E-2	2	Plant-pathogen interaction
Downregulated	3.31E-5	4.1	DNA replication
	1.01E-4	2.9	Ribosome biogenesis in eukaryotes
	1.75E-4	3.3	Homologous recombination
	2.75E-3	2.3	RNA degradation
	3.85E-3	2.9	ABC transporters
	7.73E-3	2.7	Nucleotide excision repair

D.

Grp.	Adj.Pval	Fold	Pathway (Click for more info)
Upregulated	1.86E-21	1.6	Response to chemical
	1.28E-14	1.8	Response to hormone
	1.86E-14	1.7	Response to organic substance
	5.21E-14	1.8	Response to endogenous stimulus
	2.10E-12	1.7	Cellular response to chemical stimulus
	2.76E-11	3	Cellular response to decreased oxygen levels
	2.76E-11	3	Cellular response to oxygen levels
	6.24E-11	3	Cellular response to hypoxia
	6.70E-11	1.5	Response to abiotic stimulus
	6.70E-11	2.8	Response to decreased oxygen levels
Downregulated	5.79E-19	5.1	Movement of cell or subcellular component
	5.79E-19	1.5	Cellular component organization or biogenesis
	1.62E-17	1.7	Organelle organization
	3.94E-14	5.1	Microtubule-based movement
	1.68E-13	1.3	Nucleic acid metabolic process
	1.20E-12	2.1	Chromosome organization
	4.34E-12	2.1	Ribonucleoprotein complex biogenesis
	4.42E-12	1.8	RNA processing
	4.42E-12	2.3	Ribosome biogenesis
	4.99E-12	1.4	Cellular component organization

Figure 34: Differential expression analysis of Col-0 and sua. A. Volcano plot showing the downregulated and upregulated genes in sua compared to Col-0. B. Different number of genes differentially expressed in sua compared to Col-0 C. KEGG pathways in sua compared to Col-0. D. GO Biological Process term in sua compared to Col-0.

The results of SALMON and DESeq2 also gave us the list of differentially expressed genes between the two backgrounds. However, we need to cross-check those results with a splicing analysis of *sua* to determine potential genes of interest to work on.

The splicing analysis was done using rmats (Park et al., 2013; Shen et al., 2012, 2014, version 4.1.2), which compared all replicates of Col-0 to all replicates of *sua* on the same run, giving a stronger analysis than individually pairing them and then average the results. The visualization of those data was performed by rmats2sashimiplot (https://github.com/Xinglab/rmats2sashimiplot, version 2.0.4) and InteractiVenn for the Venn diagram (Heberle et al., 2015). In total, 12785 events, described in Chapter I, were spotted by rmats but only 833 of them had an FDR value and a pvalue below 0.05, which 691 were unique events (Figure 35.A). The Intron Retention were the most prevalent events with 545 event which were statistically significant, which is commonly found in *Arabidopsis* (Filichkin et al., 2010). The Venn diagram shows that some genes present several alternative splicing events, with the gene RS41 that contains all 4 events (Figure 35.B).

A.

Type of alternative splicing	Number of events	Events with pvalue<0.05 and FDR value<0.05	Unique ASE
A3SS	2232	122	85
A5SS	1536	101	69
MXE	135	0	0
IR	4854	545	489
SE	4028	65	45
Total	12785	833	691

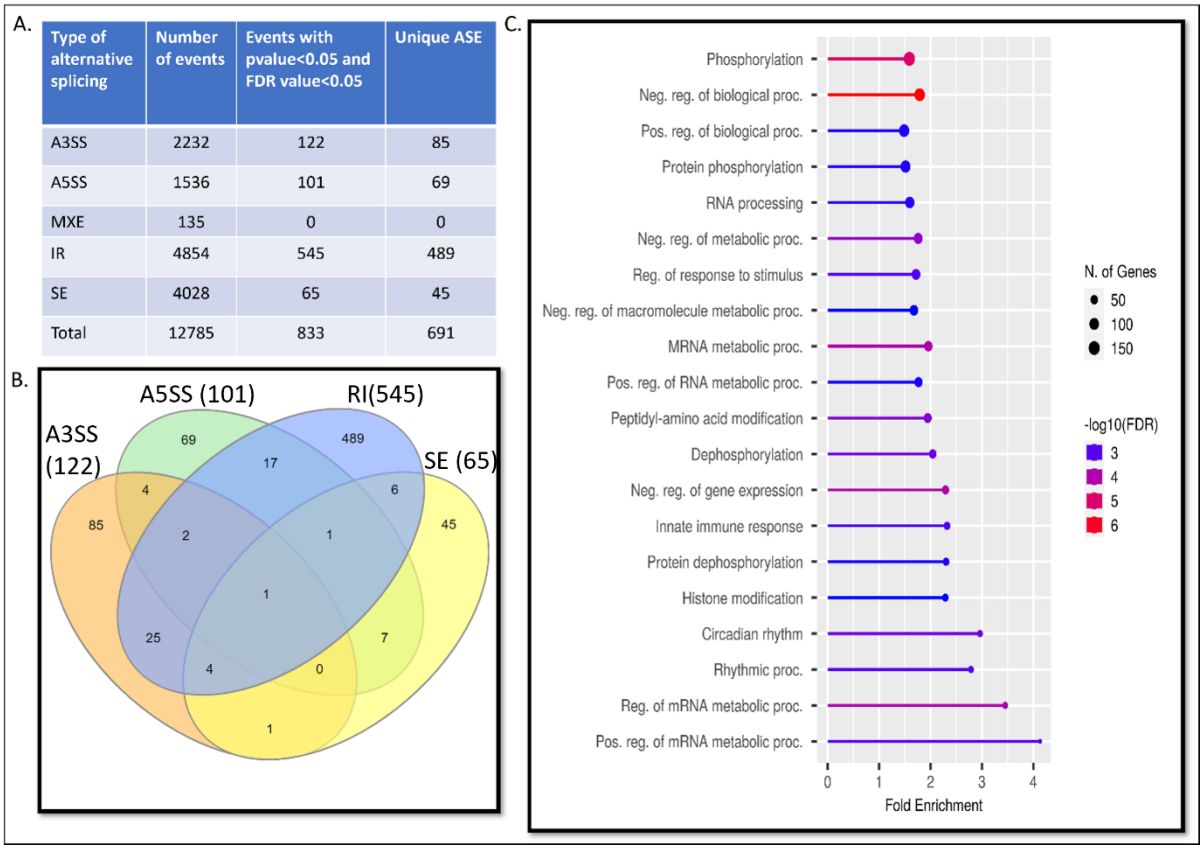

Figure 35: Summary of the alternative splicing analysis between Col-0 and sua. A. Table with the number of different events happening between the Col-0 and sua. A3SS: Alternative 3' Splice Site, A5SS: Alternative 5' Splice Site, MXE: Mutually Exclusive Exons, IR: Intron Retention, SE: Skipped Exon B. Venn diagram of the events with a p-value < 0.05. C. GO Biological Process of the genes presenting an alternative splicing between Col-0 and sua.

The GO Biological Process analysis of the genes that are alternatively spliced, with an FDR value and pvalue below 0.05, showed a completely different range of processes than the differential expression analysis (Figure 35.C). The alternatively spliced genes are mostly involved in phosphorylation, the regulation of biological processes positively or negatively, several mRNA processing steps and the circadian rhythm. Those terms are already more interesting than the previous ones, especially if those events really happen in *sua*.

Finally, the combination of the alternative splicing analysis and the differential expression analysis was done to produce a table with a list of potential candidates that are both spliced and downregulated in *sua* compared to Col-0. I first proceeded to a control by looking at the level of a gene already proven to be spliced by *SUA*: *SNC4* and *CERK1* (Zhang et al., 2014). Indeed, *ABI3* is only expressed in the siliques and the seeds (Sugliani et al., 2010), which are

not covered by the sequencing. While CERK1 could not be found, *SNC4* is indeed alternatively spliced in our results with a A3SS event and is also lowly expressed in *sua* (Figure 36), proving that the methods of analysing those data are good but still perfectible.

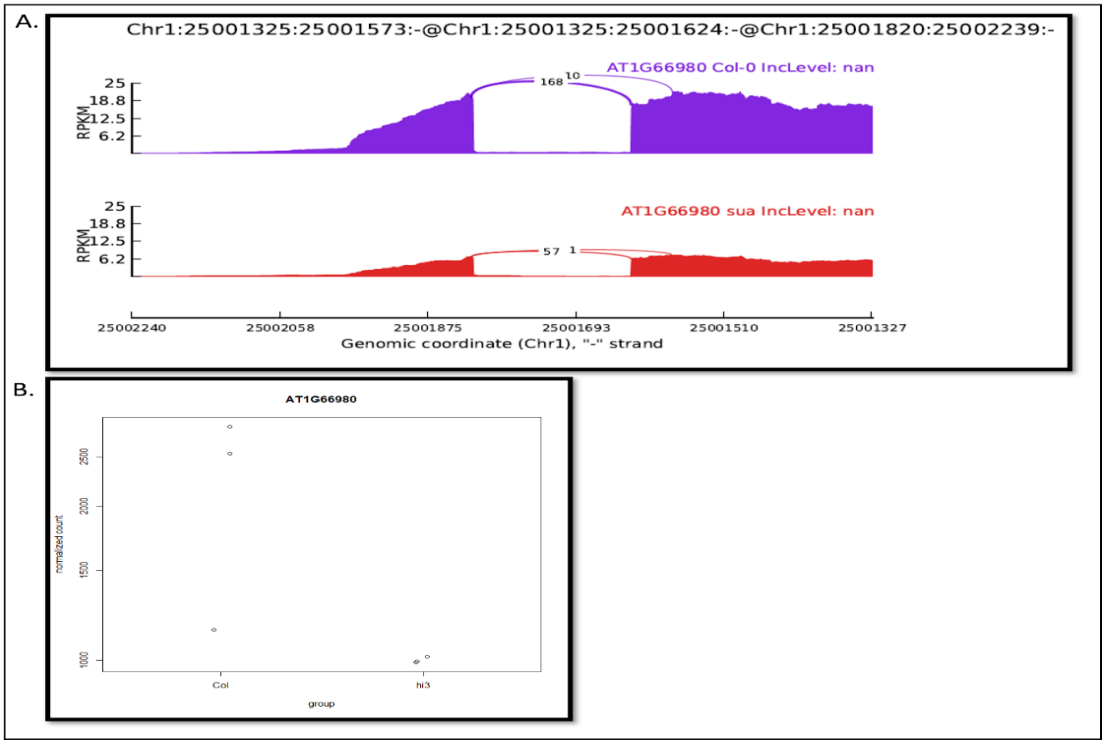

Figure 36: Analysis of SNC4. A. Sashimi plot of the A3SS event in SNC4. On top, the expression profile in Col-0 and at the bottom, in sua. B. Normalized count of SNC4 in Col-0 and sua.

I then looked at the top hits which shared the two conditions which were *AT2G46790*, a clock regulator, *AT4G35270*, a nitrate responsive transcription factor and *AT4G10120*, a sucrose phosphate synthase. Clearly, none of those could be involved with miRNAs, so I decided to look at genes either involved in the miRNA biogenesis and degradation pathways following the genes evoked in Yu et al. (2017), or nucleases, especially 3'-5' exonucleases as I hypothesized that only an 3'-5' exonuclease could degrade the poly-U tail left by *HESO1* and/or *URT1* at the 3' end of miRNAs. Among the selection, a few candidates appeared to be of interest like *HESO1* (*AT2G39740*) itself, *SGS3* (*AT5G23570*) responsible of the production of phasiRNAs, *DCL1* (*AT1G01040*) involved in the processing of the pri-miR and pre-miR and *AT5G53020*, an unknown 3'-5' exonuclease, later called *RNase X* in this thesis. Because they

are closer to the degradation step, I chose to focus on only *HESO1* and the *RNase X*, but proving the alternative splicing of the other genes could also be interesting.

HESO1 presented an A5SS event in the 5'-UTR that discriminated *HESO1.3* from its two other isoforms (Figure 37). However, in both backgrounds, the IncLevel calculated by rmats, which indicates the percentage of time the exon is kept in all the transcripts present in the sequencing data, is low with 12.2% of time the exon is kept in Col-0 and 1.4% in *sua*. That means that *HESO1.3* is the dominant isoform and apart from the downregulation of this gene in the single mutant (Figure 37.C.), *SUA* only changes the splicing from *HESO1.1* (second most abundant isoform) and *HESO1.2* (least abundant isoform) to *HESO1.3* by 10% in the WT. Overall, *HESO1* is only more expressed 1.6 times in Col-0 compared to *sua*.

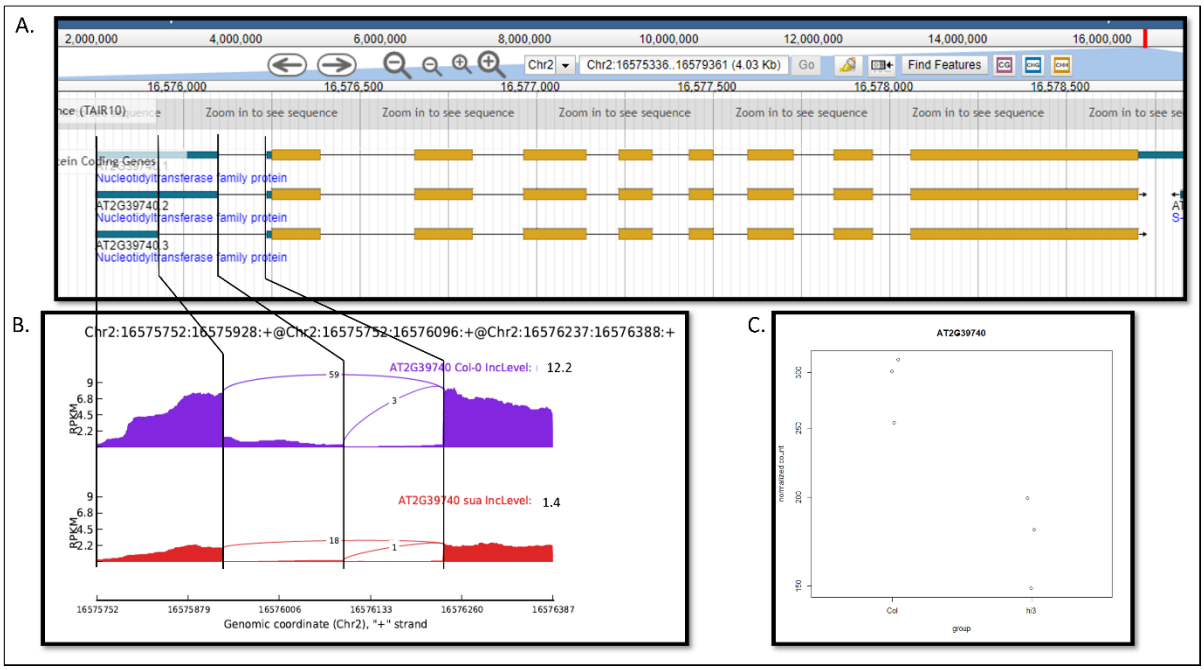

Figure 37: Analysis of HESO1. A. Map detail of HESO1 showing the 3 isoforms. B. Sashimi plot of the A5SS event. On top, the expression profile in Col-0 and at the bottom, in sua. The IncLevel value was multiplied by 100 to give a percentage and added to the plot. C. Normalized count number of HESO1 in Col-0 and sua.

The other gene of interest that I selected is *AT5G53020* (latter named *RNase X*) that is produced in 10 isoforms, making the isolation of an isoform by PCR or RT-qPCR impossible (Figure 38.B). This gene is 3.4 times more expressed in Col-0 than in *sua* (Figure 38.D) but the difference could be even higher because its level in the third replicate of Col-0 is lower than

in the other two. Three events were detected by rmats: a Skipped Exon event (Figure 38.A.), an Intron Retention event (Figure 38.C) and an Alternative 3' Splice Site event (not shown as it is only 3 nucleotides difference, and it is too small to be shown on the same figure). The first event is the skip of an exon of 150 nucleotides, which is kept only 54% of the time in Col-0 but 96% in *sua* (Figures 38.A, 38.B). On top of that, *AT5G53020.1* and mainly *AT5G53020.9*, containing this exon, are the only upregulated isoforms in *sua* compared to Col-0 (Figure 38.D), suggesting that *SUA* is crucial for the effective splicing of this exon. The second event is the retention of an 868 nucleotides long intron, which happens 45% of the time in the WT but only 1.4% in *sua* (Figures 38.B., 38.C) and the isoforms containing this intron (*AT5G53020.4*, *AT5G53020.5*, *AT5G53020.7* and *AT5G53020.6*) are less expressed in the mutant compared to the WT (Figure 38.D), suggesting again the importance of *SUA* in the correct splicing of this gene. The last event, not shown, is a A3SS of a 3-nucleotide deletion in the last coding sequence (CDS) exon in the *AT5G53020.6* and *AT5G53020.7* isoforms. This codon is CAG, coding for a Glutamine does not seem to have an impact on *AT5G53020.7*'s expression and I tend to think the IR event is more responsible to the downregulation of *AT5G53020.6* as it occurs more often than the A3SS.

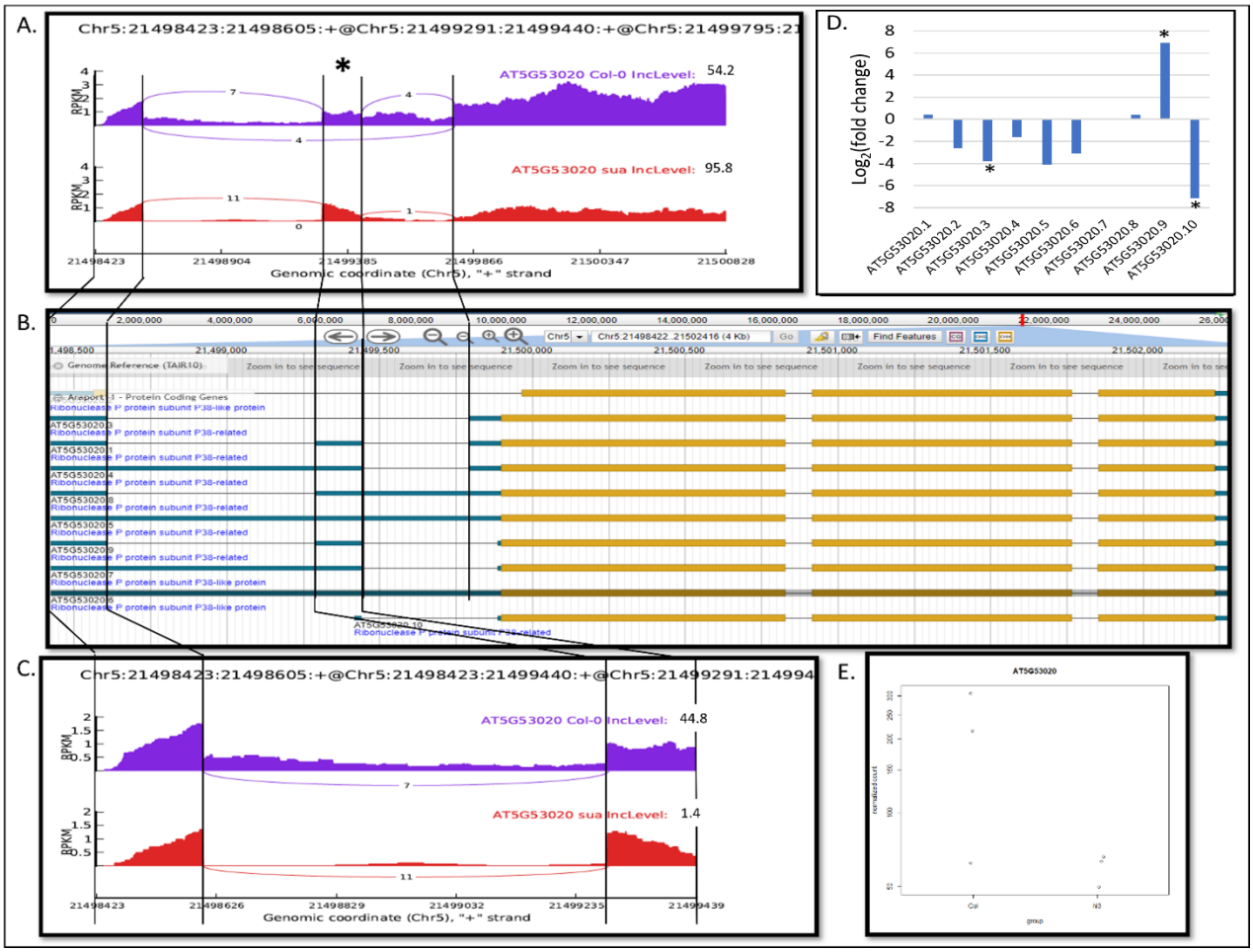

Figure 38: Analysis of AT5G53020. A. Sashimi plot of the SE event. On top, the expression profile in Col-0 and at the bottom, in sua. The IncLevel value was multiplied by 100 to give a percentage and added to the plot. The "" represent the event. B. Map detail of AT5G53020. C. Sashimi plot of the IR event. On top, the expression profile in Col-0 and at the bottom, in sua. The IncLevel value was multiplied by 100 to give a percentage and added to the plot. D. Log2(fold change) of the different AT5G53020 isoforms in sua compared to Col-0. The "*" represents a pvalue < 0.05. E. Normalized count number of AT5G53020 in Col-0 and sua.*

PCRs were done to show the difference in splicing between Col-0 and *sua* but was not successful. For *HESO1*, it is explained by the fact that the event was not unidirectional, so after 35-40 cycles of PCR, all isoforms were detected in both backgrounds. Meanwhile, it was impossible to design primers to isolate independently the many isoforms of *RNase X* (Figure 39). Taken together, those results suggest that *SUA* is responsible for the alternative splicing of an unknown 3'-5' exonuclease, *RNase X*, and may be involved in the splicing of *HESO1*. Whether this is enough to explain the small phenotype rescue of *hen1* by *hi3* is not yet clear and quantification of this change is the next step of the analysis.

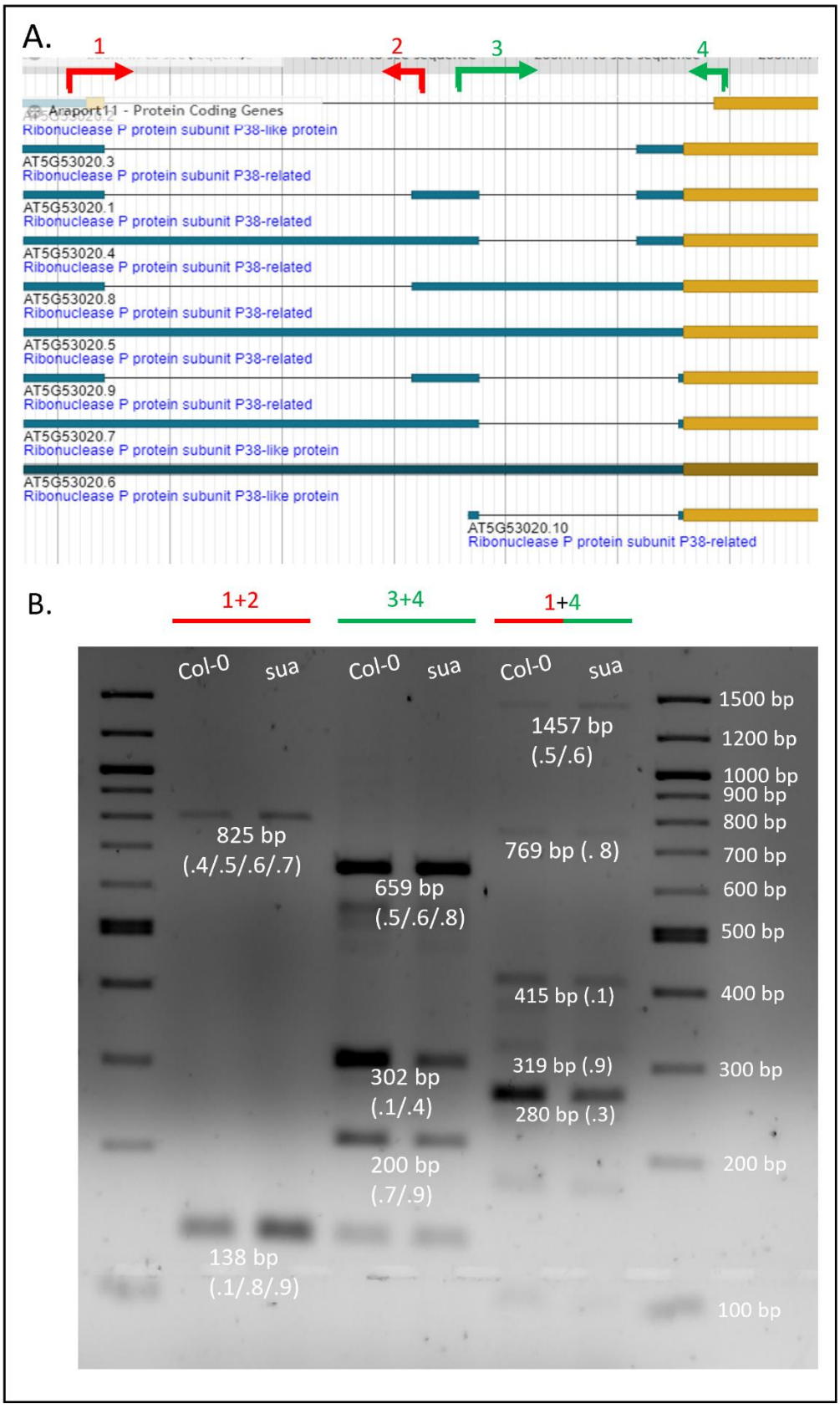

Figure 39: Isolation of the RNase X isoforms by PCR. A. Map detail of RNase X with the designed primers. B. Gel showing the results of three PCRs using different primer pairs. Product size is below the band with the expected number of the isoform amplified in brackets.

4) Verification of the downregulation of *HESO1* and *RNase X* in *sua*

Despite I was unable to prove the alternative splicing of *HESO1* and *RNase X*, I wanted to verify if, at least, those two genes are downregulated in *sua* compared to the WT. I first started with RT-qPCR to verify the level of the mRNA. Primers were designed to the CDS region to capture all possible transcripts, and I looked for the best housekeeping gene to use for normalization as different expression patterns could occur in *sua*. For that, I ordered primers for 8 housekeeping genes (HKG) used in Kudo et al. (2016) and Wang et al. (2014), performed three independent RT-qPCRs with Col-0, *sua* and *heso1* on the same plate, testing the 8 housekeeping genes and uploaded the Ct values on RefFinder (Xie et al., 2023). RefFinder combines the results of multiple tools to give the most stable housekeeping gene, in this case *EF1-α* was the best choice as it was ranked as the most stable gene by three tools (Delta CT, Normfinder and Genorm) (Figure 40).

	Ranking Order (Better--Good--Average)							
Method	1	2	3	4	5	6	7	8
Delta CT	EF1-alpha	AP2M	RBP45B	RHIP-1	Actin	VHA-H	PEX5	PP2AA3
BestKeeper	RBP45B	VHA-H	Actin	EF1-alpha	RHIP-1	AP2M	PEX5	PP2AA3
Normfinder	EF1-alpha	AP2M	RHIP-1	RBP45B	Actin	VHA-H	PEX5	PP2AA3
Genorm	AP2M | EF1-alpha		Actin	RBP45B	RHIP-1	VHA-H	PEX5	PP2AA3
Recommended comprehensive ranking	**EF1-alpha**	**AP2M**	**RBP45B**	**Actin**	**RHIP-1**	**VHA-H**	**PEX5**	**PP2AA3**

Figure 40: Identification of the best reference gene by RefFinder. RefFinder combines the results of multiple tools to give the most stable housekeeping gene.

After determining the correct HKG to use, RT-qPCRs were done to test the level of *HESO1, RNase X* and *SNC4* mRNAs in Col-0, *sua* and *heso1* (for the level of *HESO1* mRNA only). As *SNC4* is one of the validated gene to be spliced by *sua* and downregulated in *sua*, the RT-qPCR testing its level should show a lower level of mRNA in *sua* which was not significant (Figure 41.C). The same results were obtained for the mRNA level of *HESO1* and *RNase X*, which were lower in *sua* than Col-0 but the differences were not significant to validate this downregulation (Figures 41.A, 41.B). The level of *HESO1* mRNA in the *heso1* mutant was significantly lower than the WT and hi3, respectively, showing that the RT-qPCR and the primers used worked to determine the level of this mRNA (Figure 41.A).

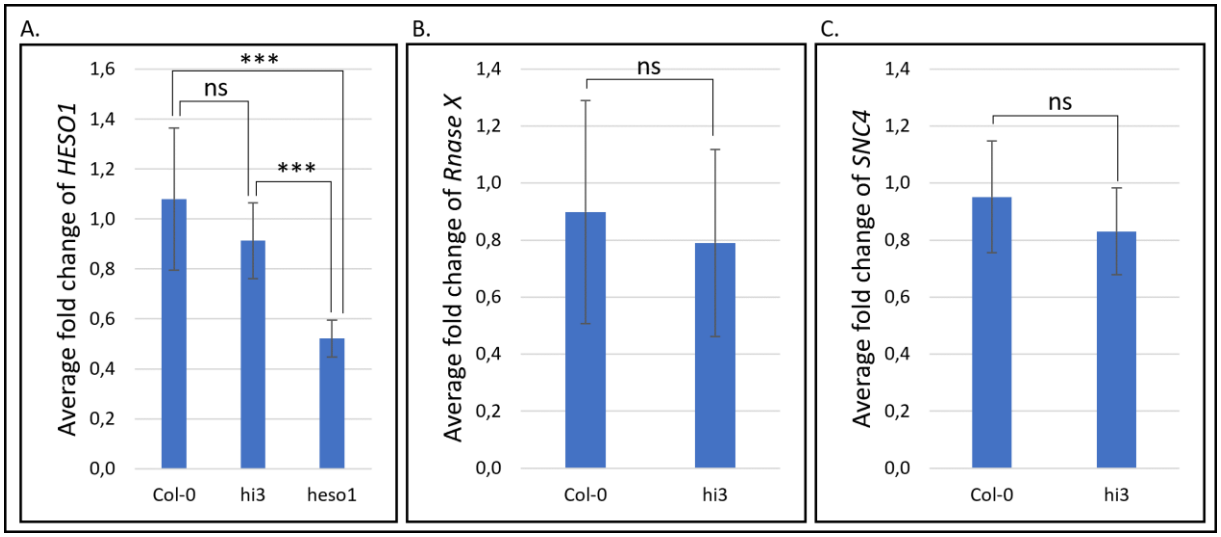

Figure 41: Graphs of the RT-qPCR. The RT-qPCRs were performed using a set of primers targeting the mRNA of interest and a set of primers targeting EF1-α for normalisation. A. RT-qPCR result of HESO1. B. RT-qPCR result of RNAse X. C. RT-qPCR result for SNC4. Asterisks represent statistical comparison and significance (two-tailed t-test, p-value < 0.05).

As previous RT-qPCR experiments, the results were not conclusive, so we decided to test the level of *in vivo* proteins with western blot. 7 µg of proteins was used and the mouse primary antibodies against *HESO1* and *RNase X* were ordered from Abmart as they already had the antibody against *RNase X* and were the fastest company to deliver. Their antibodies consist of a combination of monoclonal antibodies targeting multiple peptides antigens from the corresponding region of the target protein (Ab-mart.com). Despite receiving two pairs of primary antibodies, targeting the N-terminal and the C-terminal of the proteins of interest, I latter found that those antibodies were not specific enough and did not have time to order new ones from another company. The secondary antibody was an HRP-rabbit antibody against mouse to target the primaries. The detection of the secondary was done with the "SuperSignal" West Pico kit (Thermo Fisher Scientific) containing a mix of biotin and of peroxidase that produce rapidly a signal detectable on a scanner. As the first results using this secondary antibody were not quantifiable, I decided to use a fluorescent secondary antibody using Alexa Fluor 680 (Abcam, ab175775) and I scanned the membrane using the Odyssey scanner at 680 nm to have clearer bands than the HRP.

On both western blots, the primary antibody could not detect neither of the proteins of interest at the expected size (Figure 42) putting another end point to quantification assays.

On top of that, the primary antibodies seemed to be very unspecific, which was more visible on the images coming from the biotin/peroxidase kit (not shown).

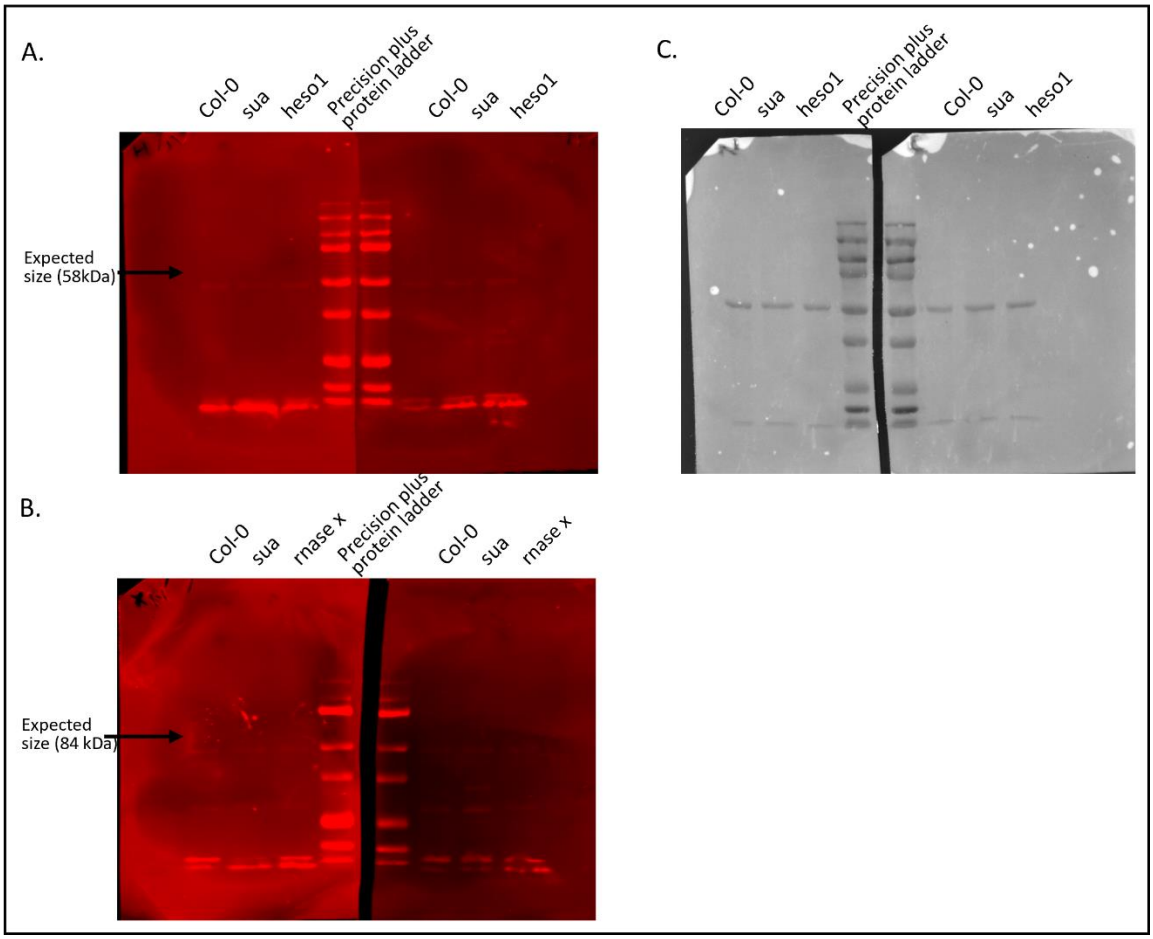

Figure 42: Western blot pictures using a fluorescent secondary antibody (Alexa Fluor 680). On all pictures, the left part to the ladder is using a primary antibody targeting the N-terminal of the protein of interest and the right part is using a primary antibody against the C-terminal of the protein of interest. The ladder is the Precision Plus Protein Dual Color and ranges at 10, 15, 20, 25, 37, 50, 75, 100, 150, 250 kDa. A. Western blot of the detection of HESO1. B. Western blot of the detection of RNase X. C. Ponceau scan for the membranes shown in A.

5) Discussion

Taken together, *SUA* seems unlikely to be involved in any miRNA pathways. Firstly, there is no changes in the level of miRNAs, pre-miRNAs or pri-miRNAs in the mutant compared to the WT, which was a prerequisite described in all the papers that showed proteins involved in the miRNA biogenesis (Fan et al., 2022; Laubinger et al., 2008; Szarzynska et al., 2009; Yang et al., 2006). However, the small reproductive phenotype rescue of *hen1* by *hi3* shall not be ignored

and experiments could be done on the reproductive part of *sua*. This was not done, as explained in the previous chapter, because working with the reproductive part of *hen1* is complicated and it was needed to compare the level of miRNAs and its precursors with the double mutant.

The sequencing of mRNAs of *sua* was not done previously and revealed partially the depth of the splicing function of *SUA* as we did not sequenced *sua* siliques and seeds to detect the splicing change in *ABI3* (Sugliani et al., 2010) or under biotic stress to detect *CERK1*'s splicing (Zhang et al., 2014) for example. However, for the last described gene spliced by *SUA*, *SNC4*, the event detected by the tool rmats is defined as an A3SS on the region neighbouring the eighth intron while the authors defined it as an intron retention. In both case, part of the intron is kept, the two transcripts exist in the WT with the intron-retaining transcript is more abundant in the *sua* mutant and an overall decrease in the level of *SNC4* transcript in *sua*. Overall, our alternative splicing analysis revealed 833 significant events with 545 IR events which are the most prevalent events in *Arabidopsis* (Filichkin et al., 2010), showcasing the importance of *SUA* in broader areas than previously described. Because of time limitations, I decided to focus on *HESO1* because of the initial yeast two-hybrid assay that led us to the study of *SUA* and an unknown 3'-5' exonuclease, named *RNase X*, that would degrade the miRNAs U-tail. Many other genes could have been selected, like *DCL1*, responsible of pri-miRNA and pre-miRNA processing, *SGS3* involved in phasiRNA production, and several endonucleases have been found to be alternatively spliced and have a reduced level of their transcripts in sua. As shown by the *ABI3* and *SNC4-CERK1* studies and its interaction with the prespliceosomal complex, *SUA* have broad roles and those sequencing data could help unveil more role of this splicing factor.

Validation of the level of *HESO1* and *RNase X* in the mutant was not yet achieved with the used methods. As the RT-qPCR results were inconclusive, as shown by *SNC4* level in *sua* compared to the WT, I decided to go for western blot. Unfortunately, Abmart's antibodies were not specific enough and did not even catch the proteins at their expected size. The splicing could have had an impact on the size in *sua*, but I should have been able to see the unaffected protein at the right size in Col-0, which was not the case. In addition, the closest bands to the expected size had the same intensity in all samples, even in the negative control.

The Ponceau staining showed an equal transfer of proteins (Figure 42.B) but whether this transfer was complete is unknown, as the activated PVDF membrane can let proteins go through it. Rather than using Ponceau or Coomassie staining, another way to normalize the band intensity is to incubate the membrane with a combination of two primary antibodies simultaneously, one targeting the protein of interest and the other targeting a housekeeping protein, which needs to be determined. The advantage of this technique is that the antibodies are produced in two different species to allow to use two different secondary antibodies with two different fluorochrome and scanned both at the same time on the Odyssey scanner (Li-cor), the software provided allowing to calculate the intensity of both fluorochromes and normalize the data with more accuracy than a Ponceau or a Coomassie staining. This was not done because I did not have time to order the antibodies but remains a valid option to test. The initial secondary antibody was received in 2008 and may have shown signs of fatigue, thus the use of another secondary antibody with a fluorochrome, which showed roughly the same results. Finally, the quantity of loaded proteins and the antibodies dilution factor may also had a huge impact on the success of this experiments, but it would not affect the accuracy of the primary antibodies whether they were at a 1:1000 or 1:10000 diluted and incubated with or without milk in the incubation buffer. I would assume that the experiment failed because of the primary antibodies and new ones should be tested. Our last possible quantification method would be northern blots but having several transcripts may affect the quantification.

I would put aside the hypothesis of *SUA* splicing *HESO1*, as the proportion of different transcripts is not that different between Col-0 and *sua* (10% difference) and the overall level is only 1.5 times more in Col-0. However, I am more confident on the splicing of *RNase X*, as we have an intron retained 98.6% of the time in *sua* while being 55.2% in Col-0 and an exon almost never skipped in *sua* compared to being kept at 54.2% in Col-0, the overall transcript level being 3.4 times lower in *sua* than Col-0. A new RT-qPCR experiment should be performed with a negative control to assess the level of transcripts of this *RNase X*, mainly to verify the primer design. Unfortunately, it is not feasible to validate the transcripts proportion because of its many isoforms making the primer design impossible to discriminate between isoforms. This *RNase X* was never studied before, thus my temporary name, and this gene will be the focus of the next chapter.

Chapter V] RNase X, the missing key of miRNA's turnover?

1) Introduction

After the splicing analysis of *sua*, I was left with one last candidate to study. This last chapter will discuss the identification of *AT5G53020*, temporally named *RNase X* because of its structure prediction making an X shape (Figure 43.A). This gene does not have a name on TAIR but is named *MNB8.8* on Uniprot. As it was not studied in plants, I will keep *RNase X* for the rest of the thesis. *RNase X* is predicted to be a Ribonuclease P protein subunit P38-like protein (*Rpp38-like* protein). In human, *Rpp38* is part of the conserved *RNase P*, composed of one RNA strand *H1* and 10 protein subunits (Eder et al., 1997; Jarrous & Altman, 2001) and it functions in tRNA processing, but also in the transcription of other small non-coding RNAs like 5S rRNA or U6 (Jarrous, 2002; Jarrous & Reiner, 2007; Reiner et al., 2006). However, the *RNase P* does not exist in plants and the closest ribonucleoprotein is *RNase MRP*, present in the nuclei and involved in the maturation of ribosomal RNA (Esakova & Krasilnikov, 2010; Kiss et al., 1992). The *RNase P* activity in plants is replaced by the protein-only *RNase P* or *PRORP* (proteinaceous RNAse P or PROtein-only RNase P) gene family with 3 proteins (*PRORP1*, *PRORP2* and *PRORP3*) in *Arabidopsis* located in organelles and in the nucleus (Bouchoucha et al., 2019; Gutmann et al., 2012). Knock-out of *PRORP1* shows lethality as well as the double mutant *prorp2/prorp3*, but not their respective single mutants, showing their essential functions and the redundancy between *PRORP2* and *PRORP3*. The authors also showed that the *PRORPs* were involved in tRNA maturation and not the *RNase MRP*, as first thought, as downregulation of *RNase MRP* does not change the level of tRNA while downregulation of the respective *PRORPs* does. Finally, they also showed that the *PRORPs* are involved, *in vivo*, in the maturation of small nucleolar RNA (snoRNA) and mitochondrial mRNA like the *RNase P* in animals (Gutmann et al., 2012).

Despite losing its initial role to the *PRORP*, the *RNase X* is still conserved in plants as shown by the phylogenetic tree provided by PANTHER (Mi et al., 2019) with the presence of the similar protein in rice, maize, poplar (*Populus trichocarpa*), or even in the moss *Physcomitrium patens* with its singular X shape (Figure 43.A). Additional analysis using ConSurf (Ashkenazy et

al., 2016) showed where the most conserved amino acids are on the structure of the *Arabidopsis RNase X*, with an average score of 69.6% of amino acid conservation between homologues of different plant species (Figure 43.B and Table S2). Whether the most conserved parts are involved in enzymatic activity needs to be investigated.

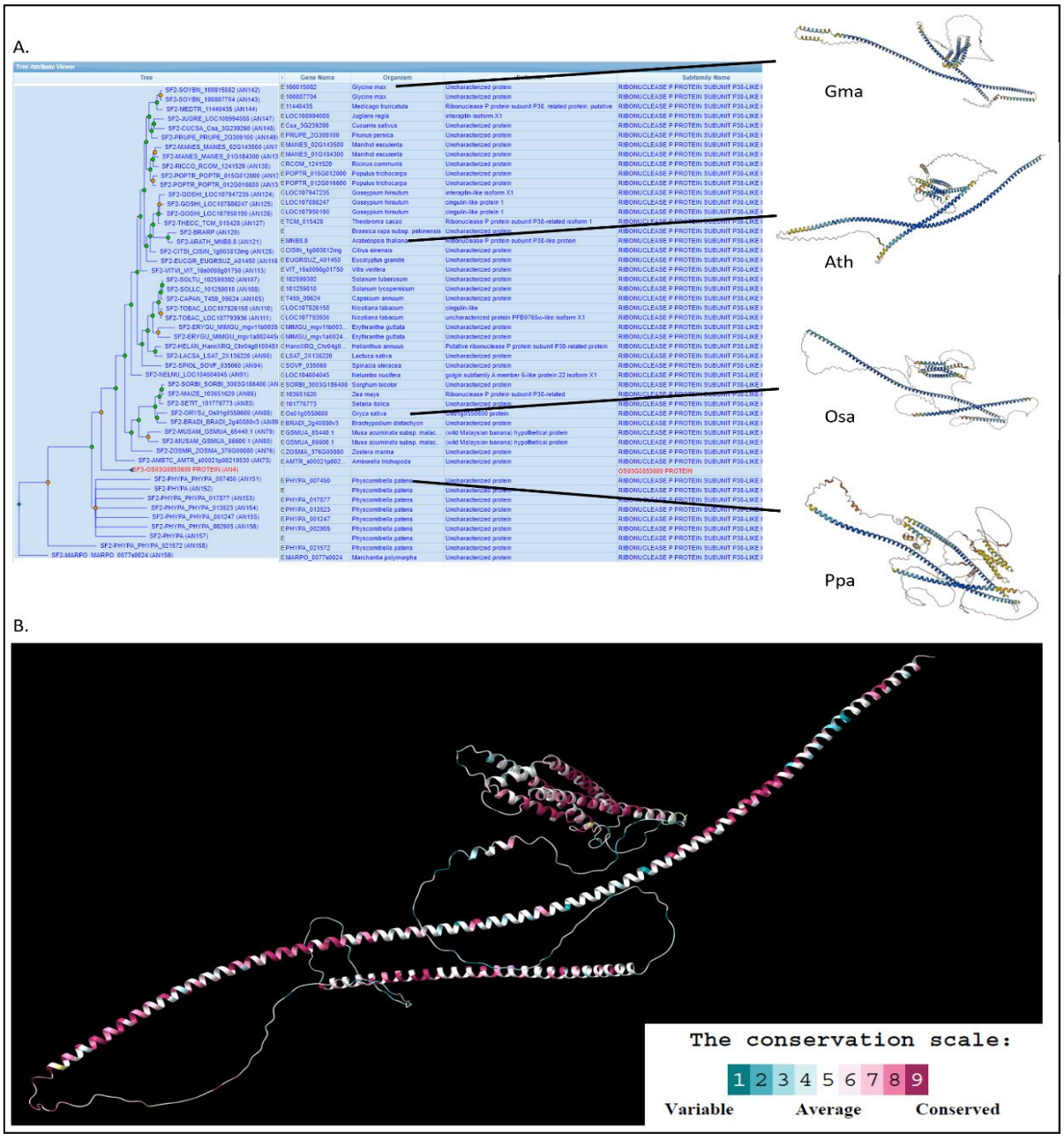

Figure 43: Conservation of the RNase X in plants. A. On the left, the phylogenetic tree provided by PANTHER and on the right, a selection of the different protein structure predicted by Alphafold. Gma: Glycine max, Ath: Arabidopsis thaliana, Osa: Oryza sativa and Ppa: Physcomitrium patens. B. Predicted structure of RNase X in Arabidopsis thaliana with a conservation filter calculated by ConSurf. The conservation was determined by sequence homology of this protein within all plants.

Additionally, RNase X does not belong to a bigger family, even if the BLASTP result of the sequence of RNase X on *Arabidopsis thaliana* genome shows a 99.45% hit with AT5G51930 (Figure 44.A). This gene is predicted to encode for a Glucose-Methanol-Choline oxidoreductase which have a completely different role from a RNase and a reverse BLASTP using AT5G51930 protein sequence does not hit with RNase X. RNase X is also not related to the PRORPs genes with an average of 18% similarity (Figure 44.B).

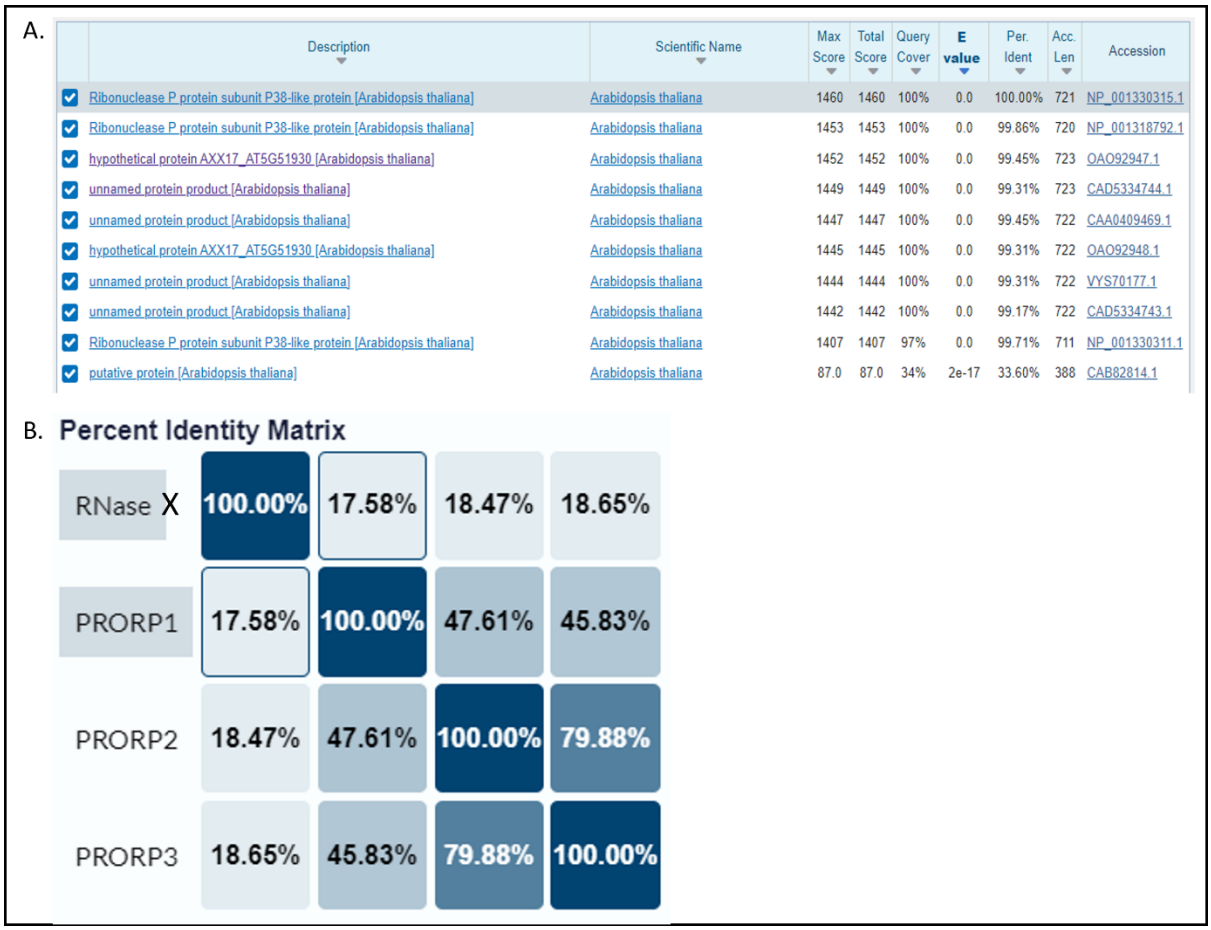

Description	Scientific Name	Max Score	Total Score	Query Cover	E value	Per. Ident	Acc. Len	Accession
Ribonuclease P protein subunit P38-like protein [Arabidopsis thaliana]	Arabidopsis thaliana	1460	1460	100%	0.0	100.00%	721	NP_001330315.1
Ribonuclease P protein subunit P38-like protein [Arabidopsis thaliana]	Arabidopsis thaliana	1453	1453	100%	0.0	99.86%	720	NP_001318792.1
hypothetical protein AXX17_AT5G51930 [Arabidopsis thaliana]	Arabidopsis thaliana	1452	1452	100%	0.0	99.45%	723	OAO92947.1
unnamed protein product [Arabidopsis thaliana]	Arabidopsis thaliana	1449	1449	100%	0.0	99.31%	723	CAD5334744.1
unnamed protein product [Arabidopsis thaliana]	Arabidopsis thaliana	1447	1447	100%	0.0	99.45%	722	CAA0409469.1
hypothetical protein AXX17_AT5G51930 [Arabidopsis thaliana]	Arabidopsis thaliana	1445	1445	100%	0.0	99.31%	722	OAO92948.1
unnamed protein product [Arabidopsis thaliana]	Arabidopsis thaliana	1444	1444	100%	0.0	99.31%	722	VYS70177.1
unnamed protein product [Arabidopsis thaliana]	Arabidopsis thaliana	1442	1442	100%	0.0	99.17%	722	CAD5334743.1
Ribonuclease P protein subunit P38-like protein [Arabidopsis thaliana]	Arabidopsis thaliana	1407	1407	97%	0.0	99.71%	711	NP_001330311.1
putative protein [Arabidopsis thaliana]	Arabidopsis thaliana	87.0	87.0	34%	2e-17	33.60%	388	CAB82814.1

Figure 44: Homology of RNase X. A. BLASTP result of RNase X sequence in Arabidopsis thaliana. B. Percent Identity Matrix of RNase X and the PRORPs.

According to the Klepikova Arabidopsis Atlas (Klepikova et al., 2016), the *RNase X* is constitutively expressed in the plant at all stages and organs except in the SAM (Shoot Apical Meristem) (Figure 45.A) while being more expressed in the hypocotyl and in the leaves (Figure 45.C). It also has similar level of expression than *HESO1* (Figure 45.B) and comparison between the two genes shows a higher level of *RNase X* in the hypocotyl and the seeds, but the latter is due to the very low expression of HESO1 in seeds (Figure 45.D).

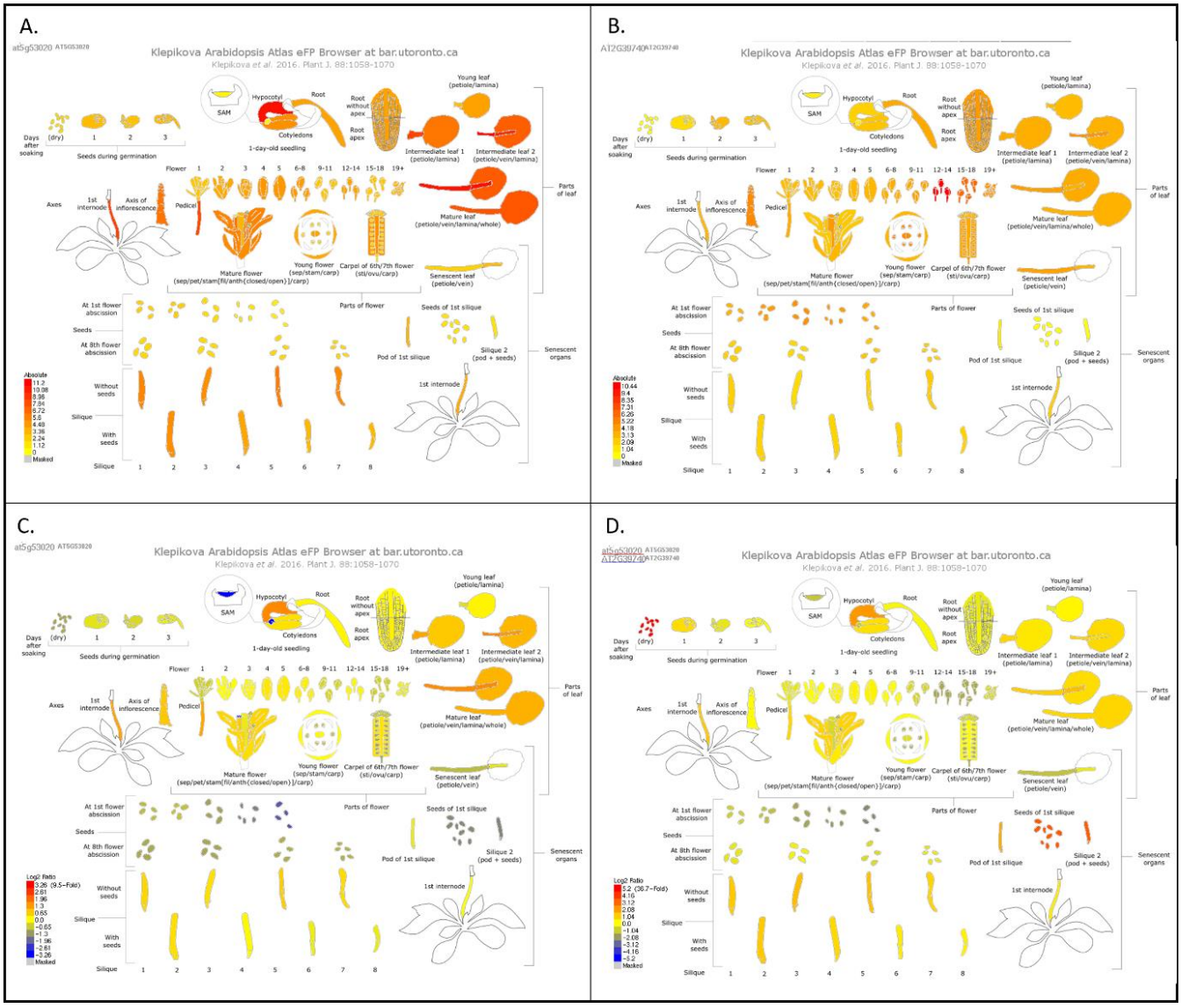

Figure 45: Expression patterns of RNase X and HESO1 using the Klepikova Arabidopsis Atlas. A. Absolute expression of RNase X. B. Absolute expression of HESO1. C. Relative expression of RNase X, calculated by comparing the expression level in one part by the overall expression level. D. Differential expression between RNase X and HESO1.

Overall, because the *PRORPs* have replaced the *RNase P* and their deletion mutants show lethality in *Arabidopsis*, the conservation of *RNase X* in plants and with an expression level similar to *HESO1*, I hypothesize that *RNase X* might be a remnant of the ancestral system and may have changed its activity. In addition, this gene was never studied before, making the next set of results novel.

2) Phenotypic analysis

Following the work previously done in chapter III, I started by looking at the phenotype of a SALK mutant of *RNase X*. I ordered the SALK line seeds (SALK_118734) and proceeded to get the homozygous mutant, which exhibited a strong phenotypic difference compared to the WT, despite not being a complete knock-out mutant as found by the mRNA sequencing results. The T-DNA insert is in the 5'-UTR and two other lines were ordered with the insert in the 5'-UTR (SALK_ 052802) and the CDS (SALK_130943) regions but never arrived (Figure 46).

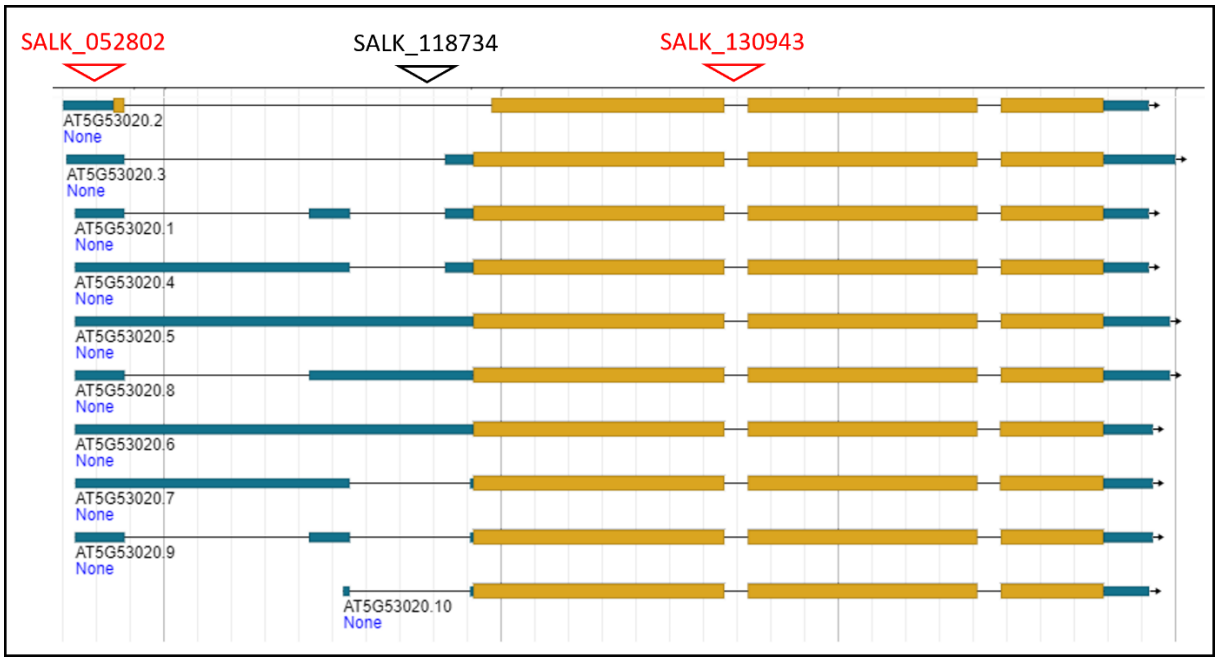

Figure 46: Location of the SALK T-DNA inserts in RNase X. The SALK line in red were ordered but did not arrive. The green boxes represent the 3'-UTR and the 5'-UTR while the yellow boxes represent the CDS, the black lines are the intronic regions.

Nevertheless, this *rnase x* mutant grows bigger in term of rosette size and leaves number than Col-0 (Figures 47.C, 47.D), exhibiting more than double the number of rosette leaves at day 38 pv, which are bigger than the WT and exhibit mild serration and more visible and abundant trichomes (Figures 47.A, 47.B). The downregulation of *RNase X* also affects the reproductive part, with longer main stem leading to an increased number of ramifications and flowers (Figure 48.A). The siliques are longer than Col-0 but contain fewer seeds (Figures 48.B, 48.C), the size of the seeds was not tested and might explain why there are fewer seeds in a bigger pod. Even if the downregulation of *RNase X* was not proven in the previous chapter, I suppose

that the small phenotypic rescue of *hen1* by *hi3* might be partially due to the incorrect splicing of *RNAse X* in the *sua* background and needs to be verified. Interestingly, the phenotype of *rnase x* is the opposite of the *hen1* phenotype and whether this is due to an overall increased level of miRNAs will be tested.

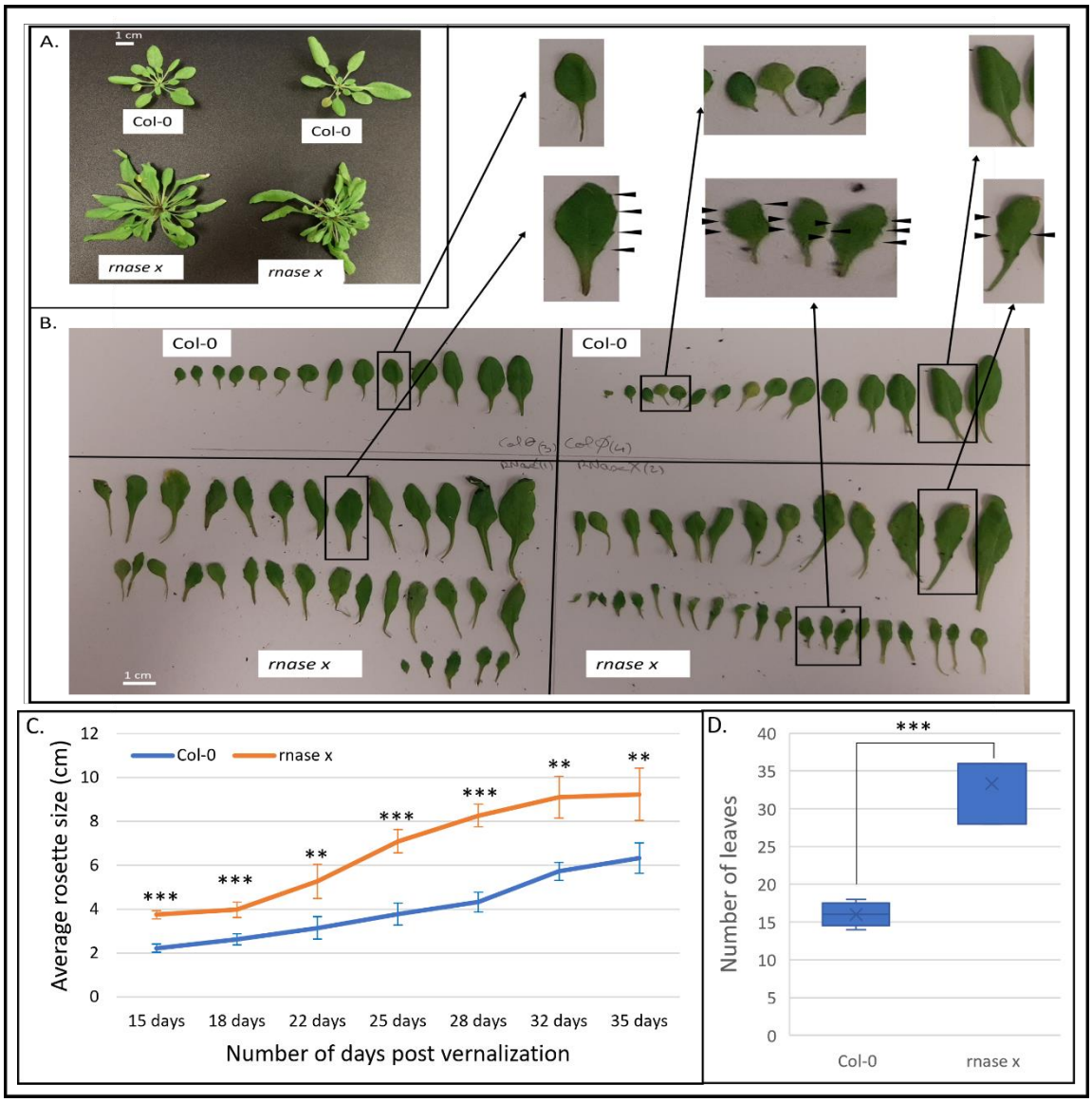

Figure 47: Vegetative phenotypic analysis. A. Picture of the cut rosette of Col-0 and rnase x at Day 38 pv. Pictures of the leaves composing the rosette in A., arrows show the serration on the leaves. C. Average rosette diameter of the different backgrounds at different timepoints after vernalization. The rosette diameter was calculated by summing the two longest rosette leaves of 4 biological replicates. D. Number of rosette leaves at Day 38 pv. The same 4 biological replicates were used. Asterisks represent statistical comparison and significance (two-tailed t-test, p-value < 0.05).

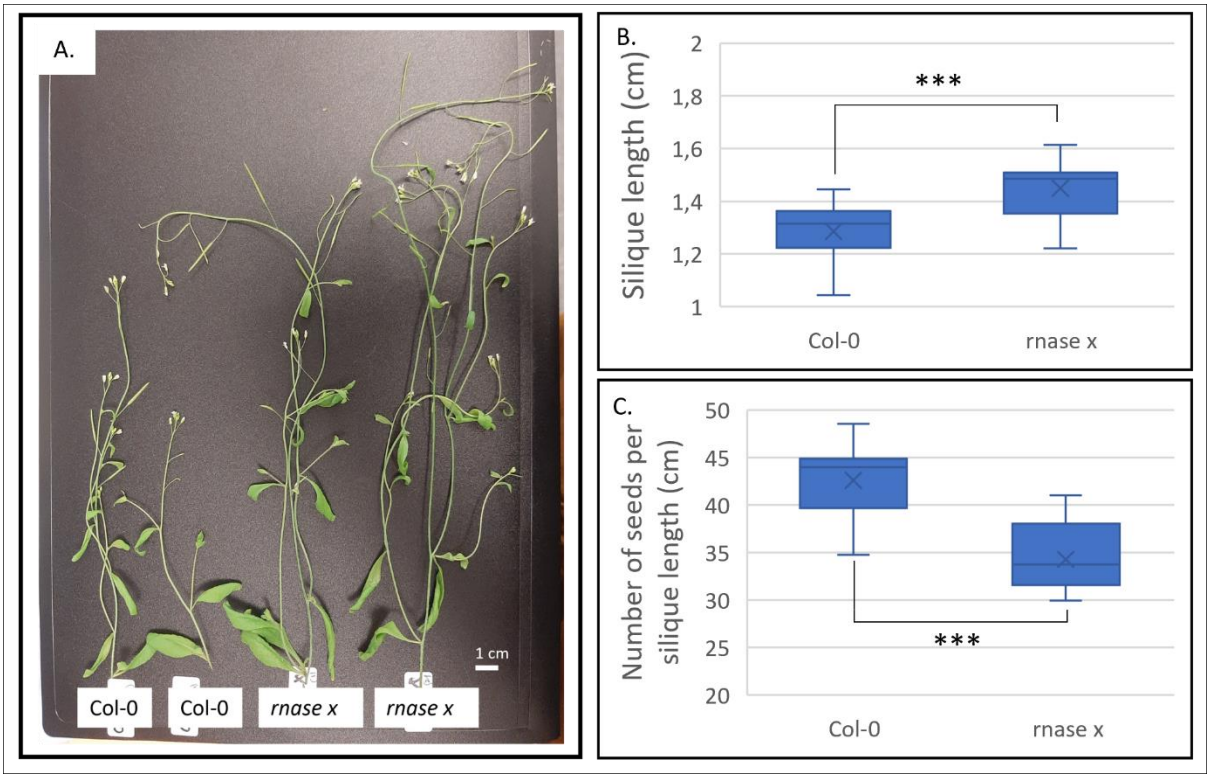

Figure 48: Reproductive phenotypic analysis. A. Picture of the stem of Col-0 and rnase x. B. Silique length of the different genotypes. 15 siliques measured C. Number of seeds divided by the length of the silique they originate from. 15 siliques measured. Asterisks represent statistical comparison and significance (two-tailed t-test, p-value < 0.05).

3) miRNAome analysis

Because crossing *rnase x* with *hen1* was not feasible in time, to test whether the phenotype of *rnase x* is related to a higher level of miRNAs, I proceeded to make sRNA libraries for sequencing and tested a few miRNAs by northern blot. Sequencing data were analysed by Dr Payet, he removed the adapters from the reads using Cutadapt (Martin, 2011), used Shortstack (Axtell, 2013) to predict the miRNAs and sent me the cleaned reads alongside Deseq2 analysis results (Table S5). I used iDep to produce the figures using the same count matrix as Deseq2 using an FDR cutoff <0.05 and a minimum fold change of 2.

The total read count after the cleaning and prediction shows a higher level of miRNAs in *rnase x* compared to Col-0 (Figure 49.A), but this should not be taken for granted as several steps in the libraries' preparation may induce biases, like PCR, adapters ligation or size selection on

the gel (Baran-Gale et al., 2015). The PCA shows a good clustering between Col-0 and *rnase x* (Figure 49.B). After differential expression analysis, 14 miRNAs are upregulated and 16 miRNAs are downregulated in *rnase x* compared to Col-0 (Figures 49.C, 49.D).

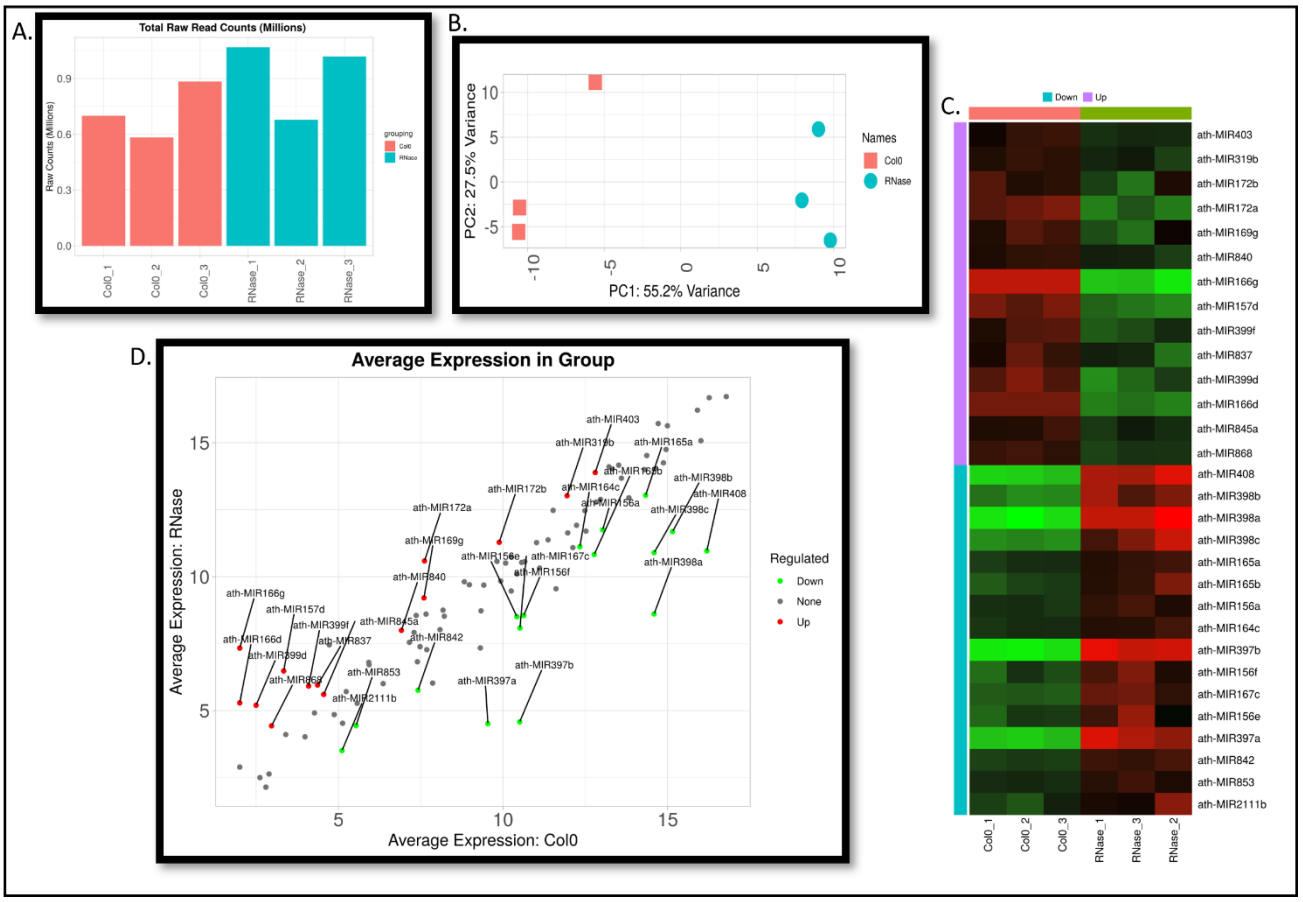

Figure 49: Analysis of the predicted miRNAs from the sRNA sequencing of Col-0 and rnase x. A. Total number of reads. B. PCA of the sequenced samples. C. Heatmap of the differentially expressed miRNAs. D. Scatter plot of the differentially expressed miRNAs.

To validate the sRNA sequencing data, I performed northern blot on 7 miRNAs, 3 were predicted to be upregulated in *rnase x* (miR166, miR172 and miR319), 3 to be downregulated (miR156, miR164c and miR408) and miR160 which was not differentially expressed acted as a control (Figures 49.C, 49.D). Unfortunately, the third biological replicate of Col-0 and the first biological replicate of *rnase x* on the northern blots are spoiling the analysis results. However, I decided to keep them on the picture and removed them in the expression calculations, like removing aberrant Ct values in RT-qPCR, to show the importance of using minimum three biological replicates (Figure 50). Overall, the results of the northern blots do

not coincide with those of the sRNA sequencing analysis apart from the upregulated miRNAs. Indeed, for those, especially miR166 and miR172, there is a 187% and 117% difference of expression between *rnase x* and Col-0. miR319 shows a slight increase in expression in both techniques while miR160 level is unchanged. However, the levels of miR156 and miR164c are, respectively, ~62% and ~63% higher in *rnase x* in the northern blot opposed to the sRNA results, miR408 level is also 47% more expressed in *rnase x* while it should be very downregulated according to the sequencing data. In retrospect, miR397 and miR398 might have been better candidates than miR164c and miR408 to test for the downregulation, as they were more downregulated in the sequencing data, and it is always interesting to test miR156 especially when testing miR172 because of the miR156-*SPL*-miR172 pathway (Schoor et al., 2021; Wu et al., 2009) (Figures 49.C, 49.D, 50).

The higher level of miR172 connects with the phenotype of *rnase x*, as the mutant is showing a faster transition from vegetative phase to reproductive stage even if the downregulation of miR156 seems to not have started yet. It would be interesting to test the level of miR156 in younger plants to assess if miR156 is already more expressed in *rnase x* than Col-0 and if it is already decreasing in the 20-day old plants that I used for northern blots. Oddly, plants overexpressing miR166 exhibit dwarfism which is the opposite of *rnase x* (Jung & Park, 2007), but the development is not only affected by miR166 and other actors like miR156 are probably impairing the effect of the high level of miR166 in *rnase x* or, more simply, miR166 is not overexpressed enough to induce dwarfism.

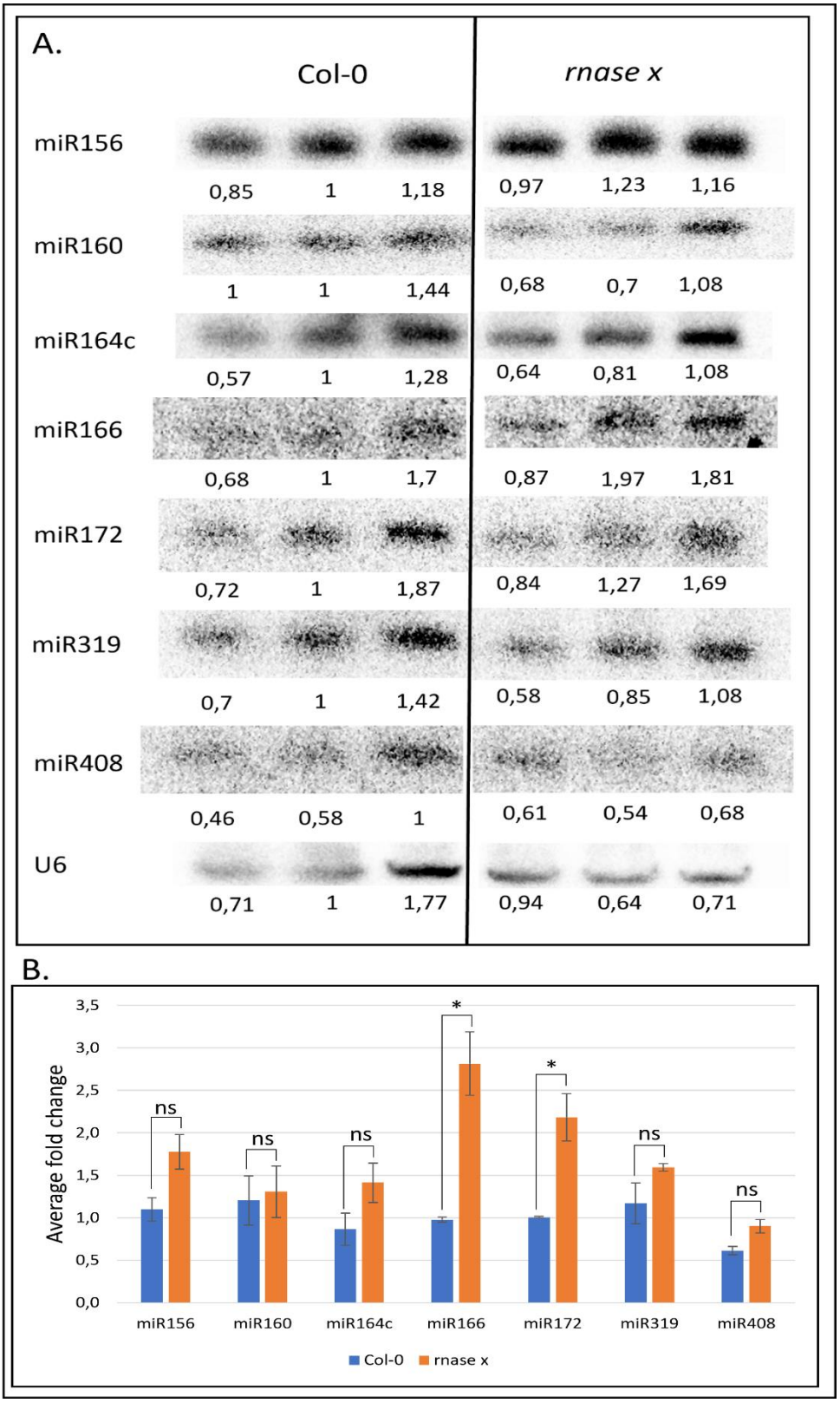

Figure 50: Northern blot analysis of some miRNAs in Col-0 and rnase x. A. Northern blots of miR156, miR160, miR164c, miR166, miR172, miR319, miR408 and U6 for loading control. 10µg of RNA loaded. B. Average expression of the different tested miRNAs in the different backgrounds, normalized by U6. Calculations for the third replicate of Col-0 and the first of

rnase x were omited. Asterisks represent statistical comparison and significance (two-tailed t-test, p-value < 0.05).

As most of the miRNAs tested by northern blot are more abundant in *rnase x* but as the mutant tested is not a complete knock-out, it is yet unclear that *RNase X* is responsible for the degradation of all miRNAs. The northern blot also showed what could be the different pri-miRs and pre-miRs with a lot of variations on the pri-miRs (Figure 51), but as showed in the previous chapter, it is unsure that the pri-miR bands does not contain other RNAs targeted by the different probes and I did not perform RT-qPCR on the pri-miRs, so even if there looks like the level of pri-miRs is higher in *rnase x*, I cannot conclude that *RNAse X* is responsible for their regulation. However, I am more confident with the pre-miRs, as they are located lower on the membrane and thus have been separated from the total RNA (Seo et al., 2020). The level of all tested pre-miRs is higher in *rnase x* compared to the WT and is indicative of either a direct regulation of *RNase X* on the pre-miRs or that *RNase X* is involved in a regulation loop of pre-miRs. Using another technique to validate the pre-miR quantity is complicated as they are rapidly processed *in vivo*, and few research groups study the pre-miRs. However, a solution was proposed by Schmittgen et al. (2008) to validate the pre-miR level by RT-qPCR despite the fact that any probes designed to amplify the pre-miR will also amplify the pri-miR, as they share the exact same sequence. After using two sets of primers at the same time, one targeting the pre-miR (thus the pri-miR) and the other targeting only the pri-miR, a subtraction of the normalized value from the first set of primers by the normalized value of the second would give the expression of the pre-miR on top of doing an electrophoresis using the products of the RT-qPCR that confirms the amplification of the pre-miR alongside a ladder as used in Lu et al. (2019). However, I did not have time to implement this method.

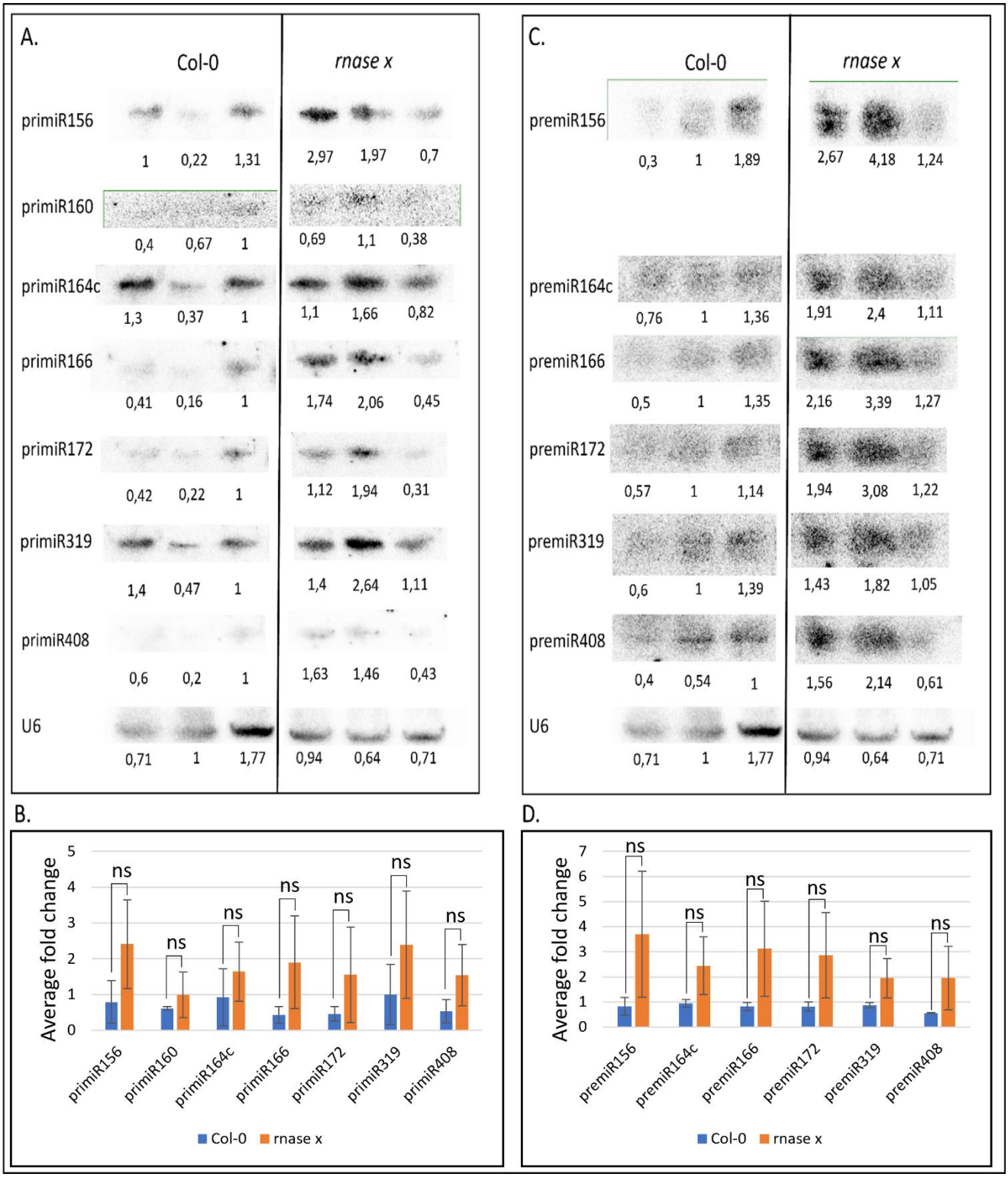

Figure 51: Northern blot analysis of some pri-miRs and pre-miRs in Col-0 and rnase x. A. Northern blots of primiR156, primiR160, primiR164c, primiR166, primiR172, primiR319, primiR408 and U6 for loading control. 10µg of RNA loaded. B. Average expression of the different tested pri-miRs in the different backgrounds, normalized by U6. C. Northern blots of premiR156, premiR164c, premiR166, premiR172, premiR319, premiR408 and U6 for loading control. 10µg of RNA loaded. B. Average expression of the different tested pre-miRs in the

different backgrounds, normalized by U6. "ns" represent statistical comparison and significance (two-tailed t-test, p-value < 0.05).

Lastly, I performed a miTRATA analysis (microRNA Truncation and Tailing Analysis) to look for a difference in the tailing/truncation pattern between the two backgrounds (Patel et al., 2016). This tool computationally detects miRNAs using the cleaned data from the sRNA sequencing, miRBase (version 21) and a reference genome (TAIR10), then determines the truncation and tailing length of each detected miRNAs and summarizes the results on bubble plots. Unfortunately, the online server was not working, but the Meyers lab performed the analysis locally after I sent them the cleaned sRNA sequencing data in tag count format. Overall, an increase in tailing length and tailing proportion but with no change in the truncation length can be observed in *rnase x* compared to Col-0 (Figure 52). Some miRNAs like miR158, partially unmethylated in Col-0, and miR159 even showed a decrease in truncation proportion of 1, 2 or 5 nucleotides in favour of increased tailing in the mutant. miR398, which was predicted to be downregulated in *rnase x*, shows a decreased tailing compared to the WT and indicates that other actors are involved, and we can theorise that *RNase X* may normally downregulate those actors. Finally, over the miRNAs tested by northern blot, miR166 showed a slight increased tailing proportion in *rnase x* compared to Col-0 and less truncation of 1 nucleotide if untailed. As the effect seems unnoticeable, we can assume that its expression level in *rnase x* is dictated by something else, like the level of AGO10 that sequester specifically miR166 to downregulate it (Zhu et al., 2011). Also, miR172 showed a very slight increase in tailing, probably because its level is increasing as the plants transition to reproductive stage, thus reducing its probability to be degraded. However, as those results are based on bioinformatics, which made predictions at different levels of analysis, there is a need to verify the tailing and truncation patterns of those miRNAs by northern blots.

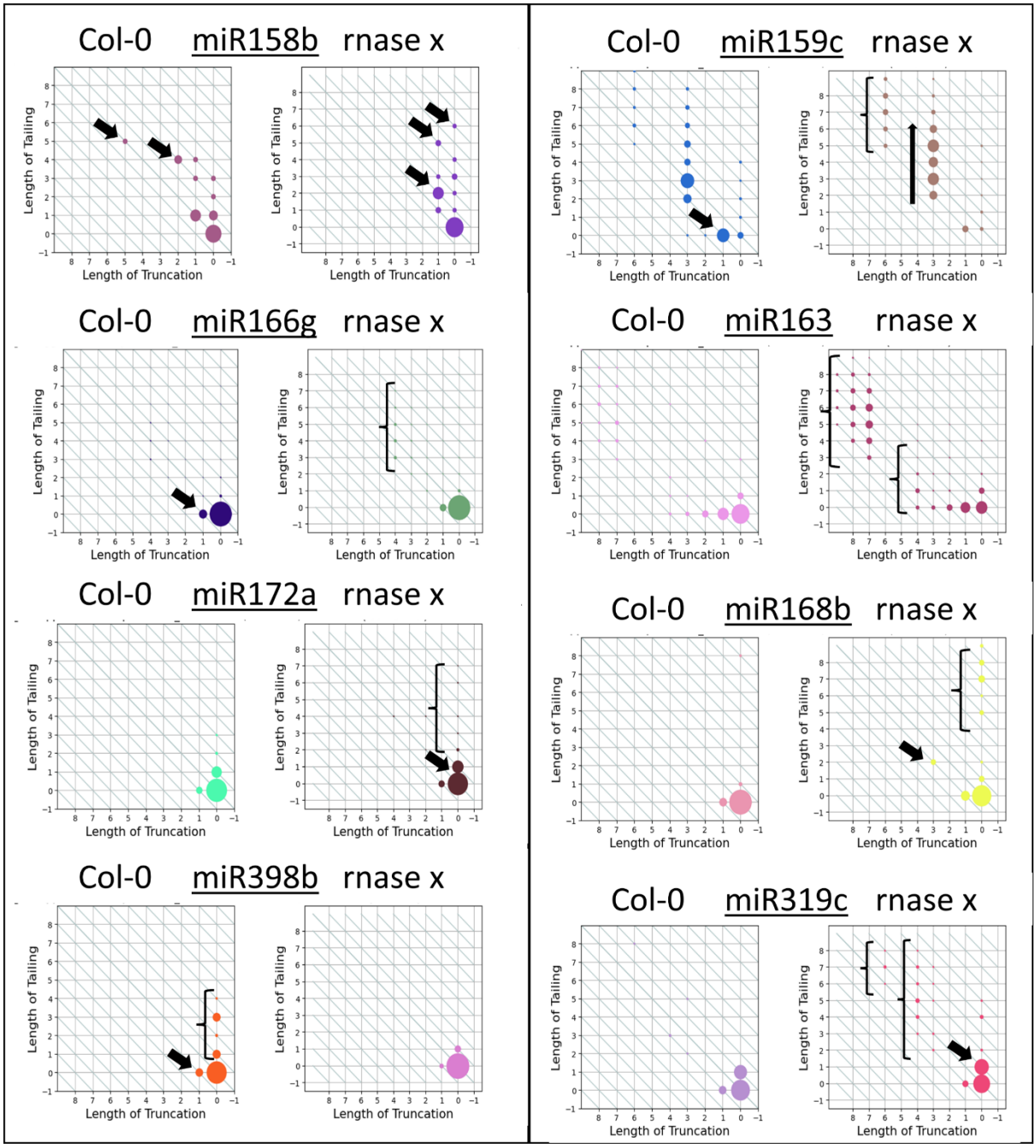

Figure 52: miTRATA analysis of some miRNAs. In the bubble plot, the bubble size corresponds to the proportion of all reads derived from that miRNA, which have modifications corresponding to the truncation length axis and tailing length axis. Arrows and brackets indicate noteworthy bubbles. Results figures were produced by the Meyers group but the brackets and arrows were added by me.

In conclusion, there is an increase in the level of most tested miRNAs and of the tailing in *rnase x* but not all miRNAs are affected that indicate that *RNase X* may have changed its

function to the degradation of a subset of urydilated miRNAs or may be involved in the regulation of pre-miRs, as showed by the overall increased level of pre-miRs in the mutant.

4) mRNA sequencing analysis

As the mutant does not contain an increased level of all miRNAs, it is also interesting to look at the gene regulation in the mutant as it may be involved in feedback loops or degrades important genes that lead to the mutant phenotype. We sent total RNA of Col-0 and *rnase x* to Novogene for mRNA sequencing using poly-A enrichment and after sequencing, they delivered the cleaned reads, that I aligned to the genome (Araport11) and quantified using SALMON (version 1.10) and Deseq2. Figures were produced using iDEP (version 1.1) using the count matrix provided by SALMON.

The quality control shows a good distribution of the data and a good clustering of the samples and a relatively uniform heatmap (Figure 53).

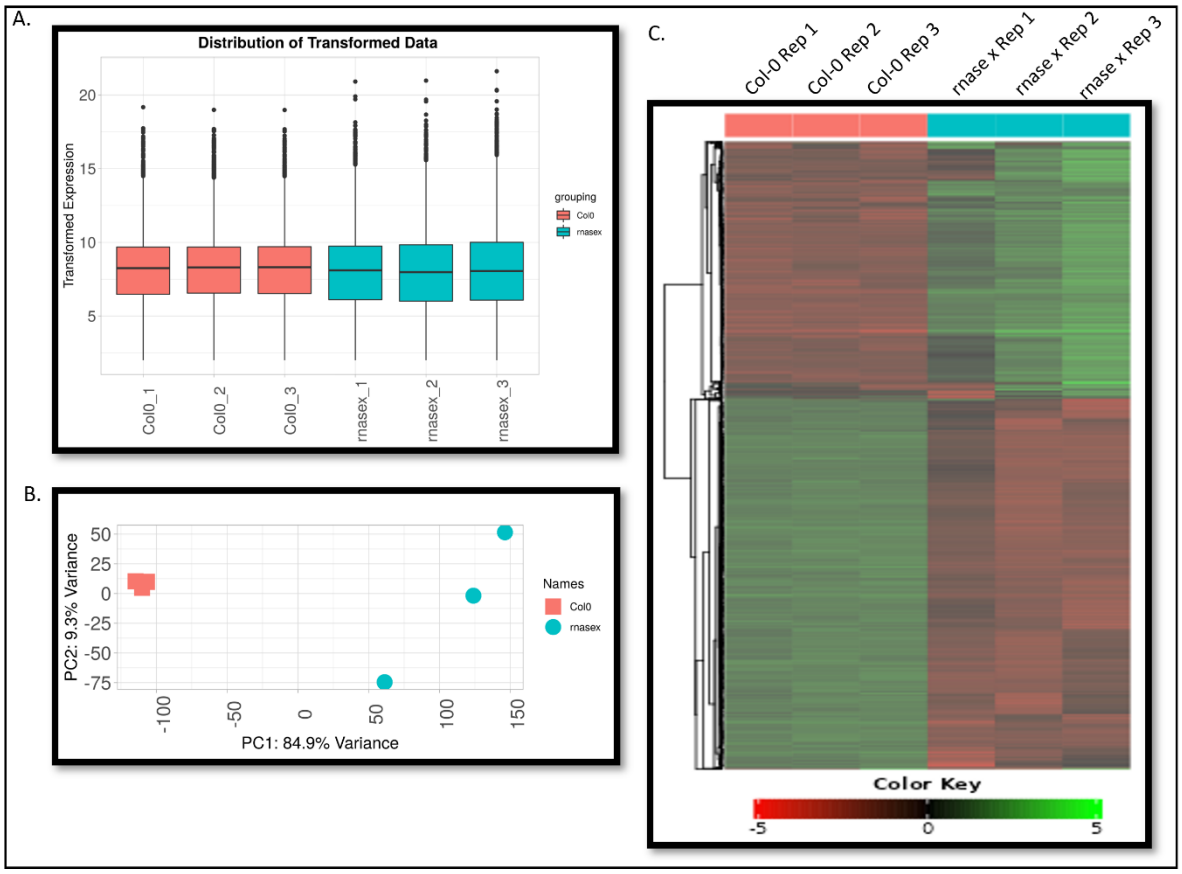

Figure 53: Analysis of the Illumina sequencing of Col-0 and rnase x. A. Distribution of the transformed data. B. PCA of the sequenced samples. C. Heatmap of the genes in Col-0 and rnase x.

After normalisation and differential expression analysis (FDR <0.01 and minimum fold change >2), 4999 genes are upregulated, and 5186 genes are downregulated in *rnase x* compared to Col-0 (Figures 54.A, 54.B). KEGG enrichment analysis shows an upregulation of the oxidative phosphorylation, hormone signal transduction or the autophagy pathways in the mutant while the most downregulated pathways are focused on the DNA with the DNA replication, the mismatch repair, and the homologous recombination. It is also noticeable to observe a downregulation of the RNA degradation pathway, showing the importance of *RNase X* (Figure 54.C). Considering the GO Biological Process, the cell killing is the most upregulated process in the mutant and may indicate a potential regulation role for *RNase X* (Figure 54.D). Apart from the hormone signalling, it seems that none of the most differentially expressed pathway could explain the *rnase x* phenotype, meaning that the increased level of some miRNAs may be the only responsible factor.

A.

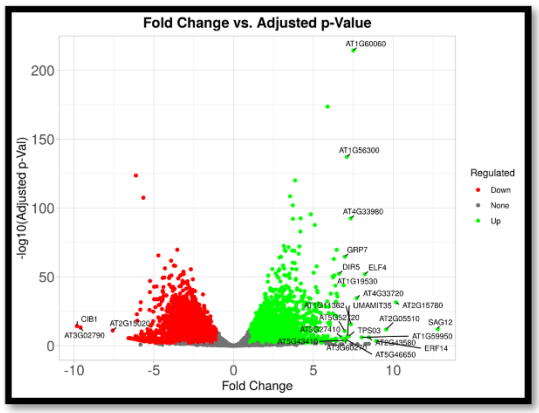

B.

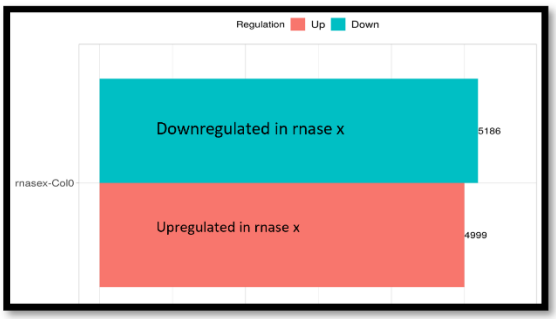

C.

Grp.	Adj.Pval	Fold	Pathway (Click for more info)
Upregulated	1.36E-8	2.3	Oxidative phosphorylation
	6.02E-6	1.7	Plant hormone signal transduction
	6.89E-3	1.7	MAPK signaling pathway-plant
	1.73E-2	2.2	Autophagy-other
Downregulated	6.07E-9	2.8	DNA replication
	1.92E-8	2.5	Homologous recombination
	6.04E-6	2.2	Nucleotide excision repair
	6.04E-6	2.7	Mismatch repair
	6.70E-6	2	Ribosome biogenesis in eukaryotes
	2.40E-5	2.2	ABC transporters
	3.63E-5	1.8	Nucleocytoplasmic transport
	4.04E-5	2.2	Aminoacyl-tRNA biosynthesis
	2.58E-3	1.8	Inositol phosphate metabolism
	3.73E-3	1.6	RNA degradation

D.

Grp.	Adj.Pval	Fold	Pathway (Click for more info)
Upregulated	1.04E-10	1.2	Response to chemical
	7.86E-8	1.3	Response to hormone
	3.88E-7	3.3	Cell killing
	3.88E-7	3.3	Killing of cells of another organism
	5.11E-7	1.3	Response to endogenous stimulus
	6.74E-7	1.4	Protein modification by small protein conjugation
	1.25E-6	1.4	Protein ubiquitination
	2.34E-6	1.2	Transport
	3.90E-6	1.9	Negative regulation of molecular function
	1.23E-5	1.2	Response to organic substance
Downregulated	2.41E-43	2.1	Chromosome organization
	1.12E-41	1.5	Organelle organization
	1.02E-40	1.4	Cellular component organization or biogenesis
	1.59E-36	1.9	DNA metabolic process
	3.04E-35	1.9	Cell cycle
	2.89E-34	1.4	Cellular component organization
	1.37E-30	3.3	Movement of cell or subcellular component
	1.15E-29	2	Cell cycle process
	4.92E-27	3.4	Microtubule-based movement
	2.43E-26	1.9	Cellular response to DNA damage stimulus

Figure 54: Differential expression analysis of Col-0 and rnase x. A. Volcano plot showing the downregulated and upregulated genes in rnase x compared to Col-0. B. Number of genes with differential expression in rnase x compared to Col-0. C. KEGG pathways in rnase x compared to Col-0. D. GO Biological Process terms in rnase x compared to Col-0.

5) Discussion

Phenotypically, *rnase x* is very interesting with a better fitness than the WT, which is odd from an evolutionary point of view, but that might change in stress conditions and explain why it the gene was conserved. More of its phenotype needs to be unveiled like the roots phenotype or looking at the microscopic level to see the trichome and if the increased biomass is due to cell expansion or cell proliferation (Song et al., 2018). As it is conserved among plants, this gene may be interesting in agronomics, especially in plants where leaves are consumed but also the fruits as the siliques are longer in the mutant. That might be due to bigger seeds but that was not tested. Besides, I suppose that the small phenotypic rescue of *hen1* by *sua* might finally be partially due to the incorrect splicing of *RNAse X* in the *sua* background because *rnase x* transition faster to the reproductive stage than Col-0 like *hi3/hen1* did compared to

hen1. From my observations, the phenotype of *rnase x* is the opposite of *hen1*'s with increased biomass, reproductive capacity, miRNA level and tailing. Obtaining the double mutant and looking at its potential phenotypic and miRNA level rescue will give another response on the implication of *RNase X* in the degradation of U-tailed miRNAs.

Over the 7 miRNAs tested by northern blots, none of them was downregulated in *rnase x* compared to Col-0 despite three of them being predicted to be at lower level by the sRNA sequencing. As the preparation of the libraries induces biases (Baran-Gale et al., 2015), the northern blot is more trustful and clearly shows the increase of miRNA and suggest the increase of pre-miR levels. On top of that, miTRATA analysis shows an increase of tailing but a decrease in truncation, which is expected from a knocked-out enzyme that would normally degrades U-tailed miRNAs. From that, we can also hypothesize that *RNase X* regulates the pre-miR level by upregulating protein(s) involved in the regulation of pre-miRs and its absence in the mutant leads to a downregulation of those and an increase of pre-miRs. The higher pre-miR level could also be due to an increase of miR162, which targets *DCL1* responsible of the pre-miR processing (Xie et al., 2003). However, the levels of pri-miRs and pre-miRs need to be determined by northern blot using a loop specific probe or a probe targeting the miRNA* or by RT-qPCR as described in Lu et al. (2019) .

While obtaining a *rnase x/hen1* double mutant would help to determine the rescue of the *hen1* background, it would also be interesting to produce a *rnase x/heso1/urt1* triple mutant to determine if the tailing is necessary for *RNase X* to work, and if it could also act redundantly or cooperatively with *SDN1* to degrade non urydilated miRNAs.

To further confirm the degradation of U-tailed miRNA by *RNase X*, an interesting experiment to do is to incubate a recombinant *RNase X* with radio labelled U-tailed miRNAs of different sizes in a timepoint experiment and observe the degradation on a resolving gel in a similar way to Zhao et al. (2012). It could also be interesting to overexpress *RNase X* in vivo and observe the phenotype, the level of miRNAs and the tailing as done in this chapter.

While most miRNAs seem to be affected in rnase x, some are not, which suggest that either *RNase X* only degrades a subset of miRNAs, or that it was not downregulated enough to degrade all miRNAs or that it cooperates with other proteins. Unfortunately, no interaction data was found on BioGRID, so it was not part of the Arabidopsis Interactome Map Project (Dreze et al., 2011) and potential interactors need to be determined, probably by computational methods. With over 10000 genes that are predicted to be differentially expressed, I did not carry out a detailed sequencing analysis of the differentially expressed mRNAs but for example, *AGO10* was found to be downregulated in *rnase x* compared to Col-0. *AGO10*'s expression is controlled by different hormones: auxin and brassinosteroids (Zhang et al., 2020) and sequester specifically miR166 to regulate shoot apical meristem development (Zhu et al., 2011). miR166 was significantly more expressed in *rnase x* but its truncation/tailing pattern was not very different from Col-0 (Figures 50, 52), showing that *RNase X* does not directly regulate its level and the mutant shows an upregulation of the hormone signalling pathway (Figure 54). Thus, *RNase X* may, in normal conditions, regulate the level of those hormones by degrading them in time, leading to a "normal" expression of *AGO10* that sequester miR166 and reduces its level. Meanwhile, in the *rnase x* mutant, those hormones are upregulated, *AGO10* level decreases and miR166 increases. This hypothesis needs to be tested *in vivo* by RT-qPCR for example.

As *RNase X* was never studied before, a lot of exciting discoveries are yet to be made. Its cellular location could be a hint of the other potential roles, especially for pre-miR regulation as the pre-miR processing is done in the nucleus, thus if *RNase X* is only expressed in the cytoplasm, as predicted on TAIR, would indicate that the increased expression of pre-miRs in the mutant is due to an indirect regulation. Unveiling its crystal structure like it was done with *SDN1* (Chen et al., 2018) would help us understand how the miRNAs are processed, determine the domains that composed this enzyme predicted by Alphafold (Jumper et al., 2021) and even unveil how it could interact with other miRNAs involved proteins like *AGO1* or *HESO1* and complement that data with protoplast two-hybrid assays (Ehlert et al., 2006) and blind docking predictions (Che et al., 2022; Liu et al., 2022). Besides, as *HESO1* and *HEN1* also work on other sRNAs (Yu et al., 2010; Zhao et al., 2012), it would also be interesting to observe the level of some siRNAs in the *rnase x* mutant by northern blot to determine if *RNase X* is also

involved in the regulation of those sRNAs, like its homologue in human which act on tRNA and other small non-coding RNAs (Jarrous & Altman, 2001; Jarrous & Reiner, 2007; Reiner et al., 2006). Finally, it could be interesting to look at the other homologous subunits of the human *RNase P* to determine if they also changed to the same role(s) as *RNase X* in plants to act redundantly or cooperatively.

Chapter VI] Discussion and conclusion

1) Determination of genes involved in the miRNA turnover

Determining the genes involved in miRNA regulation in plants is a 20-year-old question and many important genes had been found controlling their steady state level, from their protection by *HEN1* (Li et al., 2005; Yu et al., 2005), their tailing performed by *HESO1* and *URT1* (Zhao et al., 2012, Wang et al., 2015) to more recently *ATRM2* or *XRN4*, which respectively control the methylation step and the degradation of the passenger strand (Liu et al., 2020; Wang et al., 2018). However, the gene involved in the degradation of U-tailed miRNAs remains unsolved and my PhD work tried to answer this question.

The classical way to look for an unknown gene is to perform a genetic screen, but none were designed to determine the genes involved in miRNA turnover, with the preferred candidate approach more commonly used (Li et al., 2005; Liu et al., 2020; Park et al., 2002; Zhao et al., 2012). The Dalmay laboratory designed a genetic screen based on miR395, expressed on low Sulfur media, and a GFP-transgene containing a target sequence for the miRNA. When replenishing the plant, grown on low Sulfur media, with Sulfur, GFP would appear. However, plants would express faster or slower GFP recovery than the control if they contained a mutation interfering with miRNA turnover because miR395 is not produced anymore after replenishing and GFP occurs as the existing miR395 pool gets degraded. This screening allowed the previous PhD student to discovery a post transcriptional gene silencing mutant, called *msm1* (unpublished data). However, I did not manage to identify an interesting candidate despite having selected 33 of them (14 from my own screenings and 19 previously selected by the laboratory) for RT-qPCR quantification and left with 6 candidates for northern blot quantification. The main issue was the timepoint experiments that needs to be improved for a latter use. The RNA quantity was often not enough to perform a good northern blot experiment, which requires at least 5 µg of RNA, while increasing the number of timepoints cannot be done for RT-qPCR experiment due to the limitations of a 96-well plate. It also seems that replenishment of the media with Sulfur was not great because of a lot of variations

between two biological replicates at the same timepoints or with increased level of miR395 on the latter timepoint (24-48h) despite being standardized.

On the other hand, looking at candidate genes is another approach to determine a gene's function. This project is based on the SALK lines (Alonso et al., 2003) and on the Arabidopsis Interactome Map Project (Dreze et al., 2011), proposed to look at the 6 proteins that were predicted to interact with *HESO1*, with the idea that after *HESO1* is finished tailing miRNAs, it would call an enzyme that degrades U-tailed miRNAs. By crossing the 6 mutants into a *hen1* background, if one of those is involved in the degradation of miRNAs, it would rescue the characteristic *hen1* phenotype alongside an increase in miRNA level. Four of the double mutants could be obtained within the timeframe of this PhD, but only one showed a small phenotypic rescue of the reproductive stage with earlier stem production and flower production than *hen1* but did not rescue the level of miRNAs in the vegetative stage. Growing *hen1* background plants was the most difficult part of this project as it is a very sensitive background that does not produce a lot of seeds and keeping a heterozygous *hen1* plant with a homozygous version of a candidate gene rather than the F1 generation is the best way to save time and effort if the double mutant shows low fitness and if that needs to be redone.

Nevertheless, this remaining candidate gene, *SUA*, is a splicing factor involved in seed maturation and immune response (Sugliani et al., 2010; Zhang et al., 2014) but with potentially more roles as the single mutant does not exhibit a particular phenotype indicating that it acts redundantly or is involved in very specific stress conditions or timeframe. I thus hypothesized that the weak rescue in *sua/hen1* was due to incorrect splicing of one or several genes involved in miRNA steady-state level and splicing analysis led to the discovery of an unknown ribonuclease, named *RNase X*. Though, I could not confirm the predicted decreased level of *HESO1* and *RNase X* in *sua* by RT-qPCR or western blot, I decided to keep working on *RNase X* as it was never studied before, and it could offer potential research output.

RNase X was predicted to be a homologue of a human *RNase P* subunit involved in tRNA processing, which is done in plants by other complexes called the *PRORPs*, leaving *RNase X* without this function. After phenotypic analysis and measuring the increased level of some

miRNAs in the *rnase x* mutant, I hypothesized that it was involved in the miRNA turnover. After truncation/tailing analysis, it appears to be the case with increased tailing but not truncation in the mutant indicating that the miRNAs are tailed like in the WT but are not degraded in the mutant. However, over 10,000 genes are differentially expressed between WT and *rnase x* plants, therefore it is possible that another RNase that degrades U-tailed miRNAs could be downregulated in the *rnase x*. Confirmation of the degradation of U-tailed miRNA specifically by *RNase X* needs to be tested by incubating a recombinant *RNase X* with radio labelled U-tailed miRNAs of different sizes in a timepoint experiment and observe the degradation on a gel in a similar way to Zhao et al. (2012). Further confirmation can be done by crossing *rnase x* with *hen1* to observe a phenotypic rescue and increased level of miRNAs.

2) Limitations

As all PhD projects, the main limitation was time. The genetic screen was the main project, until it did not produce a candidate of interest among the 33 chosen candidates. The screen design has it flaws as it relies on a timepoint experiment and not just a single observation (like survivability in a certain media), inducing a heavy manual monitoring and is tedious due to the use of a microscope. Many factors could have biased the experiment as the Sulfur starvation response contains a lot of actors like *SLIM1* and miR395 and mutations in those actors could have influenced some results. Even though, it is possible to look at another stress response pathway involving miRNA like the Phosphate assimilation pathway with miR399, the screening can also detect other siRNAs involved gene like *msm1* (unpublished data) and increase the complexity of the results. Other problems can be raised like the fact that the control was not constantly expressing the GFP correctly and that I could have missed very late response mutants as the screening was stopped day 12 after addition of $MgSO_4$ because the leaves were covering the roots. The screenings were stopped for the timepoint experiments and after finding out that none of the candidates were valuable, we decided to stop the project instead of restarting other screenings.

Then, I focused on the candidate approach, which lead to another limitation: working with *hen1* background, as the selection of the *hen1/hiX* double mutants took almost 3 years

because of their low fitness and especially their low fertility. Moreover, I wanted all the double mutants before starting to measure their phenotype and miRNA level, losing even more time, even if in the end, none of the candidates were of interest, except for *SUA*, which was analysed before getting all the double mutants because it had a small phenotypic rescue. The biggest mistake I have made was to not keep a heterozygous *hen1* background with a homozygous *hiX*, instead of starting from the selection F1 generation. Still, the sequencing of sRNA (not shown), mRNA and the splicing analysis of *sua* was done during my last year. Selection and analysis of the *rnase x* mutant was done 5 months before my submission deadline, explaining why I did not have time to get a *rnase x/hen1* double mutant, did not have time to set up RT-qPCR and a degradation experiment and did not analyse the mRNA sequencing data in detail as I could not verify the level of candidate genes by RT-qPCR in time.

3) Wider relevance of this PhD and future work

Despite not identifying a candidate gene during my PhD, the screening assay is operational, yet perfectible, and previously allowed the discovery of *msm1*. A few more improvements need to be done on the timepoint experiment, but it could be used for the determination of genes involved in miRNA turnover or Sulfur regulation.

I also produced several sequencing datasets that need to be published with the sRNA sequencing of *sua*, *sua/hen1* and *rnase x*, the mRNA sequencing of *rnase x* and *sua*, which was requested in Zhang et al. (2014), offering a broader impact of my work. The next steps are to verify the tailing of miRNAs in the rnase x mutant and to cross it in a hen1 background to look at a potential phenotype recovery and an increase of miRNA level. If it turns out that *RNase X* is not responsible for the degradation of U-tailed miRNAs, determined by the future degradation experiment, the gene responsible for that will be in the downregulated genes in *rnase x* sequencing results, which will narrow down the potential candidates over the whole genome.

Finally, as *RNase X* is conserved in plants and looks to be of agronomical interest, studying the mutant in stress conditions and in other species like tomato, maize or even rice could be a great insight to develop better crops in a time of climate change.

Chapter VII] Material & Methods

1) Plants material and growth conditions

1.1) Growing media

Depending on the experiments, sterilised seeds were grown in different prepared media which was autoclaved to ensure sterility. Before sowing, the media was melted in the microwave before pouring in the appropriate container and left to cool down before putting the seeds.

1.1.1) Murashige and Skoog (MS) media

Murashige and Skoog (MS) media was prepared by adding 4.3 g of MS mix powder (Rédei, 2008) and 5g of Glucose [ThermoFisher Scientific, 15023021] in 1 L of dH2O. The pH was lowered to 5.7 by adding HCl before adding 8 g of phytoagar [Duchefa, 9002-18-0].

1.1.2) Low Sulfur (LS) media

Low Sulfur (LS) media was entirely made to remove all sources of Sulfur. The ingredients and their concentrations are listed in supplemental table S3.

1.2) Seeds sterilisation

For each experiment involving growth on sterile media, the seeds needed to be sterilised. This was done by incubating the seeds in 20% sodium hypochlorite [Sigma-Aldrich, 28-3100] and 0.1% Triton [Sigma-Aldrich, T8787] solution for 13 minutes with gentle shaking. After incubation, the sterilisation solution was removed, and the seeds washed six times with dH_2O.

1.3) Tissue culture

1.3.1) GFP screenings

The M2 seeds of *rdr6* and of EMS mutated *rdr6* mutants' seeds were sowed in 48 well plates (ThermoFisher Scientific, 140675) filled with 400 µl of LS media and, after two days at 4°C for vernalisation, stored upright in growth chamber in long day condition (23°C/16h light, 18°C/8h dark cycles). The plants were grown for 6 day and each plant was observed under blue light (450 nm) with the Leica MZ16 F with FluoCombi (https://www.leica.com/) and was scored according to their fluorescence at 510 nm (Table 1). The screening assays started one day before adding $MgSO_4$ in the media to verify that the plants do not express the GFP and any plants that passed the threshold score of 3 out of 5 at that moment were discarded. Then, the plants were observed at day 0, day 1, day 2, day 5, day 7, day 9 and day 12 post Sulfur addition. To accommodate the eyes to the obscurity and to the expected fluorescence, the control plate was always analysed first. The score was voice recorded using a phone and the data updated after each screening in an Excel file. Plants expressing a fluorescence score of at least 3 of out 5 at day 1 and day 2 were considered Early Response (ER) candidates and those who started expressing the appropriate score at day 7,9 and 12 were considered Late Response (LR) candidates. At the end of the screenings, candidates were first transferred in MS media for two to three weeks before being transferred in soil and grown in the same temperature and light cycle conditions.

1.3.2) Validation by RT-qPCR and northern blot experiments

For the RT-qPCR experiments, 9 plants per biological replicate for each timepoints (0h, 24h and 48h) were sterilised as above and grown on square petri dishes [ThermoFisher Scientific, 11349273] with LS media for three weeks. $MgSO_4$ was added at the 0h timepoint and the roots cut and frozen in liquid nitrogen 24h and 48h after addition. The 0h timepoint did not receive $MgSO_4$ before getting its roots cut. For the northern blots, the same protocols of sterilisation and sowing were used but with more timepoints. For some experiments, plants were first grown on MS media and transferred in LS media after 2 weeks, making sure to

gently push the roots in the media and Sulfur starved for 96h before starting the timepoint course by adding $MgSO_4$.

1.3.3) SALK mutants

Seeds for plants of interest were ordered from the Eurasian Arabidopsis Stock Centre (uNASC) (https://arabidopsis.info/) making sure to have the Col-0 background and the T-DNA insert in the corresponding genes. For all experiments involving those mutants, the seeds were sown in pots containing sterile JIC soil, disposed in tray and left for two to three days at 4°C under a protective cover for vernalisation. The trays were then moved to a grown room with long day conditions. They were watered by filling the tray with one to two cm of tap water once a week and after the protective lid was removed one week later, they were watered twice a week.

1.4) Crosses

Homozygous plants containing the T-DNA insert were grown under short day conditions for about a month to prevent asynchronous flowering of the different lines. They were then moved to long day condition to triggers the transition from vegetative phase to reproductive phase until flowers in both plants were present. Under the Leica MZ16 F microscope and visible light, the process starts with the receiving plant (i.e., the female) with the removal of opened flowers and siliques on the stem, if any are already present. Then, with forceps, the removal of the meristem buds to prevent the stem to continue growing with unwanted flowers, leaving two to three unopened flowers. The petals and stamens were delicately removed, leaving only the carpel ready to receive pollen from the donating plant (i.e., the male). From the male plant, opened flowers were picked and the petals removed to see the anthers that were them gently rubbed on the pistils of the receiving plant, several rubs were performed with different male anthers to ensure proper fertilisation. The pistils were covered to protect them from unwanted pollen and taped to differentiate them from the other. The success of the crosses could be verified three to four days later with the start of production

of a silique. Seeds were collected from those siliques, the F1 generation grown, and the plants were genotyped by PCR to verify the success of the crosses. Successful F1 lines were kept and the seeds from their self-fertilization were used to produce the F2.

1.5) Seed gathering

The plants were bagged in a semi-transparent bag (Banner, 1170535) once they have enough siliques and stopped from being watered when 60-70% of the siliques were brown. To gather the seeds, the plants were cut just above the rosette, the pot discarded and the dried siliques in the bag gently crushed to release the seeds. The content of the bag was then released on mesh round sifters of different mesh sizes on top of a folded paper. To remove as much unwanted plant material (dried siliques and leaves) as possible, the plant material was funnelled several times on the sifters until getting almost only seeds. Finally, the content was funnelled in a 1.5 ml Eppendorf tube (Starlab, S1615-5500), labelled and stored at 4°C for short to long term storage.

1.6) Phenotypic measurements

As *Arabidopsis'* rosette is not a perfect circle, I measured the two biggest leaves to measure the rosette diameter in four biological replicates of each available background. Measurements were done every three or four days from Day 15 post vernalization (pv) to Day 35 pv. Siliques were measured in three technical replicates after the plant produced at least a dozen siliques to make sure to take the longest one. 15 technical replicates were used for the comparison between Col-0 and *RNase X*.

2) Molecular work

The oligos used in this thesis are in Table S1.

2.1) RNA extraction

For all experiment involving the screening assays, RNA was extracted from roots meanwhile for the experiment involving the SALK mutants, RNA was extracted from 20-25 days old whole seedlings and snap frozen in liquid Nitrogen (LN_2). Both were extracted using the Tri Reagent protocol. Under the fume hood, frozen plant tissues in 1.5 ml Eppendorf tube were grinded in LN_2 environment with a micro pestle and 1000 µl of Tri Reagent (ThermoFisher Scientific, 11312940) was added to the tube and vortexed to dissolve the powder in solution. After a 5 minutes incubation, 200 µl of chloroform (ThermoFisher Scientific, 67-66-3) was added to the tube and mixed by inverting the tube several times. The solution was left 8 minutes at room temperature before a centrifugation at 4°C, 14000 rcf for 15min. The supernatant was then transferred to a new tube and 1000 µl of 80-100% ethanol was added, and the tube stored two hours at -80°C for the RNA to precipitate. After the precipitation step, the tube was centrifuged at 4°C, 14000 rcf for 8 minutes. The supernatant-ethanol mix was removed by carefully avoiding the newly formed pellet containing the RNA. Two subsequent washes with 950 µl 80% ethanol and centrifugation at 7500 rcf for 3 minutes at room temperature were performed. A final centrifugation of a minute at 7500 rcf was performed to pull down the maximum amount of ethanol left, removed by a finer tip (10-20 µl tips). To ensure complete removal of the ethanol, the tube was left on a heat block at 37°C, cap open, for 5 minutes or until the pellet was dried. The RNA pellet was dissolved in 15 µl dH2O, and the concentration measured by the nanodrop 8000 spectrophotometer (ThermoFisher Scientific, ND-8000-GL).

2.2) DNA extraction

A single leaf was cut and placed in 1.5 ml Eppendorf tube and snap frozen in LN_2. It was then grinded in LN_2 environment using a micro pestle. 500 µl of DNA extraction buffer (200 mM Tris HCl pH 7.5, 250 mM NaCl, 25 mM EDTA, 0.5% SDS) was added to the tube and vortexed until the plant powder was dissolved. The tube was then incubated in a hot bath at 60°C for 30 minutes, and vortexed twice during the step to ensure complete cell lysis. In the fume hood, an equal volume (500 µl) of chloroform was added and the tube centrifuged at 4°C at 15000 rcf for 5 minutes. The supernatant was transferred to fresh tube and an equal volume

(500 µl) of Isopropanol was added before putting the tube at -20°C for 30 minutes. After centrifugation at 4°C, 15000 rcf for 5 minutes, the supernatant was removed and 950 µl of 80% ethanol was added, gently dislodging the pellet. The ethanol was removed after centrifugation at 15000 rcf for 5 min and the pellet was air dried on a heat block set up at 37°C. The pellet was resuspended in 50 µl of dH_2O. In case of the presence of starch and other polysaccharides, that make the pellet hard to dissolve, the tube was centrifuged at room temperature at 15000 rcf for 5 minutes and place on ice for 2 minutes. The supernatant was transferred into a new tube and the precipitate left behind. The concentration was measured by the nanodrop.

2.3) Protein extraction

In LN_2 environment, 20-25 days old seedlings were crushed using a micro pestle. Two volume of protein extraction buffer (25 mM TRIS-HCl pH 7.6, 15 mM $MgCl_2$, 150 mM NaCl and 1 mM DTT) was added and vortexed until dissolution of the powder. The extract was incubated on ice for 30 minutes then centrifuged at 4°C, 10000 rpm for 15 minutes. The supernatant was transferred in a fresh new tube and the protein concentration was determined by Bradford assay. The Bradford assay started with a dilution series of BSA (Bovine Serum Albumin) (Sigma-Aldrich, 9048-46-8), and the samples mixed with Bradford solution (Bradford MM, 1976) incubated for 5 minutes at room temperature. The Eppendorf BioPhotometer (Eppendorf) is calibrated using the BSA and then the sample quantified at 595 nm. After quantification, the sample were diluted to a certain concentration and an equal volume of Laemmli buffer (0.125 M TRIS pH 6.8, 4% SDS, 20% Glycerol, 0.02% Bromophenol blue, 0.2 M dH_2O) was added and the proteins stored at -20°C.

2.4) DNase treatment

For the RT-qPCR, the RNA must be exempt from any trace of DNA, so the RNA was submitted to a DNase treatment, performed following the TURBO DNase protocol (Invitrogen, AM1907). For one reaction, a mix of 2.5 µl of TURBO 10x DNase buffer, 0.5 µl of TURBO DNase (1 µl per

10 µg of RNA) and a total volume of 22 µl containing dH_2O and 500 ng of RNA were mixed in a 1.5 ml Eppendorf tube and incubated on a heat block at 37°C for 30 minutes. After incubation, 2.5 µl of Inactivator was added and the content of the tube was mixed by tapping for 5 minute and then centrifuged at 10000 rcf for 1.5 minute. The supernatant (~22 µl) was transferred to a fresh tube and could be used immediately or stored at -80°C.

2.5) cDNA synthesis

For the cDNA synthesis, following the SSIV protocol (Invitrogen, 18090010), two master mixes were made. The first one containing, for one reaction, 0.5 µl of the hemiprobe (for miRNAs' quantification only) (Androvic et al., 2017) or dH_2O, 0.5 µl of dNTP and 0.5 µl of oligodT. This mix was poured in a PCR tube containing 5.65 µl of RNA, previously treated by the DNase treatment, and incubated at 65°C for 5 minutes. The second master mix was composed of, for one reaction, 2 µl of SSIV buffer, 0.5 µl 100mM DTT, 0.1 µl RNase OUT and 0.25µl of SSIV reverse transcriptase (PCR Biosystems, PB20.11-01). The PCR tube received the second mix and went through a short program in the thermocycler of 10 minutes at 50°C and 10 minutes at 80°C. The cDNA was measured by nanodrop, used immediately or stored in the fridge for short term use.

2.6) SALK genotyping PCR and gel

To genotype the SALK mutant lines, genotyping PCRs were performed. For each mutant, The SALK T-DNA insert site [http://signal.salk.edu/tdnaprimers.2.html] provided the primers sequences composed of a set of primers targeting the Wild Type (WT) and one set of primers targeting the insert (SALK). Two master mixes were prepared both containing 5.7 µl of dH_2O, 2 µl 5X Colorless GoTaq Flexi Buffer, 0.6 µl $MgCl_2$, 0.2 µl 10mM dNTPs and 0.1 µl GoTaq polymerase (Promega, M7805). Each master mixes had one set of primers; the WT master mix had 0.2 µl of Right Primer (RP) and 0.2 µl of Left Primer (LP) while the SALK master mix had 0.2 µl of RP and 0.2 µl of LB 1.3 (Left Primer 1.3). 9 µl of the master mix was transferred in a PCR tube with 1 µl of DNA and put in the thermocycler. The PCR program was composed

of a first denaturation step at 94°C for 3 min, 35 cycles of denaturation at 94° C for 30 seconds, annealing at 60° C for 30 seconds and elongation at 72° C for 2 minutes and a final extension at 72°C for 10 min before cooling down the sample at 4°C following (O'Malley et al. (2015). Once the PCR finished, the products of the WT tubes and SALK tubes were pooled according to the sample name, 4 µl of 6X loading dye (ThermoFisher Scientific, 11541575) was added to the samples before being loaded in an 2% agarose gel (10 g agarose in 500 ml 0.5X TBE) containing 7.5-10 µl Ethidium Bromide (EtBr) (Fisher Scientific, 1239-45-8) depending on the size of the gel cast. The gel went through electrophoresis at 100-120 V for 1 hour and was then scanned using the Typhoon 9500 FLA (Cytiva, 29-0002-02 AC) at 590 nm.

2.7) RT-qPCR

For mRNA RT-qPCRs, primers were designed using primer-BLAST (https://www.ncbi.nlm.nih.gov/tools/primer-blast/) ensuring a Tm close to 60°C and a product size of 100-200 nt. For miRNA RT-qPCRs, primers were designed following Androvic and al. (2017) with a Tm close to 60°C. Master mix was prepared containing for one reaction 5 µl Sybr Green Master Mix (ThermoFisher Scientific, 4344463), 0.4 µl of RP, 0.4 µl of LP and 4.2 µl of dH2O. 9 µl of the master mix was poured in each well of a 96-well plate (ThermoFisher Scientific, N8010560) and 1 µl of cDNA containing 5 ng was added to the corresponding well. 4 technical replicates were done to impair pipetting variations. The RT-qPCR program was as follow: a first step at 95°C for 2 minutes to activate the polymerase, then 40 cycles of denaturation at 95°C for 30 seconds, annealing at 60°C for 30 seconds and extension at 72°C for 60 seconds with a final extension at 72°C for 10 minutes. Ct values were collected and analysed following the Pfaffl method (Pfaffl, 2001).

2.8) Northern blot

2.8.1) Gel preparation

The first step is to prepare a denaturing 7 M Urea 15% acrylamide gel. The gel was constituted of a solution of 9.5 ml of water, 6.3 g of Urea (Fisher Scientific, 10142740), 1.5 ml of 5X TBE, 5.5 ml of 40% acrylamide bis solution 19:1 (Bio-Rad, 1610144), 7.5 µl of

Tetramethylethylenediamine (TEMED) (Sigma-Aldrich, 110-18-9) and 150 µl of 10% Ammonium Persulfate Solution (APS) (Thermo-Fisher, 17874). The solution was poured between two 1 mm glass plates (Bio-Rad, 1651824), a 1 mm comb (Bio-Rad, 1653359) placed on top and let cool down at room temperature for about 20 minutes. Once set, the two sets of plates were put in front of each other in a tank filled with 0.5X TBE and the comb removed. The wells were cleaned using a syringe to remove Urea and bits of gel trapped inside. 1-10 µg of total RNA mixed with 2X loading dye (50/50 total volume) (ThermoFisher Scientific, AM8546G) for a maximum volume of 20 µl, prewarmed at 60°C for 2 minutes, was slowly loaded in the well. The loaded gel underwent electrophoresis in a Mini-Protean Tetra Cell tank (Bio-Rad, 185-8000) at constant voltage of 90-120 V until the lowest blue line of the loading dye has reached the bottom of the gel. The gel was then transferred in a square Petri dish containing 0.5X TBE and 5 µl EtBr mix for 5 minutes and scanned using the Typhoon 9500 FLA to assure the correct loading and electrophoresis of the RNA.

2.8.2) Transference of the RNA to a nylon membrane

The transfer was done in a semi-dry transfer apparatus (ThermoFisher Scientific) by superposing three water soaked Whatman paper (ThermoFisher Scientific, 3030-335), a Hybond-NX nylon membrane (GE Healthcare Life Sciences), previously cut in the top left corner to indicate orientation, the gel and three more soaked Whatman paper as shown in Figure 55. The lid was closed and a 10-20 V courant for one hour was supplied to electrically transfer the RNA to the membrane. Another incubation of the gel in EtBr was done to validate the correct transfer of the RNA on the nylon membrane.

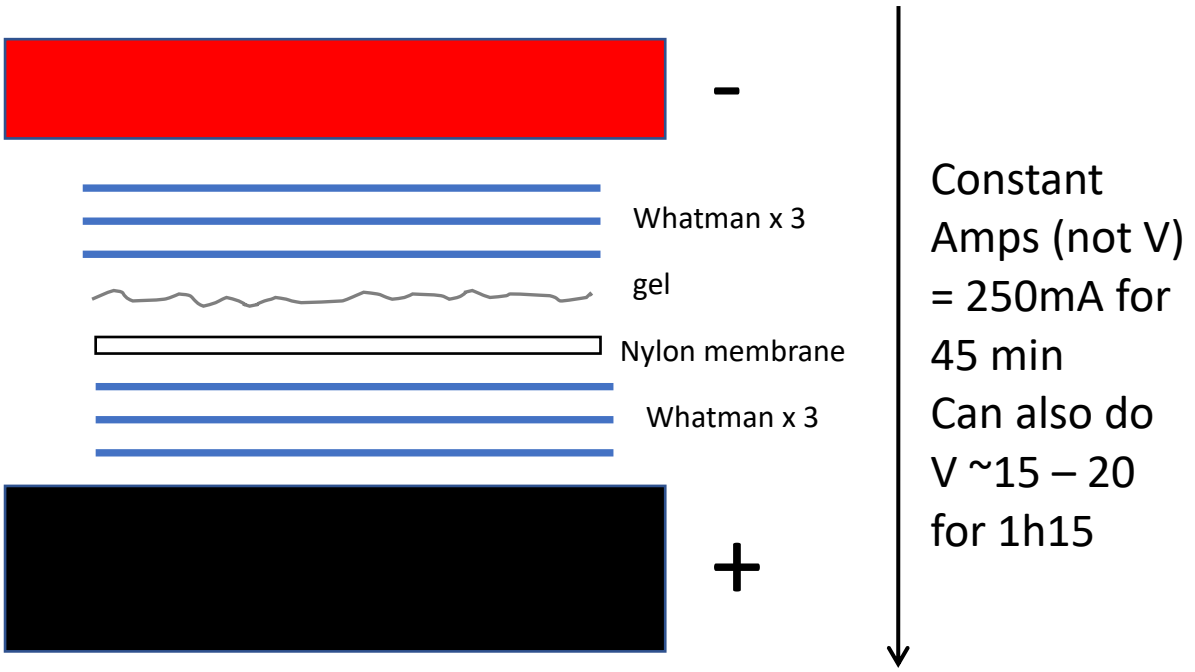

Figure 55: Semi dry transfer of the RNA from the acrylamide gel on a nylon membrane. The layout was constituted of the consecutive addition of three wet Whatman papers, one wet nylon membrane, the acrylamide gel and another three layers of wet Whatman papers. The layout underwent constant voltage of 10-20 V for about one hour.

2.8.3) Crosslinking

The RNA was chemically crosslinked to the membrane by soaking a piece of Whatman paper with a solution of 10 ml dH_2O, 122.5 µl of 12.5M 1-methylimidazole (Sigma, M50834), 10 µl of HCl (Sigma-Aldrich, H1758) and 0.373 g of EDC (1-ethyl-3-(dimethylaminopropyl)) (Thermo-Fisher, 22980). The membrane was put on top, RNA facing up, sealed in Saran wrap and left at 60°C for 90 minutes and finally rinsed with water.

2.8.4) Hybridisation

Probes targeting the miRNA of interest or U6 were labelled with γ-^{32}P (Perkin Elmer) by the T4 kinase (PNK) (New England Biolabs, M0201S). This was done by incubating on a heat block at 37°C for one hour: 2 µl of probe in 13 µl of water, 2 µl of T4 kinase buffer, 1 µl of T4 kinase and 2 µl of γ-^{32}P. In the meantime, the membrane was pre-hybridised by adding 5 ml of

ULTRAhyb-oligo buffer (Thermo-Fisher, AM8663) in a tube and put in a rotating oven (ThermoFisher Scientific) at 37° C. After the probe incubation, 30 µl of water was added to the solution and the 50 µl was transferred to the tube containing the membrane. The membrane was incubated overnight with the labelled probe at 37°C for regular probe and 60°C for LNA probe.

2.8.5) Washing the membrane

The following day, the hybridisation buffer was removed with a first rinse of 50 ml of washing solution (0.2X Saline-Sodium Citrate (SSC) and 0.1% Sodium Dodecyl Sulfate (SDS)), then, the membrane was incubated twice with 50 ml of washing solution at 37°C for 15-20 minutes, removing the solution between the two washes. A final rinse was performed, and the membrane put in a Saran wrap. Successful hybridisation was checked by using a Geiger counter. The membrane was stored in cassette (Sigma Aldrich, BAS-IP SR 2025 E) containing a Fujifilm at 4°C for exposure with variable amount of time. The Fujifilm was scanned using the Typhoon 9500 FLA at 635 nm. The intensity of the bands was measured using the ImageQuant software version 8.2.0.0 (GE Healthcare).

2.8.6) Stripping the membrane

The membrane could be reused by stripping it. This was done by incubating the membrane with a ¾ of the hybridisation tube filled with a stripping solution (0.1% SDS) at 85°C for one to two hours. The stripping of the membrane was first verified with the Geiger counter then was stored in the cassette containing the Fujifilm and later scanned to assure the correct stripping and reused up to 5 times.

2.9) sRNA library

To create sRNA library, I followed Xu et al. (2015). The 3’ HD adapters must be adenylated, and the total RNA purified by a modified version of the mirVana kit. After those preliminary

steps, the small RNA library construction can start and is a 4-day long protocol with the first day being independent while day 2,3 and 4 must be performed following each other.

2.9.1) mirVana purification of the RNA

5 µg of RNA in 50 µl of dH_2O was purified using a modified mirVana kit protocol (Ambion, AM1560) to allow a total RNA purification without using phenol. 250 µl (5X the volume of RNA) of Lysis/Binding buffer was added and the solution homogenised by pipetting. 30 µl ($1/10^{th}$ of the total volume) of Homogenate Additive was added and the mixture was left on ice for 10 minutes. Then, 412.5 µl (1.25X of the total volume) of 100% Ethanol was added and the solution transferred on a Filter Cartridge placed on a collection tube to be centrifuged at 10000 rcf for 30 seconds. After discarding the flow-through, 700 µl of miRNA Wash solution 1 was added on the filter and the tube centrifuged at 10000 rcf for 10 seconds. The flow-through was discarded and two washes of Wash solution 2/3 were performed with centrifugation at 10000 rcf for 10 seconds and a discard of the flow-through. A final centrifugation at 10000 rcf for a minute was performed to remove the maximum of residual fluids in the cartridge. The filter cartridge was transferred on a fresh collection tube and 50 µl of pre-heated (95°C) Elution solution was added and left on the filter for 2 minutes to allow the RNA to be brought in solution before centrifuging at maximum speed (~23000 rcf) for 30 seconds. The flow-through was kept and the same step was repeated with another 50 µl of Elution solution. 10 µl of 3M NaOAc ($1/10^{th}$ of the total volume) (Sigma-Aldrich, S2889) was added to the 100 µl, vortexed and left at -80°C overnight. The following day, the tube was centrifuged at maximum speed for 25 minutes and the supernatant was removed without disturbing the pellet. 700 µl of 80% Ethanol was added directly on the pellet to dislodge it. The tube was centrifuged at 7500 rcf for 3 minutes and the Ethanol removed, another centrifugation at 7500 rcf for 1 minute, to remove as much Ethanol as possible, was performed and the tube were left cap open at 37°C for 5 minutes or until the pellet was dried. The RNA pellet was eluted in 16 µl of dH_2O to allow 1 µl to be used for the Nanodrop quantification.

2.9.2) Adenylation and purification of 3’ HD adapters

The 3’ HD adapters, were adenylated using The Mth RNA ligase (NEB, E2610L). In a 1.5 ml Eppendorf tube on ice, 2 µl of the 3’ adapters, 4 µl of 10X 5’ DNA adenylation buffer, 4 µl of 10mM ATP, 4 µl of Mth ligase and 26 µl of nuclease free water were mixed and incubated at 65°C for 1 hour on a heat block. The enzyme was then inactivated by incubating the tube at 85°C for 5 minutes.

The adenylated adapters were then purified using the Oligo Clean and Concentrator 5 (Zymo-Research, D4061) following the manufacturer’s instructions. The oligonucleotides were eluted in 16 µl of dH_2O, the concentration measured with a Nanodrop and 10 µM stocks were made. To verify the adenylation, an electrophoresis on a 16% PAGE Urea gel was performed with the adapters from the stock, the adenylated adapters, and a mix of the two. After electrophoresis at 120 V for 45 minutes, the gel was incubated in a square Petri dish containing diluted EtBr for 5 minutes before being scanned on the Typhoon 9500 FLA.

2.9.3) Day 1: Addition of 5’ adapters and adenylated 3’ HD adapters to the total RNA and cDNA synthesis.

All incubations were performed in a thermocycler and the 50% PEG solution was placed at 37°C to make it easier to pipette. The first part was to ligate the adenylated 3’ HD adapters to the RNA. For that, 2 µg of purified RNA was denatured at 70°C for 2 minutes with 1.5 µl of adenylated 3’ HD adapter, then placed on ice. A mix containing 2 µl T4 RNA ligase 2 10X buffer, 0.75 µl RNAse OUT, 1 µl T4 RNA ligase 2, 3.75 µl of dH2O and 4 µl of 50% PEG solution was added to the RNA/3’HD adapter mix and incubated at 26°C for 2 hours. Once completed, 30 µl of dH2O was added to the mix and purified using the RNA Clean and Concentrator 5 kit (Zymo R1015) following the manufacturer’s instructions. 13 µl of dH2O was used to elute the RNA. 12.1 µl of RNA was then deadenylated my mixing it with 1.6 µl 10X deadenylase buffer, 0.8 µl 10mM DTT, 0.5 µl RNAse OUT (ThermoFisher Scientific, 10777019) and 1 µl 5’ deadenylase and incubated at 30°C for 30 minutes. 4 µl of 25mM EDTA was added to stop the reaction. The excess of 3’ adapters was removed by adding 2 µl 500mM Tris-HCl (pH9), 7 µl 50mM MgCl2 and 1 µl RecJ Exonuclease (NEB, M0264S) to the previous mix and incubated at

37°C for 30 minutes. The next step was to ligate the 5' HD adapters to the RNA. The required amount of 5' HD adapters was denatured at 70°C for 2 minutes and then placed on ice. A mix of 1 µl 10X T4 RNA ligase buffer, 1 µl 10mM ATP, 2 µl denatured 5' HD adapters and 1 µl T4 RNA ligase 1 (NEB, M0204S) was added to the 30 µl of RNA alongside 7 µl 50% PEG solution and incubated at 26°C for 2 hours. After incubation, 8 µl of dH2O was added to make up to 50 µl and the di-tagged RNA was purified using the RNA Clean and Concentrator 5 kit (Zymo R1015). The sample was eluted twice in 15 µl of nuclease free water. The final step was the cDNA synthesis. The 30 µl of purified di-tagged RNA was mixed with 4 µl 10X MMLV Reverse Transcription buffer, 2 µl 10mM dNTPs, 2 µl 100mM DTT, 1 µl RTP (Reverse primer) and 1 µl High performance MMLV Reverse Transcriptase (Promega, M1701) and incubated at 37°C for 20 minutes then at 85°C for 15 minutes to terminate the reaction. The cDNA could be stored at -20°C overnight or at -80°C for longer term storage.

2.9.4) Day 2: Amplification of the cDNA and selection of the miRNAs on an acrylamide gel

During day 2, the cDNA was amplified by PCR and went through gel electrophoresis to isolate the miRNAs. For each sample, 3 PCRs were simultaneously performed by mixing 9.3 µl dH2O, 0.5 µl 10mM dNTPs, 4 µl 5X High fidelity Phusion buffer, 1 µl 10µM Illumina RP-1 primer, 0.2 µl Phusion DNA polymerase (NEB, M0530S), 4 µl cDNA and 1 µl 10µM Illumina reverse index primer. The PCRs were set up as: 30 seconds at 98°C, n cycles of 10 seconds at 98°C, 30 seconds at 55°C, 15 seconds at 72°C and a final amplification at 72°C for 10 minutes to finish the program with a final hold at 10°C. The number of cycle n was 12, 14 and 16 cycles and was done to determine the best number of cycles if more amplification was needed. Then, the sample went through gel electrophoresis in an 8% PAGE gel made by pouring, between 2 glass plates, 10 ml of dH2O, 1.5 ml 5X TBE, 3 ml 40% Acrylamide bis 19:1, 150 µl APS and 7.5 µl TEMED, left for 1 hour to solidify, then was transferred in a tank filled with 0.5X TBE. The 20 µl of cDNA was mixed with 4 µl of 5X Novek loading dye ($1/5^{th}$ of total volume) and 20 µl were loaded, using long fine tips, in 3 wells according to their number of cycles in the PCR, the leftovers were combined and loaded in a 4^{th} well. 10 µl of 20bp ladder was also loaded at each end of the gel. The electrophoresis was performed at 120 V for approximately 1.5 to 2

hours until the higher light blue dye has reached the bottom of the gel. After electrophoresis, the gel was stained in a square Petri dish containing 50 ml 0.5X TBE and 5 µl Sybr Gold (ThermoFisher Scientific, S11494), covered with foil, for 2 minutes, put on a glass plate and scanned using the Typhoon 9500 FLA set up at 473 nm. The contrast and luminosity of the image was modified using ImageJ (FIJI), to allow the visibility of the bands of interest, and the image was printed at the actual size of the gel. The bands of interest were at 145-150 bp, so between the 3rd and 4th bands of the ladder, which start at 200 bp. A rectangle was drawn around those bands and between the second and third wells to ease the transfer of the gel in the tubes. By putting the glass with the gel on the print, the gel was cut using a razor blade following the rectangle. The cut gel was transferred in a punctured 0.5 ml Eppendorf tube in a 2 ml collection Eppendorf tube. The rest of the gel was scanned again to ensure the correct excision and cut again if necessary. The tube was centrifuged at maximum speed for 5 minutes to shred and collect the gel in the 2 ml tube. 400 µl of 1X NEB-2 buffer (100µl per lane) (NEB, B7002S) was added in the tube was left on a shaking plate at 150 rpm at 4°C overnight.

2.9.5) Day 3: Purification of the cDNA and re-selection of the miRNAs on an acrylamide gel

The third day consist in the purification the cDNA from the gel and perform another gel electrophoresis to ensure the correct isolation of the miRNA bands from the rest of the cDNA. Using a cut P1000 tip, the gel was transferred onto a Spin-X column placed on a collection tube and centrifuged at 2600 rpm for 5 minutes at 4°C. Roughly 400 µl of the elute was transferred into a new 2 ml Eppendorf tube and 40 µl of 3M NaOAc, 2.5 µl Glycoblue and 1300 µl of 100% chilled Ethanol was added to the mix. After being vortexed, the tube was placed at –80°C for 4-5 hours (could be left overnight but not preferable). After this incubation, the tube was centrifuged at maximum speed for 20 minutes at 4C and the supernatant removed without disturbing the pellet. 700 µl of 80% Ethanol was added to the pellet to dislodge it and the tube centrifuged at maximum speed for 2 minutes at room temperature. The Ethanol was removed without disturbing the pellet and another centrifugation at maximum speed for 1 minute was performed to pull down the maximum of the Ethanol which was removed using a finer tip. The tube was then left, cap open, at 37°C

for 5 minutes or until the pellet was dried. The pellet was finally resuspended in 15 µl nuclease free water and mixed with 3.75 µl 5x Novek loading dye. An 8% PAGE gel was set up and 5 µl of the sample was loaded in 3 wells while the leftover was loaded in a 4th well. 10 µl of 20 bp ladder was loaded at each end of the gel and the electrophoresis performed at 125 V for 1.5 hours or until the higher light blue dye has reached the bottom of the gel. As performed during day 2, the gel was stained in Sybr Gold/0.5X TBE for 2 minutes and scanned using the Typhoon 9500 FLA set up at 475nm. The image was corrected using ImageJ and printed in real size. The bands between the 3rd and 4th ladder bands, starting from the top, were cut and moved in a punctured 0.5 ml Eppendorf tube placed in a collecting 2 ml Eppendorf tube to be centrifuged at maximum speed for 5 minutes. 400 µl of 1X NEB-2 buffer (100 µl per lane) was added in the tube was left on a shaking plate at 150 rpm at 4°C overnight.

2.9.6) Day 4: Purification of the cDNA

The fourth and final day of the sRNA library construction was for the purification of the cDNA. As during day 3, using a cut P1000 tip, the gel was transferred onto a Spin-X column placed on a collection tube and centrifuged at 2600 rpm for 5 minutes at 4°C. Roughly 400 µl of the elute was transferred into a new 2 ml Eppendorf tube and 40 µl of 3M NaOAc, 2.5 µl Glycoblue and 1300 µl of 100% chilled Ethanol was added to the mix. After being vortexed, the tube was placed at –80°C for 4-5 hours (could be left overnight but not preferable). After this incubation, the tube was centrifuged at maximum speed for 20 minutes at 4C and the supernatant removed without disturbing the pellet. 700 µl of 80% Ethanol was added to the pellet to dislodge it and the tube centrifuged at maximum speed for 2 minutes at room temperature. The Ethanol was removed without disturbing the pellet and another centrifugation at maximum speed for 1 minute was performed to pull down the maximum of the Ethanol which was removed using a finer tip. The tube was then left, cap open, at 37°C for 5 minutes or until the pellet was dried. The pellet was finally resuspended in 15 µl nuclease free water and was stored at -80°C.

To ensure the purity and equal concentration of all the samples, a final 8% PAGE gel electrophoresis was performed with all samples by loading in the gel a mix of 1 µl of the cDNA library, 2 µl of 5X Novek dye and 7 µl of dH2O. The gel was stained in Sybr Gold/0.5X TBE and

scanned using the Typhoon 9500 FLA, and the quantification of the bands done using ImageQuant. The samples were sent to Earlham Institute for sequencing.

2.10) mRNA sequencing

Total RNA extracted from 20-25 days old whole plants using the same protocol previously described was cleaned using the Zymo RNA cleaning and concentrator kit (R1015) and quantified using the nanodrop 8000 spectrophotometer to verify that the requirements were met and then sent for sequencing to Novogene. They prepared the libraries using a poly-A enrichment and binding Illumina adapters, sequenced the samples, removed the adapters and the low-quality reads, and send the results.

2.11) Western blot

2.11.1) Antibodies

The primary antibodies were ordered at Abmart (Q5XET5 for HESO1, Q9LVV0 for RNase X) and are a combination of multiples monoclonal antibodies targeting the proteins of interest. Two secondary antibodies were tested, both from Abcam and targeting the primary mouse antibody, an HRP-conjugated rabbit antibody (ab6728) and a fluorescent goat antibody (ab145775).

2.11.2) Gel preparation

The western blot gel is made of the superposition of two gels, the resolving gel and the stacking gel. First, a 10% resolving gel was made on ice by mixing 7.9 ml of water, 5 ml of 1.5M TRIS pH8.8, 0.2 ml of SDS, 6.7 ml of 30% acrylamide/bis solution, 10 µl of TEMED and 200 µl of 10% APS. The solution was poured between two 1mm glass plates for ~80% of the total volume the glass plates can received. Isopropanol was then slowly added on top of the gel to create a flat top limit. After ~30min of solidification, the isopropanol was removed, and the top of the glass plates washed with water and dried using a tissue. Then a 5% stacking gel was

made with of 3.3 ml of dH2O, 1.5 ml of 0.5M TRIS pH6.8, 60 µl of 10% SDS, 1 ml of 30% acrylamide bis solution, 6 µl of TEMED and 60 µl of 10% APS and poured on top of the resolving gel. Combs were fitted on top of the gel and let set up for solidification for 30-45 minutes. Once set, the two sets of plates were put in front of each other in a tank filled with 0.5X TBE.

2.11.3) Gel electrophoresis

5-10 µg of protein/Laemmli buffer (50%/50%) in a volume of maximum 20 µl was pre-heated at 95°C for 5 minutes before being loaded in the gels with fine tips. 5 µl of visible protein ladder (Biorad, #1610374S) was added in one of the well to assess the progression of the electrophoresis. The migration of the proteins was done in 1X SDS-PAGE running buffer (Stock 10X: 30.28 g of TRIS, 144.13 g of Glycine, 10 g of SDS, qsp 1 L dH_2O) at 100 V in the stacking gel and switched to a higher voltage (150-200 V) once in the resolving gel. The end of the electrophoresis was determined by looking at the protein marker.

2.11.4) Transference of the proteins

Proteins were transferred from the gel to a PVDF membrane, pre-activated by soaking it in 100% Methanol. Like the northern blot transference step (Figure 55), three layers of soaked Whatman papers, the PVDF membrane, the gel and three layers of Whatman papers were superposed in a semi-dry transfer apparatus. The stock 10X transfer solution was made of 58.2 g of TRIS, 29.3 g of Glycine, 12.5 ml of 10% SDS in 1 L of water and the pH set at 9.2. For the soaking of the Whatman papers and membrane, a 1X solution was prepared and used. Once the apparatus closed, it went through 1 hour of continuous current at 20 V. Validation of the transfer was done by incubating the membrane in Ponceau solution for 5 minutes and scanning it using the Syngene G:Box scanner (Syngene) and the GeneSys software version 1.5.7.0 for capturing. Quantification of total proteins can be done at this step by quantifying the bands of the different samples with Fiji.

2.11.5) Blocking

For the blocking step, three buffer were made: The stock 10X TBS (10 ml TRIS pH7.5, 8.766 g NaCl and 1 L of dH_2O), fresh TBS-T (100 ml of 10X stock TBS, 1 ml of Tween 20 and 900 ml of water) and fresh TBS-T, 5% milk (100 ml of 10X stock TBS, 5 g of powder milk (MARVEL stores) and 900 ml of dH_2O). The membrane was washed in TBS-T until Ponceau was gone, then covered with TBS-T with milk and shaken at room temperature for about one hour. A last wash in TBS-T for 2 minutes was done and the membrane could either be stored in the fridge in TBS-T or immediately incubated with the primary antibody.

2.11.6) Incubation with antibodies

10 µl of primary antibody was diluted in 10 ml of TBS-T (1:1000) with 1% milk and added on top on the membrane in a square Petri dish and left shaking overnight at 4°C. The following day, the antibody solution was removed, and the membrane washed three times by shaking the membrane in TBS-T for 15 minutes at room temperature.

The membrane was then incubated at room temperature for at least one hour with a solution of 10 ml TBS-T with milk and 1 µl of the secondary antibody (1:10000). The membrane was then washed three times like with the primary antibody.

2.11.7) Detection

As two different secondary antibodies were used, two detection method were used. Detection of the HRP antibody was done using the SuperSignal West Pico Plus Chemiluminescent Substrate kit (ThermoFisher Scientific, 34579). The membrane was incubated for 5 minutes in a mix of 5 ml substrate and 5 ml stable peroxide, then moved in Saran wrap to be scanned immediately in the Syngene G:Box scanner. The fluorescent

antibody (Abcam, ab175775) was detected directly after its incubation using the Odyssey scanner at 680nm.

3) Bioinformatics

3.1) sRNA sequencing analysis

The cleaning of the sRNA analysis was performed by Dr Rocky PAYET. In short, the adapters were removed from the sequences using Cutadapt (Martin, 2011) and an additional 4 nucleotides were removed from both end. The reads were then aligned to the genome (Araport 11) and miRNAs were predicted by Shortstack (Axtell, 2013) on the default settings with miRbase (Griffiths-Jones, (2006), version 21). Results were then normalized using Deseq2 (Love et al., 2014)and figures produced with iDep (Ge et al., (2018),version 1.1) using the cleaned data, following all default parameters apart for the specie set to *A.thaliana* (TAIR10) and for the DEG analysis with an FDR cutoff <0.05 instead of <0.5. For the miTRATA analysis, the cleaned reads files were converted in tag count format using the script provided by the authors (Patel et al., 2016) and the analysis was done locally by the Meyers lab, as the online server was not working, using TAIR10 and miRbase version 22.

3.2) mRNA sequencing analysis

Novogene sent the data after removing the adapters and the low count reads. Upon receiving the data, the genome was indexed using SALMON (Patro et al., 2017) with Araport 11 reference cDNA and reads were aligned on the genome and quantified using SALMON in mapping-based mode. Results were then normalized using DeSeq2 (Love et al., 2014) and figures produced with iDep (Ge et al., 2018) following all default parameters apart for the specie set to *A.thaliana* (TAIR10) and for the DEG analysis with an FDR cutoff <0.01 instead of <0.5.

3.3) Alternative splicing analysis

Alternative splicing analysis was performed using rmats (Park et al., 2013; Shen et al., 2012, 2014, version 4.1.2) using the FASTQ files containing the mRNA sequencing reads and Araport 11 as the genome. All samples were processed at the same time and the results were converted into sashimi plots using rmats2sashimiplot (https://github.com/Xinglab/rmats2sashimiplot). Other figures were done using iDep (Ge et al., 2018) using the same parameters as used in mRNA sequencing analysis. Venn diagram was done using InteractiVenn (Heberle et al., 2015).

Chapter VIII] Legal acknowledgements

This work was supported by the UKRI-BBSRC Norwich Research Park Biosciences Doctoral Training Partnership, and we thank the Salk Institute Genomic Analysis Laboratory for providing the sequence-indexed Arabidopsis TDNA insertion mutants.

Chapter IX] References

Aklilu, E. (2021). Review on forward and reverse genetics in plant breeding. *All Life*, *14*(1), 127–135. https://doi.org/10.1080/26895293.2021.1888810

Albaqami, M., & Reddy, A. S. N. (2018). Development of an in vitro pre-mRNA splicing assay using plant nuclear extract. *Plant Methods*, *14*(1), 1–12. https://doi.org/10.1186/S13007-017-0271-6/FIGURES/5

Ali, G. S., Palusa, S. G., Golovkin, M., Prasad, J., Manley, J. L., & Reddy, A. S. N. (2007). Regulation of Plant Developmental Processes by a Novel Splicing Factor. *PLOS ONE*, *2*(5), e471. https://doi.org/10.1371/JOURNAL.PONE.0000471

Alisch, R. S., Jin, P., Epstein, M., Caspary, T., & Warren, S. T. (2007). Argonaute2 Is Essential for Mammalian Gastrulation and Proper Mesoderm Formation. *PLOS Genetics*, *3*(12), e227. https://doi.org/10.1371/JOURNAL.PGEN.0030227

Alonso, J. M., & Ecker, J. R. (2006). Moving forward in reverse: Genetic technologies to enable genome-wide phenomic screens in Arabidopsis. In *Nature Reviews Genetics* (Vol. 7, Issue 7, pp. 524–536). https://doi.org/10.1038/nrg1893

Alonso, J. M., Stepanova, A. N., Leisse, T. J., Kim, C. J., Chen, H., Shinn, P., Stevenson, D. K., Zimmerman, J., Barajas, P., Cheuk, R., Gadrinab, C., Heller, C., Jeske, A., Koesema, E., Meyers, C. C., Parker, H., Prednis, L., Ansari, Y., Choy, N., … Ecker, J. R. (2003). Genome-wide insertional mutagenesis of Arabidopsis thaliana. *Science*, *301*(5633), 653–657. https://doi.org/10.1126/science.1086391

Ameres, S. L., & Zamore, P. D. (2013). Diversifying microRNA sequence and function. *Nature Reviews Molecular Cell Biology 2013 14:8*, *14*(8), 475–488. https://doi.org/10.1038/nrm3611

Androvic, P., Valihrach, L., Elling, J., Sjoback, R., & Kubista, M. (2017). Two-tailed RT-qPCR: a novel method for highly accurate miRNA quantification. *Nucleic Acids Research*, *45*(15). https://doi.org/10.1093/NAR/GKX588

Ashkenazy, H., Abadi, S., Martz, E., Chay, O., Mayrose, I., Pupko, T., & Ben-Tal, N. (2016). ConSurf 2016: an improved methodology to estimate and visualize evolutionary conservation in macromolecules. *Nucleic Acids Research*, *44*(Web Server issue), W344. https://doi.org/10.1093/NAR/GKW408

Auerbach, D., & Stagljar, I. (2005). Yeast Two-Hybrid Protein-Protein Interaction Networks. *Proteomics and Protein-Protein Interactions*, 19–31. https://doi.org/10.1007/0-387-24532-4_2

Aukerman, M. J., & Sakai, H. (2003). Regulation of Flowering Time and Floral Organ Identity by a MicroRNA and Its APETALA2-Like Target Genes. *The Plant Cell*, *15*(11), 2730. https://doi.org/10.1105/TPC.016238

Aung, K., Lin, S. I., Wu, C. C., Huang, Y. T., Su, C. L., & Chiou, T. J. (2006). pho2, a phosphate overaccumulator, is caused by a nonsense mutation in a microRNA399 target gene. *Plant Physiology*, *141*(3), 1000–1011. https://doi.org/10.1104/pp.106.078063

Axtell, M. J. (2013). ShortStack: Comprehensive annotation and quantification of small RNA genes. *RNA*, *19*(6), 740. https://doi.org/10.1261/RNA.035279.112

Axtell, M. J., & Meyers, B. C. (2018). Revisiting criteria for plant microRNA annotation in the Era of big data. In *Plant Cell* (Vol. 30, Issue 2, pp. 272–284). American Society of Plant Biologists. https://doi.org/10.1105/tpc.17.00851

Axtell, M. J., Snyder, J. A., & Bartel, D. P. (2007). Common Functions for Diverse Small RNAs of Land Plants. *The Plant Cell*, *19*(6), 1750. https://doi.org/10.1105/TPC.107.051706

Bail, S., Swerdel, M., Liu, H., Jiao, X., Goff, L. A., Hart, R. P., & Kiledjian, M. (2010). Differential regulation of microRNA stability. *RNA*, *16*(5), 1032–1039. https://doi.org/10.1261/rna.1851510

Bajczyk, M., Lange, H., Bielewicz, D., Szewc, L., Bhat, S. S., Dolata, J., Kuhn, L., Szweykowska-Kulinska, Z., Gagliardi, D., & Jarmolowski, A. (2020). SERRATE interacts with the nuclear exosome targeting (NEXT) complex to degrade primary miRNA precursors in Arabidopsis. *Nucleic Acids Research*, *48*(12), 6839–6854. https://doi.org/10.1093/NAR/GKAA373

Balcells, I., Cirera, S., & Busk, P. K. (2011). Specific and sensitive quantitative RT-PCR of miRNAs with DNA primers. *BMC Biotechnology*, *11*, 70. https://doi.org/10.1186/1472-6750-11-70

Baran-Gale, J., Lisa Kurtz, C., Erdos, M. R., Sison, C., Young, A., Fannin, E. E., Chines, P. S., & Sethupathy, P. (2015). Addressing bias in small RNA library preparation for sequencing: A new protocol recovers microRNAs that evade capture by current methods. *Frontiers in Genetics*, *6*(DEC), 174833. https://doi.org/10.3389/FGENE.2015.00352/BIBTEX

Bartel, D. P. (2004). MicroRNAs: Genomics, Biogenesis, Mechanism, and Function. In *Cell* (Vol. 116, Issue 2, pp. 281–297). Cell Press. https://doi.org/10.1016/S0092-8674(04)00045-5

Bartel, D. P. (2009). MicroRNAs: Target Recognition and Regulatory Functions. *Cell*, *136*(2), 215–233. https://doi.org/10.1016/J.CELL.2009.01.002

Baskerville, S., & Bartel, D. P. (2005). Microarray profiling of microRNAs reveals frequent coexpression with neighboring miRNAs and host genes. *RNA*, *11*(3), 241–247. https://doi.org/10.1261/RNA.7240905

Becklin, K. M., Anderson, J. T., Gerhart, L. M., Wadgymar, S. M., Wessinger, C. A., & Ward, J. K. (2016). Examining Plant Physiological Responses to Climate Change through an Evolutionary Lens. *Plant Physiology*, *172*(2), 635–649. https://doi.org/10.1104/PP.16.00793

Behzadnia, N., Golas, M. M., Hartmuth, K., Sander, B., Kastner, B., Deckert, J., Dube, P., Will, C. L., Urlaub, H., Stark, H., & Lührmann, R. (2007). Composition and three-dimensional EM structure of double affinity-purified, human prespliceosomal A complexes. *The EMBO Journal*, *26*(6), 1737–1748. https://doi.org/10.1038/SJ.EMBOJ.7601631

Ben-Dov, C., Hartmann, B., Lundgren, J., & Valcárcel, J. (2008). Genome-wide analysis of alternative pre-mRNA splicing. *Journal of Biological Chemistry*, *283*(3), 1229–1233. https://doi.org/10.1074/jbc.R700033200

Benes, V., & Castoldi, M. (2010). Expression profiling of microRNA using real-time quantitative PCR, how to use it and what is available. *Methods (San Diego, Calif.)*, *50*(4), 244–249. https://doi.org/10.1016/J.YMETH.2010.01.026

Bernstein, E., Caudy, A. A., Hammond, S. M., & Hannon, G. J. (2001). Role for a bidentate ribonuclease in the initiation step of RNA interference. *Nature*, *409*(6818), 363–366. https://doi.org/10.1038/35053110

Bernstein, E., Kim, S. Y., Carmell, M. A., Murchison, E. P., Alcorn, H., Li, M. Z., Mills, A. A., Elledge, S. J., Anderson, K. V., & Hannon, G. J. (2003). Dicer is essential for mouse development. *Nature Genetics 2003 35:3*, *35*(3), 215–217. https://doi.org/10.1038/ng1253

Bi, D., Cheng, Y. T., Li, X., & Zhang, Y. (2010). Activation of Plant Immune Responses by a Gain-of-Function Mutation in an Atypical Receptor-Like Kinase. *Plant Physiology*, *153*(4), 1771. https://doi.org/10.1104/PP.110.158501

Bohmert, K., Camus, I., Bellini, C., Bouchez, D., Caboche, M., & Banning, C. (1998). AGO1 defines a novel locus of Arabidopsis controlling leaf development. *EMBO Journal*, *17*(1), 170–180. https://doi.org/10.1093/emboj/17.1.170

Bonnal, S., Martínez, C., Förch, P., Bachi, A., Wilm, M., & Valcárcel, J. (2008). RBM5/Luca-15/H37 Regulates Fas Alternative Splice Site Pairing after Exon Definition. *Molecular Cell*, *32*(1), 81–95. https://doi.org/10.1016/j.molcel.2008.08.008

Bouchoucha, A., Waltz, F., Bonnard, G., Arrivé, M., Hammann, P., Kuhn, L., Schelcher, C., Zuber, H., Gobert, A., & Giegé, P. (2019). Determination of protein-only RNase P interactome in Arabidopsis mitochondria and chloroplasts identifies a complex between PRORP1 and another NYN domain nuclease. *The Plant Journal*, *100*(3), 549–561. https://doi.org/10.1111/TPJ.14458

Boyes, D. C., Zayed, A. M., Ascenzi, R., McCaskill, A. J., Hoffman, N. E., Davis, K. R., & Görlach, J. (2001). Growth Stage–Based Phenotypic Analysis of Arabidopsis: A Model for High Throughput Functional Genomics in Plants. *The Plant Cell*, *13*(7), 1499–1510. https://doi.org/10.1105/TPC.010011

Bradford MM. (1976). A rapid and sensitive method for the quantitation of microgram quantities of protein utilizing the principle of protein-dye binding. *Analytical Biochemistry*, *72*(1–2), 248–254. https://doi.org/10.1006/ABIO.1976.9999

Carvalho, R. F., Carvalho, S. D., & Duque, P. (2010). The Plant-Specific SR45 Protein Negatively Regulates Glucose and ABA Signaling during Early Seedling Development in Arabidopsis. *Plant Physiology*, *154*(2), 772–783. https://doi.org/10.1104/PP.110.155523

Cerutti, L., Mian, N., & Bateman, A. (2000). Domains in gene silencing and cell differentiation proteins: The novel PAZ domain and redefinition of the Piwi domain. *Trends in Biochemical Sciences*, *25*(10), 481–482. https://doi.org/10.1016/S0968-0004(00)01641-8

Chamala, S., Feng, G., Chavarro, C., & Barbazuk, W. B. (2015). Genome-wide identification of evolutionarily conserved alternative splicing events in flowering plants. *Frontiers in Bioengineering and Biotechnology*, *3*(MAR), 133308. https://doi.org/10.3389/FBIOE.2015.00033/BIBTEX

Chang, H. M., Triboulet, R., Thornton, J. E., & Gregory, R. I. (2013). A role for the Perlman syndrome exonuclease Dis3l2 in the Lin28–let-7 pathway. *Nature 2013 497:7448*, *497*(7448), 244–248. https://doi.org/10.1038/nature12119

Charlesworth, D., & Vekemans, X. (2005). How and when did Arabidopsis thaliana become highly self-fertilising. *BioEssays : News and Reviews in Molecular, Cellular and Developmental Biology*, *27*(5), 472–476. https://doi.org/10.1002/BIES.20231

Chatterjee, S., Fasler, M., Büssing, I., & Großhans, H. (2011). Target-Mediated Protection of Endogenous MicroRNAs in C. elegans. *Developmental Cell*, *20*(3), 388–396. https://doi.org/10.1016/j.devcel.2011.02.008

Chatterjee, S., & Großhans, H. (2009). Active turnover modulates mature microRNA activity in Caenorhabditis elegans. *Nature*, *461*(7263), 546–549. https://doi.org/10.1038/nature08349

Che, X., Chai, S., Zhang, Z., & Zhang, L. (2022). Prediction of ligand binding sites using improved blind docking method with a Machine Learning-Based scoring function. *Chemical Engineering Science*, *261*, 117962. https://doi.org/10.1016/J.CES.2022.117962

Chen, C., Ridzon, D. A., Broomer, A. J., Zhou, Z., Lee, D. H., Nguyen, J. T., Barbisin, M., Xu, N. L., Mahuvakar, V. R., Andersen, M. R., Lao, K. Q., Livak, K. J., & Guegler, K. J. (2005). Real-time quantification of microRNAs by stem-loop RT-PCR. *Nucleic Acids Research*, *33*(20). https://doi.org/10.1093/NAR/GNI178

Chen, D., Yan, W., Fu, L. Y., & Kaufmann, K. (2018). Architecture of gene regulatory networks controlling flower development in Arabidopsis thaliana. *Nature Communications*, *9*(1), 1–13. https://doi.org/10.1038/s41467-018-06772-3

Chen, J., Liu, L., You, C., Gu, J., Ruan, W., Zhang, L., Gan, J., Cao, C., Huang, Y., Chen, X., & Ma, J. (2018). Structural and biochemical insights into small RNA 3' end trimming by Arabidopsis SDN1. *Nature Communications*, *9*(1). https://doi.org/10.1038/s41467-018-05942-7

Chen, J., Teotia, S., Lan, T., & Tang, G. (2021). MicroRNA Techniques: Valuable Tools for Agronomic Trait Analyses and Breeding in Rice. *Frontiers in Plant Science*, *12*, 744357. https://doi.org/10.3389/FPLS.2021.744357/BIBTEX

Chen, Q. ju, Zhang, L. peng, Song, S. ren, Wang, L., Xu, W. ping, Zhang, C. xi, Wang, S. ping, Liu, H. feng, & Ma, C. (2022). vvi-miPEP172b and vvi-miPEP3635b increase cold tolerance of grapevine by regulating the corresponding MIRNA genes. *Plant Science*, *325*, 111450. https://doi.org/10.1016/J.PLANTSCI.2022.111450

Chen, X., Liu, J., Cheng, Y., & Jia, D. (2002). HEN1 functions pleiotropically in Arabidopsis development and acts in C function in the flower. *Development*, *129*(5), 1085–1094.

Cheng, Y. J., Shang, G. D., Xu, Z. G., Yu, S., Wu, L. Y., Zhai, D., Tian, S. L., Gao, J., Wang, L., & Wang, J. W. (2021). Cell division in the shoot apical meristem is a trigger for miR156 decline and vegetative phase transition in Arabidopsis. *Proceedings of the National Academy of Sciences of the United States of America*, *118*(46). https://doi.org/10.1073/PNAS.2115667118/-/DCSUPPLEMENTAL

Cooper, G. M. (2000). *Protein Degradation*. https://www.ncbi.nlm.nih.gov/books/NBK9957/

Daines, B., Wang, H., Wang, L., Li, Y., Han, Y., Emmert, D., Gelbart, W., Wang, X., Li, W., Gibbs, R., & Chen, R. (2011). The Drosophila melanogaster transcriptome by paired-end RNA sequencing. *Genome Research*, *21*(2), 315–324. https://doi.org/10.1101/GR.107854.110

Dalmadi, Á., Miloro, F., Bálint, J., Várallyay, É., & Havelda, Z. (2021). Controlled RISC loading efficiency of miR168 defined by miRNA duplex structure adjusts ARGONAUTE1 homeostasis. *Nucleic Acids Research*, *49*(22), 12912–12928. https://doi.org/10.1093/NAR/GKAB1138

Dalmay, T., Hamilton, A., Rudd, S., Angell, S., & Baulcombe, D. C. (2000). An RNA-dependent RNA polymerase gene in arabidopsis is required for posttranscriptional gene silencing mediated by a

transgene but not by a virus. *Cell*, *101*(5), 543–553. https://doi.org/10.1016/S0092-8674(00)80864-8

Dalmay, T., Horsefield, R., Braunstein, T. H., & Baulcombe, D. C. (2001). SDE3 encodes an RNA helicase required for post-transcriptional gene silencing in Arabidopsis. *EMBO Journal*, *20*(8), 2069–2077. https://doi.org/10.1093/emboj/20.8.2069

Delhaize, E., & Randall, P. J. (1995). Characterization of a phosphate-accumulator mutant of Arabidopsis thaliana. *Plant Physiology*, *107*(1), 207–213. https://doi.org/10.1104/pp.107.1.207

Denli, A. M., Tops, B. B. J., Plasterk, R. H. A., Ketting, R. F., & Hannon, G. J. (2004). Processing of primary microRNAs by the Microprocessor complex. *Nature 2004 432:7014*, *432*(7014), 231–235. https://doi.org/10.1038/nature03049

Derrien, B., Baumberger, N., Schepetilnikov, M., Viotti, C., De Cillia, J., Ziegler-Graff, V., Isono, E., Schumacher, K., & Genschik, P. (2012). Degradation of the antiviral component ARGONAUTE1 by the autophagy pathway. *Proceedings of the National Academy of Sciences of the United States of America*, *109*(39), 15942–15946. https://doi.org/10.1073/PNAS.1209487109/SUPPL_FILE/PNAS.201209487SI.PDF

Dikaya, V., El Arbi, N., Rojas-Murcia, N., Muniz Nardeli, S., Goretti, D., & Schmid, M. (2021). Insights into the role of alternative splicing in plant temperature response. *Journal of Experimental Botany*, *72*(21), 7384–7403. https://doi.org/10.1093/JXB/ERAB234

Djami-Tchatchou, A. T., Sanan-Mishra, N., Ntushelo, K., & Dubery, I. A. (2017). Functional roles of microRNAs in agronomically important plants-potential as targets for crop improvement and protection. *Frontiers in Plant Science*, *8*, 242053. https://doi.org/10.3389/FPLS.2017.00378/BIBTEX

Dobin, A., Davis, C. A., Schlesinger, F., Drenkow, J., Zaleski, C., Jha, S., Batut, P., Chaisson, M., & Gingeras, T. R. (2013). STAR: ultrafast universal RNA-seq aligner. *Bioinformatics*, *29*(1), 15. https://doi.org/10.1093/BIOINFORMATICS/BTS635

Dong, Q., Hu, B., & Zhang, C. (2022). microRNAs and Their Roles in Plant Development. *Frontiers in Plant Science*, *13*. https://doi.org/10.3389/FPLS.2022.824240

Dong, Z., Han, M. H., & Fedoroff, N. (2008). The RNA-binding proteins HYL1 and SE promote accurate in vitro processing of pri-miRNA by DCL1. *Proceedings of the National Academy of Sciences of the United States of America*, *105*(29), 9970. https://doi.org/10.1073/PNAS.0803356105

Dorone, Y., Boeynaems, S., Flores, E., Jin, B., Hateley, S., Bossi, F., Lazarus, E., Pennington, J. G., Michiels, E., De Decker, M., Vints, K., Baatsen, P., Bassel, G. W., Otegui, M. S., Holehouse, A. S., Exposito-Alonso, M., Sukenik, S., Gitler, A. D., & Rhee, S. Y. (2021). A prion-like protein regulator of seed germination undergoes hydration-dependent phase separation. *Cell*, *184*(16), 4284-4298.e27. https://doi.org/10.1016/J.CELL.2021.06.009/ATTACHMENT/ABD9D5DF-1B47-4480-8147-F411A5FDBA7C/MMC4.XLSX

Drechsel, G., Kahles, A., Kesarwani, A. K., Stauffer, E., Behr, J., Drewe, P., Rätsch, G., & Wachter, A. (2013). Nonsense-Mediated Decay of Alternative Precursor mRNA Splicing Variants Is a Major Determinant of the Arabidopsis Steady State Transcriptome. *The Plant Cell*, *25*(10), 3726–3742. https://doi.org/10.1105/TPC.113.115485

Dreze, M., Carvunis, A.-R., Charloteaux, B., Galli, M., Pevzner, S. J., Tasan, M., Ahn, Y.-Y., Balumuri, P., Barabasi, A.-L., Bautista, V., Braun, P., Byrdsong, D., Chen, H., Chesnut, J. D., Cusick, M. E., Dangl, J. L., de los Reyes, C., Dricot, A., Duarte, M., … Yazaki, J. (2011). Evidence for Network Evolution in an Arabidopsis Interactome Map. *Science*, *333*(6042), 601–607. https://doi.org/10.1126/science.1203877

Dreze, M., Monachello, D., Lurin, C., Cusick, M. E., Hill, D. E., Vidal, M., & Braun, P. (2010). High-quality binary interactome mapping. *Methods in Enzymology*, *470*(C), 281–315. https://doi.org/10.1016/S0076-6879(10)70012-4

Earley, K., Smith, M. R., Weber, R., Gregory, B. D., & Poethig, R. S. (2010). An endogenous F-box protein regulates ARGONAUTE1 in Arabidopsis thaliana. *Silence*, *1*(1), 1–10. https://doi.org/10.1186/1758-907X-1-15/FIGURES/6

Eder, P. S., Kekuda, R., Stolc, V., & Altman, S. (1997). Characterization of two scleroderma autoimmune antigens that copurify with human ribonuclease P. *Proceedings of the National Academy of Sciences of the United States of America*, *94*(4), 1101. https://doi.org/10.1073/PNAS.94.4.1101

Ehlert, A., Weltmeier, F., Wang, X., Mayer, C. S., Smeekens, S., Vicente-Carbajosa, J., & Dröge-Laser, W. (2006). Two-hybrid protein–protein interaction analysis in Arabidopsis protoplasts: establishment of a heterodimerization map of group C and group S bZIP transcription factors. *The Plant Journal*, *46*(5), 890–900. https://doi.org/10.1111/J.1365-313X.2006.02731.X

Esakova, O., & Krasilnikov, A. S. (2010). Of proteins and RNA: The RNase P/MRP family. *RNA*, *16*(9), 1725. https://doi.org/10.1261/RNA.2214510

Eulalio, A., Huntzinger, E., & Izaurralde, E. (2008). GW182 interaction with Argonaute is essential for miRNA-mediated translational repression and mRNA decay. *Nature Structural & Molecular Biology 2008 15:4*, *15*(4), 346–353. https://doi.org/10.1038/nsmb.1405

Fabian, M. R., & Sonenberg, N. (2012). The mechanics of miRNA-mediated gene silencing: A look under the hood of miRISC. In *Nature Structural and Molecular Biology* (Vol. 19, Issue 6, pp. 586–593). https://doi.org/10.1038/nsmb.2296

Fan, L., Gao, B., Xu, Y., Flynn, N., Le, B., You, C., Li, S., Achkar, N., Manavella, P. A., Yang, Z., & Chen, X. (2022). Arabidopsis AAR2, a conserved splicing factor in eukaryotes, acts in microRNA biogenesis. *Proceedings of the National Academy of Sciences of the United States of America*, *119*(41), e2208415119. https://doi.org/10.1073/PNAS.2208415119/SUPPL_FILE/PNAS.2208415119.SD04.XLSX

Fang, Y., & Spector, D. L. (2007). Identification of Nuclear Dicing Bodies Containing Proteins for MicroRNA Biogenesis in Living Arabidopsis Plants. *Current Biology : CB*, *17*(9), 818. https://doi.org/10.1016/J.CUB.2007.04.005

F.H. CRICK. (1958). *'On protein synthesis' | Wellcome Collection*. https://wellcomecollection.org/works/z3d5fnyg

Fields, S., & Song, O. K. (1989). A novel genetic system to detect protein-protein interactions. *Nature*, *340*(6230), 245–246. https://doi.org/10.1038/340245a0

Filichkin, S. A., Priest, H. D., Givan, S. A., Shen, R., Bryant, D. W., Fox, S. E., Wong, W. K., & Mockler, T. C. (2010). Genome-wide mapping of alternative splicing in Arabidopsis thaliana. *Genome Research*, *20*(1), 45–58. https://doi.org/10.1101/GR.093302.109

Filichkin, S., Priest, H. D., Megraw, M., & Mockler, T. C. (2015). Alternative splicing in plants: directing traffic at the crossroads of adaptation and environmental stress. *Current Opinion in Plant Biology*, *24*, 125–135. https://doi.org/10.1016/J.PBI.2015.02.008

Forman, J. J., & Coller, H. A. (2010). The code within the code: microRNAs target coding regions. *Cell Cycle*, *9*(8), 1533–1541. https://doi.org/10.4161/CC.9.8.11202

Franco-Zorrilla, J. M., Valli, A., Todesco, M., Mateos, I., Puga, M. I., Rubio-Somoza, I., Leyva, A., Weigel, D., García, J. A., & Paz-Ares, J. (2007). Target mimicry provides a new mechanism for regulation of microRNA activity. *Nature Genetics 2007 39:8*, *39*(8), 1033–1037. https://doi.org/10.1038/ng2079

Frankiw, L., Baltimore, D., & Li, G. (2019). Alternative mRNA splicing in cancer immunotherapy. *Nature Reviews Immunology 2019 19:11*, *19*(11), 675–687. https://doi.org/10.1038/s41577-019-0195-7

Frey, K., & Pucker, B. (2020). Animal, Fungi, and Plant Genome Sequences Harbor Different Non-Canonical Splice Sites. *Cells 2020, Vol. 9, Page 458*, *9*(2), 458. https://doi.org/10.3390/CELLS9020458

Fromm, B., Keller, A., Yang, X., Friedlander, M. R., Peterson, K. J., & Griffiths-Jones, S. (2020). Quo vadis microRNAs? In *Trends in Genetics*. Elsevier Ltd. https://doi.org/10.1016/j.tig.2020.03.007

Frydman, J. (2003). Folding of Newly Translated Proteins In Vivo: The Role of Molecular Chaperones. *Https://Doi.Org/10.1146/Annurev.Biochem.70.1.603*, *70*, 603–648. https://doi.org/10.1146/ANNUREV.BIOCHEM.70.1.603

Fujii, H., Chiou, T. J., Lin, S. I., Aung, K., & Zhu, J. K. (2005). A miRNA involved in phosphate-starvation response in Arabidopsis. *Current Biology*, *15*(22), 2038–2043. https://doi.org/10.1016/j.cub.2005.10.016

Gandikota, M., Birkenbihl, R. P., Höhmann, S., Cardon, G. H., Saedler, H., & Huijser, P. (2007). The miRNA156/157 recognition element in the 3′ UTR of the Arabidopsis SBP box gene SPL3 prevents early flowering by translational inhibition in seedlings. *The Plant Journal*, *49*(4), 683–693. https://doi.org/10.1111/J.1365-313X.2006.02983.X

Ge, S. X., Son, E. W., & Yao, R. (2018). iDEP: an integrated web application for differential expression and pathway analysis of RNA-Seq data. *BMC Bioinformatics 2018 19:1*, *19*(1), 1–24. https://doi.org/10.1186/S12859-018-2486-6

Ghini, F., Rubolino, C., Climent, M., Simeone, I., Marzi, M. J., & Nicassio, F. (2018). Endogenous transcripts control miRNA levels and activity in mammalian cells by target-directed miRNA degradation. *Nature Communications 2018 9:1*, *9*(1), 1–15. https://doi.org/10.1038/s41467-018-05182-9

Giaever, G., Chu, A. M., Ni, L., Connelly, C., Riles, L., Véronneau, S., Dow, S., Lucau-Danila, A., Anderson, K., André, B., Arkin, A. P., Astromoff, A., El Bakkoury, M., Bangham, R., Benito, R., Brachat, S., Campanaro, S., Curtiss, M., Davis, K., … Johnston, M. (2002). Functional profiling of

the Saccharomyces cerevisiae genome. *Nature*, *418*(6896), 387–391. https://doi.org/10.1038/nature00935

Gibilisco, L., Zhou, Q., Mahajan, S., & Bachtrog, D. (2016). Alternative Splicing within and between Drosophila Species, Sexes, Tissues, and Developmental Stages. *PLOS Genetics*, *12*(12), e1006464. https://doi.org/10.1371/JOURNAL.PGEN.1006464

Gratani, L. (2014). Plant Phenotypic Plasticity in Response to Environmental Factors. *Advances in Botany*, *2014*, 1–17. https://doi.org/10.1155/2014/208747

Griffiths-Jones, S. (2006). miRBase: the microRNA sequence database. *Methods in Molecular Biology (Clifton, N.J.)*, *342*, 129–138. https://doi.org/10.1385/1-59745-123-1:129

Grimson, A., Farh, K. K. H., Johnston, W. K., Garrett-Engele, P., Lim, L. P., & Bartel, D. P. (2007). MicroRNA Targeting Specificity in Mammals: Determinants beyond Seed Pairing. *Molecular Cell*, *27*(1), 91–105. https://doi.org/10.1016/j.molcel.2007.06.017

Guerra, D., Crosatti, C., Khoshro, H. H., Mastrangelo, A. M., Mica, E., & Mazzucotelli, E. (2015). Post-transcriptional and post-translational regulations of drought and heat response in plants: A spider's web of mechanisms. *Frontiers in Plant Science*, *6*(FEB), 123379. https://doi.org/10.3389/FPLS.2015.00057/BIBTEX

Gutmann, B., Gobert, A., & Giegé, P. (2012). PRORP proteins support RNase P activity in both organelles and the nucleus in Arabidopsis. *Genes & Development*, *26*(10), 1022. https://doi.org/10.1101/GAD.189514.112

Hackenberg, M., Shi, B. J., Gustafson, P., & Langridge, P. (2013). Characterization of phosphorus-regulated miR399 and miR827 and their isomirs in barley under phosphorus-sufficient and phosphorus-deficient conditions. *BMC Plant Biology*, *13*(1), 214. https://doi.org/10.1186/1471-2229-13-214

Hacquard, T., Clavel, M., Baldrich, P., Lechner, E., Pérez-Salamó, I., Schepetilnikov, M., Derrien, B., Dubois, M., Hammann, P., Kuhn, L., Brun, D., Bouteiller, N., Baumberger, N., Vaucheret, H., Meyers, B. C., & Genschik, P. (2022). The Arabidopsis F-box protein FBW2 targets AGO1 for degradation to prevent spurious loading of illegitimate small RNA. *Cell Reports*, *39*(2). https://doi.org/10.1016/j.celrep.2022.110671

Han, J., Lee, Y., Yeom, K. H., Kim, Y. K., Jin, H., & Kim, V. N. (2004). The Drosha-DGCR8 complex in primary microRNA processing. *Genes & Development*, *18*(24), 3016. https://doi.org/10.1101/GAD.1262504

Han, J., & Mendell, J. T. (2023). MicroRNA turnover: a tale of tailing, trimming, and targets. *Trends in Biochemical Sciences*, *48*(1), 26–39. https://doi.org/10.1016/J.TIBS.2022.06.005

Han, M. H., Goud, S., Song, L., & Fedoroff, N. (2004). The Arabidopsis double-stranded RNA-binding protein HYL1 plays a role in microRNA-mediated gene regulation. *Proceedings of the National Academy of Sciences of the United States of America*, *101*(4), 1093. https://doi.org/10.1073/PNAS.0307969100

Hao, K., Wang, Y., Zhu, Z., Wu, Y., Chen, R., & Zhang, L. (2022). miR160: An Indispensable Regulator in Plant. *Frontiers in Plant Science*, *13*. https://doi.org/10.3389/FPLS.2022.833322

Hayer, K. E., Pizarro, A., Lahens, N. F., Hogenesch, J. B., & Grant, G. R. (2015). Benchmark analysis of algorithms for determining and quantifying full-length mRNA splice forms from RNA-seq data. *Bioinformatics*, *31*(24), 3938–3945. https://doi.org/10.1093/BIOINFORMATICS/BTV488

He, L., & Hannon, G. J. (2004). MicroRNAs: Small RNAs with a big role in gene regulation. In *Nature Reviews Genetics* (Vol. 5, Issue 7, pp. 522–531). https://doi.org/10.1038/nrg1379

Heberle, H., Meirelles, V. G., da Silva, F. R., Telles, G. P., & Minghim, R. (2015). InteractiVenn: A web-based tool for the analysis of sets through Venn diagrams. *BMC Bioinformatics*, *16*(1), 1–7. https://doi.org/10.1186/S12859-015-0611-3

Hetzer, M., Bilbao-Cortés, D., Walther, T. C., Gruss, O. J., & Mattaj, I. W. (2000). GTP hydrolysis by Ran is required for nuclear envelope assembly. *Molecular Cell*, *5*(6), 1013–1024. https://doi.org/10.1016/S1097-2765(00)80266-X

Ho, P. T. B., Clark, I. M., & Le, L. T. T. (2022). MicroRNA-Based Diagnosis and Therapy. *International Journal of Molecular Sciences*, *23*(13). https://doi.org/10.3390/IJMS23137167

Hollister, J. D., Smith, L. M., Guo, Y. L., Ott, F., Weigel, D., & Gaut, B. S. (2011). Transposable elements and small RNAs contribute to gene expression divergence between Arabidopsis thaliana and Arabidopsis lyrata. *Proceedings of the National Academy of Sciences of the United States of America*, *108*(6), 2322–2327. https://doi.org/10.1073/pnas.1018222108

Hutvágner, G., McLachlan, J., Pasquinelli, A. E., Bálint, É., Tuschl, T., & Zamore, P. D. (2001). A cellular function for the RNA-interference enzyme Dicer in the maturation of the let-7 small temporal RNA. *Science (New York, N.Y.)*, *293*(5531), 834–838. https://doi.org/10.1126/SCIENCE.1062961

Ibrahim, F., Rymarquis, L. A., Kim, E. J., Becker, J., Balassa, E., Green, P. J., & Cerutti, H. (2010). Uridylation of mature miRNAs and siRNAs by the MUT68 nucleotidyltransferase promotes their degradation in Chlamydomonas. *Proceedings of the National Academy of Sciences of the United States of America*, *107*(8), 3906–3911. https://doi.org/10.1073/pnas.0912632107

Iki, T., Yoshikawa, M., Nishikiori, M., Jaudal, M. C., Matsumoto-Yokoyama, E., Mitsuhara, I., Meshi, T., & Ishikawa, M. (2010). In Vitro Assembly of Plant RNA-Induced Silencing Complexes Facilitated by Molecular Chaperone HSP90. *Molecular Cell*, *39*(2), 282–291. https://doi.org/10.1016/J.MOLCEL.2010.05.014

Iwakawa, H. oki, & Tomari, Y. (2013). Molecular insights into microRNA-mediated translational repression in plants. *Molecular Cell*, *52*(4), 591–601. https://doi.org/10.1016/j.molcel.2013.10.033

Jacob, F., & Monod, J. (1961). Genetic regulatory mechanisms in the synthesis of proteins. In *Journal of Molecular Biology* (Vol. 3, Issue 3, pp. 318–356). Academic Press. https://doi.org/10.1016/S0022-2836(61)80072-7

Jarrous, N. (2002). Human ribonuclease P: subunits, function, and intranuclear localization. *RNA*, *8*(1), 1. https://doi.org/10.1017/S1355838202011184

Jarrous, N., & Altman, S. (2001). Human Ribonuclease P. *Methods in Enzymology*, *342*, 93–100. https://doi.org/10.1016/S0076-6879(01)42538-9

Jarrous, N., & Reiner, R. (2007). Human RNase P: a tRNA-processing enzyme and transcription factor. *Nucleic Acids Research*, *35*(11), 3519–3524. https://doi.org/10.1093/NAR/GKM071

Jeffares, D. C., Penkett, C. J., & Bähler, J. (2008). Rapidly regulated genes are intron poor. *Trends in Genetics*, *24*(8), 375–378. https://doi.org/10.1016/j.tig.2008.05.006

Jia, J., Long, Y., Zhang, H., Li, Z., Liu, Z., Zhao, Y., Lu, D., Jin, X., Deng, X., Xia, R., Cao, X., & Zhai, J. (2020). Post-transcriptional splicing of nascent RNA contributes to widespread intron retention in plants. *Nature Plants 2020 6:7*, *6*(7), 780–788. https://doi.org/10.1038/s41477-020-0688-1

Jover-Gil, S., Candela, H., Robles, P., Aguilera, V., Barrero, J. M., Micol, J. L., & Ponce, M. R. (2012). The MicroRNA pathway genes AGO1, HEN1 and HYL1 participate in leaf proximal-distal, venation and stomatal patterning in arabidopsis. *Plant and Cell Physiology*, *53*(7), 1322–1333. https://doi.org/10.1093/pcp/pcs077

Jumper, J., Evans, R., Pritzel, A., Green, T., Figurnov, M., Ronneberger, O., Tunyasuvunakool, K., Bates, R., Žídek, A., Potapenko, A., Bridgland, A., Meyer, C., Kohl, S. A. A., Ballard, A. J., Cowie, A., Romera-Paredes, B., Nikolov, S., Jain, R., Adler, J., … Hassabis, D. (2021). Highly accurate protein structure prediction with AlphaFold. *Nature 2021 596:7873*, *596*(7873), 583–589. https://doi.org/10.1038/s41586-021-03819-2

Jung, J. H., & Park, C. M. (2007). MIR166/165 genes exhibit dynamic expression patterns in regulating shoot apical meristem and floral development in Arabidopsis. *Planta*, *225*(6), 1327–1338. https://doi.org/10.1007/S00425-006-0439-1/FIGURES/7

Kant, S., Peng, M., & Rothstein, S. J. (2011). Genetic regulation by NLA and microRNA827 for maintaining nitrate-dependent phosphate homeostasis in Arabidopsis. *PLoS Genetics*, *7*(3), e1002021. https://doi.org/10.1371/journal.pgen.1002021

Kataoka, T., Hayashi, N., Yamaya, T., & Takahashi, H. (2004). Root-to-shoot transport of sulfate in Arabidopsis. Evidence for the role of SULTR3;5 as a component of low-affinity sulfate transport system in the root vasculature. *Plant Physiology*, *136*(4), 4198–4204. https://doi.org/10.1104/pp.104.045625

Kataoka, Y., Takeichi, M., & Uemura, T. (2001). Developmental roles and molecular characterization of a Drosophila homologue of Arabidopsis Argonaute1, the founder of a novel gene superfamily. *Genes to Cells*, *6*(4), 313–325. https://doi.org/10.1046/J.1365-2443.2001.00427.X

Kawashima, C. G., Yoshimoto, N., Maruyama-Nakashita, A., Tsuchiya, Y. N., Saito, K., Takahashi, H., & Dalmay, T. (2009). Sulphur starvation induces the expression of microRNA-395 and one of its target genes but in different cell types. *Plant Journal*, *57*(2), 313–321. https://doi.org/10.1111/j.1365-313X.2008.03690.x

Kervestin, S., & Jacobson, A. (2012). NMD: a multifaceted response to premature translational termination. *Nature Reviews Molecular Cell Biology 2012 13:11*, *13*(11), 700–712. https://doi.org/10.1038/nrm3454

Ketting, R. F., Fischer, S. E. J., Bernstein, E., Sijen, T., Hannon, G. J., & Plasterk, R. H. A. (2001). Dicer functions in RNA interference and in synthesis of small RNA involved in developmental timing in C. elegans. *Genes & Development*, *15*(20), 2654. https://doi.org/10.1101/GAD.927801

Khan, G. A., Bouraine, S., Wege, S., Li, Y., Carbonnel, M. De, Berthomieu, P., Poirier, Y., & Rouached, H. (2014). Coordination between zinc and phosphate homeostasis involves the transcription factor PHR1, the phosphate exporter PHO1, and its homologue PHO1;H3 in Arabidopsis. *Journal of Experimental Botany*, *65*(3), 871–884. https://doi.org/10.1093/jxb/ert444

Kirschner, S., Woodfield, H., Prusko, K., Koczor, M., Gowik, U., Hibberd, J. M., & Westhoff, P. (2018). Expression of SULTR2;2, encoding a low-affinity sulphur transporter, in the Arabidopsis bundle sheath and vein cells is mediated by a positive regulator. *Journal of Experimental Botany*, *69*(20), 4897–4906. https://doi.org/10.1093/jxb/ery263

Kiss, T., Marshallsay, C., & Filipowicz, W. (1992). 7-2/MRP RNAs in plant and mammalian cells: association with higher order structures in the nucleolus. *The EMBO Journal*, *11*(10), 3737. https://doi.org/10.1002/J.1460-2075.1992.TB05459.X

Klepikova, A. V., Kasianov, A. S., Gerasimov, E. S., Logacheva, M. D., & Penin, A. A. (2016). A high resolution map of the Arabidopsis thaliana developmental transcriptome based on RNA-seq profiling. *The Plant Journal*, *88*(6), 1058–1070. https://doi.org/10.1111/TPJ.13312

Knouf, E. C., Wyman, S. K., & Tewari, M. (2013). The Human TUT1 Nucleotidyl Transferase as a Global Regulator of microRNA Abundance. *PLoS ONE*, *8*(7), e69630. https://doi.org/10.1371/journal.pone.0069630

Krol, J., Busskamp, V., Markiewicz, I., Stadler, M. B., Ribi, S., Richter, J., Duebel, J., Bicker, S., Fehling, H. J., Schübeler, D., Oertner, T. G., Schratt, G., Bibel, M., Roska, B., & Filipowicz, W. (2010). Characterizing Light-Regulated Retinal MicroRNAs Reveals Rapid Turnover as a Common Property of Neuronal MicroRNAs. *Cell*, *141*(4), 618–631. https://doi.org/10.1016/j.cell.2010.03.039

Kudo, T., Sasaki, Y., Terashima, S., Matsuda-Imai, N., Takano, T., Saito, M., Kanno, M., Ozaki, S., Suwabe, K., Suzuki, G., Watanabe, M., Matsuoka, M., Takayama, S., & Yano, K. (2016). Identification of reference genes for quantitative expression analysis using large-scale RNA-seq data of Arabidopsis thaliana and model crop plants. *Genes & Genetic Systems*, *91*(2), 111–125. https://doi.org/10.1266/GGS.15-00065

Kumar, S., Verma, S., & Trivedi, P. K. (2017). Involvement of small RNAs in phosphorus and sulfur sensing, signaling and stress: Current update. *Frontiers in Plant Science*, *8*, 237019. https://doi.org/10.3389/FPLS.2017.00285/BIBTEX

Kurihara, Y. (2017). Activity and roles of Arabidopsis thaliana XRN family exoribonucleases in noncoding RNA pathways. *Journal of Plant Research*, *130*(1), 25–31. https://doi.org/10.1007/s10265-016-0887-z

Lai, E. C. (2002). Micro RNAs are complementary to 3' UTR sequence motifs that mediate negative post-transcriptional regulation. *Nature Genetics 2002 30:4*, *30*(4), 363–364. https://doi.org/10.1038/ng865

Landthaler, M., Yalcin, A., & Tuschl, T. (2004). The human DiGeorge syndrome critical region gene 8 and Its D. melanogaster homolog are required for miRNA biogenesis. *Current Biology : CB*, *14*(23), 2162–2167. https://doi.org/10.1016/J.CUB.2004.11.001

Laubinger, S., Sachsenberg, T., Zeller, G., Busch, W., Lohmann, J. U., Rätsch, G., & Weigel, D. (2008). Dual roles of the nuclear cap-binding complex and SERRATE in pre-mRNA splicing and microRNA processing in Arabidopsis thaliana. *Proceedings of the National Academy of Sciences of the United States of America*, *105*(25), 8795. https://doi.org/10.1073/PNAS.0802493105

Lauressergues, D., Couzigou, J. M., San Clemente, H., Martinez, Y., Dunand, C., Bécard, G., & Combier, J. P. (2015). Primary transcripts of microRNAs encode regulatory peptides. *Nature 2015 520:7545*, *520*(7545), 90–93. https://doi.org/10.1038/NATURE14346

Lauressergues, D., Ormancey, M., Guillotin, B., San Clemente, H., Camborde, L., Duboé, C., Tourneur, S., Charpentier, P., Barozet, A., Jauneau, A., Le Ru, A., Thuleau, P., Gervais, V., Plaza, S., & Combier, J. P. (2022). Characterization of plant microRNA-encoded peptides (miPEPs) reveals molecular mechanisms from the translation to activity and specificity. *Cell Reports*, *38*(6), 110339. https://doi.org/10.1016/J.CELREP.2022.110339

Lee, H., Yoo, S. J., Lee, J. H., Kim, W., Yoo, S. K., Fitzgerald, H., Carrington, J. C., & Ahn, J. H. (2010). Genetic framework for flowering-time regulation by ambient temperature-responsive miRNAs in Arabidopsis. *Nucleic Acids Research*, *38*(9), 3081–3093. https://doi.org/10.1093/nar/gkp1240

Lee, J. H., Ryu, H. S., Chung, K. S., Posé, D., Kim, S., Schmid, M., & Ahn, J. H. (2013). Regulation of temperature-responsive flowering by MADS-box transcription factor repressors. *Science*, *342*(6158), 628–632. https://doi.org/10.1126/SCIENCE.1241097/SUPPL_FILE/PAPV2.PDF

Lee, R. C., Feinbaum, R. L., & Ambros, V. (1993). The C. elegans heterochronic gene lin-4 encodes small RNAs with antisense complementarity to lin-14. *Cell*, *75*(5), 843–854. https://doi.org/10.1016/0092-8674(93)90529-Y

Lee, Y., Ahn, C., Han, J., Choi, H., Kim, J., Yim, J., Lee, J., Provost, P., Rådmark, O., Kim, S., & Kim, V. N. (2003). The nuclear RNase III Drosha initiates microRNA processing. *Nature 2003 425:6956*, *425*(6956), 415–419. https://doi.org/10.1038/nature01957

Li, C., & Zhang, B. (2016). MicroRNAs in Control of Plant Development. In *Journal of Cellular Physiology* (Vol. 231, Issue 2, pp. 303–313). Wiley-Liss Inc. https://doi.org/10.1002/jcp.25125

Li, J., Yang, Z., Yu, B., Liu, J., & Chen, X. (2005). Methylation protects miRNAs and siRNAs from a 3'-end uridylation activity in Arabidopsis. *Current Biology*, *15*(16), 1501–1507. https://doi.org/10.1016/j.cub.2005.07.029

Li, Q., Gao, Y., & Yang, A. (2020). Sulfur Homeostasis in Plants. *International Journal of Molecular Sciences*, *21*(23), 1–16. https://doi.org/10.3390/IJMS21238926

Li, S., Li, M., Liu, K., Zhang, H., Zhang, S., Zhang, C., & Yu, B. (2020). MAC5, an RNA-binding protein, protects pri-miRNAs from SERRATE-dependent exoribonuclease activities. *Proceedings of the National Academy of Sciences of the United States of America*, *117*(38), 23982–23990. https://doi.org/10.1073/PNAS.2008283117/SUPPL_FILE/PNAS.2008283117.SD02.XLSX

Liang, G., Li, Y., He, H., Wang, F., & Yu, D. (2013). Identification of miRNAs and miRNA-mediated regulatory pathways in Carica papaya. *Planta*, *238*(4), 739–752. https://doi.org/10.1007/S00425-013-1929-6/FIGURES/7

Liang, G., & Yu, D. (2010). Reciprocal regulation among miR395, APS and SULTR2;1 in Arabidopsis thaliana. *Plant Signaling and Behavior*, *5*(10), 1257–1259. https://doi.org/10.4161/psb.5.10.12608

Licausi, F., Ohme-Takagi, M., & Perata, P. (2013). APETALA2/Ethylene Responsive Factor (AP2/ERF) transcription factors: mediators of stress responses and developmental programs. *New Phytologist*, *199*(3), 639–649. https://doi.org/10.1111/NPH.12291

Lilienbaum, A. (2013). Relationship between the proteasomal system and autophagy. *International Journal of Biochemistry and Molecular Biology*, *4*(1), 1. /pmc/articles/PMC3627065/

Lin, S. I., Chiang, S. F., Lin, W. Y., Chen, J. W., Tseng, C. Y., Wu, P. C., & Chiou, T. J. (2008). Regulatory Network of MicroRNA399 and PHO2 by Systemic Signaling. *Plant Physiology*, *147*(2), 732–746. https://doi.org/10.1104/PP.108.116269

Lin, W. Y., Lin, Y. Y., Chiang, S. F., Syu, C., Hsieh, L. C., & Chiou, T. J. (2018). Evolution of microRNA827 targeting in the plant kingdom. *New Phytologist*, *217*(4), 1712–1725. https://doi.org/10.1111/nph.14938

Liu, Q., Wang, F., & Axtell, M. J. (2014). Analysis of Complementarity Requirements for Plant MicroRNA Targeting Using a Nicotiana benthamiana Quantitative Transient Assay. *The Plant Cell*, *26*(2), 741–753. https://doi.org/10.1105/TPC.113.120972

Liu, Y., Gao, W., Wu, S., Lu, L., Chen, Y., Guo, J., Men, S., & Zhang, X. (2020). AtXRN4 Affects the Turnover of Chosen miRNA*s in Arabidopsis. *Plants 2020, Vol. 9, Page 362*, *9*(3), 362. https://doi.org/10.3390/PLANTS9030362

Liu, Y., Yang, S., Khan, A. R., & Gan, Y. (2023). TOE1/TOE2 Interacting with GIS to Control Trichome Development in Arabidopsis. *International Journal of Molecular Sciences 2023, Vol. 24, Page 6698*, *24*(7), 6698. https://doi.org/10.3390/IJMS24076698

Liu, Y., Yang, X., Gan, J., Chen, S., Xiao, Z. X., & Cao, Y. (2022). CB-Dock2: improved protein–ligand blind docking by integrating cavity detection, docking and homologous template fitting. *Nucleic Acids Research*, *50*(W1), W159–W164. https://doi.org/10.1093/NAR/GKAC394

Lobbes, D., Rallapalli, G., Schmidt, D. D., Martin, C., & Clarke, J. (2006). SERRATE: a new player on the plant microRNA scene. *EMBO Reports*, *7*(10), 1052. https://doi.org/10.1038/SJ.EMBOR.7400806

Long, Y., Stahl, Y., Weidtkamp-Peters, S., Postma, M., Zhou, W., Goedhart, J., Sánchez-Pérez, M. I., Gadella, T. W. J., Simon, R., Scheres, B., & Blilou, I. (2017). In vivo FRET–FLIM reveals cell-type-specific protein interactions in Arabidopsis roots. *Nature 2017 548:7665*, *548*(7665), 97–102. https://doi.org/10.1038/nature23317

Long, Y., Stahl, Y., Weidtkamp-Peters, S., Smet, W., Du, Y., Gadella, T. W. J., Goedhart, J., Scheres, B., & Blilou, I. (2018). Optimizing FRET-FLIM labeling conditions to detect nuclear protein interactions at native expression levels in living Arabidopsis roots. *Frontiers in Plant Science*, *9*, 334379. https://doi.org/10.3389/FPLS.2018.00639/BIBTEX

Lorković, Z. J., & Barta, A. (2002). Genome analysis: RNA recognition motif (RRM) and K homology (KH) domain RNA-binding proteins from the flowering plant Arabidopsis thaliana. *Nucleic Acids Research*, *30*(3), 623–635. https://doi.org/10.1093/NAR/30.3.623

Love, M. I., Huber, W., & Anders, S. (2014). Moderated estimation of fold change and dispersion for RNA-seq data with DESeq2. *Genome Biology*, *15*(12), 1–21. https://doi.org/10.1186/S13059-014-0550-8/FIGURES/9

Lu, D., Yamawaki, T., Zhou, H., Chou, W. Y., Chhoa, M., Lamas, E., Escobar, S. S., Arnett, H. A., Ge, H., Juan, T., Wang, S., & Li, C. M. (2019). Limited differential expression of miRNAs and other small RNAs in LPS-stimulated human monocytes. *PLOS ONE*, *14*(3), e0214296. https://doi.org/10.1371/JOURNAL.PONE.0214296

Mallory, A. C., Bartel, D. P., & Bartel, B. (2005). MicroRNA-Directed Regulation of Arabidopsis AUXIN RESPONSE FACTOR17 Is Essential for Proper Development and Modulates Expression of Early Auxin Response Genes. *The Plant Cell*, *17*(5), 1360. https://doi.org/10.1105/TPC.105.031716

Maniatis, T., & Tasic, B. (2002). Alternative pre-mRNA splicing and proteome expansion in metazoans. *Nature 2002 418:6894*, *418*(6894), 236–243. https://doi.org/10.1038/418236a

Maple, J., & Møller, S. G. (2007). *Mutagenesis in Arabidopsis*. 197–206. https://doi.org/10.1007/978-1-59745-257-1_14

Marquez, Y., Brown, J. W. S., Simpson, C., Barta, A., & Kalyna, M. (2012). Transcriptome survey reveals increased complexity of the alternative splicing landscape in Arabidopsis. *Genome Research*, *22*(6), 1184. https://doi.org/10.1101/GR.134106.111

Martin, M. (2011). Cutadapt removes adapter sequences from high-throughput sequencing reads. *EMBnet.Journal*, *17*(1), 10–12. https://doi.org/10.14806/EJ.17.1.200

Maruyama-Nakashita, A., Nakamura, Y., Tohge, T., Saito, K., & Takahashi, H. (2006). Arabidopsis SLIM1 is a central transcriptional regulator of plant sulfur response and metabolism. *Plant Cell*, *18*(11), 3235–3251. https://doi.org/10.1105/tpc.106.046458

Marzi, M. J., Ghini, F., Cerruti, B., De Pretis, S., Bonetti, P., Giacomelli, C., Gorski, M. M., Kress, T., Pelizzola, M., Muller, H., Amati, B., & Nicassio, F. (2016). Degradation dynamics of microRNAs revealed by a novel pulse-chase approach. *Genome Research*, *26*(4), 554. https://doi.org/10.1101/GR.198788.115

Matera, A. G., & Wang, Z. (2014). A day in the life of the spliceosome. *Nature Reviews Molecular Cell Biology 2014 15:2*, *15*(2), 108–121. https://doi.org/10.1038/nrm3742

Matlin, A. J., Clark, F., & Smith, C. W. J. (2005). Understanding alternative splicing: towards a cellular code. *Nature Reviews Molecular Cell Biology 2005 6:5*, *6*(5), 386–398. https://doi.org/10.1038/nrm1645

McGrath, S. P., & Zhao, F. J. (1996). Sulphur uptake, yield responses and the interactions between nitrogen and sulphur in winter oilseed rape (Brassica napus). *The Journal of Agricultural Science*, *126*(1), 53–62. https://doi.org/10.1017/s0021859600088808

Mee, Y. P., Wu, G., Gonzalez-Sulser, A., Vaucheret, H., & Poethig, R. S. (2005). Nuclear processing and export of microRNAs in Arabidopsis. *Proceedings of the National Academy of Sciences of the United States of America*, *102*(10), 3691. https://doi.org/10.1073/PNAS.0405570102

Mei, Q., Li, X., Meng, Y., Wu, Z., Guo, M., Zhao, Y., Fu, X., & Han, W. (2012). A Facile and Specific Assay for Quantifying MicroRNA by an Optimized RT-qPCR Approach. *PLoS ONE*, *7*(10). https://doi.org/10.1371/JOURNAL.PONE.0046890

Meister, G., Landthaler, M., Peters, L., Chen, P. Y., Urlaub, H., Lührmann, R., & Tuschl, T. (2005). Identification of novel argonaute-associated proteins. *Current Biology*, *15*(23), 2149–2155. https://doi.org/10.1016/j.cub.2005.10.048

Meyers, B. C., Axtell, M. J., Bartel, B., Bartel, D. P., Baulcombe, D., Bowman, J. L., Cao, X., Carrington, J. C., Chen, X., Green, P. J., Griffiths-Jones, S., Jacobsen, S. E., Mallory, A. C., Martienssen, R. A., Poethig, R. S., Qi, Y., Vaucheret, H., Voinnet, O., Watanabe, Y., … Zhui, J. K. (2008). Criteria for annotation of plant microRNAs. In *Plant Cell* (Vol. 20, Issue 12, pp. 3186–3190). American Society of Plant Biologists. https://doi.org/10.1105/tpc.108.064311

Mi, H., Muruganujan, A., Huang, X., Ebert, D., Mills, C., Guo, X., & Thomas, P. D. (2019). Protocol Update for Large-scale genome and gene function analysis with PANTHER Classification System (v.14.0). *Nature Protocols*, *14*(3), 703. https://doi.org/10.1038/S41596-019-0128-8

Miya, A., Albert, P., Shinya, T., Desaki, Y., Ichimura, K., Shirasu, K., Narusaka, Y., Kawakami, N., Kaku, H., & Shibuya, N. (2007). CERK1, a LysM receptor kinase, is essential for chitin elicitor signaling in Arabidopsis. *Proceedings of the National Academy of Sciences of the United States of America*, *104*(49), 19613–19618. https://doi.org/10.1073/PNAS.0705147104

Modepalli, V., Fridrich, A., Agron, M., & Moran, Y. (2018). The methyltransferase HEN1 is required in Nematostella vectensis for microRNA and piRNA stability as well as larval metamorphosis. *PLoS Genetics*, *14*(8). https://doi.org/10.1371/JOURNAL.PGEN.1007590

Moran, Y., Agron, M., Praher, D., & Technau, U. (2017). The evolutionary origin of plant and animal microRNAs. In *Nature Ecology and Evolution* (Vol. 1, Issue 3, pp. 1–8). Nature Publishing Group. https://doi.org/10.1038/s41559-016-0027

Nagarajan, V. K., Jones, C. I., Newbury, S. F., & Green, P. J. (2013). XRN 5'→3' exoribonucleases: Structure, mechanisms and functions. In *Biochimica et Biophysica Acta - Gene Regulatory Mechanisms* (Vol. 1829, Issues 6–7, pp. 590–603). NIH Public Access. https://doi.org/10.1016/j.bbagrm.2013.03.005

Nath, M., & Tuteja, N. (2016). NPKS uptake, sensing, and signaling and miRNAs in plant nutrient stress. In *Protoplasma* (Vol. 253, Issue 3, pp. 767–786). Springer-Verlag Wien. https://doi.org/10.1007/s00709-015-0845-y

Nodine, M. D., & Bartel, D. P. (2010). MicroRNAs prevent precocious gene expression and enable pattern formation during plant embryogenesis. *Genes and Development*, *24*(23), 2678–2692. https://doi.org/10.1101/gad.1986710

Nozawa, M., Fujimi, M., Iwamoto, C., Onizuka, K., Fukuda, N., Ikeo, K., & Gojobori, T. (2016). Evolutionary Transitions of MicroRNA-Target Pairs. *Genome Biology and Evolution*, *8*(5), 1621–1633. https://doi.org/10.1093/GBE/EVW092

O'Malley, R. C., Barragan, C. C., & Ecker, J. R. (2015). A User's Guide to the Arabidopsis T-DNA Insertional Mutant Collections. *Methods in Molecular Biology (Clifton, N.J.)*, *1284*, 323. https://doi.org/10.1007/978-1-4939-2444-8_16

Ooms, J. J. J., Léon-Kloosterziel, K. M., Bartels, D., Koornneef, M., & Karssen, C. M. (1993). Acquisition of Desiccation Tolerance and Longevity in Seeds of Arabidopsis thaliana (A Comparative Study Using Abscisic Acid-Insensitive abi3 Mutants). *Plant Physiology*, *102*(4), 1185–1191. https://doi.org/10.1104/PP.102.4.1185

Pan, Q., Shai, O., Lee, L. J., Frey, B. J., & Blencowe, B. J. (2008). Deep surveying of alternative splicing complexity in the human transcriptome by high-throughput sequencing. *Nature Genetics 2008 40:12*, *40*(12), 1413–1415. https://doi.org/10.1038/ng.259

Papp, I., Mette, M. F., Aufsatz, W., Daxinger, L., Schauer, S. E., Ray, A., Van Der Winden, J., Matzke, M., & Matzke, A. J. M. (2003). Evidence for Nuclear Processing of Plant Micro RNA and Short Interfering RNA Precursors. *Plant Physiology*, *132*(3), 1382. https://doi.org/10.1104/PP.103.021980

Park, J. H., & Shin, C. (2014). MicroRNA-directed cleavage of targets: mechanism and experimental approaches. *BMB Reports*, *47*(8), 417. https://doi.org/10.5483/BMBREP.2014.47.8.109

Park, J. W., Tokheim, C., Shen, S., & Xing, Y. (2013). Identifying differential alternative splicing events from RNA sequencing data using RNASeq-MATS. *Methods in Molecular Biology*, *1038*, 171–179. https://doi.org/10.1007/978-1-62703-514-9_10/FIGURES/00102

Park, W., Li, J., Song, R., Messing, J., & Chen, X. (2002). CARPEL FACTORY, a Dicer Homolog, and HEN1, a Novel Protein, Act in microRNA Metabolism in Arabidopsis thaliana. *Current Biology : CB*, *12*(17), 1484. https://doi.org/10.1016/S0960-9822(02)01017-5

Patel, P., Ramachandruni, S. D., Kakrana, A., Nakano, M., & Meyers, B. C. (2016). miTRATA: a web-based tool for microRNA Truncation and Tailing Analysis. *Bioinformatics*, *32*(3), 450–452. https://doi.org/10.1093/BIOINFORMATICS/BTV583

Patro, R., Duggal, G., Love, M. I., Irizarry, R. A., & Kingsford, C. (2017). Salmon provides fast and bias-aware quantification of transcript expression. *Nature Methods 2017 14:4*, *14*(4), 417–419. https://doi.org/10.1038/nmeth.4197

Peng, T., Qiao, M., Liu, H., Teotia, S., Zhang, Z., Zhao, Y., Wang, B., Zhao, D., Shi, L., Zhang, C., Le, B., Rogers, K., Gunasekara, C., Duan, H., Gu, Y., Tian, L., Nie, J., Qi, J., Meng, F., … Tang, G. (2018). A Resource for Inactivation of MicroRNAs Using Short Tandem Target Mimic Technology in Model and Crop Plants. *Molecular Plant*, *11*(11), 1400–1417. https://doi.org/10.1016/J.MOLP.2018.09.003

Pfaff, J., Hennig, J., Herzog, F., Aebersold, R., Sattler, M., Niessing, D., & Meister, G. (2013). Structural features of Argonaute-GW182 protein interactions. *Proceedings of the National Academy of Sciences of the United States of America*, *110*(40), E3770–E3779. https://doi.org/10.1073/PNAS.1308510110/SUPPL_FILE/PNAS.201308510SI.PDF

Pfaffl, M. W. (2001). A new mathematical model for relative quantification in real-time RT–PCR. *Nucleic Acids Research*, *29*(9), e45. https://doi.org/10.1093/NAR/29.9.E45

Posé, D., Verhage, L., Ott, F., Yant, L., Mathieu, J., Angenent, G. C., Immink, R. G. H., & Schmid, M. (2013). Temperature-dependent regulation of flowering by antagonistic FLM variants. *Nature 2013 503:7476*, *503*(7476), 414–417. https://doi.org/10.1038/nature12633

Pramanik, D., Shelake, R. M., Kim, M. J., & Kim, J. Y. (2021). CRISPR-Mediated Engineering across the Central Dogma in Plant Biology for Basic Research and Crop Improvement. *Molecular Plant*, *14*(1), 127–150. https://doi.org/10.1016/J.MOLP.2020.11.002/ATTACHMENT/B00068A0-6FC5-4557-BE4B-893B33B4FDBC/MMC1.PDF

Pushpendra K. Gupta. (2015). *MicroRNAs and target mimics for crop improvement on JSTOR*. https://www.jstor.org/stable/24905528

Rajagopalan, R., Vaucheret, H., Trejo, J., & Bartel, D. P. (2006). A diverse and evolutionarily fluid set of microRNAs in Arabidopsis thaliana. *Genes & Development*, *20*(24), 3407–3425. https://doi.org/10.1101/GAD.1476406

Ramachandran, V., & Chen, X. (2008). Degradation of microRNAs by a family of exoribonucleases in Arabidopsis. *Science*, *321*(5895), 1490–1492. https://doi.org/10.1126/science.1163728

Raza, A., Charagh, S., Karikari, B., Sharif, R., Yadav, V., Mubarik, M. S., Habib, M., Zhuang, Y., Zhang, C., Chen, H., Varshney, R. K., & Zhuang, W. (2023). miRNAs for crop improvement. *Plant Physiology and Biochemistry*, *201*, 107857. https://doi.org/10.1016/J.PLAPHY.2023.107857

Reddy, A. S. N., Marquez, Y., Kalyna, M., & Barta, A. (2013). Complexity of the Alternative Splicing Landscape in Plants. *The Plant Cell*, *25*(10), 3657. https://doi.org/10.1105/TPC.113.117523

Rédei, G. P. (2008). Murashige & Skoog Medium (MS1). *Encyclopedia of Genetics, Genomics, Proteomics and Informatics*, 1290–1290. https://doi.org/10.1007/978-1-4020-6754-9_10971

Reiner, R., Ben-Asouli, Y., Krilovetzky, I., & Jarrous, N. (2006). A role for the catalytic ribonucleoprotein RNase P in RNA polymerase III transcription. *Genes & Development*, *20*(12), 1621–1635. https://doi.org/10.1101/GAD.386706

Reinhart, B. J., Slack, F. J., Basson, M., Pasquinelll, A. E., Bettlnger, J. C., Rougvle, A. E., Horvitz, H. R., & Ruvkun, G. (2000). The 21-nucleotide let-7 RNA regulates developmental timing in Caenorhabditis elegans. *Nature*, *403*(6772), 901–906. https://doi.org/10.1038/35002607

Reinhart, B. J., Weinstein, E. G., Rhoades, M. W., Bartel, B., & Bartel, D. P. (2002). MicroRNAs in plants. *Genes & Development*, *16*(13), 1616. https://doi.org/10.1101/GAD.1004402

Rhoades, M. W., Reinhart, B. J., Lim, L. P., Burge, C. B., Bartel, B., & Bartel, D. P. (2002). Prediction of plant microRNA targets. *Cell*, *110*(4), 513–520. https://doi.org/10.1016/S0092-8674(02)00863-2

Rogers, K., & Chen, X. (2013). Biogenesis, Turnover, and Mode of Action of Plant MicroRNAs. *The Plant Cell*, *25*(7), 2383. https://doi.org/10.1105/TPC.113.113159

Ross-Macdonald, P., Coelho, P. S. R., Roemer, T., Agarwal, S., Kumar, A., Jansen, R., Cheung, K. H., Sheehan, A., Symonlatis, D., Umansky, L., Heldtman, M., Nelson, F. K., Iwasaki, H., Hager, K., Gerstein, M., Miller, P., Roeder, G. S., & Snyder, M. (1999). Large-scale analysis of the yeast genome by transposon tagging and gene disruption. *Nature*, *402*(6760), 413–418. https://doi.org/10.1038/46558

Saiyed, A. N., Vasavada, A. R., & Johar, S. R. K. (2022). Recent trends in miRNA therapeutics and the application of plant miRNA for prevention and treatment of human diseases. *Future Journal of Pharmaceutical Sciences 2022 8:1*, *8*(1), 1–20. https://doi.org/10.1186/S43094-022-00413-9

Samynathan, R., Venkidasamy, B., Shanmugam, A., Ramalingam, S., & Thiruvengadam, M. (2023). Functional role of microRNA in the regulation of biotic and abiotic stress in agronomic plants. *Frontiers in Genetics*, *14*, 1272446. https://doi.org/10.3389/FGENE.2023.1272446/BIBTEX

Schmittgen, T. D., Lee, E. J., Jiang, J., Sarkar, A., Yang, L., Elton, T. S., & Chen, C. (2008). Real-time PCR quantification of precursor and mature microRNA. *Methods (San Diego, Calif.)*, *44*(1), 31. https://doi.org/10.1016/J.YMETH.2007.09.006

Schoor, J. K. Vander, Hecht, V., Aubert, G., Burstin, J., & Weller, J. L. (2021). Defining the components of the miRNA156-SPL-miR172 aging pathway in pea and their expression relative to changes in leaf morphology. *BioRxiv*, 2021.08.22.457055. https://doi.org/10.1101/2021.08.22.457055

Schwarz, D. S., Hutvágner, G., Du, T., Xu, Z., Aronin, N., & Zamore, P. D. (2003). Asymmetry in the assembly of the RNAi enzyme complex. *Cell*, *115*(2), 199–208. https://doi.org/10.1016/S0092-8674(03)00759-1

Seo, P. J., Park, M. J., Lim, M. H., Kim, S. G., Lee, M., Baldwin, I. T., & Park, C. M. (2012). A Self-Regulatory Circuit of CIRCADIAN CLOCK-ASSOCIATED1 Underlies the Circadian Clock Regulation of Temperature Responses in Arabidopsis. *The Plant Cell*, *24*(6), 2427–2442. https://doi.org/10.1105/TPC.112.098723

Seo, Y., Kim, S. S., Kim, N., Cho, S., Park, J. B., & Kim, J. H. (2020). Development of a miRNA-controlled dual-sensing system and its application for targeting miR-21 signaling in tumorigenesis. *Experimental & Molecular Medicine 2020 52:12*, *52*(12), 1989–2004. https://doi.org/10.1038/s12276-020-00537-z

Shang, X., Cao, Y., & Ma, L. (2017). Alternative Splicing in Plant Genes: A Means of Regulating the Environmental Fitness of Plants. *International Journal of Molecular Sciences 2017, Vol. 18, Page 432*, *18*(2), 432. https://doi.org/10.3390/IJMS18020432

Shen, S., Park, J. W., Huang, J., Dittmar, K. A., Lu, Z. X., Zhou, Q., Carstens, R. P., & Xing, Y. (2012). MATS: a Bayesian framework for flexible detection of differential alternative splicing from RNA-Seq data. *Nucleic Acids Research*, *40*(8), e61–e61. https://doi.org/10.1093/NAR/GKR1291

Shen, S., Park, J. W., Lu, Z. X., Lin, L., Henry, M. D., Wu, Y. N., Zhou, Q., & Xing, Y. (2014). rMATS: Robust and flexible detection of differential alternative splicing from replicate RNA-Seq data. *Proceedings of the National Academy of Sciences of the United States of America*, *111*(51), E5593–E5601. https://doi.org/10.1073/PNAS.1419161111/SUPPL_FILE/PNAS.1419161111.SD05.XLS

Sheu-Gruttadauria, J., Pawlica, P., Klum, S. M., Wang, S., Yario, T. A., Schirle Oakdale, N. T., Steitz, J. A., & MacRae, I. J. (2019). Structural Basis for Target-Directed MicroRNA Degradation. *Molecular Cell*, *75*(6), 1243-1255.e7. https://doi.org/10.1016/j.molcel.2019.06.019

Shi, R., & Chiang, V. L. (2005). Facile means for quantifying microRNA expression by real-time PCR. *BioTechniques*, *39*(4), 519–524. https://doi.org/10.2144/000112010

Shin, H., Shin, H. S., Dewbre, G. R., & Harrison, M. J. (2004). Phosphate transport in Arabidopsis: Pht1;1 and Pht1;4 play a major role in phosphate acquisition from both low- and high-phosphate environments. *Plant Journal*, *39*(4), 629–642. https://doi.org/10.1111/j.1365-313X.2004.02161.x

Sibley, C. R., Blazquez, L., & Ule, J. (2016). Lessons from non-canonical splicing. *Nature Reviews Genetics 2016 17:7*, *17*(7), 407–421. https://doi.org/10.1038/nrg.2016.46

Simkin, A., Geissler, R., McIntyre, A. B. R., & Grimson, A. (2020). Evolutionary dynamics of microRNA target sites across vertebrate evolution. *PLoS Genetics*, *16*(2). https://doi.org/10.1371/JOURNAL.PGEN.1008285

Singh, A., Gautam, V., Singh, S., Sarkar Das, S., Verma, S., Mishra, V., Mukherjee, S., & Sarkar, A. K. (2018). Plant small RNAs: advancement in the understanding of biogenesis and role in plant development. In *Planta* (Vol. 248, Issue 3, pp. 545–558). Springer Verlag. https://doi.org/10.1007/s00425-018-2927-5

Song, J., Wang, X., Song, B., Gao, L., Mo, X., Yue, L., Yang, H., Lu, J., Ren, G., Mo, B., & Chen, X. (2019). Prevalent cytidylation and uridylation of precursor miRNAs in Arabidopsis. *Nature Plants 2019 5:12*, *5*(12), 1260–1272. https://doi.org/10.1038/s41477-019-0562-1

Song, Z., Zhang, L., Wang, Y., Li, H., Li, S., Zhao, H., & Zhang, H. (2018). Constitutive expression of mir408 improves biomass and seed yield in arabidopsis. *Frontiers in Plant Science*, *8*, 312958. https://doi.org/10.3389/FPLS.2017.02114/BIBTEX

Spanudakis, E., & Jackson, S. (2014). The role of microRNAs in the control of flowering time. *Journal of Experimental Botany*, *65*(2), 365–380. https://doi.org/10.1093/JXB/ERT453

Speth, C., Szabo, E. X., Martinho, C., Collani, S., zur Oven-Krockhaus, S., Richter, S., Droste-Borel, I., Macek, B., Stierhof, Y. D., Schmid, M., Liu, C., & Laubinger, S. (2018). Arabidopsis RNA processing factor SERRATE regulates the transcription of intronless genes. *ELife*, *7*. https://doi.org/10.7554/ELIFE.37078

Srere, P. A. (1999). Protein interactions. *Methods (San Diego, Calif.)*, *19*(2), 193. https://doi.org/10.1074/mcp.m100037-mcp200

Stepien, A., Knop, K., Dolata, J., Taube, M., Bajczyk, M., Barciszewska-Pacak, M., Pacak, A., Jarmolowski, A., & Szweykowska-Kulinska, Z. (2017). Posttranscriptional coordination of splicing and miRNA biogenesis in plants. *Wiley Interdisciplinary Reviews. RNA*, *8*(3). https://doi.org/10.1002/WRNA.1403

Sugliani, M., Brambilla, V., Clerkx, E. J. M., Koornneef, M., & Soppe, W. J. J. (2010). Conserved Splicing Factor SUA Controls Alternative Splicing of the Developmental Regulator ABI3 in Arabidopsis. *The Plant Cell*, *22*(6), 1936–1946. https://doi.org/10.1105/TPC.110.074674

Swinburne, I. A., & Silver, P. A. (2008). Intron Delays and Transcriptional Timing during Development. *Developmental Cell*, *14*(3), 324. https://doi.org/10.1016/J.DEVCEL.2008.02.002

Syed, N. H., Kalyna, M., Marquez, Y., Barta, A., & Brown, J. W. S. (2012). Alternative splicing in plants – coming of age. *Trends in Plant Science*, *17*(10), 616–623. https://doi.org/10.1016/J.TPLANTS.2012.06.001

Szarzynska, B., Sobkowiak, L., Pant, B. D., Balazadeh, S., Scheible, W. R., Mueller-Roeber, B., Jarmolowski, A., & Szweykowska-Kulinska, Z. (2009). Gene structures and processing of Arabidopsis thaliana HYL1-dependent pri-miRNAs. *Nucleic Acids Research*, *37*(9), 3083–3093. https://doi.org/10.1093/NAR/GKP189

Szweykowska-Kulinska, Z., Jarmolowski, A., & Vazquez, F. (2013). The crosstalk between plant microRNA biogenesis factors and the spliceosome. *Plant Signaling & Behavior*, *8*(11). https://doi.org/10.4161/PSB.26955

Takahashi, H., Watanabe-Takahashi, A., Smith, F. W., Blake-Kalff, M., Hawkesford, M. J., & Saito, K. (2000). The roles of three functional sulphate transporters involved in uptake and translocation of sulphate in Arabidopsis thaliana. *Plant Journal*, *23*(2), 171–182. https://doi.org/10.1046/j.1365-313X.2000.00768.x

Takahashi, H., Yamazaki, M., Sasakura, N., Watanabe, A., Leustek, T., De Almeida Engler, J., Engler, G., Van Montagu, M., & Saito, K. (1997). Regulation of sulfur assimilation in higher plants: A sulfate transporter induced in sulfate-starved roots plays a central role in Arabidopsis thaliana. *Proceedings of the National Academy of Sciences of the United States of America*, *94*(20), 11102–11107. https://doi.org/10.1073/pnas.94.20.11102

Teng, C., Zhang, C., Guo, F., Song, L., & Fang, Y. (2023). Advances in the Study of the Transcriptional Regulation Mechanism of Plant miRNAs. *Life 2023, Vol. 13, Page 1917*, *13*(9), 1917. https://doi.org/10.3390/LIFE13091917

Teotia, S., & Tang, G. (2015). To Bloom or Not to Bloom: Role of MicroRNAs in Plant Flowering. *Molecular Plant*, *8*(3), 359–377. https://doi.org/10.1016/J.MOLP.2014.12.018

Thornton, J. E., Du, P., Jing, L., Sjekloca, L., Lin, S., Grossi, E., Sliz, P., Zon, L. I., & Gregory, R. I. (2014). Selective microRNA uridylation by Zcchc6 (TUT7) and Zcchc11 (TUT4). *Nucleic Acids Research*, *42*(18), 11777–11791. https://doi.org/10.1093/nar/gku805

To, A., Valon, C., Savino, G., Guilleminot, J., Devic, M., Giraudat, J., & Parcy, F. (2006). A Network of Local and Redundant Gene Regulation Governs Arabidopsis Seed Maturation. *The Plant Cell*, *18*(7), 1642–1651. https://doi.org/10.1105/TPC.105.039925

Todesco, M., Rubio-Somoza, I., Paz-Ares, J., & Weigel, D. (2010). A Collection of Target Mimics for Comprehensive Analysis of MicroRNA Function in Arabidopsis thaliana. *PLoS Genetics*, *6*(7), 1–10. https://doi.org/10.1371/JOURNAL.PGEN.1001031

Tsai, H. L., Li, Y. H., Hsieh, W. P., Lin, M. C., Ahn, J. H., & Wu, S. H. (2014). HUA ENHANCER1 is involved in posttranscriptional regulation of positive and negative regulators in Arabidopsis photomorphogenesis. *Plant Cell*, *26*(7), 2858–2872. https://doi.org/10.1105/tpc.114.126722

Tu, B., Liu, L., Xu, C., Zhai, J., Li, S., Lopez, M. A., Zhao, Y., Yu, Y., Ramachandran, V., Ren, G., Yu, B., Li, S., Meyers, B. C., Mo, B., & Chen, X. (2015). Distinct and Cooperative Activities of HESO1 and URT1 Nucleotidyl Transferases in MicroRNA Turnover in Arabidopsis. *PLoS Genetics*, *11*(4). https://doi.org/10.1371/JOURNAL.PGEN.1005119

Tworak, A., Urbanowicz, A., Podkowinski, J., Kurzynska-Kokorniak, A., Koralewska, N., & Figlerowicz, M. (2016). Six Medicago truncatula Dicer-like protein genes are expressed in plant cells and upregulated in nodules. *Plant Cell Reports*, *35*(5), 1043. https://doi.org/10.1007/S00299-016-1936-8

Ustianenko, D., Hrossova, D., Potesil, D., Chalupnikova, K., Hrazdilova, K., Pachernik, J., Cetkovska, K., Uldrijan, S., Zdrahal, Z., & Vanacova, S. (2013). Mammalian DIS3L2 exoribonuclease targets the uridylated precursors of let-7 miRNAs. *RNA*, *19*(12), 1632. https://doi.org/10.1261/RNA.040055.113

Vaucheret, H., Vazquez, F., Crété, P., & Bartel, D. P. (2004). The action of ARGONAUTE1 in the miRNA pathway and its regulation by the miRNA pathway are crucial for plant development. *Genes & Development*, *18*(10), 1187. https://doi.org/10.1101/GAD.1201404

Versaw, W. K., & Harrison, M. J. (2002). A chloroplast phosphate transporter, PHT2;1, influences allocation of phosphate within the plant and phosphate-starvation responses. *Plant Cell*, *14*(8), 1751–1766. https://doi.org/10.1105/tpc.002220

Voinnet, O. (2009). Origin, Biogenesis, and Activity of Plant MicroRNAs. *Cell*, *136*(4), 669–687. https://doi.org/10.1016/J.CELL.2009.01.046

Wan, J., Zhang, X. C., Neece, D., Ramonell, K. M., Clough, S., Kim, S. Y., Stacey, M. G., & Stacey, G. (2008). A LysM receptor-like kinase plays a critical role in chitin signaling and fungal resistance in Arabidopsis. *The Plant Cell*, *20*(2), 471–481. https://doi.org/10.1105/TPC.107.056754

Wang, B. B., & Brendel, V. (2006). Genomewide comparative analysis of alternative splicing in plants. *Proceedings of the National Academy of Sciences of the United States of America*, *103*(18), 7175–7180. https://doi.org/10.1073/PNAS.0602039103/SUPPL_FILE/02039TABLE4.PDF

Wang, D., Lu, M., Miao, J., Li, T., Wang, E., & Cui, Q. (2009). Cepred: Predicting the Co-Expression Patterns of the Human Intronic microRNAs with Their Host Genes. *PLOS ONE*, *4*(2), e4421. https://doi.org/10.1371/JOURNAL.PONE.0004421

Wang, E. T., Sandberg, R., Luo, S., Khrebtukova, I., Zhang, L., Mayr, C., Kingsmore, S. F., Schroth, G. P., & Burge, C. B. (2008). Alternative isoform regulation in human tissue transcriptomes. *Nature 2008 456:7221*, *456*(7221), 470–476. https://doi.org/10.1038/nature07509

Wang, H., Wang, J., Jiang, J., Chen, S., Guan, Z., Liao, Y., & Chen, F. (2014). Reference genes for normalizing transcription in diploid and tetraploid Arabidopsis. *Scientific Reports 2014 4:1*, *4*(1), 1–8. https://doi.org/10.1038/srep06781

Wang, J., Mei, J., & Ren, G. (2019). Plant microRNAs: Biogenesis, homeostasis, and degradation. *Frontiers in Plant Science*, *10*, 433008. https://doi.org/10.3389/FPLS.2019.00360/BIBTEX

Wang, J. W., Czech, B., & Weigel, D. (2009). miR156-Regulated SPL Transcription Factors Define an Endogenous Flowering Pathway in Arabidopsis thaliana. *Cell*, *138*(4), 738–749. https://doi.org/10.1016/j.cell.2009.06.014

Wang, J. W., Wang, L. J., Mao, Y. B., Cai, W. J., Xue, H. W., & Chen, X. Y. (2005). Control of Root Cap Formation by MicroRNA-Targeted Auxin Response Factors in Arabidopsis. *The Plant Cell*, *17*(8), 2204. https://doi.org/10.1105/TPC.105.033076

Wang, X., Wang, Y., Dou, Y., Chen, L., Wang, J., Jiang, N., Guo, C., Yao, Q., Wang, C., Liu, L., Yu, B., Zheng, B., Chekanova, J. A., Ma, J., & Ren, G. (2018). Degradation of unmethylated miRNA/miRNA*s by a DEDDy-type 3′ to 5′ exoribonuclease Atrimmer 2 in Arabidopsis. *Proceedings of the National Academy of Sciences of the United States of America*, *115*(28), E6659–E6667. https://doi.org/10.1073/PNAS.1721917115/-/DCSUPPLEMENTAL

Wang, X., Zhang, S., Dou, Y., Zhang, C., Chen, X., Yu, B., & Ren, G. (2015). Synergistic and Independent Actions of Multiple Terminal Nucleotidyl Transferases in the 3′ Tailing of Small RNAs in Arabidopsis. *PLOS Genetics*, *11*(4), e1005091. https://doi.org/10.1371/JOURNAL.PGEN.1005091

Wei, S. J., Chai, S., Zhu, R. M., Duan, C. Y., Zhang, Y., & Li, S. (2020). HUA ENHANCER1 Mediates Ovule Development. *Frontiers in Plant Science*, *11*, 533172. https://doi.org/10.3389/FPLS.2020.00397/BIBTEX

Weidtkamp-Peters, S., & Stahl, Y. (2017). The use of FRET/FLIM to study proteins interacting with plant receptor kinases. *Methods in Molecular Biology*, *1621*, 163–175. https://doi.org/10.1007/978-1-4939-7063-6_16/FIGURES/5

Will, C. L., & Lührmann, R. (2011). Spliceosome Structure and Function. *Cold Spring Harbor Perspectives in Biology*, *3*(7), a003707. https://doi.org/10.1101/CSHPERSPECT.A003707

Willmann, R., Lajunen, H. M., Erbs, G., Newman, M. A., Kolb, D., Tsuda, K., Katagiri, F., Fliegmann, J., Bono, J. J., Cullimore, J. V., Jehle, A. K., Götz, F., Kulik, A., Molinaro, A., Lipka, V., Gust, A. A., & Nürnberger, T. (2011). Arabidopsis lysin-motif proteins LYM1 LYM3 CERK1 mediate bacterial peptidoglycan sensing and immunity to bacterial infection. *Proceedings of the National*

Academy of Sciences of the United States of America, *108*(49), 19824–19829. https://doi.org/10.1073/PNAS.1112862108

Winzeler, E. A., Shoemaker, D. D., Astromoff, A., Liang, H., Anderson, K., Andre, B., Bangham, R., Benito, R., Boeke, J. D., Bussey, H., Chu, A. M., Connelly, C., Davis, K., Dietrich, F., Dow, S. W., El Bakkoury, M., Foury, F., Friend, S. H., Gentalen, E., … Davis, R. W. (1999). Functional characterization of the S. cerevisiae genome by gene deletion and parallel analysis. *Science*, *285*(5429), 901–906. https://doi.org/10.1126/science.285.5429.901

Wu, G. (2013). Plant MicroRNAs and Development. In *Journal of Genetics and Genomics* (Vol. 40, Issue 5, pp. 217–230). https://doi.org/10.1016/j.jgg.2013.04.002

Wu, G., Park, M. Y., Conway, S. R., Wang, J. W., Weigel, D., & Poethig, R. S. (2009). The sequential action of miR156 and miR172 regulates developmental timing in Arabidopsis. *Cell*, *138*(4), 750. https://doi.org/10.1016/J.CELL.2009.06.031

Wu, G., & Poethig, R. S. (2006). Temporal Regulation of Shoot Development in Arabidopsis Thaliana By Mir156 and Its Target SPL3. *Development (Cambridge, England)*, *133*(18), 3539. https://doi.org/10.1242/DEV.02521

Wu, X., Shi, Y., Li, J., Xu, L., Fang, Y., Li, X., & Qi, Y. (2013). A role for the RNA-binding protein MOS2 in microRNA maturation in Arabidopsis. *Cell Research 2013 23:5*, *23*(5), 645–657. https://doi.org/10.1038/cr.2013.23

Xiao, Y., Liu, T. M., & MacRae, I. J. (2023). A tiny loop in the Argonaute PIWI domain tunes small RNA seed strength. *EMBO Reports*, *24*(6). https://doi.org/10.15252/EMBR.202255806

Xie, F., Wang, J., & Zhang, B. (2023). RefFinder: a web-based tool for comprehensively analyzing and identifying reference genes. *Functional and Integrative Genomics*, *23*(2), 1–5. https://doi.org/10.1007/S10142-023-01055-7/FIGURES/2

Xie, K., Wu, C., & Xiong, L. (2006). Genomic Organization, Differential Expression, and Interaction of SQUAMOSA Promoter-Binding-Like Transcription Factors and microRNA156 in Rice. *Plant Physiology*, *142*(1), 280. https://doi.org/10.1104/PP.106.084475

Xie, Z., Kasschau, K. D., & Carrington, J. C. (2003). Negative feedback regulation of Dicer-Like1 in Arabidopsis by microRNA-guided mRNA degradation. *Current Biology*, *13*(9), 784–789. https://doi.org/10.1016/S0960-9822(03)00281-1

Xu, P., Billmeier, M., Mohorianu, I., Green, D., Fraser, W. D., & Dalmay, T. (2015). An improved protocol for small RNA library construction using High Definition adapters. *Methods in Next Generation Sequencing*, *2*(1). https://doi.org/10.1515/MNGS-2015-0001

Yan, K., Liu, P., Wu, C. A., Yang, G. D., Xu, R., Guo, Q. H., Huang, J. G., & Zheng, C. C. (2012). Stress-Induced Alternative Splicing Provides a Mechanism for the Regulation of MicroRNA Processing in Arabidopsis thaliana. *Molecular Cell*, *48*(4), 521–531. https://doi.org/10.1016/j.molcel.2012.08.032

Yang, A., Shao, T. J., Bofill-De Ros, X., Lian, C., Villanueva, P., Dai, L., & Gu, S. (2020). AGO-bound mature miRNAs are oligouridylated by TUTs and subsequently degraded by DIS3L2. *Nature Communications 2020 11:1*, *11*(1), 1–13. https://doi.org/10.1038/s41467-020-16533-w

Yang, G. D., Yan, K., Wu, B. J., Wang, Y. H., Gao, Y. X., & Zheng, C. C. (2012). Genomewide analysis of intronic microRNAs in rice and Arabidopsis. *Journal of Genetics*, *91*(3), 313–324. https://doi.org/10.1007/S12041-012-0199-6/TABLES/3

Yang, L., Liu, Z., Lu, F., Dong, A., & Huang, H. (2006). SERRATE is a novel nuclear regulator in primary microRNA processing in Arabidopsis. *The Plant Journal*, *47*(6), 841–850. https://doi.org/10.1111/J.1365-313X.2006.02835.X

Yang, L., Wu, G., & Poethig, R. S. (2012). Mutations in the GW-repeat protein SUO reveal a developmental function for microRNA-mediated translational repression in Arabidopsis. *Proceedings of the National Academy of Sciences of the United States of America*, *109*(1), 315–320. https://doi.org/10.1073/PNAS.1114673109/SUPPL_FILE/PNAS.201114673SI.PDF

Yang, X., Ren, W., Zhao, Q., Zhang, P., Wu, F., & He, Y. (2014). Homodimerization of HYL1 ensures the correct selection of cleavage sites in primary miRNA. *Nucleic Acids Research*, *42*(19), 12224. https://doi.org/10.1093/NAR/GKU907

Yang, Z., Ebright, Y. W., Yu, B., & Chen, X. (2006). HEN1 recognizes 21–24 nt small RNA duplexes and deposits a methyl group onto the 2′ OH of the 3′ terminal nucleotide. *Nucleic Acids Research*, *34*(2), 667. https://doi.org/10.1093/NAR/GKJ474

Yi, R., Qin, Y., Macara, I. G., & Cullen, B. R. (2003). Exportin-5 mediates the nuclear export of pre-microRNAs and short hairpin RNAs. *Genes & Development*, *17*(24), 3011. https://doi.org/10.1101/GAD.1158803

Yoshimoto, N., Takahashi, H., Smith, F. W., Yamaya, T., & Saito, K. (2002). Two distinct high-affinity sulfate transporters with different inducibilities mediate uptake of sulfate in Arabidopsis roots. *Plant Journal*, *29*(4), 465–473. https://doi.org/10.1046/j.0960-7412.2001.01231.x

Yu, B., Bi, L., Zhai, J., Agarwal, M., Li, S., Wu, Q., Ding, S. W., Meyers, B. C., Vaucheret, H., & Chen, X. (2010). siRNAs compete with miRNAs for methylation by HEN1 in Arabidopsis. *Nucleic Acids Research*, *38*(17), 5844. https://doi.org/10.1093/NAR/GKQ348

Yu, B., Yang, Z., Li, J., Minakhina, S., Yang, M., Padgett, R. W., Steward, R., & Chen, X. (2005). Methylation as a Crucial Step in Plant microRNA Biogenesis. *Science (New York, N.Y.)*, *307*(5711), 932. https://doi.org/10.1126/SCIENCE.1107130

Yu, H., & Gerstein, M. (2006). Genomic analysis of the hierarchical structure of regulatory networks. *Proceedings of the National Academy of Sciences of the United States of America*, *103*(40), 14724–14731. https://doi.org/10.1073/pnas.0508637103

Yu, Y., Ji, L., Le, B. H., Zhai, J., Chen, J., Luscher, E., Gao, L., Liu, C., Cao, X., Mo, B., Ma, J., Meyers, B. C., & Chen, X. (2017). ARGONAUTE10 promotes the degradation of miR165/6 through the SDN1 and SDN2 exonucleases in Arabidopsis. *PLOS Biology*, *15*(2), e2001272. https://doi.org/10.1371/JOURNAL.PBIO.2001272

Yu, Y., Jia, T., & Chen, X. (2017). The 'how' and 'where' of plant microRNAs. *New Phytologist*, *216*(4), 1002–1017. https://doi.org/10.1111/NPH.14834

Yuan, J., Wang, X., Qu, S., Shen, T., Li, M., & Zhu, L. (2023). The roles of miR156 in abiotic and biotic stresses in plants. *Plant Physiology and Biochemistry*, *204*, 108150. https://doi.org/10.1016/J.PLAPHY.2023.108150

Zhai, J., Zhao, Y., Simon, S. A., Huang, S., Petsch, K., Arikit, S., Pillay, M., Ji, L., Xie, M., Cao, X., Yu, B., Timmermans, M., Yang, B., Chen, X., & Meyersa, B. C. (2013). Plant MicroRNAs Display Differential 3' Truncation and Tailing Modifications That Are ARGONAUTE1 Dependent and Conserved Across Species. *The Plant Cell*, *25*(7), 2417–2428. https://doi.org/10.1105/TPC.113.114603

Zhan, X., Qian, B., Cao, F., Wu, W., Yang, L., Guan, Q., Gu, X., Wang, P., Okusolubo, T. A., Dunn, S. L., Zhu, J. K., & Zhu, J. (2015). An Arabidopsis PWI and RRM motif-containing protein is critical for pre-mRNA splicing and ABA responses. *Nature Communications 2015 6:1*, *6*(1), 1–12. https://doi.org/10.1038/ncomms9139

Zhang, B., Wang, L., Zeng, L., Zhang, C., & Ma, H. (2015). Arabidopsis TOE proteins convey a photoperiodic signal to antagonize CONSTANS and regulate flowering time. *Genes & Development*, *29*(9), 975–987. https://doi.org/10.1101/GAD.251520.114

Zhang, C., Fan, L., Le, B. H., Ye, P., Mo, B., & Chen, X. (2020). Regulation of ARGONAUTE10 Expression Enables Temporal and Spatial Precision in Axillary Meristem Initiation in Arabidopsis. *Developmental Cell*, *55*(5), 603-616.e5. https://doi.org/10.1016/J.DEVCEL.2020.10.019

Zhang, C., Hughes, M., & Clarke, P. R. (1999). Ran-GTP stabilises microtubule asters and inhibits nuclear assembly in Xenopus egg extracts. *Journal of Cell Science*, *112*(14), 2453–2461. https://doi.org/10.1242/JCS.112.14.2453

Zhang, W., Murphy, C., & Sieburth, L. E. (2010). Conserved RNaseII domain protein functions in cytoplasmic mRNA decay and suppresses Arabidopsis decapping mutant phenotypes. *Proceedings of the National Academy of Sciences of the United States of America*, *107*(36), 15981–15985. https://doi.org/10.1073/pnas.1007060107

Zhang, Y., Ma, Y., Liu, R., & Li, G. (2022). Genome-Wide Characterization and Expression Analysis of KH Family Genes Response to ABA and SA in Arabidopsis thaliana. *International Journal of Molecular Sciences*, *23*(1), 511. https://doi.org/10.3390/IJMS23010511/S1

Zhang, Z., Hu, F., Sung, M. W., Shu, C., Castillo-González, C., Koiwa, H., Tang, G., Dickman, M., Li, P., & Zhang, X. (2017). RISC-interacting clearing 3'- 5' exoribonucleases (RICEs) degrade uridylated cleavage fragments to maintain functional RISC in Arabidopsis thaliana. *ELife*, *6*. https://doi.org/10.7554/ELIFE.24466

Zhang, Z., Liu, Y., Ding, P., Li, Y., Kong, Q., & Zhang, Y. (2014). Splicing of Receptor-Like Kinase-Encoding SNC4 and CERK1 is Regulated by Two Conserved Splicing Factors that Are Required for Plant Immunity. *Molecular Plant*, *7*(12), 1766. https://doi.org/10.1093/MP/SSU103

Zhao, D., Wei, M., Shi, M., Hao, Z., & Tao, J. (2017). Identification and comparative profiling of miRNAs in herbaceous peony (Paeonia lactiflora Pall.) with red/yellow bicoloured flowers. *Scientific Reports*, *7*(1), 1–13. https://doi.org/10.1038/srep44926

Zhao, F. J., Hawkesford, M. J., & McGrath, S. P. (1999). Sulphur assimilation and effects on yield and quality of wheat. *Journal of Cereal Science*, *30*(1), 1–17. https://doi.org/10.1006/jcrs.1998.0241

Zhao, Q., Leung, S., Corbett, A. H., & Meier, I. (2006). Identification and Characterization of the Arabidopsis Orthologs of Nuclear Transport Factor 2, the Nuclear Import Factor of Ran. *Plant Physiology*, *140*(3), 869. https://doi.org/10.1104/PP.105.075499

Zhao, Y., Mo, B., & Chen, X. (2012). Mechanisms that impact microRNA stability in plants. *RNA Biology*, *9*(10), 1218–1223. https://doi.org/10.4161/RNA.22034

Zhao, Y., Yu, Y., Zhai, J., Ramachandran, V., Dinh, T. T., Meyers, B. C., Mo, B., & Chen, X. (2012). HESO1, a nucleotidyl transferase in Arabidopsis, uridylates unmethylated miRNAs and siRNAs to trigger their degradation. *Current Biology : CB*, *22*(8), 689. https://doi.org/10.1016/J.CUB.2012.02.051

Zhou, B., Luo, Q., Shen, Y., Wei, L., Song, X., Liao, H., Ni, L., Shen, T., Du, X., Han, J., Jiang, M., Feng, S., & Wu, G. (2023). Coordinated regulation of vegetative phase change by brassinosteroids and the age pathway in Arabidopsis. *Nature Communications 2023 14:1*, *14*(1), 1–18. https://doi.org/10.1038/s41467-023-38207-z

Zhu, H., Hu, F., Wang, R., Zhou, X., Sze, S. H., Liou, L. W., Barefoot, A., Dickman, M., & Zhang, X. (2011). Arabidopsis Argonaute 10 specifically sequesters miR166/165 to regulate shoot apical meristem development. *Cell*, *145*(2), 242. https://doi.org/10.1016/J.CELL.2011.03.024

Zhu, K., Chen, F., Liu, J., Chen, X., Hewezi, T., & Cheng, Z. M. M. (2016). Evolution of an intron-poor cluster of the CIPK gene family and expression in response to drought stress in soybean. *Scientific Reports*, *6*. https://doi.org/10.1038/SREP28225

Zhu, W., Schlueter, S. D., & Brendel, V. (2003). Refined Annotation of the Arabidopsis Genome by Complete Expressed Sequence Tag Mapping. *Plant Physiology*, *132*(2), 469–484. https://doi.org/10.1104/PP.102.018101

Zipprich, J. T., Bhattacharyya, S., Mathys, H., & Filipowicz, W. (2009). Importance of the C-terminal domain of the human GW182 protein TNRC6C for translational repression. *RNA*, *15*(5), 781. https://doi.org/10.1261/RNA.1448009

Zuo, Y. (2001). Exoribonuclease superfamilies: structural analysis and phylogenetic distribution. *Nucleic Acids Research*, *29*(5), 1017–1026. https://doi.org/10.1093/nar/29.5.1017